University of Southampton
FACULTY OF PHYSICAL SCIENCES AND ENGINEERING
ELECTRONICS AND COMPUTER SCIENCE

Outage Analysis and Optimization for Wireless Multiuser Relay Networks

by

Bo Zhang

A thesis submitted for the degree of
Doctor of Philosophy
at the University of Southampton

November 2014

Supervisor: *Prof. Lajos Hanzo*
Dipl Ing, M.Sc, Ph.D, DSc, FIET, FIEEE, FREng
Supervisor: *Dr. Mohammed El-Hajjar*
M.Sc, Ph.D, MIEEE
Southampton Wireless Group
Electronics and Computer Science
University of Southampton
Southampton SO17 1BJ
United Kingdom

𝔇edicated to my family

UNIVERSITY OF SOUTHAMPTON

ABSTRACT

FACULTY OF PHYSICAL SCIENCES AND ENGINEERING
ELECTRONICS AND COMPUTER SCIENCE

Outage Analysis and Optimization for Wireless Multiuser Relay Networks

by Bo Zhang

In this thesis, we propose a suite of schemes for wireless multiuser relay networks, where multiple source nodes (SNs) and relay nodes (RNs) share the spectral resources and hence we take into the account the co-channel interference (CCI). Our objective is to deal with both the channel fading and CCI in order to improve the attainable outage performance.

Firstly, we consider the opportunistic relay selection (ORS) design in the scenario, where multiple RNs are available for assisting the transmission of a single SN, while CCI is imposed by other SNs in the network. We design the single-user-detection-aided (SUD-aided) and multi-user-detection based successive-interference-cancellation-aided (MUD-SIC-aided) systems, where multiple-user detection (MUD) receivers using successive interference cancellation (SIC) at the destination node (DN) are adopted to combat co-channel interference. In SUD-aided system, we employ single-user detection (SUD) at the RNs and MUD-SIC at the DN. In MUD-SIC-aided system, we employ MUD-SIC at both the RNs and DN. We present the outage analysis of both systems based on an outage-optimised ORS scheme, implying that the proposed ORS scheme provides the best outage performance. We show that the traditional ORS scheme proposed for SUD receivers based on the highest SNR criterion is not outage-optimal, when employing MUD-SIC in the presence of CCI. Hence, we propose a novel ORS scheme based on a best-effort detection (BED) criterion that outperforms the traditional ORS scheme. Furthermore, considering the effects of the outdated channel state information (CSI), an improved BED-ORS is proposed for enhancing the robustness towards CSI imperfections.

Then, we study the scenario, where multiple SNs are coordinated to share a RN. In this case, network coding (NC) may be invoked at the RN, which treats the CCI from other SNs as useful messages and superimposes them to reduce the time slots required for relaying, therefore achieving higher spectral efficiency. However, NC systems may not always be beneficial in cooperative communications, where the detrimental interference of the undesired SNs, often referred to as network coding noise (NC noise), may outweigh the benefits of NC. In previous works, the outage performance was only evaluated numerically for several case studies. Against this background, we propose a systematically analytical framework for evaluating the

outage performance for a multi-unicast NC-aided network, where each DN extracts the information of the desired SN from the NC signal forwarded by the RN. As our main contribution, we present the outage analysis of this system in the presence of NC noise and the closed-form analytical outage probability expressions are derived for an arbitrary number of SN-DN pairs. We show that if NC is employed, the quality of the worst SN-DN link may dominate the outage performance of every SNs.

We then consider a two-hop network, where multiple SNs transmit to a DN with the aid of a RN and we assume the direct link between the SNs and the DN is weak. In this scenario, we show that the NC-aided relaying is not preferred and hence the buffer-aided relaying (BAR) is advocated for improving the uplink. The RN is equipped with a buffer, which is capable of storing multiple frames received from the SNs. During each time slot, the proposed protocol activates either the SN-RN hop or the RN-DN hop, depending on the channel quality of each hop and the buffer state at the RN. In order to optimise the hop selection for the network, we design a hop quality metric (HQM) and propose a multi-user buffer-aided-relaying uplink (MU-BR-UL) protocol. The benefits of the proposed protocol is analysed in terms of the end-to-end outage probability and the end-to-end transmission delay. Then, the optimal power allocation is proposed for minimizing the end-to-end outage probability under the total power constraint. Furthermore, the impact of the buffer size, the number of users and the relay position on the achievable outage performance are characterized. The results indicate that the outage performance is significantly improved when the proposed power allocation is utilized in the MU-BR-UL protocol.

Finally, we consider a new family of networks, in which the SNs and RNs have energy harvesting (EH) capability, which allows the nodes to harvest energy from the environments and convert it to electrical energy for wireless transmissions. The EH removes the constraints of relying on a battery for constant power supply, but also demands novel energy usage policy (EUP) design for effectively utilizing the random power supply gleaned from the EH system. We start with the point-to-point (P2P) network and by effectively exploiting the statistics of the energy arrival rates, we propose novel search algorithms for designing the EUP, which achieve a significantly better outage performance than the state-of-the-art designs reported in the literature. Based on the proposed methods in P2P network, we design novel EUPs for space-division-multiple-access (SDMA) and SDMA-based relay sharing networks. We show that the proposed EUPs significantly outperforms the state-of-the-art benchmarks in terms of outage performance.

Declaration of Authorship

I, **Bo Zhang**, declare that the thesis entitled

Outage Analysis and Optimization for Wireless Multiuser Relay Networks

and the work presented in it are my own and have been generated by me as the result of my own original research. I confirm that:

1. This work was done wholly or mainly while in candidature for a research degree at this University;
2. Where any part of this thesis has previously been submitted for a degree or any other qualification at this University or any other institution, this has been clearly stated;
3. Where I have consulted the published work of others, this is always clearly attributed;
4. Where I have quoted from the work of others, the source is always given. With the exception of such quotations, this thesis is entirely my own work;
5. I have acknowledged all main sources of help;
6. Where the thesis is based on work done by myself jointly with others, I have made clear exactly what was done by others and what I have contributed myself;
7. Parts of this work have been published, as seen in the list of publications.

Signed:

Date:

Acknowledgements

I would like to give my sincere thank to my supervisor Professor Lajos Hanzo for his professional supervision, his great support and great patience with me throughout these four years. His passion towards research, diligence and positive altitudes towards life inspired me and would encourage me after my graduation.

I would also like to thank my supervisor Dr. Mohammed El-Hajjar for his guidance. He helped me to discover my potential at research with constructive discussions and encouragements. I cannot complete this thesis without him and I am very grateful.

I want to say thanks to my parents. As their single child, I have been away for four years, during which they suffer a lot and endure lots of difficulties. But they conquered the difficulties and supported me. I would also thank my fiancee, Jinyu Yang for her company and support along this journey.

I also appreciate the friendship with everyone in our group, for their help, company and smile. I know there is a long list of names to mention and I am afraid of missing any one of them: Professor Sheng Chen, Professor Lie-Liang Yang, Dr. Soon Xin Ng, Dr. Rob Maunder, Dr. Rong Zhang, Dr. Shaoshi Yang, Dr. Chen Dong, Dr. Shuai Wang, Dr. Jie Zhang, Dr. Ping Yang, Dr. Li Wang, Dr. Xinyi Xu, Dr. Jiao Feng, Dr. Dandan Liang and Dr. Shida Zhong, Dr. Hong Chen, Dr. Hui Zhang, Dr. Liang Li, Dr. Chao Xu, Dr. Zhengming Kong, Dr. Taihai Chen and two Doctors named Jiayi Zhang, Dr. Wei Wu, Dr. Xiaojie Ju, Dr. Hung Viet Hguyen, Dr. Hoang Anh Ngo, An Li, Fan Jin, Meng Chen, Wenbo Zhang, Zunaira Barbar, Antony Thomas, Dimitrios Alanis, Panagiotis Botsinis, Ning Zheng, Xuan Li, Abdulah Jeza Aljohani, Professor Jing Lei, Professor Gan Liu, Hongming Zhang, Imran Ahmed, Feilong Wu. My housemates Dr. Jiankang Zhang, Dr. Yongkai Huo, Dr. Lilin Dan, Chuan Zhu and Kent Chuang. My badminton guys Dr. Jing Zuo, Dr. Haiping Huang, Dr. Fang Xu, Jia Shi, Wei Liang, Jie Hu, Hua Sun and Tao Wang. The guys playing both wireless and basketball next to me Dr. Fucheng Yang, Dr. Li Li, Xin Zuo, Peichang Zhang, Junyi Jiang.

Many thanks to all of you.

Contents

List of First-Author Publications

Journal Paper

1. **B. Zhang, H. Chen, M. El-Hajjar, R. Maunder and L. Hanzo**, Distributed Multiple-Component Turbo Codes for Cooperative Networks, IEEE Signal Processing Letters, In Press.
2. **B. Zhang, M. El-Hajjar and L. Hanzo**, Opportunisitc Relay Selection in Interference Contaminated Cooperative Networks, IEEE Transactions on Vehicular Technology, In Press.
3. **B. Zhang, J. Hu, Y. Huang, M. El-Hajjar and L. Hanzo**, Outage Analysis of Superposition Modulation Aided Network Coded Cooperation in the Presence of Network Coding Noise, IEEE Transactions on Vehicular Technology, Accepted.
4. **B. Zhang, C. Dong, M. El-Hajjar and L. Hanzo,** Buffer-Aided Relaying for Multi-user Uplink: Outage Analysis and Power Allocation, Submitted for Publication.
5. **B. Zhang, C. Dong, M. El-Hajjar and L. Hanzo,** Outage Analysis and Optimization for Energy Harvesting Networks with Finite Energy Buffer, Prepared for Submission.
6. **B. Zhang, C. Dong, M. El-Hajjar and L. Hanzo,** Distributed Energy Usage Policy Optimization for Multiple Access Energy Harvesting Networks. Prepared for Submission.

List of Symbols

General Notations

P_t	The instantaneous transmit power, the unit is Watt (W).
P_{out}	The outage probability.
R	The transmission rate of the transceiver.
γ_{ij}	The instantaneous SNR of the channel between node i and j.
$\bar{\gamma}_{ij}$	The average SNR of the channel between node i and j.
γ_{th}	The received SNR required for successful decoding defined as $\gamma_{th} = 2^R - 1$.
N_0	The noise power at the receiver.
T	The transition matrix of the discrete Markov chain.
π	The steady state probability vector of the discrete Markov chain.

Opportunistic Relay Selection Networks

K	The number of relay nodes.
M	The number of interferers.
D_s	The decoding set of relay nodes successfully decode the message.
c_l	The candidate node's index in the decoding set D_s.
P_e^1	The packet error ratio of the broadcast phase.
P_e^2	The packet error ratio of the relaying phase.
y_j^p	The signal received by the j-th node in the p-th phase.
$h_{i,j}^p$	The channel coefficient between node i and j in the p-th phase.
n_j^p	The noise at node j in the p-th phase.
$d_{i,j}$	The distance between node i and node j.
$P_{e,ij}$	The packet error ratio of the channel between node i and j.
γ_0	The received instantaneous SNR at a SIC receiver.
γ_i, $i > 0$	The received instantaneous SIR at a SIC receiver.
$\gamma_{(i)}$	The ordered received instantaneous SNR and INRs at a SIC receiver.
$\hat{h}$	The outdated channel coefficient.

ρ	The correlation coefficient between the outdated channel coefficient and the actual channel coefficient.
$P_f^{c_l}$	In the presence of outdated channel state information, the probability of avoiding an outage by candidate c_l as the probability that the actual decoding outcome is success, conditioned on the prediction being a success.
$I_0(\cdot)$	Zero-order modified Bessel function of the first kind.

Superposition Modulation Aided Relaying Networks

$h_{i,j}$	The channel coefficient between node i and j.
x_k	The signal transmitted by the k-th source node.
γ_k^p	The received instantaneous SNR at a k-th destination node in the p-th phase.
F_s	The forwarding set includes all the SNs, whose signals have been successfully decoded by the RN.
x_r	The signal transmitted by the relay node.

Buffer-Aided Relaying Networks

B	The size of the data buffer at the relay node.
b	The number of data frame in the buffer.
$\bar{b}$	The average number of data frame in the buffer.
V_b	The buffer state, where the number of data frame in the buffer is b.
$\bar{d}$	The average time duration that a frame is stored in the buffer.
P_{del}	The probability mass function of the delay.
W	The position-state matrix, where the specific element in the i-th row and j-th column is the probability that the frame is at the $(i-1)$-th position in the buffer and the buffer is at the state of V_{j-1}.
P_{del}	The total power budget of the source nodes and the relay node.

Energy Harvesting Networks

G_{sd}	The average channel gain between the source node and the destination node.
B_E	The amount of energy stored in the energy buffer, the unit is Joule (J).
B_T	The energy buffer state defined as $B_T = B/T_E$, the unit is Watt (W).
B_{max}	The upperbound of the energy buffer state, the unit is Watt (W).
P_{in}	The instantaneous energy arrival rate, the unit is Watt (W).
$\overline{P}_{in}$	The average energy arrival rate, the unit is Watt (W).
P_{th}	The threshold transmit power for successful decoding defined as $P_{th} = \gamma_{th}/G_{sd}$, the unit is Watt (W).

P_d	The desired transmit power in one-dimensional search. the unit is Watt (W).
T_E	The recharging cycle: the duration of a fading block of the energy arrival rate, the unit is second (sec).
T_C	The duration of a fading block of the wireless channels, the unit is second (sec).
ε_P	The discrete step size of the DMC model for the energy buffer state, the unit is Joule (J).
l	The discrete energy buffer state defined as $l = \lfloor B_T/\varepsilon_P \rfloor$.
$L_{\max}$	The discrete upperbound of the energy buffer state defined as $L_{\max} = \lfloor B_{\max}/\varepsilon_P \rfloor$.
L_{in}	The discrete instantaneous energy arrival rate defined as $L_{in} = \lfloor P_{in}/\varepsilon_P \rfloor$.
$\overline{L}_{in}$	The discrete instantaneous energy arrival rate defined as $L_{in} = \lfloor \overline{P}_{in}/\varepsilon_P \rfloor$.
L_t	The discrete instantaneous transmit power defined as $L_t = \lfloor P_t/\varepsilon_P \rfloor$.
L_{th}	The discrete decoding threshold defined as $L_{th} = \lfloor P_{th}/\varepsilon_P \rfloor$.
L_d	The discrete desired transmit power in one-dimensional search defined as $L_{th} = \lfloor P_d/\varepsilon_P \rfloor$.

Chapter 1

Introduction

1.1 Motivations

When designing wireless communication networks, we aim for answering the following three questions:

1. How to guarantee reliability for transmissions over the hostile wireless channel?
2. How to share the precious spectral resources among multiple users?
3. How to prolong the battery-recharge span both of the users and of the networks?

Since the conception of the information theory in the 1940s, the first question was pursued by thousands of researchers. At the time of writing, the state-of-the-art channel coding is capable of theoretically approaching the Shannon capacity for transmission over Gaussian and ergodic channels [1, 2], which is the maximum achievable rate while maintaining an arbitrarily low error probability. Hence, from a system designer's perspective, the data rate over each link of the wireless network may be capable of theoretically approaching the channel capacity.

Although the detrimental effects of noise are mitigated by channel coding in the context of the single-user transmission link, interference tends to preclude the handicap for reliable transmissions, when multiple users have to share the wireless spectrum, which is a precious limited resource in practice. In order to avoid the co-channel interference (CCI), the second-, third- and fourth-generation (4G) commercial cellular networks have invoked various orthogonal multiple access schemes, including the frequency-division multiple access (FDMA), the classic code-division multiple access (CDMA), time-division multiple access (TDMA) as well as the orthogonal-FDMA (OFDMA) [3]. At the time of writing we are entering the fifth-generation (5G) era. However, the ever-increasing amount of user devices requires both more spectrum as well as improvement of the spectral efficiency. Therefore, the philosophy of sacrificing the spectral efficiency in order to avoid the CCI may no longer be attractive.

The non-orthogonal space-division multiple access (SDMA) has been shown to achieve higher spectral efficiency than the orthogonal counterparts of TDMA, CDMA and OFDMA, albeit more sophisticated interference-cancellation (IC) mechanisms should be adopted for achieving the spectral efficiency improvements [4]. In the 4G systems, multiple antennas have been used for facilitating the multiple-input-multiple-output (MIMO) schemes, which may cancel the interference with the aid of the increased degree-of-freedom. Compared to single-input-single-output (SISO) schemes, we have a higher degree-of-freedom in the MIMO schemes, which allows us to recover both the desired signals and the interference [4]. In networks where the user devices have a limited size and hence they are less amenable to the employment to MIMOs, relaying has been introduced for constructing distributed MIMO systems, which exploit the cooperating antennas of spatially distributed single-antenna-aided wireless nodes [5, 6]. In the first part of this treatise, our focus is on the family of spectrum-sharing techniques invoked in the context of relaying networks, where novel IC schemes are proposed and analyzed in Chapters 2-4.

Then, in Chapter 5, we aim for prolonging the wireless nodes/networks lifetime, while guaranteeing a certain quality-of-service (QoS). Although a significant amount of work has been contributed to topic of "using the energy more efficiently" via capacity-achieving channel coding and efficient multiple access protocols, a major limitation of prolonging the network lifetime is the limited battery capacity, since the nodes can only operate for a finite duration until the battery becomes depleted. Fundamentally, the energy stored in the batteries is gleaned from the main's supply, which in turn relies on burning the coal, oil as well as from renewable energy sources like solar power or wind power. Instead of relying on the conventional procedure, which creates a gap between the power generation step and the power utilization step, the class of energy harvesting (EH) techniques allows a single node to harvest to use it for its utilizations [7]. To elaborate, EH refers to harnessing energy from the environment and converting it to electrical energy, which is then used for powering the nodes. Wireless communication is our major concern and the energy usage policy design for EH-aided wireless networks has become a hot topic [8, 9]. Hence in the second part of this treatise, we will design energy usage policies for EH-aided wireless networks in Chapter 5.

Before elaborating further on the new contributions of this thesis in Section 1.3, the related state-of-the-art is introduced in the next section.

1.2 Related Works

1.2.1 Outage Probability and Diversity Techniques

The wireless channels exhibit fading, where the ergodic capacity and outage capacity constitute a pair of salient performance measures for characterizing transmissions over

fading channels [4]. When a packet is transmitted over the ergodic fading channels, where the packet's duration spans across ergodic realizations of fading channel, the ergodic capacity is a reasonable performance measure. In this case, the packets can be successfully received by the destination as long as 'perfect capacity-achieving' channel coding is applied and the transmitted data rate is lower than the ergodic channel capacity [1, 10].

However, when a packet is transmitted over a *non-ergodic slow fading channel*, where the fading envelope is quasi-static across the entire packet, error-free transmissions cannot be guaranteed, even if powerful channel coding is applied[1]. *In this case, the instantaneous channel capacity is a random variable, and an outage occurs if the data rate is higher than the instantaneous channel capacity.* The so-called p-outage capacity is defined as the achievable data rate, at which the resultant outage probability (OP) is p. Hence, in slow fading channels, the outage probability is a reasonable performance measure and its analysis as well as optimization constitutes the focus of the thesis.

If the packets are transmitted over slow-fading channels, the OP may be quite high, when the channel experiences a deep fade. However, providing reliable transmission at high data rates is one of the important objectives of wireless communications, which motivates us to investigate sophisticated diversity techniques for the sake of improving the OP [4]. The most intuitive understanding of diversity techniques is "Do not put all eggs (signals) in the same basket (fading channel)." By sending signals that carry the same information through independent fading temporal-, frequency- and spatial-domain channels, multiple independently faded replicas of the same information are obtained at the receiver. In this case, the probability that all independent replicas suffer from in deep fading is greatly reduced and hence the OP may be substantially improved. Diversity techniques aiming for combating the effects of fading in order to achieve a high reliability have been proposed for both the temporal-, frequency- and spatial-domains [4, 10]. The corresponding implementations are forward error correction (FEC) coding, multi-carrier systems and MIMO systems in the context of temporal-, frequency- and spatial-diversity [4, 10].

Recently, in order to facilitate spatial diversity for networks, where the nodes have a limited size that preclude the employment of efficient MIMOs, distributed MIMOs have received extensive research attention since 2003 [5,6, 11]. Explicitly, relay-aided networks are capable of achieving spatial diversity for the sake of eliminating the correlation of signals, when multiple antennas cannot be used by the mobile nodes owning to their compact size. In recent years, various techniques have been proposed

[1] Adaptive modulation and coding relying on the accessibility of near-instantaneous channel state information at the transmitter (CSIT) may be guaranteeing error-free transmission. In practice, the CSIT may either be erroneous or outdated, and sophisticated CSI feedback design is required.

for improving the performance of wireless relaying in the context of distributed MIMO networks, which are briefly reviewed in the following two sections.

1.2.2 Single-Source Relaying Networks

The milestones of single-source relaying networks are listed in Table 1.1. The contributions disseminated during 2003 and 2004 proposed various orthogonal relaying schemes, including the amplify-and-forward (AF) [6], decode-and-forward (DF) [11] as well as the coded-cooperation schemes [12]. Later in 2005, more bandwidth-efficient relaying schemes were proposed relying on limited feedback aided automatic-repeat-request (ARQ) [13] and on non-orthogonal signaling [14], respectively. In 2006, more contributions started to focus on the multiple-source based scenario, as it will be revealed in the next section. On the other hand, a variety of relay selection schemes were proposed during the post-2006 era in order to achieve a higher diversity order. Among them, the single best relay selection of [15], opportunistic relay selection (ORS) [16] and multiple relay selection [17] were intensively analysed in the literature, since they are capable of achieving the maximum attainable diversity order, hence exhibit a considerable SNR gain, while relying on simpler synchronization mechanisms than their distributed space-time code (DSTC) counterparts [11].

Table 1.1 Milestones of Single-Source Relaying Networks

Year	Authors	Summary
2003	J. N. Laneman and G. W. Wornell [11]	DSTC was proposed and compared to repetition-based relaying, where the DSTCs were shown to achieve a higher spectral efficiency. The diversity multiplexing tradeoff (DMT) of orthogonal-DF relaying scheme was analysed, where the source node (SN) does not transmit during the relaying phase.
	A. Sendonaris, E. Erkip, and B. Aazhang [18, 19]	The system design of cooperative networks was proposed and its outage performance was analysed in the context of cellular networks.
2004	J. Laneman, D. Tse, and G. W. Wornell [6]	Both fixed and selective AF/DF relaying schemes operating without any feedback, as well as incremental relaying schemes relying on a limited feedback received from the destination node (DN) were conceived for a two-user cooperative scenario. They were also compared in terms of their OP and diversity order. It was shown that for the fixed-DF relaying scheme, they achieve the full-diversity order of 2.

Table 1.1 Milestones of Single-Source Relaying Networks

Year	Authors	Summary
	A. Stefanov and E. Erkip [12]	Coded cooperation was proposed. It was shown for two-user cooperative scenario that even if the inter-user channel quality was severely degraded, coded cooperation was still capable of providing substantial diversity and coding gains over its non-cooperative counterpart.
	M. Janani, A. Hedayat, T. E. Hunter, and A. Nosratinia [20]	Further coded cooperation contributions were made by Hunter as well as Nosratinia [21] and the attainable OP was analysed in [22].
2005	B. Zhao and M. C. Valenti [13]	Exploiting the limited feedback gleaned from the receivers, a DF-based cooperative automatic-repeat-request (CARQ) scheme was proposed for transmissions over orthogonal time slots. This CARQ may be viewed as a space-time generalization of the classic HARQ scheme relying on time-diversity. The CARQ regime relying on multiple retransmissions was shown to significantly improve the associated energy-latency trade-off, when compared to conventional multi-hop protocols.
	K. Azarian, H. ElGamal, and P. Schniter [14]	Non-orthogonal AF (NAF) and dynamic-DF (DDF) relaying schemes were proposed and the DMT of both systems was analysed. Firstly, in the down-link (DL) broadcast channel, the NAF was shown to outperform Laneman's orthogonal-DF DSTC-aided relaying schemes [11]. The DDF was shown to achieve the optimal tradeoff for multiplexing gains $0 \leq r \leq 1/N$, in the presence of $(N-1)$ relay nodes (RNs). Secondly, in the up-link (UL) cooperative multiple access (CMA) channel, the CMA-NAF scheme was proposed to achieve the optimal DMT. The authors highlighted the superiority of their schemes in the context of half-duplex cooperative systems by eliminating the need for orthogonal subspace constraint adopted in [6, 11–13, 18–20].

Table 1.1 Milestones of Single-Source Relaying Networks

Year	Authors	Summary
2006	A. Bletsas, A. Khisti, D. P. Reed, and A. Lippman [23]	ORS was proposed and shown to achieve the same DMT as DSTCs. However, the mutual information conveyed by ORS (by the best replica) was lower than that of DSTCs relying on all replicas. Moreover, the relay selection requires less-stringent synchronisation among the RNs and relied on a distributed architecture [16, 23].

1.2.3 Spectrum Sharing in Multi-Source Relaying Networks

In previous contributions, the focus was on the design of single-source relaying networks, while the effects of CCI be typically ignored [13,16,17]. However, this idealized scenario does not represent practical networks supporting simultaneous multi-source transmissions. As mentioned before, the family of orthogonal multiple access schemes aims for minimizing the CCI with the aid of *interference avoidance*, where the SNs are assigned orthogonal resources for their transmission. Nonetheless, unintended CCI may exist due to imperfect synchronization and control.

In order to more efficiently exploit the limited spectral resources, orthogonal multiple access scheme may be replaced by their non-orthogonal counterparts, which inevitably introduce CCI. Recently, the authors of [24–27] addressed the outage analysis of dual-hop relaying systems in the presence of CCI at the RNs or DNs or in fact at both. Their analysis was based on receivers utilizing either single-user detection (SUD) or interference suppression [28].

Instead of suppressing the interference, the interference-cancellation (IC) techniques at the receivers are capable of jointly/iteratively recovering the interference signals, and then canceling them. Hence the system's operation becomes effectively noise limited [28]. The IC idea may be implemented at the RNs and the DNs. In Fig. 1.1, we categorize different IC solution proposed for multi-source relaying networks as:

1. **IC used at the DN**: Carefully designed inter-SN coding may be adopted at the RNs, and IC is only invoked at the DNs. In this case, the RNs may superimpose the signals received from multiple SNs and forward the composite signal simultaneously [29, 30], which promises a higher bandwidth efficiency. In this category, a relay is shared among multiple SNs and the network coding (NC) based relay sharing techniques have been most widely studied [29–31]. Since NC is also deemed to be a promising candidate for recovering the multiplexing

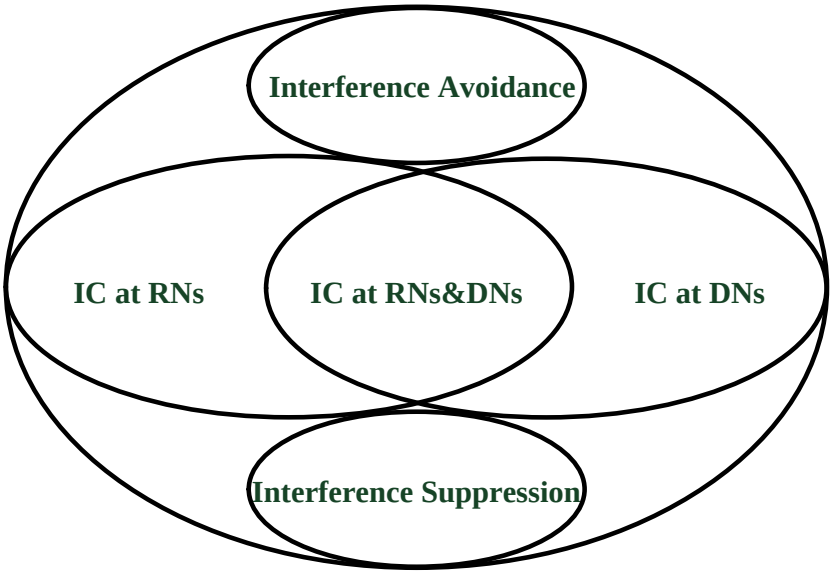

Figure 1.1: Solutions in Multi-Source Relaying Networks

loss of relaying networks, numerous research contributions have been devoted to this area [32–37]. Some of the salient research efforts in NC-CC have been summarised in Table 1.2.

2. **IC employed both at the RN and at the DN**: Compared to spectrum sharing relying on NC-based relay sharing [29–31], this is a less well-explored area, even though it may be viewed as a more natural evolution from single-SN relaying networks, where the RNs are not shared among multiple SNs. In this scenario, multiple SN-RN-DN links share the spectrum by transmitting simultaneously and therefore inflicting CCI upon each other. In each SN-RN-DN link, there is a single SN, where the RNs treat the signals received from other SN-RN-DN links as interference. Hence IC may be invoked at the RN and only the desired signal is forwarded to its intended DN, which also adopts IC for removing the interference arriving from other SN-RN-DN links. The design and analysis of this solution is considered in Chapter 2 and its performance is compared to that of its counterpart using IC at the DN in Chapter 3.
3. **IC only at the RN**: The RNs decode the signals arriving from multiple SNs relying on an IC algorithm and no inter-SN coding is employed. The signals gleaned from different SNs are forwarded via orthogonal channels, so that no IC is necessitated at the DN. As shown in Chapter 3 and Chapter 4, this scheme is preferred when the direct link between a SN and its DN is weak. Hence relaying is required for providing the uplink.

Table 1.2 Milestones of Network-Coded Multi-Source Relaying Networks

Year	Authors	Summary
2005	E. G. Larsson and B. R. Vojcic [38]	Superposition modulation and multi-user detection were applied in cooperative networks, where a linear-combination based superposition modulation aided scheme was shown to outperform the conventional time-multiplexing DF relaying arrangement.
2006	Y. Chen, S. Kishore, and L. Jing [39]	Binary linear NC constructed over the Galois Field $GF(2)$ was applied to both a distributed antenna system as well as to a cooperative multi-user system. It was shown that cooperative network coding scheme was capable of achieving a better outage performance than its conventional cooperative counterpart, achieving a diversity order of M, which is the number of cooperating users.
	S. Katti, H. Rahul, W. Hu, D. Katabi, M. Médard, and J. Crowcroft [29]	An architecture was proposed for wireless mesh networks delivering unicast traffic, as well as dynamic and potentially bursty flows. A range of practical issues concerning the integration of NC into existing networks were also considered. The hardware prototype constructed achieved a network throughput gain spanning from a few percent to way above 100%, depending on the traffic pattern, congestion level and transport protocol.
	S. Zhang, S. C. Liew, and P. P. Lam [33]	The concept of physical-layer network coding (PL-NC) was proposed, which required two time slots to exchange information for two users. By constrast, the previous proposed NC schemes required three time slots. The authors assumed perfect symbol-level and carrier-phase synchronisation, as well as the employment of power control, so that the frames received from the pair of users would arrive at the relay with the same phase and amplitude. Furthermore, it should also be noted that the relay mapped the superposition of electromagnetic signals to the Galois Field $GF(2^n)$ using the additions of digital bit streams.

Table 1.2 Milestones of Network-Coded Multi-Source Relaying Networks

Year	Authors	Summary
	T. Ho, M. Medard, R. Koetter, D. R. Karger, M. Effros, J. Shi, and B. Leong [40]	Distributed random linear NC (RL-NC) was proposed for the transmission and compression of information in general multisource multicast networks. The network nodes independently and randomly selected linear mappings from the inputs onto the output links over a finite field. It was shown that RL-NC may approaching the capacity with a probability exponentially approaching unity upon with increasing code length. It was also demonstrated that RL-NC was capable of achieving a compression in a network. Furthermore, a bound was derived concerning the required field size for centralised NC operating in general multicast networks.
2007	T. Fuja, J. Kliewer, and D. Costello [31]	It was shown for a two-user cooperative scenario using simulation, that the binary linear NC scheme constituted a substantial coding gain over other cooperative diversity techniques, including those based on time multiplexing [5, 6, 20, 21] and superposition modulation [32].
	S. Katti, S. Gollakota, and D. Katabi [30]	The PL-NC proposed in [33] was implemented in a 2-user-1-relay scenario using a hardware soft-radio defined prototype[2]. For PL-NC to become practical, the authors had to address two challenges. Firstly, the channel-induced distortions had to be eliminated before canceling the interfering signal. Secondly, imperfect synchronisation resulted in a time shift between the two signals. Both users had to align the known signal with the interference in the received signal before they could cancel the interference.

[2]The PL-NC was also referred to as analog network coding (ANC) by the authors in [30]. However, the terminology "ANC" is used in a wider sense, where the superposition-based NC was referred to as ANC in some of the literature, e.g. [41]. Therefore, throughout this contribution, we consider PL-NC to be a special case of ANC.

Table 1.2 Milestones of Network-Coded Multi-Source Relaying Networks

Year	Authors	Summary
2008	T. Wang and G. B. Giannakis [34]	The concept of complex-field NC was proposed. In contrast to binary NC constructed over the Galois field [39], where the network's throughput was limited as the number of sources increases in the M-SN-1-RN-1-DN wireless multiple access relay channel, complex-field NC may always be capable of achieving a throughput as high as 1/2 symbol per source per channel use.
2010	M. Xiao and M. Skoglundn [36]	Random linear NC [40] was not guaranteed to exist for finite alphabet sizes, hence cannot guarantee achieving the diversity order of $(2M-1)$. For an M-user scenario, dynamic NC[3] was proposed, where a non-binary finite-field based linear-combination was adopted over $GF(2^n)$. The resultant diversity order was $(2M-1)$, which was higher than that of the schemes operating without NC or with the aid of the binary NC schemes of [31,39]. Its performance bounds were analysed in [42].
	S. Sharma, Y. Shi, J. Liu, Y. T. Hou, and S. Kompella [41]	It was shown that employing NC may not always benefit cooperative communication (CC) in the context of analog-NC-aided AF relaying. The concept of NC noise was introduced. Both the signal aggregation employed at a RN and the signal extraction used at a DN were analysed. It was shown that the NC noise imposed at each DN of a multi-session environment would increase with the number of cooperating sessions. Therefore it is capable of entirely eroding the advantage of NC in cooperative communications. The analog-NC-aided DF relaying performance was also analysed by Sharma, et. al [43].

[3]Please note that, the DNC does exhibit randomness, which stems entirely from the channel coefficients. This is the fundamental difference between DNC and RL-NC [40].

Table 1.2 Milestones of Network-Coded Multi-Source Relaying Networks

Year	Authors	Summary
2011	B. Nazer and M. Gastpar [44]	The compute-and-forward (CF) based NC philosophy was proposed for achieving significantly increased rates in a network, using the idea of lattice codes. Explicitly, the SNs map messages from a finite field into lattice points, and transmit these over the channel. Each RN observes a noise linear combination of these lattice points and attempts to decode an integer combination of them. After decoding these linear combinations, the RNs send them towards the DNs. The DNs map the received equations of lattice points back into the linear equation over a finite field. Finally, the original messages from the finite field may be recovered.
2012	J. L. Rebelatto, B. F. Uchoa-Filho, Y. Li, and B. Vucetic [37]	The generalised dynamic NC regime based on [36] was proposed. An analogy with the maximum distance separable codes was established. Specifically, Reed-Solomon codes were used as a design example.
2013	V. T. Muralidharan and B. S. Rajan [45]	A PL-NC scheme was proposed for the M-SN-1-RN-1-DN wireless multiple access relay channel was proposed. In phase-1 the SNs transmitted, while in phase-2 all the SNs and the RN transmitted. After phase-1 the RN had to decode the messages of the SNs and transmitted a many-to-one function of the decoded messages. It was shown that if certain parameters were chosen appropriately, the proposed decoder may offer the maximum diversity order of 2. The simulation results provided indicated that the proposed PL-NC scheme offered a substantial gain over [34].
2014	Chen, Z., Fan, P., Letaief. K. Ben. [46]	The author investigated a multi-source multi-cast network with the aid of an arbitrary number of relays using CF-based NC idea [44]. The fundamental limit is found for the maximal common multicast throughput of all SNs. It was shown that the CF strategy outperforms conventional DF strategy.

Table 1.2 Milestones of Network-Coded Multi-Source Relaying Networks

Year	Authors	Summary
	Di Renzo, M. [47]	The author provided a mathematical framework for the analysis for networks with an arbitrary number of SNs and RNs with the aid of NC over non-binary Galois field. The repetition-based and relay selection cooperation are investigated for NC-based relaying networks. It was shown that repetition-based protocols are capable of achieving full-diversity if the Galois field size is sufficiently large and the network code satisfies the maximum distance separable property. Also, it was shown that if the number of active RNs is no fewer than the number of SNs, the relay selection are capable of achieving full- diversity.

1.2.4 Wireless Energy Harvesting Networks

All the previously reported research relies on a battery at the transceiver to provide a constant power supply. However, the finite battery capacity implies a fundamental limitation on the network's lifetime. Energy harvesting refers to harnessing energy gleaned from the environment or from other energy sources and converting it to electrical energy [7]. If the harvested energy source is periodically available, the wireless transceiver can be powered perpetually. However, the energy harvested from the environment is random rather than constant, which requires sophisticated energy usage policy design in order to efficiently utilize the harvested energy. This has become a "hot topic" in recent years and the most representative contributions are summarised in Table 1.3.

Table 1.3 Milestones of Energy Harvesting Networks

Year	Authors	Summary
2009	Lei, J., Yates, R., & Greenstein, L. [48]	Assuming that the messages for transmission arrive at the sensor by obeying a memoryless Poisson process, the optimal online energy usage policy was derived using a dynamic programming framework, which maximizes the average reward rate of a point-to-point (P2P) link.

Table 1.3 Milestones of Energy Harvesting Networks

Year	Authors	Summary
2010	Sharma, V., Mukherji, U., Joseph, V., & Gupta, S. [49]	For a P2P link with a EH-SN, the authors found the energy management policies that maximize the data rate, when the data queue at the EH-SN remains stable. The energy management policies that minimize the mean delay in the queue were also derived.
	Medepally, B., & Mehta, N. B. [50]	The authors considered a network in which EH nodes volunteer to serve as amplify-and-forward RNs for a non-EH SN. The symbol error rate was derived for both stationary and for ergodic EH processes, and the optimal static transmit power at the EH RNs was also derived.
2011	Ozel, O., Tutuncuoglu, K., Yang, J., Ulukus, S., & Yener, A. [8]	Under the idealized simplifying assumption of having both the non-causal channel state information (CSI) and energy harvesting information (EHI) of the energy arrival rate at the transmitter, the optimal offline energy usage policies were designed either for throughput maximization or for completion time minimization in a P2P network communicating over fading channels. The optimal online policies were also designed with the aid of a stochastic dynamic programming technique.
	Li, H., Jaggi, N., & Sikdar, B. [51]	In a wireless sensor network relying on EH nodes, the authors considered a range of scheduling problems by either selecting the SN to directly transmit their data to the DN or by using a RN to assist, given an estimate of the current network state. The optimal scheduling problem was formulated and solved as a Markov decision process (MDP), assuming that the complete state information conceiving the RNs is available at the SNs. The idealized simplifying assumption of having perfect full state information was removed and the problem was formulated as a partially observable Markov decision process (POMDP).

Table 1.3 Milestones of Energy Harvesting Networks

Year	Authors	Summary
2012	Yang, J., & Ulukus, S. [52]	As an evolution of [8], the authors considered the optimal packet scheduling problem in a P2P network having an EH-SN, while both the data packets and the harvested energy were assumed to arrive at the source node randomly. The time for delivering all packets was minimized by adapting the transmission rate both according to the traffic load and to the energy available in the energy buffer. The optimal off-line scheduling policy was provided.
	Yang, J., & Ulukus, S. [53]	As an evolution of [52], the optimal packet scheduling problem in a two-EH-SN multiple access communication system was considered. The optimal off-line policy was found by minimizing the time required for all packets to be delivered from the pair of EH-SNs to the destination.
2013	Huang, C., Zhang, R., & Cui, S. [54]	The authors considered a three-node Gaussian relay channel using decode-and-forward relaying associated with a EH-SN, a EH-RN and a DN. Assuming that both the energy arrival time and the harvested amount are known in advance, the optimal off-line policy was determined for maximizing the throughput over a finite time-horizon of N transmission blocks for both delay-constrained and for delay-tolerant scenarios.
	Luo, S., Zhang, R., & Lim, T. J. [55]	The authors considered the so-called "energy half-duplex constraint", in which a pair of rechargeable energy storage devices are assumed to be available and at any given time, only one of them is being recharged. The energy harvesting rate is assumed to be a random variable that is constant over the time interval of interest. A "save-then-transmit" protocol was proposed based on the best-effort policy, where the energy stored in the buffer is used up in support of each individual transmission event. The optimal "save-ratio" that minimizes the outage probability was also derived. The diversity order associated with a random power arrival process was shown to be the same as that of constant power, but the OP difference can be large.

Table 1.3 Milestones of Energy Harvesting Networks

Year	Authors	Summary
	Zlatanov, N., Schober, R., & Hadzi-Velkov, Z. [56]	The asymptotically-optimal policy was proposed for an infinite energy buffer and it was shown to minimise the OP by allowing the EH-SN to transmit at a constant power, which is equal to the average energy arrival rate supplied by the EH-SN, when sufficient energy is stored in the energy buffer. By contrast, if insufficient energy is stored in the energy buffer, the SN would switch to the best-effort policy. When the size of the energy buffer approaches infinity, it was shown that the OP would approach that of the constant-power system.
2014	Huang, C., Zhang, R., & Cui, S. [57]	The authors considered the optimal power allocation for OP minimization in P2P fading channels relying on an EH-SN. For the non-causal ESI case, the globally optimal off-line power allocation was obtained by a forward search algorithm. Moreover, for the case associated with causal EHI, both the optimal and suboptimal online power allocation algorithms were proposed.
	Xu, J., & Zhang, R. [58]	The authors considered the fundamental tradeoff between maximizing the energy efficiency and bandwidth efficiency in the context of a P2P additive white Gaussian noise (AWGN) channel associated with an EH-SN, which assumes having a practical on-off transmitter model relying on non-ideal circuit power. The optimal off-line policy derived for maximizing the average throughput over a finite time-horizon is derived as a two-phase transmission regime, where the EE-maximizing on-off and the SE-maximizing power allocation is adopted in the first and second phase, respectively.

1.3 Thesis Outline and Novel Contributions

Fig.1.2 illustrates the thesis structure, where the first part in Chapters 2, 3 and 4 assumes that the nodes are equipped with batteries having a finite capacity and

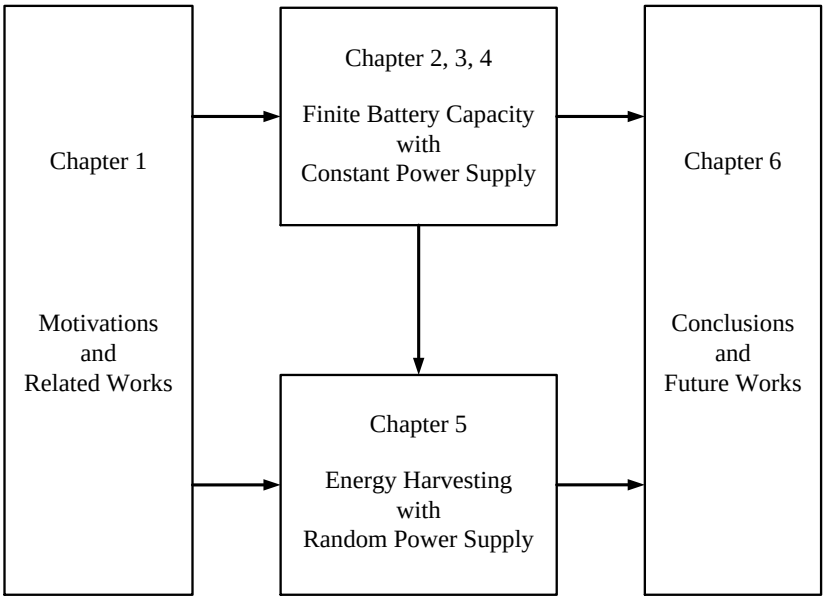

Figure 1.2: Solutions in Multi-Source Relaying Networks

the second part in Chapter 5 assumes that the nodes are equipped with an energy-harvesting system. Specifically, novel IC schemes are proposed for multi-source relaying networks in Chapters 2, 3 and 4. The corresponding OP analysis and its optimization are also considered. The second part of the thesis assumes that the nodes are equipped with EH capability, where the OP analysis and optimization of P2P, SDMA and multi-source relaying networks are detailed in Chapter 5.

Chapter 2: The multi-user-detection (MUD) based IC technique is introduced at both the RNs and the DNs in multi-SN relaying networks employing relay selection. We first analyse the outage performance of the proposed systems and define the design criteria for outage-optimal ORS schemes adopting MUD-SIC receivers at the DN. Then, in order to demonstrate the outage improvements introduced by successive-interference-cancellation (SIC) receivers, we design a novel best-effort-detection based ORS (BED-ORS) scheme based on a best-effort-detection criterion. We demonstrate that the proposed BED-ORS regime is capable of achieving a better outage performance than the traditional ORS scheme originally designed for SUD receivers [59]. Furthermore, in order to enhance the robustness of ORS against outdated CSI imposed by a realistic delayed feedback, we design an improved BED-ORS, which relies on the associated statistical information concerning the SN-DN and RN-DN channels for avoiding outage events associated with the highest possible probability. We demonstrate that the improved BED-ORS is more robust against outdated CSI than the conventional BED-ORS.

Chapter 3: The NC technique is introduced at the RNs and IC is implemented at the DNs. As discussed in Section 1.2.3, various NC-based multi-SN relaying schemes

have been conceived and the authors demonstrated their superiority over conventional relaying schemes. We consider the scheme proposed in [43], which extracts the information of the desired SN from the composite signal forwarded by the RN and as our main contribution, we present the outage analysis of this system in the presence of NC noise. More explicitly, the closed-form analytical OP expressions are derived for an arbitrary number of SN-DN pairs with the aid of accurate approximations. Simulation results are also provided for confirming the analytical results, which validates our analysis.

Chapter 4: An IC technique is introduced at the RNs, while the DN relies on low-complexity single-user detectors. As shown in Chapter 3, when relaying is introduced for improving the quality of the uplink, the direct links between the SNs and the DN may be weak. Therefore, the NC-based relay sharing schemes may perform worse than the conventional cooperative networks. Therefore, we adopt a time-multiplexing cooperative scheme, where the RN uses a higher rate for re-encoding the message from multiple SNs so that the relaying phase is shared among multiple SNs simultaneously, while dispensing with the direct links. In this case, buffer-aided relaying is proposed, which exploits the associated hop-selection diversity. The system design, the OP analysis as well as the delay analysis of the buffer-aided multi-user uplink is detailed.

Chapter 5: In this chapter, EH-based wireless nodes are used for replacing both the conventional SNs and the RNs in the network, where the new challenge is to optimize the energy usage policy (EUP) according to the random power supply provided by the EH devices. Firstly, an analytical framework is proposed for investigating the OP of a EH-P2P network, in which a EH-SN equipped with a finite energy buffer transmits to a DN. Secondly, we investigate the optimal EUP conceived for minimizing the OP of a P2P-EH network. Thirdly, we also extend the proposed DMC framework to more general non-orthogonal EH-networks, where a SDMA network and a SDMA-aided two-hop relay sharing network are investigated, as our specific case studies. Explicitly, we propose a distributed EUP optimization (DEUPO) protocol, in which each EH-SN is capable of optimizing its own policy using both the local statistics of the fading channel and the related energy arrival model.

Chapter 6: In this chapter we offer our conclusions and then provide design guidelines as well as a range of future research ideas.

Chapter 2

Opportunistic Relay Selection in Multi-Relay Wireless Networks[1]

As discussed in Chapter 1, cooperative communication is capable of providing spatial diversity for single-antenna aided wireless devices [13], where one or more nodes act as relays for other communicating nodes. Hence, relay selection [17] is an important factor that affects the performance of a cooperative system. As the coordination and synchronization of multiple simultaneously transmitting relay nodes (RNs) constitutes a challenge, opportunistic relay selection (ORS) [16] may be preferred, which achieves the maximum attainable diversity at a lower implementation complexity than its counterpart operating without relay selection. Explicitly, the ORS scheme may select a specific RN from multiple candidate RNs to retransmit the signal from the source node (SN) that facilitates the highest instantaneous signal-to-noise power ratio (SNR) at the destination node (DN) [16]. In this way, a diversity order equal to the number of RNs K can be achieved[2] [16]. Recently, several improved ORS algorithms have been proposed for different scenarios. In [60], the authors investigated the optimal highest-SNR-based relay selection, the geometry-based relay selection and the random relay selection for uniformly distributed sensor nodes, where they have shown that for all proposed schemes, the SNR variance at the DN converges to zero as the number of RNs increases, which substantially mitigates the effects of fading. In [61], an ORS was designed for selecting multiple rather than a single relay, in order to achieve an improved end-to-end throughput.

However, practical networks suffer from the deleterious effects of co-channel interference (CCI), which was not considered in the previous literature [13, 16, 17, 60, 61]. Recently, a dual-hop cooperative relaying scheme adopting single-user detection

[1] Part of the work in this chapter has been published in: B. Zhang, M. El-Hajjar and L. Hanzo, Opportunistic Relay Selection for Cooperative Relaying in Co-Channel Interference Contaminated Networks, IEEE Transactions on Vehicular Technology, 2013.

[2] If the direct link between the SN and the DN is considered, a maximum diversity order of $(K+1)$ may be achieved.

(SUD) receivers was conceived for mitigating the CCI [24,27,59]. The authors of [59] showed that the traditional ORS based on the highest-SNR criterion is "outage-optimal" in dual-hop relaying system adopting SUD receivers. However, the SUD receivers treat CCI as noise, while the structured nature of the interference is not exploited. In contrast to SUD, multi-user detection (MUD) relying on successive interference cancellation (SIC) [4] may achieve better outage performance, at the cost of a moderate implementational complexity [4]. In [62], MUD-SIC receivers were introduced into a cooperative network relying on multiple SNs, RNs and DNs, where the transmission rates were optimised for a scenario of multiple RNs accessing the channel simultaneously.

The classic MUD-SIC has been routinely adopted at the detection and decoding stage as well as for improving the outage performance of both the multi-user uplink as well as of P2P schemes in the presence of interference. However, it has not been intrinsically amalgamated with any ORS design scheme as a medium access control (MAC) layer protocol in the existing literature. Therefore, the first research question we consider can be stated as: *how to design outage-optimal ORS using MUD-SIC receivers*? Furthermore, the outage performance of ORS may degrade due to having a realistic delayed feedback, where the relay selection decisions are based on realistic outdated channel state information (CSI)[3] [63, 64]. However, previous research found in the open literature only considered ORS schemes either using outdated-CSI assuming interference-free scenarios [63–65] or assuming perfect-CSI in the presence of CCI [59,66]. Therefore, our second research question is stated as: *how to mitigate the outage performance degradation under realistic outdated-CSI for the ORS scheme using MUD-SIC receivers?*

Against this background, in this chapter, we first review the outage-optimal ORS design in interference-free multi-relay networks, where the SUD receivers are adopted at both the RNs and at the DN. It is plausible that the *highest SNR criterion* is outage-optimal [16]. Then, we investigate the outage-optimal ORS design conceived for multi-relay networks operating in the presence of CCI and propose a pair of novel schemes, where we employ MUD-SIC receivers at the DN and we consider relaying networks subjected to CCI.

We consider a pair of single-SN multi-RN systems employing MUD-SIC receivers at the DN. In the first system, which we refer to as our *SUD-aided scheme*, we employ SUD receivers at the RNs. By contrast, in the second system, which we refer to as our *MUD-SIC-aided scheme*, we employ MUD-SIC receivers at both the DN and the RNs. Although a single SN-DN pair is considered in our system, the ORS scheme proposed may be generalised to practical multi-user networks comprised of multiple SNs, e.g. in a cellular network, where multiple SN-DN pairs in a cell may be assigned

[3]In this chapter, the CSI is defined as the instantaneous channel coefficient capturing the effects of the pathloss and fading.

orthogonal channels so that the ORS may be implemented separately for each SN-DN pair, while the CCI is dominated by inter-cell interference. Then, we address the above-mentioned open problems in the context of the proposed system models and the corresponding novel contributions of this chapter are summarized as follows:

- We analyse the outage performance of the proposed systems and define the criteria to be satisfied in order to arrive at an outage-optimal ORS scheme for the class of systems adopting MUD-SIC receivers at the DN. We show that the conventional ORS scheme proposed for SUD receivers based on the highest SNR criterion is not outage-optimal, when employing a MUD-SIC receiver in the presence of CCI. Hence, we design a novel outage-optimal best-effort-detection-based-ORS (BED-ORS) scheme, which intrinsically integrates the SIC algorithm into ORS. We demonstrate that the proposed BED-ORS is capable of achieving a better outage performance than the traditional ORS scheme that was originally designed for SUD receivers [59].
- In order to enhance the robustness of ORS considering the outdated CSI due to delayed feedback, we design an improved BED-ORS (I-BED-ORS), which relies on the statistical information concerning the SN-DN and RN-DN channels in order to minimize the outage probability. We demonstrate that the I-BED-ORS is more robust against outdated-CSI than BED-ORS.

The rest of the chapter is organized as follows. In Section 2.1, the outage-optimal ORS designed for multi-RN networks is reviewed in the absence of CCI, where the outage performance is analysed. In Section 2.2 we analyse the outage performance of multi-RN networks in the presence of realistic CCI and propose a pair of two systems adopting MUD-SIC receivers at the DN, where the outage-optimal ORS scheme is designed. In Section 2.3 we present our simulation results, followed by our conclusions in Section 2.4.

2.1 ORS Design for Interference-free Networks

In this section we review the state-of-the-art in ORS design conceived for minimising the end-to-end outage probability (OP) for interference-free networks, which lays the foundation for Section 2.2, where we consider realistic networks operating in the presence of CCI. Again, the OP analysis of ORS design in the context of interference-free networks is well documented in [16,67]. Therefore this section serves as background knowledge.

2.1.1 System Model

We consider a network comprised of a SN, K RNs and a DN, as shown in Fig. 2.1. Each node is equipped with a single antenna and operates in a half-duplex mode. We assume a Rayleigh block fading channel model, where the fading coefficient remains

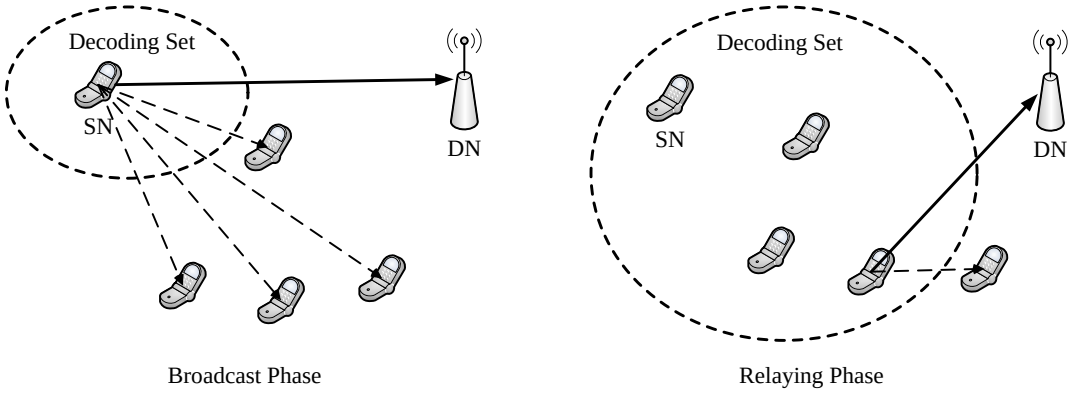

Figure 2.1: System Model of ORS without CCI

constant for the duration of a packet and then it is faded independently from one packet to another both in time and space. The noise at the receivers is modelled by independent zero-mean circularly symmetric complex Gaussian random variables.

The classic cooperation process includes the **broadcast phase** and the **relaying phase**. In the broadcast phase, the SN transmits its data to both the RNs and the DN, where the signals received by the RNs and the DN are given by

$$y_k^1 = h_{s,k}^1 x_s + n_k^1, \quad k = 1, \ldots, K \tag{2.1}$$

$$y_d^1 = h_{s,d}^1 x_s + n_d^1 \tag{2.2}$$

with y_j^p being the signal received by the j-th node in the p-th phase[4], $h_{i,j}^p$ is the instantaneous channel coefficient or the CSI between node i and j in the p-th phase representing the effects of the pathloss and Rayleigh fading, x_s is the signal transmitted by the SN with its power normalised to 1, while n_j^p is the noise at node j during the p-th phase. Similar to [13,16], we adopt the notion of *decoding set*, denoted by D_s, which includes all nodes having the knowledge of the SN's original codeword. The nodes are assumed to have perfect receiver-side CSI for recovering the codewords. Naturally, before the broadcast phase, only SN is in the D_s. After the initial transmission, the RNs which receive adequate information for decoding successfully would join D_s. In practice, the transmitted codewords may add cyclic redundancy check (CRC) bits for error detection, where the RN may detect the errors after channel decoding. Again, only the specific RNs that successfully decoded the message are included in the decoding set D_s and only these RNs may be selected as the relaying nodes in order to avoid error propagation [16, 23], which is illustrated in Fig. 2.1.

[4] $p = 1$ represents the broadcast phase and $p = 2$ stands for the relaying phase.

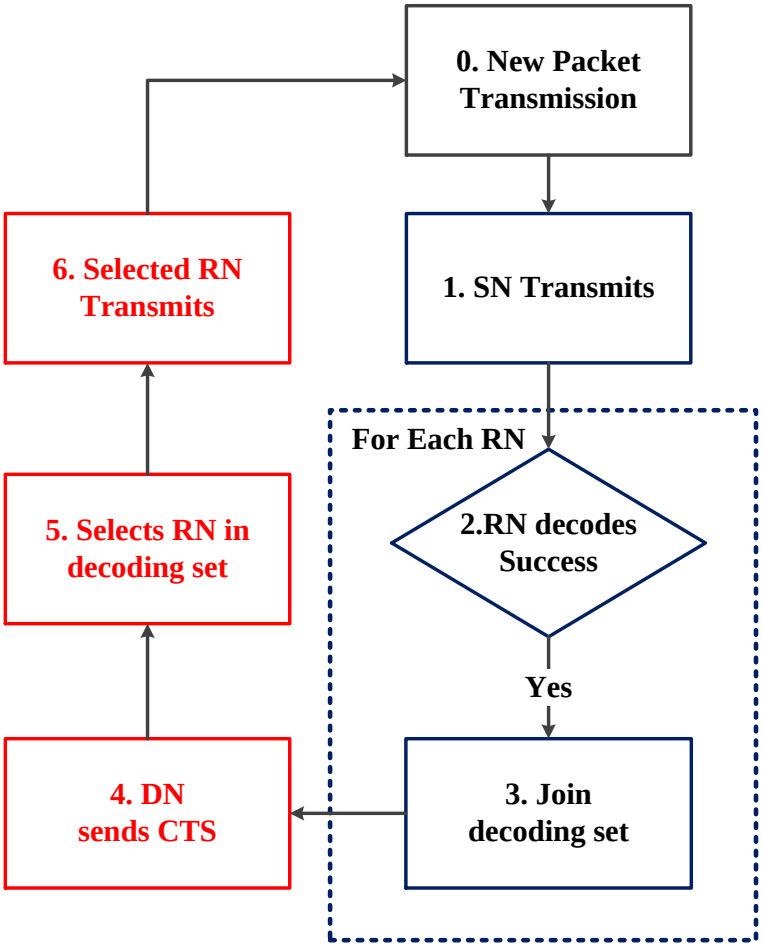

Figure 2.2: Flowchart of ORS scheme without CCI

During the relaying phase, the optimum node $k^\star$ is assumed to be selected by the ORS scheme for relaying and the signal received at the DN is given by

$$y_d^2 = h_{k^\star,d}^2 x_s + n_d^2. \tag{2.3}$$

Specifically, the DN broadcasts a clear-to-send (CTS) signal and all RNs listen. It is assumed that each RN acquires perfect transmitter-side CSI by estimating the CSI during the reception of the CTS signal. In the next section, the ORS design relying on selecting the optimal node $k^\star$ is investigated.

2.1.2 Opportunistic Relay Selection Design

The ORS scheme selecting a single RN for relaying was shown to be outage-optimal for decode-forward (DF) relaying by the authors of [16, 23]. Specifically, the selected RN is the one in the decoding set D_s having the highest instantaneous SNR at the

DN, which is shown to be outage-optimal. The flowchart of the ORS scheme is characterized in Fig. 2.2, which is described as follows:

1. **Initial transmission**: the SN broadcasts its message to all RNs and to the DN as shown in Block 1 of Fig. 2.2, while the RNs and the DN listen.
2. **Decoding set update**: All RNs attempt to decode the signal buffered during the SN's broadcast phase, as shown in Block 2 of Fig. 2.2. If a RN successfully decodes the received signal, it is capable of regenerating the original message and therefore joins D_s, as shown in Block 3 of Fig. 2.2.
3. **ORS at DN**: The specific potential transmit node within D_s, which has the highest instantaneous SNR at the DN is selected as the retransmission node in Block 5 of Fig. 2.2. This can be realized without requiring global CSI at each node with the aid of an uncoordinated/distributed algorithm or it may be coordinated by a central control node. A practical option is to employ distributed timers [16, 23], where each node estimates its own instantaneous SNR at the DN by estimating the CSI during the reception of the CTS signals broadcast by the DN in Block 4 of Fig. 2.2. On the basis of the time division duplex (TDD) protocol, it may be assumed that the uplink channel is identical to the downlink channel. The RN will then initiate the count-down timer, which is inversely proportional to the instantaneous SNR levels and then joins the contention. Therefore, the timer of the RN having the highest SNR at the DN runs out first. As soon as the timer runs out, the RN broadcasts a flag to announce itself as the transmitting node. After receiving the flag, the other RNs would reset their timers and remain silent.
4. **Relaying**: The node selected in Step 3 above re-encodes the message and re-transmits it, as shown in Block 6 of Fig. 2.2. The DN attempts to decode the message and a new packet's transmission initiates.

2.1.3 Outage Analysis

An outage is defined as the event, where the received SNR experienced at the DN is lower than the predefined threshold γ_{th} that has to be exceeded for successful decoding. If idealized perfect capacity-achieving channel coding is assumed, this threshold is $\gamma_{th} = 2^R - 1$, where R is the maximum achievable transmission rate of the SN [4]. When no packet-combining techniques are invoked at the receiver and the erroneous packets are discarded, the OP P_{out} is equal to the probability that both the broadcast and the relaying phases are in outage. Hence, we have

$$P_{out} = P_e^1 P_e^2, \tag{2.4}$$

where P_e^1 denotes the packet error ratio (PER) of the direct transmission in the broadcast phase, while P_e^2 represents the PER of the retransmission in the relaying

phase. As the classic point-to-point (P2P) transmission is a basic building block of the single-SN-multi-RN network, we first present the P2P PER analysis and then we deduce the OP of the network considered based on the P2P PER analysis.

Since a Rayleigh-distributed block fading channel is assumed, the instantaneous SNR for transmission over the SN-DN channel obeys the exponential distribution of $f_{\bar{\gamma}_{sd}}(\gamma) = \frac{1}{\bar{\gamma}_{sd}} \exp(-\frac{\gamma}{\bar{\gamma}_{sd}})$ and the PER of the broadcast phase P_e^1 may be expressed as

$$\begin{aligned} P_e^1 &= P_{e,sd} \\ &= \Pr\{\gamma_{sd} < \gamma_{th}\} \\ &= 1 - \exp\{-\frac{\gamma_{th}}{\bar{\gamma}_{sd}}\}. \end{aligned} \tag{2.5}$$

By contrast, the retransmission phase OP P_e^2 in Eq. (2.4) may be expressed as

$$P_e^2 = \sum_{D_s} \Pr\{D_s\} P_e(D_s), \tag{2.6}$$

where $Pr\{D_s\}$ is the probability that D_s is the decoding set after the broadcast phase and $P_e(D_s)$ is the PER of the retransmission conditioned on the cardinality of the decoding set D_s. Since each RN's decoding status is either error-free or erroneous, there are 2^K combinations of D_s. Hence, $\Pr\{D_s\}$ can be formulated as [67]

$$\Pr\{D_s\} = \prod_{i \in D_s} (1 - P_{e,si}) \prod_{j \notin D_s} P_{e,sj}, \tag{2.7}$$

where i and $P_{e,si}$ denote the i-th node in the decoding set and the error probability of its reception during the SN's broadcast phase, respectively. Since the selected RN is the one that has the highest SNR at the DN, $P_e(D_s)$ is given by the product of probabilities, where the transmissions from every node in D_s to the DN fails and hence $P_e(D_s)$ is represented as

$$P_e(D_s) = \prod_{i \in D_s} P_{e,id}, \tag{2.8}$$

where $P_{e,id}$ denotes the OP at the DN, when the i-th node of the decoding set is selected for transmission, which may be expressed as

$$\begin{aligned} P_{e,id} &= \Pr\{\gamma_{id} < \gamma_{th}\} \\ &= 1 - \exp\{-\frac{\gamma_{th}}{\bar{\gamma}_{id}}\}. \end{aligned} \tag{2.9}$$

By substituting Eq. (2.5)-(2.9) into Eq. (2.4), the e2e OP is obtained in closed-form for the ORS scheme using DF relaying in the absence of CCI.

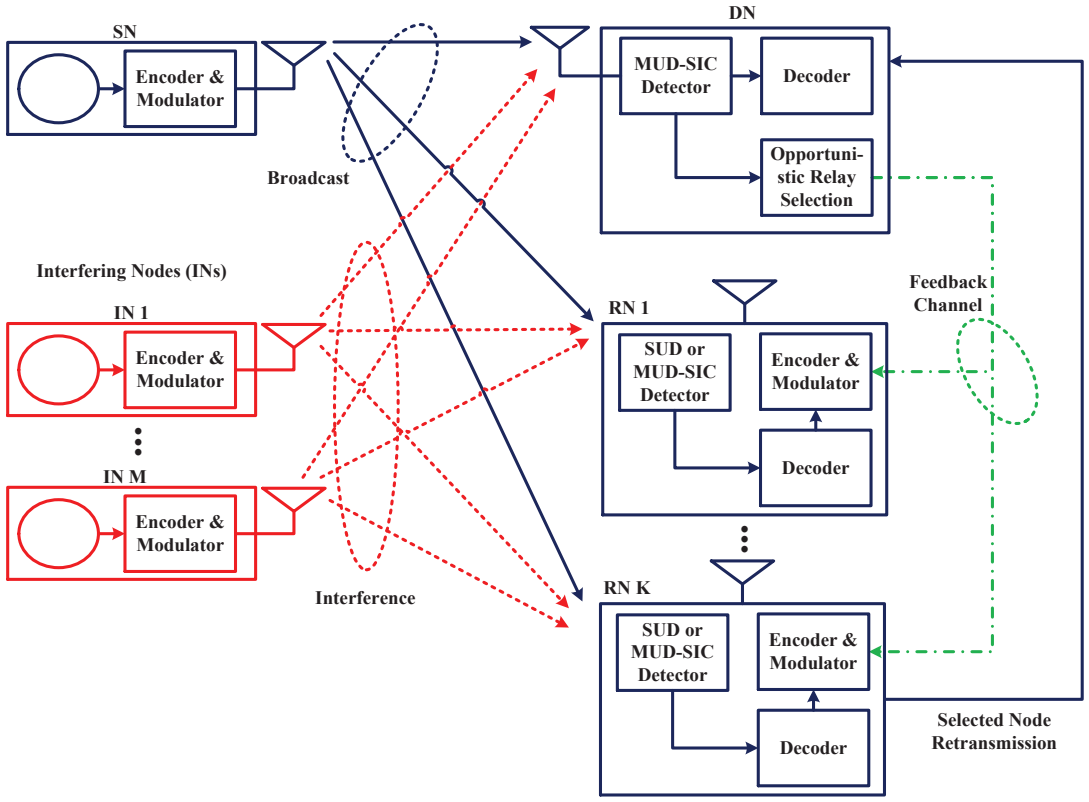

Figure 2.3: Schematic of the proposed SUD-aided and MUD-SIC-aided schemes, the RNs in the SUD-aided scheme employ the SUD receivers, while RNs in the MUD-SIC-aided scheme employ the MUD-SIC receivers.

2.2 ORS Design with CCI

2.2.1 System Model

Having considered the CCI-free scenario in Section 2.1, let us now consider a network comprised of a SN, K RNs and a DN, where M interfering nodes (INs) may access the channel concurrently. Each node is equipped with a single antenna and operates in a half-duplex mode. The system model is illustrated in Fig. 2.3, where $\{RN_1, RN_2, \ldots, RN_K\}$ form the RN set and $\{IN_1, IN_2, \ldots, IN_M\}$ form the IN set.

Similar to the scheme described in Section 2.1 for an interference-free scenario, the RNs may listen to the SN's message and then the specific RNs that successfully decoded the SN's message, may retransmit it. Again, we assume a Rayleigh-distributed block fading channel model, where the fading coefficient remains constant for the duration of a packet and then varies independently from one transmission to another both in time and space. As for the CCI-free scenario, we assume that a perfect capacity-achieving code is used and circularly symmetric complex Gaussian symbols are transmitted. Therefore, throughout this chapter the packet loss ratio (PLR) is identical to the OP. The nodes have perfect receiver-side CSI during both the detection and decoding process, while the transmitter-side CSI may be estimated by

evaluating the statistics of the received CTS signal broadcast by the DN.

As illustrated in Fig. 2.3, the communication between the SN and the DN is performed in two phases: the classic broadcast phase and the relaying phase. The general case of multiple relaying phases is feasible, but in this chapter only a single retransmission may be invoked, which is suitable for low-delay applications. Similar to CCI-free scenario of Section 2.1, we also adopt the notion of *decoding set*, denoted here by D_s, which includes all nodes that successfully decoded the SN's signal. Before the broadcast phase only the SN is in the decoding set D_s. Then, after the broadcast phase, the specific RNs, which successfully decodes the message would join D_s. The criterion used for determining whether the RN may join the decoding set is based on whether it successfully passes the CRC check. Alternatively, we may check whether the mutual information between the SN and the RN is above a threshold. Again, we assume using the CRC-based method. The number of CRC parity bits is assumed to be significantly lower than that of the transmitted data bits. The RNs joining the decoding set would notify the DN by sending their acknowledgment (ACK) or non-acknowledgment (NACK) flags. In the relaying phase, a node is selected from the decoding set D_s for retransmission with the aid of a feedback channel, as illustrated in Fig. 2.3. It is assumed that both the feedback channel as well as the ACK/NACK flags are error-free.

In the broadcast phase, the SN transmits its data to both the RNs and the DN, which also receives interfering signals from M INs. If the retransmission phase is necessitated and the optimum node $k^\star$ is assumed to be selected by the ORS scheme for retransmission, then the signals received by the RNs and the DN are given by:

$$y_k^1 = h_{s,k}^1 x_s + \sum_{m=1}^{M} h_{m,k}^1 x_m^1 + n_k^1, \quad k = 1, \ldots, K \tag{2.10}$$

$$y_d^1 = h_{s,d}^1 x_s + \sum_{m=1}^{M} h_{m,d}^1 x_m^1 + n_d^1 \tag{2.11}$$

$$y_d^2 = h_{k^\star,d}^2 x_s + \sum_{m=1}^{M} h_{m,d}^2 x_m^2 + n_d^2, \tag{2.12}$$

where y_j^p is the signal received by the j-th node in the p-th phase[5], $h_{i,j}^p$ is the CSI between node i and j in the p-th phase considering the effects of the pathloss, shadowing and Rayleigh fading, x_s is the signal transmitted by the SN with its power normalised to 1, while n_j^p is the noise at node j in the p-th phase. We assume that the fading channel coefficients and the noise are independent zero-mean circularly symmetric complex Gaussian random variables.

[5] $p = 1$ represents the broadcast phase and $p = 2$ stands for the retransmission phase.

Table 2.1: System Parameters

Number of relay nodes	K
Number of interferers	M
Channel model	Rayleigh block fading
Pathloss exponent	$\beta = 3.0$
Channel correlation coefficient	$\rho = 0.95 - 1.0$
Received instantaneous SNR	γ_0
Received instantaneous INR	$\gamma_1, \ldots, \gamma_M$
SIC-ordered received SNR and INR	$\gamma_{(1)} \geq \gamma_{(2)} \geq \cdots \geq \gamma_{(M+1)}$

At the RNs and the DN, the receiver has to detect the signals transmitted from the desired node[6]. The SUD schemes are assumed to have perfect CSI, while the MUD-SIC receiver is assumed to be perfectly synchronised with the SN and the INs so that perfect CSI of the SN and the INs are also available. In the MUD-SIC receiver illustrated in Fig. 3.2, both the desired signal as well as the interfering signals are extracted from the composite received signal. In each iteration, the SIC decoder removes the interference imposed by the successfully decoded signals from the current composite received signal. This process relies on re-encoding the decoded bit sequence, then re-modulating it with the appropriate amplitude and phase adjustment relying on perfect CSI and finally subtracting it from the CCI-infected composite signal. The signal that cannot be error-freely decoded is not subtracted from the composite received signal. It is assumed that the error propagation due to erroneous decoding can be avoided with the aid of the CRC check. The basic system parameters used throughout this chapter are listed in Table 2.1.

2.2.2 Outage Analysis

The previous contributions of [26,68] have analysed the OP of dual-hop relaying systems operating in the presence of multiple interferers. The authors of [26] considered the interference both at the RNs and the DN, where a single RN was considered. Furthermore, in [26], an interference-limited scenario was considered, while the effects of noise were neglected. Against this background, in this section, we extend the analysis of point-to-point Rayleigh fading channels of a single link to the scenario of multiple interferers. Additionally, the effects of the noise were also considered. We also generalize the scenario to multiple RNs.

In the presence of CCI, an outage is defined as the event, where the received signal-to-interference-noise power ratio (SINR) experienced at the DN is lower than the predefined threshold γ_{th} that has to be exceeded for successful decoding. Again, we assume that no packet-combining techniques are employed at the DN, where the

[6]The desired node is the SN in the broadcast phase and the RNs selected for the retransmission phase.

erroneous packets are discarded. Therefore, the OP P_{out} is given by:

$$P_{out} = P_e^1 P_e^2, \tag{2.13}$$

where P_e^1 denotes the PER of the broadcast phase, while P_e^2 denotes the PER of the relaying phase. Given the PER of a P2P link, the end-to-end OP of the system may be deduced from P_e^1 and P_e^2, which obeys the same formulation in the absence of CCI as detailed in Section 2.1:

$$P_e^2 = \sum_{D_s} Pr\{D_s\} P_e(D_s), \tag{2.14}$$

and $Pr\{D_s\}$ is given by

$$Pr\{D_s\} = \prod_{i \in D_s} (1 - P_{e,si}) \prod_{j \notin D_s} P_{e,sj}. \tag{2.15}$$

However, the exact expressions of P_e^1 and P_e^2 would be different. In this chapter, the SUD-aided system treats the interference as noise at the RNs and the corresponding $P_{e,si}$ will be given in Section 2.2.2.1, while the $P_{e,si}$ of the MUD-SIC-aided system is provided in Section 2.2.2.2.

2.2.2.1 Analysis of SUD

At the SUD receiver all interferences are treated as Gaussian noise. Therefore, the SINR at the receiver is expressed as

$$SINR = \frac{\gamma_0}{1 + \sum_{m=1}^{M} \gamma_m} \triangleq Y = \frac{\gamma_0}{1 + X}, \tag{2.16}$$

where γ_0 is the SNR of the desired signal and γ_m denotes the interference-to-noise power ratio (INR) of the m-th interfering signal. Since Rayleigh block fading is assumed, each γ_m obeys to the exponential distribution of $f_{\gamma_m}(\gamma) = \frac{1}{\bar{\gamma}_m} e^{-\frac{\gamma}{\bar{\gamma}_m}}$. For convenience of notation, X, Y denote the INR and SINR, respectively. The INR component $\sum_{m=1}^{M} \gamma_m$ is of hypo-exponential distribution, while its probability density function deduced in Theorem 2 of [16] is as follows:

$$f_X(x) = \sum_{i=1}^{g(A)} \sum_{j=1}^{r_i(A)} \chi_{i,j}(A) \frac{\bar{\gamma}_{(i)}^j}{(j-1)} x^{(j-1)} e^{-x/\bar{\gamma}_{(i)}}, \tag{2.17}$$

where $A = diag\{\gamma_1, \gamma_2, \ldots \gamma_M\}$. $g(A)$ is the number of distinct diagonal elements of A and $\bar{\gamma}_{(1)} > \bar{\gamma}_{(2)} > \cdots > \bar{\gamma}_{(g(A))}$ and $r_i(A)$ is the number of eigenvectors of $\bar{\gamma}_{(i)}$, while $\chi_{i,j}(A)$ is the (i,j)-th characteristic coefficient of A, which are defined in Eq. (29) of [16].

If perfect capacity-achieving coding is adopted, an outage occurs, when the transmission rate R is higher than the channel capacity given by $C = \log_2(1+Y)$. Equivalently, an outage occurs when the received SINR is below the threshold $\gamma_{th} = 2^R - 1$. Therefore, the PER is expressed as $P_e = Pr\{Y < \gamma_{th}\}$ and its detailed expression is formulated as follows:

$$\begin{aligned} P_e^{SUD}(\bar{\gamma}_0, \bar{\gamma}_1, \ldots \bar{\gamma}_M) &= Pr\{\frac{\gamma_0}{1+X} < \gamma_{th}\} = \int_0^{+\infty} Pr\{\gamma_0 < \gamma_{th}(1+x)\} f_X(x) dx \\ &= \int_0^{+\infty} (1 - e^{(-\frac{\gamma_{th}(1+x)}{\bar{\gamma}_0})}) \sum_{i=1}^{g(A)} \sum_{j=1}^{r_i(A)} \chi_{i,j}(A) \frac{\bar{\gamma}_{(i)}^j}{(j-1)} x^{(j-1)} e^{-x/\bar{\gamma}_{(i)}} dx \\ &= 1 - \sum_{i=1}^{g(A)} \sum_{j=1}^{r_i(A)} \chi_{i,j}(A) e^{(-\frac{\gamma_{th}}{\bar{\gamma}_0})} (1 + \frac{\bar{\gamma}_{(i)}}{\bar{\gamma}_0} \gamma_{th})^{-j}. \end{aligned} \tag{2.18}$$

2.2.2.2 Analysis of MUD-SIC

The OP analysis of MUD-SIC reception over Rayleigh-distributed block fading channels was provided in [69] for the special case of equal-rate links, where the uplink rate of each user is identical. The PER of each user is given by [69] using the optimal decoding order, which requires that the signal having the highest SNR is decoded, re-encoded, re-modulated and subtracted in each decoding iteration. A tight upper-bound of the per-user PER is deduced in [69] and formulated in Eq. (28) of [69]. In our system, we focus on the PER performance of the desired user. Without loss of generality, we set the index of the desired user as 0 and its PER expression is given in Eq. (2.19). Explicitly, π represents the possible decoding order of SIC, while $\pi(i) = 0$ indicates that the desired signal is decoded during the i-th decoding iteration[7]. Therefore, in the presence of M interferers, there are $(M+1)!$ possible decoding orders. The explicit definitions of A_v, $\bar{\lambda}_v$ and ϕ_i seen in Eq.(2.19) are given in Eq. (23) of [69]. It should be noted that the closed form expression of Eq. (2.19) may be readily evaluated for small M, but the number of possible decoding orders and the associated computational complexity of the analytical results becomes formidable, hence computer simulations may be preferred for evaluating:

$$\begin{aligned} P_e^{MUD-SIC}(\gamma_0, \gamma_1, \ldots \gamma_M) &\leq \frac{1}{(M+1)!} \sum_{\pi} \left[\sum_{i=0}^{\pi^{-1}(0)} (1 - \sum_{v=j}^{M} A_v e^{\frac{-\gamma_{th}}{\lambda_v}}) \right] \prod_{i=0}^{M} \frac{1}{\phi_i \bar{\gamma}_i}, \\ \phi_i = \frac{\sum_{u=1}^{i} \bar{\gamma}_u^{-1}}{i}, \quad \lambda_v &= \frac{1-(v-j)\gamma_{th}}{v}, \quad \bar{\lambda}_v = \frac{\lambda_v}{\phi_v}, \quad A_v = \prod_{u=j, u\neq v}^{n} \frac{\bar{\lambda}_v}{\bar{\lambda}_v - \bar{\lambda}_u}. \end{aligned} \tag{2.19}$$

[7]Note that the first iteration is indexed by 0

2.2.2.3 End-to-End Outage Analysis

Firstly, a MUD-SIC receiver is adopted at the DN in both the SUD-aided and in the MUD-SIC-aided schemes. Again, the per-user PER performance of a multi-user uplink system using a MUD-SIC receiver at the DN was characterised in [69] in the absence of relaying, where the uplink rate of each user was assumed to be identical. More specifically, the PER of each user is presented in [69] using the optimal decoding order, where the signal having the highest SNR is decoded, re-encoded, re-modulated and subtracted in each decoding iteration. A tight upper-bound of the per-user PER is given in Eq. (28) of [69]. In our system, we focus our attention on the PER performance of the desired user. We set the index of the SN to 0 and P_e^1 is given in Eq. (2.20), where $\bar{\gamma}_0$ represents the average SNR of the SN at the DN, while $\bar{\gamma}_1, \ldots \bar{\gamma}_M$ represents the average INR of the M interferers at the DN, respectively, yielding:

$$P_e^1 = P_e^{MUD-SIC}(\bar{\gamma}_0, \bar{\gamma}_1, \ldots \bar{\gamma}_M) \leq \frac{1}{(M+1)!} \sum_{\pi} \left[\sum_{i=0}^{\pi^{-1}(0)} (1 - \sum_{v=j}^{M} A_v e^{\frac{-\gamma_{th}}{\bar{\lambda}_v}}) \right] \prod_{i=0}^{M} \frac{1}{\phi_i \bar{\gamma}_i}, \tag{2.20}$$

where the definitions of the parameters used are as follows:

$$\phi_i = \frac{\sum_{u=1}^{i} \bar{\gamma}_u^{-1}}{i}, \quad \bar{\lambda}_v = \frac{1 - (v-j)\gamma_{th}}{v\phi_v}, \quad A_v = \prod_{u=j, u\neq v}^{n} \frac{\bar{\lambda}_v}{\bar{\lambda}_v - \bar{\lambda}_u}. \tag{2.21}$$

On the other hand, the PER of the retransmission phase P_e^2 may be expressed as

$$P_e^2 = \sum_{D_s} Pr\{D_s\} P_e(D_s, \bar{\gamma}_1, \ldots, \bar{\gamma}_M), \tag{2.22}$$

where $Pr\{D_s\}$ is the probability that D_s is the decoding set in the broadcast phase, which may be formulated as

$$\Pr\{D_s\} = \prod_{i \in D_s} (1 - P_{e,si}) \prod_{j \notin D_s} P_{e,sj}, \tag{2.23}$$

where i and $P_{e,si}$ denote the i-th node in the decoding set and the error probability of its reception during the SN's broadcast phase, respectively. In this chapter, the SUD-aided scheme treats the interference as noise at the RNs and the corresponding $P_{e,si}$ is given by Eq. (21) of [26]. The $P_{e,si}$ of the MUD-SIC-aided scheme is in the form of Eq. (2.20), while the SNR and the INRs should be replaced by the values at the i-th RN. Therefore, the multiplication term $Pr\{D_s\}$ in Eq. (2.22) depends only on the SN-RN channel quality and on specific choice of the receiver adopted at the RNs, namely, whether the SUD or MUD-SIC receiver is used. Therefore, $\Pr\{D_s\}$ does not depend on the ORS design. By contrast, the expression of $P_e(D_s, \bar{\gamma}_1, \ldots, \bar{\gamma}_M)$ in

Eq. (2.22) depends on the ORS design, where D_s is the decoding set and $\bar{\gamma}_1, \ldots, \bar{\gamma}_M$ represent the average INR of the M interferers at the DN.

An outage-optimal ORS scheme achieves an OP $P_e^{opt}(D_s, \bar{\gamma}_1, \ldots, \bar{\gamma}_M)$, which is equal to the probability that transmissions from all the nodes in the decoding set D_s to the DN fails [16]. However, $P_e^{opt}(D_s, \bar{\gamma}_1, \ldots, \bar{\gamma}_M)$ cannot be simply decomposed into the form of $\prod_{i \in D_s} P_{e,id}(\bar{\gamma}_{id}, \bar{\gamma}_1, \ldots, \bar{\gamma}_M)$ as adopted in [16], where $P_{e,id}(\bar{\gamma}_{id}, \bar{\gamma}_1, \ldots, \bar{\gamma}_M)$ denotes the error probability at the DN, when the i-th node of the decoding set is selected for transmission. This is because even though the ORS may rely on mutually independent SNRs as determined by $\bar{\gamma}_{id}$ and the independent fading of the current packet, the INRs represented by $\gamma_1, \ldots, \gamma_M$ are fixed for the fading realisations of the current packet, regardless of which node is selected from the decoding set. Therefore, this results in correlated error probabilities $P_{e,id}(\bar{\gamma}_{id}, \bar{\gamma}_1, \ldots, \bar{\gamma}_M)$ for each node in the decoding set, when the MUD-SIC receivers are adopted at the DN. Therefore, it remains an open challenge to deduce the closed-form expression of $P_e^{opt}(D_s, \bar{\gamma}_1, \ldots, \bar{\gamma}_M)$, which is left for our future investigation. Instead, the focus of this chapter is to conceive a beneficial ORS scheme, which achieves the optimal OP, when the MUD-SIC receiver is adopted at the DN.

2.2.3 Opportunistic Relay Selection Design

The design criterion of ORS is to achieve the optimal $P_e^{opt}(D_s, \gamma_1, \ldots, \gamma_M)$, which again, denotes the probability that the transmissions from all the nodes in the decoding set D_s to the DN failed. Therefore, an outage-optimal ORS should satisfy the following condition: *if the specific retransmission by the node selected from the set D_s cannot be successfully decoded at the DN, then a retransmission by any other node picked from the set D_s would not be decoded successfully either*[8].

When the SUD decoder is employed at the DN in the presence of multiple interferers, the optimal relay selection scheme is the same as that of the interference-free scenario [16], because the ORS scheme simply appoints the particular node having the highest instantaneous SNR at the DN **[59]**. This results in the highest instantaneous received SINR $Y_{raw} = \gamma_{id}/(\sum_{j=1}^{M} \gamma_j)$, which is denoted as **raw SINR** at the DN and therefore achieves the lowest OP. However, if the more powerful MUD-SIC receiver is employed at the DN, the OP of relay selection is no longer determined by the raw SINR. This is due to the fact that some interfering signals may be decoded and removed from the composite signal and hence the **effective SINR** of the desired signal may be iteratively enhanced, which is formulated as $Y_{eff} = \gamma_{id}/(\sum_{j=k+1}^{M} \gamma_j)$, where k indicates that the desired signal is decoded in the k-th iteration, given that

[8]It should be noted that although we use the terminology of relay selection, the SN itself may be selected for retransmission as well, if no RNs decoded the message successfully during the broadcast phase or if the SN's retransmission may facilitate a better decoding result at DN compared to the RNs.

the previous $(k-1)$ interfering signals are successfully decoded. The SIC scheme relies on the power-based ranking of all-received signal components and it is at its best, when the received power levels are clearly distinguishable. Therefore, appointing the particular node having the highest SNR at the DN for retransmission may be detrimental, because the MUD-SIC receiver of the DN cannot reliably detect and decode the desired signal or the interference. Instead, we propose the BED-ORS scheme based on the *best-effort detection* criterion, which is implemented in the formally specified Algorithm 2.2.3.1.

The philosophy of the BED-ORS is as follows: Retransmission by a node in the decoding set D_s may result in one of two decoding outcomes at the DN: success or failure. If the DN has the perfect knowledge of CSI for the links between each node in the decoding set and the DN as well as that of the links between the interferers and the DN, it may predict the decoding outcome of every node in the decoding set by invoking *SIC testing*, as described in Algorithm 1. Hence, the node that facilitates successful decoding at the DN may be selected.

2.2.3.1 Algorithm Design

The proposed BED-ORS tests all candidates in the D_s until the decoding outcome of a candidate is successful and hence selected, or no candidates results in a successful decoding outcome. Therefore, it is outage-optimal by virtue of ensuring that if the node selected cannot facilitate successful decoding, any other nodes in D_s would not be decoded successfully either. It should be noted that the proposed BED-ORS does not invoke the MUD-SIC decoding process. The DN may utilise MUD-SIC for decoding the bits or symbols at the physical layer in order to recover the information transmitted. However, the BED-ORS is a MAC layer algorithm, which initates the MUD-SIC process and relies only on the processing of the SNRs and INRs. From the physical layer's perspective, the CSI of the channels between all RNs and the DN, as well as those of the channels between all INs and the DN are required by the MUD-SIC detecting stage. However, the physical layer SNRs and INRs, have to be fed into the MAC layer and then exploited at the ORS stage, as it will be shown later with the aid of our simulation results.

Algorithm 1: Best-Effort Detection Based ORS (BED-ORS)

1. **INR ordering**: Following the broadcast phase, we assume that $(L-1)$ RNs successfully decode the SN's message. Hence, there are L candidate nodes in D_s, including the SN. We denote the decoding set D_s as $\{c_1, c_2, \ldots, c_L\}$. The DN ranks the received INR of the M interfering signals $\{\gamma_1, \gamma_2, \ldots, \gamma_M\}$ in descending order and the re-ordered **INR queue** is denoted as $\{\gamma_{(1)}, \gamma_{(2)}, \ldots, \gamma_{(M)}\}$, where $\gamma_{(1)} \geq \gamma_{(2)} \geq \cdots \geq \gamma_{(M)}$, $\forall i \in [1, M]$.

Then, for each node in D_s, the DN carries out the SNR ordering and SIC testing, as described below.

2. **SNR ordering**: The DN selects a candidate node c_l from D_s and inserts its received SNR γ_{c_l} in the INR queue, keeping the new queue, which is referred to as **SIC queue** $\gamma_{(1)} \geq \gamma_{(2)} \geq \cdots \geq \gamma_{(M+1)}$ in a descending order. This is the optimal decoding order for equal-rate scenario of the SN-RN and RN-DN links, which is formally proven in [69].
3. **SIC testing**: Firstly, for each position i in the INR queue, an SNR upper threshold γ_i^u and an SNR lower threshold γ_i^l are calculated as $\gamma_i^u = \frac{\gamma_{(i-1)}}{\gamma_{th}} - \sum_{j=i}^{M} \gamma_{(j)} - 1$ and $\gamma_i^l = \gamma_{th}(\sum_{j=i}^{M} \gamma_{(j)} + 1)$ for the SIC testing step, where γ_{th} is the predefined threshold to be exceeded for successful decoding. The bounds are derived as follows: if the SNR of a candidate node is inserted at position i, in order to facilitate successful decoding, a necessary condition is that we have $\frac{\gamma_{(i-1)}}{\gamma_{c_l} + \sum_{j=i}^{M} \gamma_{(j)} + 1} \geq \gamma_{th}$ and $\frac{\gamma_{c_l}}{\sum_{j=i}^{M} \gamma_{(j)} + 1} \geq \gamma_{th}$, where the first inequality ensures that the SINR of the signal at position $(i-1)$ exceeds γ_{th} and therefore it is decoded successfully. By contrast, the second inequality ensures that the SINR of the candidate's signal exceeds γ_{th}. Please note the condition is not a sufficient condition, because it also relies on the decoding outcomes of the preceding signals in the SIC queue.
   Denoting that after the SNR ordering, γ_{c_l} is inserted at position k. A failure is declared, when the SINR of the signal in the $i-th$ $(i < k)$ decoding iteration does not exceed γ_{th}, therefore none of the signals following in the queue (including the candidate signal) can be decoded, because their SINR is even lower. Otherwise, if each i-th signal $(i \leq k)$ in the SIC queue is successfully decoded, and $\gamma_k^u \geq \gamma_{c_l} \geq \gamma_k^l$ is satisfied, a successfully decoding outcome may be declared.
4. **Node selection**: If the decoding outcome predicted for c_l is success, c_l is selected as the transmitting node and the node's index is sent by the DN through a feedback channel to the would-be-transmit node. Otherwise, the DN selects another candidate node, which has not been tested yet and repeats steps 2 and 3 above. If the decoding outcome predicted for all nodes in D_s is failure, an outage event is declared.

An example of having two RNs in the decoding set and two INs is formulated as follows: The received SNRs of RN_1 and RN_2 at the DN are $\gamma_{c_1} = 9$ and $\gamma_{c_2} = 4$, respectively. The received INRs of IN_1 and IN_2 at the DN are $\gamma_1 = 2$ and $\gamma_2 = 8$, respectively. The transmission rate is $R = 1.0$bit/sec/Hz, therefore the resultant SINR decoding threshold is $\gamma_{th} = 2^R - 1 = 1$. In this example, Algorithm 2.2.3.1 operates as follows:

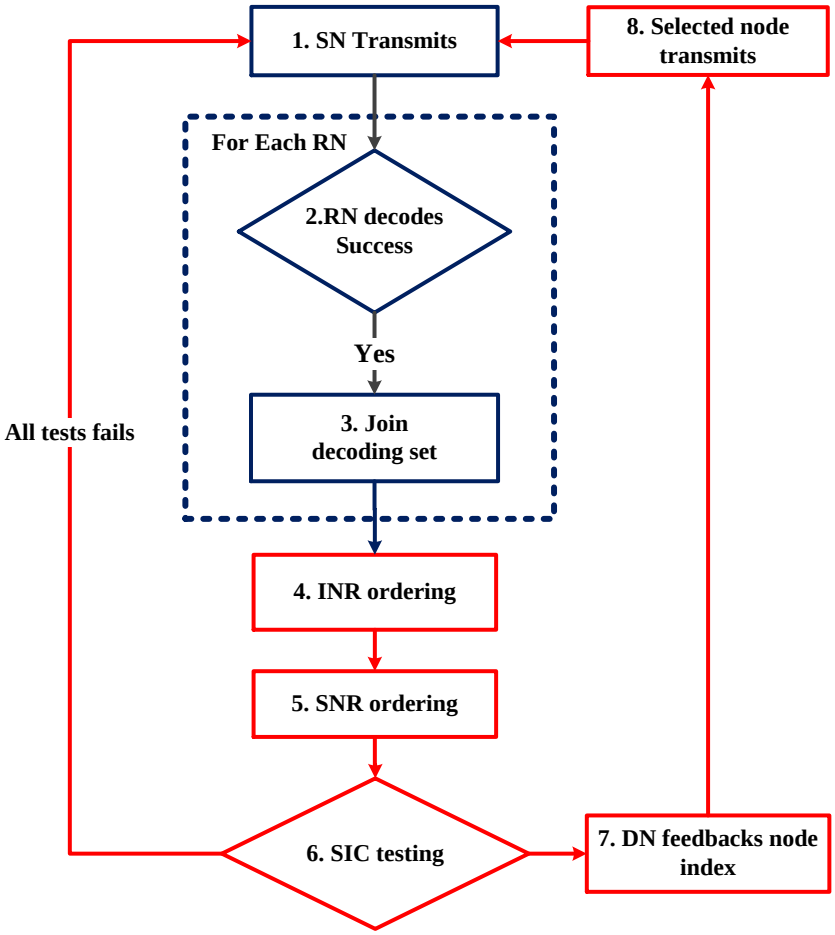

Figure 2.4: Flowchart of the ORS relying on MUD-SIC

1. **INR ordering**: The **INR queue** relies on ordering γ_1 and γ_2 from high to low as $\{8, 2\}$.
2. **SNR ordering**: For RN_1, the **SNR queue** is formed by inserting $\gamma_{c_1} = 9$ into the INR queue as $\{9, 8, 2\}$, where $\gamma_{c_1} = 9$ is inserted at the first position. For RN_1, the SNR queue is formed as $\{8, 4, 2\}$, where the $\gamma_{c_2} = 4$ is inserted at the second position.
3. **SIC testing**: For RN_1, the SIC testing evaluates $\frac{9}{8+2+1} < 1 = \gamma_{th}$. Therefore, a decoding failure is declared by the CRC. By contrast, for RN_2, both $\frac{8}{4+2+1} \geq 1$ and $\frac{4}{2+1} \geq 1$ are satisfied, therefore a successful decoding outcome is declared.
4. **Node selection**: According to the SIC testing outcomes, RN_2 is selected for relaying the signal.

However, if we rely only on selecting the highest-SNR node for relaying, which is RN_1 in the example, the system would be in outage even though selecting RN_2 is optimal.

Based on Algorithm 1, the mechanism of the proposed scheme is illustrated in Fig. 2.4, which is described as follows:

1. **Initial transmission**: the SN broadcasts its message to all RNs and to the DN as shown in Block 1 of Fig. 2.4, while the RNs and the DN listen.
2. **Decoding set update**: All RNs attempt to decode the signal received during the SN's broadcast phase, as shown in Block 2 of Fig. 2.4. If a RN decodes successfully, it is capable of flawlessly regenerating the original message and therefore joins D_s, as shown in Block 3 of Fig. 2.4. Meanwhile, the successful RN sends a relay-request-to-send (RRTS) signal to the DN, indicating that it is capable of retransmitting the SN's message.
3. **ORS at DN**: The ORS scheme is detailed in Algorithm 1, as shown in Blocks 4-7 of Fig. 2.4. It should be noted that the global knowledge of the instantaneous CSI is required at the DN for implementing ORS, which is acquired at the DN by evaluating the statistics of the RRTS signal arriving from each node in the decoding set D_s, as well as the interfering signals. By implementing Algorithm 1, the retransmitting node is selected.
4. **Relaying**: The node selected in Step 3 above re-encodes the message and transmits it, as shown in Block 8 of Fig. 2.4. The DN would then try to decode the message and a new packet's transmission is initiated by the SN in Block 1 of Fig. 2.4.

In order to support SIC decoding at the physical layer, the MAC layer of the ORS scheme originally proposed in [16] should be re-designed. The DN has the knowledge of the interference power, hence it may serve as the central controller, which requires the CSI of the channels spanning from all candidate RNs to the DN. Therefore, we may summarise the MAC layer design conceived for our BED-ORS as follows. If a RN decodes the data, it sends a RRTS message and the DN hence becomes capable of estimating the channel spanning from all candidate RNs to the DN. Then the relay selection is carried out by using Algorithm 1. Finally, the DN sends a relay-clear-to-send (RCTS) message, which includes the selected RN's identity.

Since in the MAC layer protocol proposed in [16] no interference is considered, the RNs contend to access the channel by setting up distributed timers at the RNs, where the RN having the highest SNR at the DN may be selected. Therefore, the contention period is independent of the number of RNs equipped with back-off timers. However, when there is CCI at the DN and the MUD-SIC is adopted, a practical issue arises from the fact that the CSI of the channels spanning from all candidate RNs to the DN has to be known at the DN. Therefore, each RN has to send a RRTS message to the DN for CSI estimation. Hence the total period required for the RRTS messaging is proportional to the number of candidate RNs. Therefore, the number

of participating RNs should be appropriately controlled in order to avoid exceedingly high overall delays during the relay selection phase.

2.2.3.2 Complexity Analysis

Compared to the traditional ORS scheme based on the highest received SNR/SINR [16, 59], the proposed BED-ORS imposes a higher complexity at the DN. Assuming K RNs and M INs, the worst-case in terms of the ORS implementation complexity is that the decoding set includes $(K+1)$ candidates in D_s, where all RNs decode successfully after the broadcast phase. Considering the merge sorting algorithm of [70], the INR ordering of Algorithm 1 requires approximately $M\log_2 M - M + 1$ comparison operations, while the associated threshold calculation requires $2(M+1)$ division operations and $(M-1)$ addition operations. The worst-case complexity of the SNR-based ordering requires $(K+1)\log_2 M$ comparison operations for inserting a candidate' SNR into the INR queue $(K+1)$ times[9]. The SIC testing requires two comparison operations. Therefore, the overall number of computations for Algorithm 1's worst-case scenario are $(K+M+1)\cdot\log_2 M - M + 2(K+1) + 1$ comparison operations, $2(M-1)$ additions and $2(M+1)$ divisions. By comparison, the traditional ORS scheme [16, 59] requires at most K comparison operations in order to select the node particular from D_s having the highest SNR. For example, for $K = M = 4$, the numbers of comparison, addition and division operations required by Algorithm 1 in the worst-case are approximately $25, 6, 10$, respectively, while the traditional ORS scheme requires at most four comparison operations.

It should be noted that even though the BED-ORS introduces a higher implementation complexity, it is negligible compared to the complexity imposed by the decoding process at the physical layer. For example, a state-of-the-art low complexity turbo decoder design [71] requires multiple add-compare-select (ACS) operations per bit per iteration. Assuming a frame length of 1000 bits, a turbo decoder using 4 ACS operations and 4 iterations requires 16000 ACS operations for decoding a frame. By contrast, since the BED-ORS is based on a frame-by-frame mechanism, it requires 25 comparison, 6 addition and 10 division operations for a frame, assuming a scenario of 4 RNs and 4 INs. Therefore, the BED-ORS involves a much lower complexity than the decoding process. We considered the classic cellular uplink scenario. If fixed RNs are installed by the operators, the RNs may indeed have sufficient processing capability to adopt MUD-SIC receivers. On the other hand, if user-cooperation is adopted, where the RNs are mobile users, our SUD receivers may be adopted at the RN. Although the proposed ORS scheme imposes an increased implementation complexity, it exhibits significant OP improvements, as evidenced in Section 2.3, where the implementation issues are discussed in more detail.

[9] All K RNs successfully decode the SN's signal and join D_s, therefore the size of D_s is $(K+1)$.

2.2.4 System Optimisation for a Realistic Outdated CSI

In the previous discussions, perfect CSI was assumed to be available both at the RNs and at the DN in the BED-ORS scheme. However, if the channel's coherence time is shorter than the time required for processing the relay selection plus the delay of feeding back the selected node index by the DN, the CSI used for ORS may become outdated and hence may be different from the actual CSI. As a result, the accuracy of the predictions may degrade. In this case, if the predicted decoding outcomes of multiple nodes in the decoding sets indicate decoding success, it is optimal to select the one, where the probability of actual decoding success is maximized. *Therefore, it should be emphasised that in the presence of a realistic outdated-CSI, the ORS scheme is not guaranteed to be outage-optimal. Nevertheless, we may be able to design an ORS scheme that maximises the probability of avoiding outages or, alternatively, it minimises the probability of outage [66].* Therefore, we define the *probability of avoiding an outage* of candidate c_l as the probability that the actual decoding outcome is success, conditioned on the prediction being a success, denoted as $P_f^{c_l}$. The candidate $c_\star$ having the highest probability of avoiding an outage is selected as follows: $c_\star = arg\max_{c_l \in D_s}\{P_f^{c_l}\}$.

In order to acquire $P_f^{c_l}$ for each $c_l \in D_s$, we have to evaluate the impact of outdated CSI. Using a similar approach as in [63], the correlation coefficient between the actual channel coefficient h and the outdated channel coefficient $\hat{h}$ is defined as ρ. Therefore, we have [63]: $h = \rho\hat{h} + \sqrt{1-\rho^2}v$, where $v \sim CN(0,1)$ and ρ is assumed to be a constant in this chapter. The actual SNR γ conditioned on its estimate $\hat{\gamma}$ obeys a non-central chi-square distribution with two degrees of freedom and the probability density function of the SNR is expressed as [63]

$$f_{\gamma|\hat{\gamma}}(\gamma|\hat{\gamma}) = \frac{1}{\bar{\gamma}(1-\rho^2)} e^{-\frac{\gamma+\rho^2\hat{\gamma}}{\bar{\gamma}(1-\rho^2)}} I_0\left(\frac{2\rho\sqrt{\gamma\hat{\gamma}}}{\bar{\gamma}(1-\rho^2)}\right), \tag{2.24}$$

where $\bar{\gamma}$ denotes the average SNR and $I_0(\cdot)$ is the zero-order modified Bessel function of the first kind. In our analysis we assume that the CSIs of the candidates in the decoding set are outdated, while the CSIs of the interferers are perfect. Therefore, γ_i^l and γ_i^u defined in Step 1 of Algorithm 1 are not outdated. Then, the candidate c_l's *probability of avoiding an outage* $P_f^{c_l}$ may be expressed as [72]

$$P_f^{c_l} = Pr\{\gamma_k^l \leq \gamma_{c_l}|\hat{\gamma}_{c_l}\} Pr\{\gamma_{c_l} \leq \gamma_k^u|\hat{\gamma}_{c_l}\}, \tag{2.25}$$

$$Pr\{\gamma_{c_l} \leq \gamma_k^u|\hat{\gamma}_{c_l}\} = \int_0^{\gamma_k^u} f_{\gamma_{c_l}|\hat{\gamma}_{c_l}}(\gamma_{c_l}|\hat{\gamma}_{c_l}) d\gamma_{c_l} = 1 - Q_1(\lambda, b_u) \tag{2.26}$$

$$Pr\{\gamma_k^l \leq \gamma_{c_l}|\hat{\gamma}_{c_l}\} = 1 - \int_0^{\gamma_k^l} f_{\gamma_{c_l}|\hat{\gamma}_{c_l}}(\gamma_{c_l}|\hat{\gamma}_{c_l}) d\gamma_{c_l} = Q_1(\lambda, b_l), \tag{2.27}$$

where $Q_1(\lambda, b)$ is the Marcum Q-function of order 1, while λ, b_u and b_l are defined as [72]:

$$\lambda = \rho\sqrt{\frac{2\hat{\gamma}_{c_l}}{\bar{\gamma}_{c_l}(1-\rho^2)}}, b_u = \left(\frac{2\gamma_k^u}{\bar{\gamma}_{c_l}(1-\rho^2)}\right)^2, b_l = \left(\frac{2\gamma_k^l}{\bar{\gamma}_{c_l}(1-\rho^2)}\right)^2. \tag{2.28}$$

Hence, in order to achieve the lowest OP, Algorithm 1 may be revised as follows:

Algorithm 2: I-BED-ORS using outdated-CSI

1. **INR ordering**: The same procedure of INR ordering is implemented as in Algorithm 1.
2. **SNR ordering**: The DN selects a candidate node c_l and the same procedure of SNR ordering is implemented as in Algorithm 1.
3. **SIC testing**: The same procedure of SIC testing is implemented as in Algorithm 1. Additionally, the probability of avoiding an outage $P_f^{c_l}$ is calculated using Eq. (2.25-2.28).
4. **Node selection**: For every candidate node c_l in D_s, the DN estimates the decoding outcomes and selects the node $c_{l^\star}$ of highest probability of avoiding an outage obeying $c_{l^\star} = \max_{c_l \in D_s} P_f^{c_l}$. Then, this node's index is sent by the DN to the relevant RN via a feedback channel.

As shown in Eqs. (2.25)-(2.28), the calculation of the probability $P_f^{c_l}$ of avoiding an outage involves integration and may be computationally expensive. As ρ and $\bar{\gamma}_{c_l}$ are statistical parameters which are assumed to be known so that λ is known at the DN, a look-up table connecting the values of $Q_1(\lambda, b)$ and b may facilitate an affordable implementational complexity.[10]

2.3 Numerical Results

In this section, we evaluate the performance of the proposed systems in terms of the associated OP. In all our simulations, we consider a topology comprising K RNs, all placed halfway along the line between the SN and DN and we set the channel's pathloss exponent to 3. Additionally, we assume that all nodes in the network use an identical transmit power. The time-averaged SNR of the SN-DN channel is denoted as $\bar{\gamma}_{s,d}$. Therefore, the SNR of the channel between any two nodes is $\bar{\gamma}_{i,j} = (d_{i,j}/d_{s,d})^{-\alpha}\bar{\gamma}_{s,d}$, where $d_{i,j}$ denotes the distance between node i and node j, while α is the channel's pathloss exponent. The channels are assumed to be subjected to independent Rayleigh block fading. Throughout the simulations, the transmission rate of each SN is $R_T = 0.5$ bit per second per Hz (bit/s/Hz).

[10] More practically, even if ρ and $\bar{\gamma}_{c_l}$ are unknown at the DN, a heuristic method may be implemented by selecting the $c_{l^\star} = \max_{c_l \in D_s} \min(\gamma_k^u - \gamma_{c_l}, \gamma_{c_l} - \gamma_k^l)$.

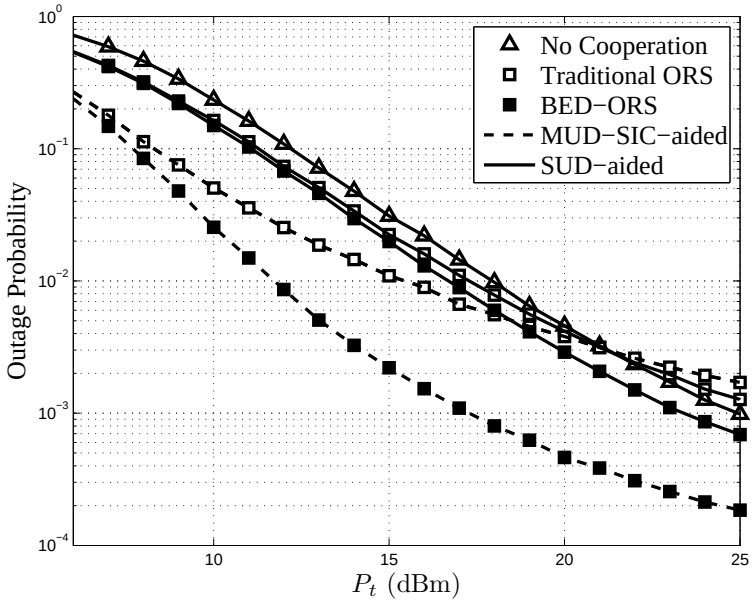

Figure 2.5: OP of different schemes versus the SN-DN link SNR for transmissions over block Rayleigh fading channels for SIR= 0dB, $R_T = 0.5$bit/s/Hz, $K = 2$ RNs and $M = 4$ INs. The traditional ORS scheme is based on the highest SNR criterion, while the proposed BED-ORS scheme is implemented by Algorithm 1 assuming perfect CSI.

1) Effects of ORS Criteria: We compare the OP performance of the traditional ORS scheme based on the *highest received SNR/SINR* criterion to that of the proposed BED-ORS scheme based on the *best-effort detection* criterion described in Algorithm 1. It is also assumed that the average signal-to-interference power ratio (SIR) for each IN is 0dB[11]. The number of RNs and INs is 2 and 4, respectively. Fig. 2.5 shows the OP of both the proposed MUD-SIC-aided scheme and of the SUD-aided arrangement. *The traditional ORS of Fig.* 2.5 *relies on a simple combination of the MUD-SIC with ORS [16], which does not exploit the knowledge of the INRs during the relay selection process.* When the traditional ORS scheme based on the *highest received SNR* criterion is used, it is observed in Fig. 2.5 that modest OP improvement is achieved by both the MUD-SIC-aided scheme and by the SUD-aided arrangement over the non-cooperative system, when the transmit power is within the range 4dBm to 21dBm. However, this trend no longer holds for higher SN-DN SNRs, where the employment of cooperation seems to be detrimental in terms of the OP, as shown in Fig. 2.5.

The reason for this behaviour was provided in Section 2.2.3. In this case, selecting a RN having a lower SNR at the DN may be preferred, where the strong interfering signals may be successfully decoded and subtracted, resulting in an improved SINR

[11]The average SIR is measured at the RNs in the broadcast phase, while at the DN the SIR in the broadcast phase for current setting is approximate $-9dB$. For simplicity, we use SIR at RNs in the broadcast phase to measure interference power.

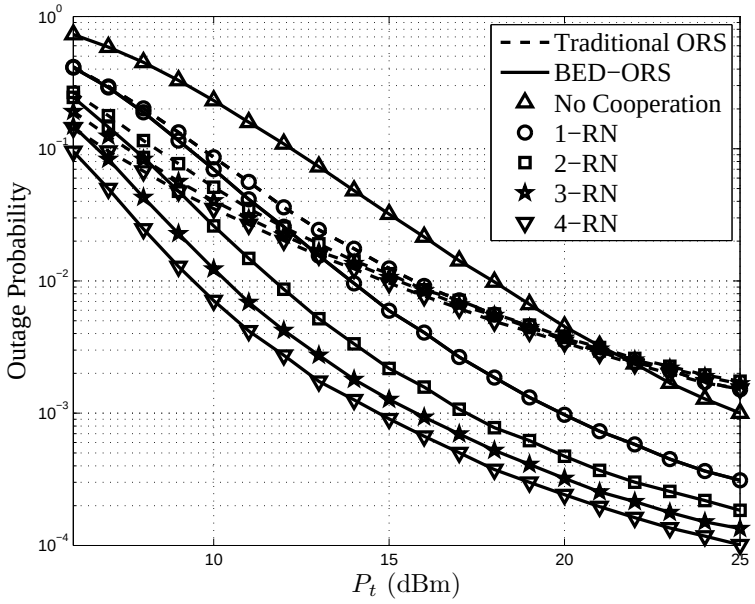

Figure 2.6: OP versus the SN-DN link SNR for transmissions over block Rayleigh fading channels with SIR= 0dB, $R_T = 0.5$bit/s/Hz, $M = 4$ INs and $K = 1$ to 4 RNs. The MUD-SIC-aided scheme is adopted. The traditional ORS scheme is based on the highest SNR criterion, while the proposed BED-ORS scheme is implemented by Algorithm 1 assuming perfect CSI.

for the desired signal and hence facilitating a higher probability of successful decoding, which is the philosophy behind the BED-ORS scheme. Fig. 2.5 illustrates that both the MUD-SIC-aided and SUD-assisted schemes using the BED-ORS regime of Algorithm 1 outperform the non-cooperative system for all the SNRs considered. For example, at $P_l = 10^{-3}$ a substantial gain of about $7.5dB$ is achieved by the MUD-SIC-aided scheme relying on two RNs over the non-cooperative system, while only a $1.8dB$ gain is attained by the SUD-aided scheme.

2) Effects of the Number of Relays, Interferers and Interference Power: Let us now we evaluate the performance of our proposed systems for different number of RNs and INs. Firstly, the number of INs is fixed to $M = 4$ and the number of RNs is increased from $K = 1$ to 4. It is observed in Fig. 2.6 that as the number of RNs increases, the outage performance of the MUD-SIC-aided scheme adopting the proposed BED-ORS scheme was improved gradually as a benefit of increased spatial diversity, which outperforms the traditional ORS scheme.

Then, the number of RNs is fixed to $K = 2$ and the number of INs increases from $M = 1$ to 4. It is observed in Fig. 2.7 that the proposed BED-ORS scheme always achieves a better OP than the traditional ORS, regardless of the number of INs. However, when the number of INs is $M = 1$ or 2, the outage performance of traditional ORS is very close to that of BED-ORS. The reason is that when the number of INs is relatively small and the resultant SINR is sufficiently high, the

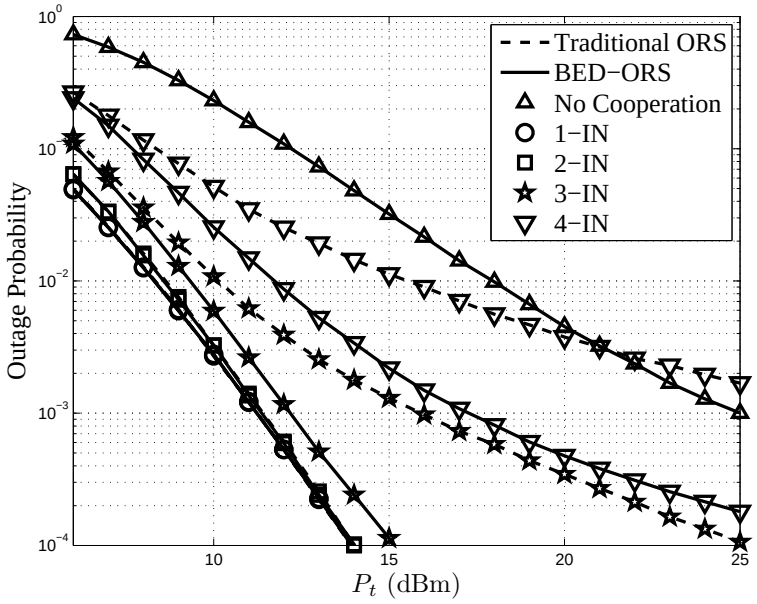

Figure 2.7: OP versus the SN-DN link SNR for transmissions over block Rayleigh fading channels with SIR= 0dB, $R_T = 0.5$bit/s/Hz, $K = 2$ RNs and $M = 1$ to 4 INs. The MUD-SIC-aided scheme is adopted. The traditional ORS scheme is based on the highest SNR criterion, while the proposed BED-ORS scheme is implemented by Algorithm 1 assuming perfect CSI.

performance of a MUD-SIC receiver and a SUD receiver is identical, where both of them are capable of approaching the OP of the interference-free scenario, in which the traditional ORS based on highest SNR criteria presented in Section 2.1 is outage-optimal.

The effects of interference power are evaluated in Fig. 2.8, where a SN assisted by $K = 2$ RNs and $M = 4$ INs is considered. We consider $SIR = 0, 6, 12$ dB, respectively. The dashed lines represent the performance of traditional-ORS, while the solid lines indicate the OP of the BED-ORS under different SIR levels. It is observed that the BED-ORS scheme achieves better outage performance than traditional ORS. It is also observed that at low SNRs, a higher SIR may result in a degraded OP, because the probability of the interference being successfully decoded and removed is small at a low INR. Assuming a constant SIR, as the SNR increases, the INR increases correspondingly and therefore achieving a higher probability of decoding and removing the interference, which in turns results in an improved OP.

On the other hand, Fig. 2.9 illustrates the importance of employing the more powerful MUD-SIC receiver at the DN in the presence of interference. If the DN adopts SUD receivers, the OP improvement achieved by enhancing the SN-DN link quality erodes at moderate SNRs and the system operates in the interference-limited region, indicated by the dotted lines. The proposed SUD-aided scheme and MUD-SIC-aided scheme, which are represented by the dashed lines and solid lines respectively, are

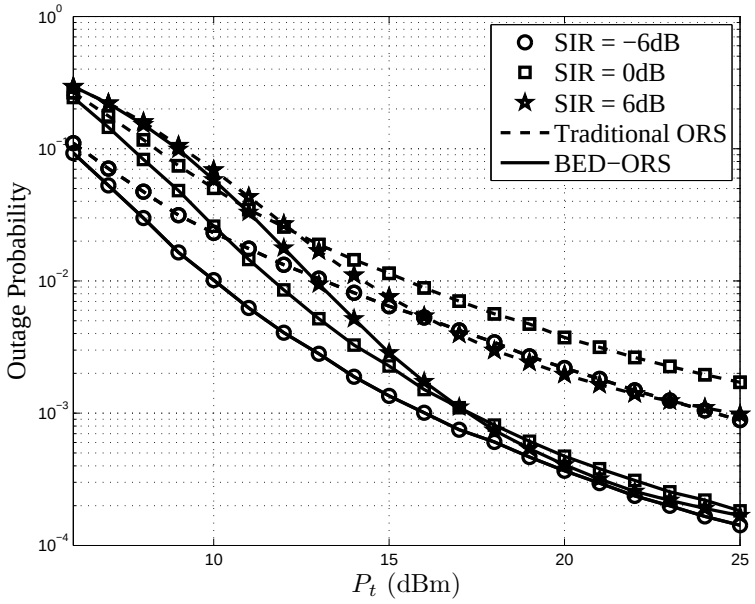

Figure 2.8: OP versus the SN-DN link SNR for transmissions over block Rayleigh fading channels with SIR= −6dB, 0dB and 6dB, $R_T = 0.5$bit/s/Hz, $K = 2$ RNs and $M = 4$ INs. The MUD-SIC-aided scheme is adopted. The traditional ORS scheme is based on the highest SNR criterion, while the proposed BED-ORS scheme is implemented by Algorithm 1 assuming perfect CSI.

capable of achieving an improved OP, with the aid of MUD-SIC receivers at the DN. We may conclude that in the presence of interference, adopting the MUD-SIC receiver at the DN guarantees a reduced OP. As the SUD receivers exhibit a lower implementation complexity than the MUD-SIC receivers, the SUD-aided scheme may be preferred for low-complexity RNs, provided that the OP degradation remains tolerable. Fig. 2.8 illustrates an example associated with $SIR = 12$dB, where the degradation of the SUD-aided scheme is approximately 1.2dB at $PLR = 10^{-3}$ compared to the MUD-SIC-aided scheme.

Practically, the decoding complexity of the MUD-SIC increases at most linearly with the number of interferers. Therefore, we are capable of controlling the number of interferers actually decoded by the MUD-SIC receivers. In other words, we may process a limited number of strong interferers using MUD-SIC, while treating the remaining interferers as noise. In this way, we may remove the most detrimental components and strike a balance between the OP achieved and the complexity imposed.

3) Effects of Outdated CSI and Using I-BED-ORS: Fig. 2.10 illustrates the OP of the ORS proposed in Sec. 2.2.4. If the CSI is outdated and the DN employs the sub-optimum Algorithm 1 based on perfect CSI, the OP may severely degrade, as shown in Fig. 2.10. By contrast, when the I-BED-ORS implemented in Algorithm 2 is used, the OP may be substantially improved, as seen in Fig. 2.10.

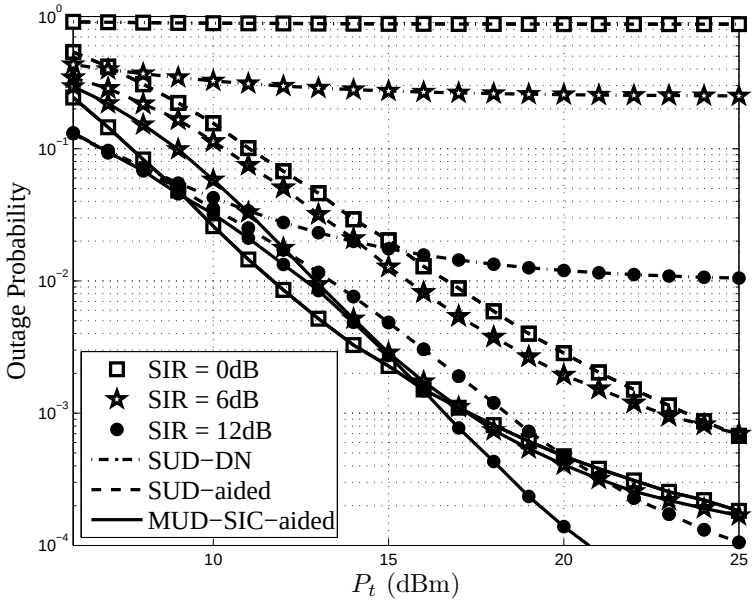

Figure 2.9: OP versus the SN-DN link SNR for transmissions over block Rayleigh fading channels with SIR= 0dB, 6dB and 12dB, $R_T = 0.5$bit/s/Hz, $K = 2$ RNs and $M = 4$ INs. **The MUD-SIC-aided and SUD-sided schemes are compared.** The BED-ORS scheme is implemented by Algorithm 1 assuming perfect CSI.

However, as the correlation coefficient ρ decreases and the reliability of the outdated CSI drops, the OP of the optimised ORS using Algorithm 2 degrades. It may be concluded that the accuracy of the CSI used for ORS is critical for the achievable OP of cooperative systems adopting MUD-SIC receivers.

2.4 Conclusions

In this chapter, we proposed a pair of systems adopting MUD-SIC receivers at the DN, namely, both the MUD-SIC-aided system and the SUD-aided system. The outage-optimal BED-ORS of Section 2.2.3.1 was proposed for both systems based on a best-effort detection criterion. The proposed systems were shown to outperform both the non-cooperative system and the system employing SUD receivers at the DN, while the MUD-SIC-aided scheme achieved significant OP improvements with the aid of the BED-ORS. Additionally, an optimised BED-ORS scheme was designed, which was shown to have an improved robustness against a degraded CSI accuracy, as imposed for example by outdated CSIs.

For a single-SN-multi-RN scenario, the ORS scheme is capable of exploiting the full diversity order. However, the resultant improvement was achieved at the cost of multiplexing loss. For example, an additional TS is required for relaying the SN's message because of the usual half-duplex constraint. Therefore, compared to non-cooperative schemes, the ORS scheme suffers from a factor two throughput penalty. By comparison, the proposed MUD-SIC scheme may accommodate the multiplexing

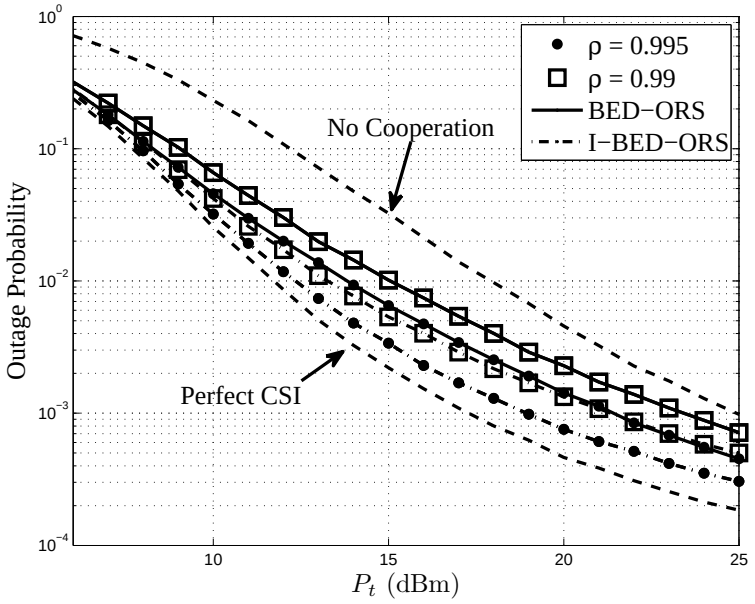

Figure 2.10: OP versus the SN-DN link SNR for transmissions over block Rayleigh fading channels with outdated CSI, where correlation coefficient $\boldsymbol{\rho = 0.99, 0.995}$. SIR= **0**dB, $\boldsymbol{R_T = 0.5}$bit/s/Hz, $\boldsymbol{K = 2}$ RNs and $\boldsymbol{M = 4}$ INs. **The BED-ORS is implemented by Algorithm 1 and I-BED-ORS is implemented by Algorithm 2.** Only the performance of the MUD-SIC-aided scheme is illustrated because it exhibits highest outage improvements towards the non-cooperative counterparts.

loss by allowing multiple SN-DN pairs to share the spectrum simultaneously. For example, assuming that there are two SN-DN pairs in the network, the two SN-RN-DN links may have simultaneously access to the spectrum, while imposing CCI on each other. When using both coordinated synchronization and receivers equipped with a MUD-SIC detection capability, both SN-DN pairs may benefit from the diversity gain achieved by ORS, while eliminating the multiplexing loss.

In Table 2.2, we compare both the OP and the decoding complexity of different schemes. The system configurations are as follows: SIR= 0dB, $R_T = 0.5$bit/s/Hz, $K = 2$ RNs and $M = 4$ INs. A turbo decoder requires 4 ACS operations per bit per iteration and 4 iterations as well as a frame length of 1000 bits is considered. The traditional ORS scheme is based on the highest SNR criterion, while the proposed BED-ORS scheme is implemented by Algorithm 1 of Section 2.2.3 assuming perfect CSI. The decoding complexity is quantified by the number of ACS operations required both at a RN as well as required at the DN.

It is shown in Table 2.2 that if the traditional-ORS algorithm is invoked, both the SUD-assisted and the MUD-SIC-aided schemes may be outperformed by the no-cooperation based benchmarker at $P_{out} = 10^{-3}$. Therefore, the BED-ORS algorithm proposed is indispensable in order to glean a beneficial diversity gain from multiple RNs.

Target OP		@10^{-2}	@10^{-3}	RN ACSs	DN ACSs
Traditional-ORS	SUD-aided	6.3	20.1	16000	48000
Traditional-ORS	MUD-SIC-aided	5.6	15.4	48000	48000
BED-ORS	SUD-aided	4.5	12.4	16000	48000
BED-ORS	MUD-SIC-aided	0.7	6.3	48000	48000
No Cooperation		7.0	14.0	0	48000

Table 2.2: Summary of transmit power P_t in dBm and achievable OP of different ORS schemes.

When equipped with the proposed BED-ORS algorithm, the MUD-SIC-aided scheme outperforms its SUD-aided counterpart by 3.8 dB at $P_{out} = 10^{-2}$, which is increased to 6.1dB at $P_{out} = 10^{-3}$, albeit this is achieved at the price of higher decoding complexity quantified in terms of the number of ACS operations at the RN. The decoding complexity imposed on each RN in the MUD-SIC-aided scheme increases linearly as the number of INs M increases, while the decoding complexity of the SUD-aided scheme remains constant, because it simply treats the interference as noise.

Therefore, it may be concluded that the MUD-SIC-aided schemes are beneficial, when multiple INs are present in the network. However, if the number of **spectrum sharing** SN-DN pairs increases, the MUD-SIC-aided schemes combined with BED-ORS algorithm eventually develop an error floor, when the MUD-SIC operates in the interference-limited high-SNR region, as observed from the numerical results of Fig. 2.7.

In order to mitigate the above-mentioned multiplexing loss and strike a tradeoff between the reliability and throughput, the **relay-sharing** philosophy will be exploited in the next chapter, where multiple SNs share the RNs in order to reduce the multiplexing loss, while maintaining the maximum attainable diversity gain at high SNRs.

Chapter 3

Superposition Modulation Aided Network Coded Cooperation[1]

As discussed in Chapter 2, opportunistic relay selection is capable of providing spatial diversity for single-antenna aided wireless devices. However, compared to non-cooperative schemes, the conventional ORS scheme of Section 2.1 suffered from a factor two multiplexing loss, owning to having a separate broadcast and cooperative phase. The scheme proposed in Chapter 2 was capable of eliminating the multiplexing loss by allowing multiple SN-DN pairs to share the spectrum simultaneously, albeit this is achieved at the cost of introducing co-channel interference (CCI). This CCI was mitigated by the successive interference cancellation based multi-user detector (MUD-SIC) of Section 2.2.

This MUD-SIC-aided scheme constitutes a conventional technique of CCI mitigation [28], which exhibits lower complexity than the optimal maximum-likelihood (ML) detector. Despite its reduced complexity, it was shown to be capable of approaching the capacity of the multi-user access channel, provided that the channel state information (CSI) is known at the transmitters [4]. However, if the CSI is unavailable at the transmitters, the outage performance of the MUD-SIC may be dominated by the residual CCI at high SNRs, as observed in [69] for multi-user channels and confirmed in Fig. 2.7 for multi-user relay channels. In order to mitigate this residual CCI at high SNRs, we have the following two options:

1. We adopt the high-complexity ML detection at both the relay nodes (RNs) and at the destination nodes (DNs).

[1]Part of the work in this chapter has been published in the collaborative work: B. Zhang, J. Hu, Y. Huang, M. El-Hajjar and L. Hanzo, Outage Analysis of Superposition Modulation Aided Network Coded Cooperation in the Presence of Network Coding Noise, IEEE Transactions on Vehicular Technology, 2014.

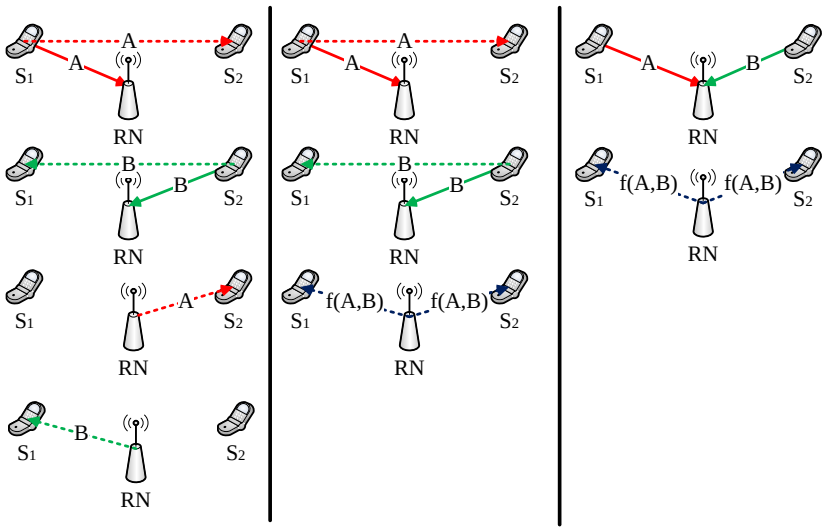

Figure 3.1: Comparison of the MABC and TDBC schemes for a two-SN scenario.

2. We specifically design signals relayed with the aid of network coding by the RNs, in order to facilitate the DNs to fully cancel the CCI instead of canceling it at the RNs.

In Chapter 4 we will opt for adopting the ML detection and compare it to its MUD-SIC counterparts, while in this chapter we will use the second design option of employing the network coding idea.

A beneficial scheme leading to a multiplexing gain may be conceived with the aid of network coding (NC) [73], which was originally conceived for wired networks and was later extended to wireless networks, where multiple SNs exchange their information via RNs. Most contributions were proposed for two-way relaying scenarios, where a pair of SNs exchange their information via a single RN [29] [30].

Before NC was invented and applied to wireless networks, the conventional two-way relaying schemes required four time slots (TSs) for exchanging the information between a pair of SNs, as shown in the 1-st column of Fig. 3.1. Specifically, in the first two TSs of broadcast phase, the SNs S_1 and S_2 send their messages A and B to the RN, respectively. Then, the RN uses another pair of TSs during the relaying phase to forward the messages A to S_2 and B to S_1, respectively. If the spatially separated channels have independent fading, the conventional scheme shown in Fig. 3.1 is capable of achieving a diversity order of $D = 2$ relying on the two signals received during the broadcast phase and the relaying phase, respectively. The bandwidth efficiency of the conventional scheme is 2 channel use per source.

By contrast, the two-way relaying schemes invoking NC may rely on less than four TSs for exchanging the information between a pair of SNs. According to the number of TSs required, two different categories of NC may be conceived for two-way relaying systems, which are discussed as follows:

1) The **time-division broadcast** (TDBC) scheme proposed in [29] reduces the number of TSs to three, which is shown in the 2-nd column of Fig. 3.1. Specifically, in the broadcast phase, the SNs S_1 and S_2 send their messages A and B to the RN in two TSs, which is identical to that of the conventional TDMA scheme. However, in the relaying phase, instead of using two TSs for forwarding the messages, the RN superimposes the messages A and B received using a function $f(A, B)$ and forwards the combined message in a single TS. Though there are numerous designs for the mix function $f(A, B)$, the classic XOR [29] and superposition-modulation (SPM) [38] operation function may fully exploit the diversity gain of TDBC scheme. Using the SPM as an example and assuming the RN may successful decode both messages A and B, then the mix function is

$$f(A, B) = A + B. \tag{3.1}$$

After receiving the mixed message contaminated by receiver's noise represented as

$$y_{rs_1} = h_{rs_1}(A + B) + n_{s_1}, \tag{3.2}$$

where h_{rs_1} is the channel coefficient of the channels spanning from the RN to the S_1, and n_{s_1} represents the receiver noise at S_1. Then, based on perfect channel estimation of h_{rs_1}, S_1 may cancel the self-interference of A using

$$y_{rs_1} - h_{rs_1}A = h_{rs_1}B + n_{s_1} \tag{3.3}$$

and arrive at a signal of message B contaminated only by the receiver noise. The same operations may be done at S_2. As the channels between the RN and S_1 and that between the S_1 and S_2 are mutually independent, the TDBC scheme is capable of achieving a diversity order of two, while using three TSs rather than four TSs compared to the conventional scheme.

2) The **multiple-access broadcast (MABC)** scheme proposed in [30] requires 2 TSs to exchange the information between 2 SNs, which is shown in the 3-rd column of Fig. 3.1. The fundamental difference between MABC and TDBC schemes is that MABC allows 2 SNs to access the channel simultaneously in the broadcast phase, where the RN receives the combined signal of

$$y_r = h_{s_1r}A + h_{s_2r}B + n_r. \tag{3.4}$$

In the relaying phase, the RN amplifies and forwards the composite signal to both SNs, where S_1 receives

$$y_{s_1} = h_{rs_1}G_{AF}y_r + n_{s_1}, \tag{3.5}$$

with G_{AF} being the power amplification factor at the RN. Then, based on the perfect channel estimation of $h_{rs_1}$and h_{s_1r}, S_1 becomes capable of canceling the self-interference of A using

$$y_{s_1} - h_{rs_1}G_{AF}h_{s_1r}A = h_{rs_1}G_{AF}h_{s_2r}B + (h_{rs_1}G_{AF}n_r + n_{s_1}). \tag{3.6}$$

As a result, we arrive at a signal containing the message B contaminated only by the receiver noise n_{s_1} and the amplified noise $h_{rs_1}G_{AF}n_r$.

The MABC requires two TSs for exchanging the information of two SNs, hence having a bandwidth efficiency of one channel use per SN [30]. However, the MABC scheme cannot be readily generalised to multiple SN based scenarios, since the SNs cannot readily overhear each other. Furthermore, due to the half-duplex constraint, the MABC scheme cannot exploit the direct links, which leads to a reduced diversity gain. As we will discuss later in Fig. 3.2, for M SN-DN pairs, a bandwidth efficiency of $(1+1/M)$ channel use per source is achieved using $(M+1)$ TSs, which approaches the bandwidth efficiency of one achieved by the MABC scheme, as M increases. Furthermore, the TDBC scheme may be capable of exploiting the diversity of the direct links, which is not the case for the MABC scheme due to the half-duplex constraint. In this treatise, we adopt the TDBC based NC-CC scheme of Fig. 3.2, where multiple SN-DN pairs share a single RN.

On the other hand, according to the detection technique adopted at the RNs, the family of NC schemes may also be categorised into digital network coding (DNC) [29] and analog network coding (ANC) [30], where the DNC adopts the decode-and-forward (DF) relaying strategy, while the ANC adopts the amplify-and-forward (AF) scheme. The ANC has been widely studied as a benefit of its appealing simplicity, where the RN amplifies and forwards the analog signals received from all SNs. On the other hand, DNC is capable of correcting the source-relay (SR) link's errors at the RNs by flawlessly regenerating and retransmitting the SNs' signals and therefore eliminating the noise-amplification-induced performance limitation of the ANC scheme. Both ANC and DNC are capable of compressing the potentially redundant source sequences, hence reducing either the required number of time-slots in time-division multiple access (TDMA) or the required bandwidth [74–76]. The performance of ANC has been widely studied in the literature, with an emphasis on bidirectional transmissions between a pair of SNs. The outage performance of ANC for bidirectional transmissions is studied from different aspects in the literature, including the optimal power allocation [77, 78], adaptive AF/DF scheme [79], relay selection [80] and multi-hop relaying [81].

SPM [32] constitutes a promising technique of realizing TDBC-based NC-CC mechanisms, where the signals received by the RN are superimposed on a symbol-by-symbol basis. The outage performance of SPM-NC-CC has been studied in [82]

for the scenario of two-user cooperation. The authors of [83] analysed the outage performance of a superposition-modulated network-coded cooperative communication (SPM-NC-CC) system supporting multiple SN-DN pairs sharing a common RN. However, it was assumed in [83] that the destination node (DN) cancels the effects of the unwanted SNs' signals by perfectly recovering them. However, the authors of [83] consider AF relaying, while we considered DF relaying, which is capable of mitigating the relay-induced error-propagation.

Sharma *et al.* point out in [43] that the employment of network-coded cooperative communication (NC-CC) systems may not always be beneficial, because the detrimental interference of the undesired SNs, which is often referred to as *network coding noise (NC noise)*, may outweigh the benefits of NC, as the number of sessions[2] involved in NC increases. Sharma *et al.* [84] have addressed the joint "session-grouping and relay-selection" problem in the context of dual-hop NC-CC systems, while adopting the optimisation criterion of requiring the *highest sum-rate of all sessions*. On the other hand, the authors of [85] proposed a joint-rate and power-control scheme for maximising the data rates of a NC-CC network, where a single RN assists two S-D pairs, while the authors of [86] jointly optimise the power allocation and group assignment. The main objective of [84–86] is to maximise the total information rate of all the SN-DN pairs in the network.

The maximised achievable rates obtained in [84–86] rely on instantaneous rate adaptation, albeit the packet-outage probability was not considered. When the knowledge of the instantaneous channel state information (CSI) is unavailable at the transmitters for rate adaptation, the packet-outage probability becomes non-negligible [43]. Sharma *et al.* also analysed [43] the effects of NC noise on the achievable rate, but the effects of NC noise on the outage performance were evaluated only by simulations, rather than analytically.

Against this background, *we consider the SPM-NC-CC scheme, where each DN extracts the information of the desired SN from the SPM signal forwarded by the RN and as our main contribution, we present the outage analysis of this system assuming a DF relay node (RN) and consider the effects of NC noise. More explicitly, the analytical outage probability expressions are derived for an arbitrary number of SN-DN pairs with the aid of tight lower-bounds. Simulation results are also provided for validating the analytical results. Furthermore, the lower-bounds and upper-bounds of the outage probability are analysed and the diversity order is shown to be 2 for an arbitrary number of SN-DN pairs. It is also revealed that the quality of the worst overheard source is the dominant factor imposed on the outage performance. Finally, we use the closed-form outage probability (OP) lower-bound for designing a relay selection scheme for SPM-NC-CC systems.*

[2]We use the terminology of *session* as defined in [43], where a session represents the transmissions from a source to its destination.

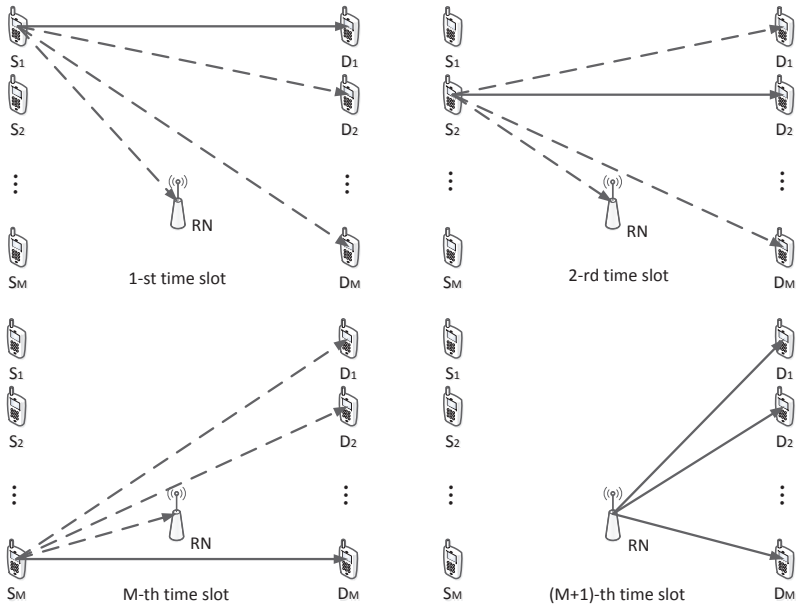

Figure 3.2: Schematic of the SPM-NC-CC scheme.

The chapter is organized as follows. Our system model is introduced in Section 3.1. Then we derive a tight lower-bound approximation of the outage probability and determine the diversity order in Section 3.2. In Section 3.3, we use the outage expressions derived for designing the relay selection scheme of our SPM-NC-CC and then in Section 3.4 we compare the simulation as well as analytical results and characterize the performance of the proposed relay selection scheme. Our conclusions are presented in Section 3.5.

3.1 System Model

We consider a network comprised of M SN-DN pairs $\{(S_1, D_1), \ldots, (S_M, D_M)\}$ and a single RN, as shown in Fig. 3.2, where each node is equipped with a single antenna and operates in a half-duplex mode. We denote the set of the SNs as $S_t = \{S_1, S_2, ..., S_M\}$. A SPM-NC-CC scheme employing $(M+1)$ TSs for the transmission of M packets from the SNs to the DNs using TDMA is considered in this paper. During the k-th TS of the first M TSs, the SN S_k broadcasts its packet to all the DNs and the RN, while all other SNs remain silent. We refer to the first M TSs as the broadcast phase, where the signals received at the DN D_k and the RN may be expressed as

$$y_{s_i d_k} = \sqrt{P_s} h_{s_i d_k} x_i + n_k^i \tag{3.7}$$

$$y_{s_i r} = \sqrt{P_s} h_{s_i r} x_i + n_r^i, \tag{3.8}$$

where P_s is the transmit power of the SNs, $h_{s_i d_k}$ and $h_{s_i r}$ are the channel coefficients capturing the effects of both the fading as well as the pathloss between the SN S_i and

the DN D_k as well as between the SN S_i and the RN, respectively. Furthermore, x_i is the signal transmitted by S_i and its power is normalized to 1, while n_k and n_r denote the additive white Gaussian noise (AWGN) at the DNs and the RN, respectively.

The RN overhears the M signals transmitted by the SNs and tries to decode them. In order to avoid error propagation, the RN superimposes the signals, which have been successfully decoded as well as re-encoded and then forwards the composite signal in the $(M+1)$-st TS termed as the *relay phase*. We assume that a perfect error detection code is employed to identify whether the signal is correctly decoded. We define the set of SNs, whose signals have been successfully decoded by the RN as the *forwarding set*, which is denoted as F_s and its size is denoted as $|F_s|$. Therefore, the forwarding set F_s satisfies $F_s \subseteq S_t$ and $|F_s| \leq M$.

We assume that an equal amount of transmit power is allocated to each SN in the forwarding set. The composite signal transmitted by the RN may be expressed as $x_r = \frac{1}{|F_s|} \sum_{S_i \in F_s} x_i$, while the signal received by D_k may be formulated as

$$y_{rd_k} = \sqrt{P_r} h_{rd_k} x_r + n_k^r. \tag{3.9}$$

where P_r represents the transmit power of the RN.

If we have $S_k \in F_s$, the DN D_k is capable of extracting x_k from y_{rd_k} by subtracting the overheard signals after weighting them using the appropriate gain factors. In our analysis we rely on perfect channel estimation. We assume that the information of the weighting and gain factors is forwarded by the RN to D_k error-freely. The noise-contaminated signal extracted by D_k is expressed as

$$\begin{aligned} \hat{y}_{rd_k} &= y_{rd_k} - \frac{\sqrt{P_r}}{|F_s|} \sum_{S_i \in F_s, i \neq k} \frac{h_{rd_k}}{h_{s_i d_k}} y_{s_i d_k} \\ &= \frac{\sqrt{P_r}}{|F_s|} h_{rd_k} \left(x_k - \sum_{S_i \in F_s, i \neq k} \frac{1}{h_{s_i d_k}} n_k^i \right) + n_k^r. \end{aligned} \tag{3.10}$$

Therefore, the signal of S_k at D_k may be contaminated by multiple noise terms, as shown in Eq. (3.10), which results in an increased noise power and was referred to as *Network Coding Noise* in [43].

In order to further elaborate on the system model, we present an example for three SN-DN pairs in Fig. 3.3. The decoding process and the signal components received at the destination D_1 in the example of Fig. 3.3 are presented in Fig. 3.4 and Fig. 3.5, respectively. During the broadcast phase, the three SNs S_1, S_2 and S_3 transmit the messages A, B and C, where the signals received by D_1 are represented in the first three columns at the left hand side of Fig. 3.4. The block of A, B, C and N stands for the signals and the noise components in the received signal, while the

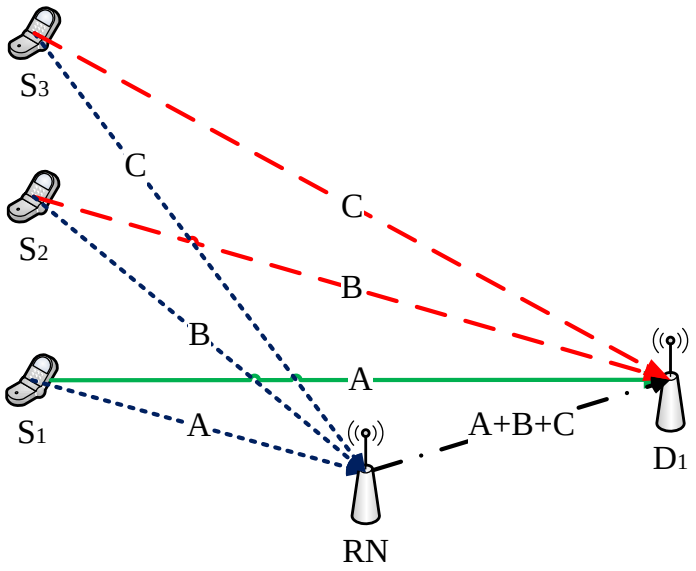

Figure 3.3: System model of an example of three SN-DN pairs.

size of the block represents the associated power. The block A, B and C are having unequal power due to the different fading coefficients of the channels spanning from S_1, S_2 and S_3 to D_1. Assuming that an equal transmit power P_t is used by all SNs, the signal power received for A, B and C is equal to $|h_{s_1d_1}|^2P_t$, $|h_{s_2d_1}|^2P_t$ and $|h_{s_3d_1}|^2P_t$, respectively.

We assume that the RN decodes all of them successfully in this example. During the relay phase, the RN re-encodes the messages and superimposes them as well as transmits to all DNs, where the signal received by D_1 is represented in the 4-th columns at left-hand side of Fig. 3.4. The decoding process of A at D_1 is illustrated at the bottom of Fig. 3.4. Firstly, based on perfect channel estimation, D_1 is capable of scaling up the signals received from S_2 as well as S_3, and then extracting A from the superimposed signal, in which the CCI of B and C is removed, as shown on the right-hand side of Fig. 3.4. Then, maximum ratio combining (MRC) is invoked for combining the extracted signal with that received during the first TS. Finally, the processed signal is fed into the decoder.

The different components of the signal extracted from the superposed signal is illustrated in Fig. 3.5. The signal power of A remains unchanged, while the unwanted signals of B and C are removed at the cost of an increased noise power during the scaling and subtraction process presented in Eq. (3.10), which results in the so-called *network coding noise* (NC-noise). Therefore, compared to the conventional two-way relaying NC scheme illustrated in Fig. 3.1, network coding noise is engendered by the imperfect overhearing links at the DNs, while in the two-way relaying NC schemes, the DNs may perfectly cancel the interference, because they serve as the SNs of the interference signal. It should be also noted that the two-way relaying scheme relying

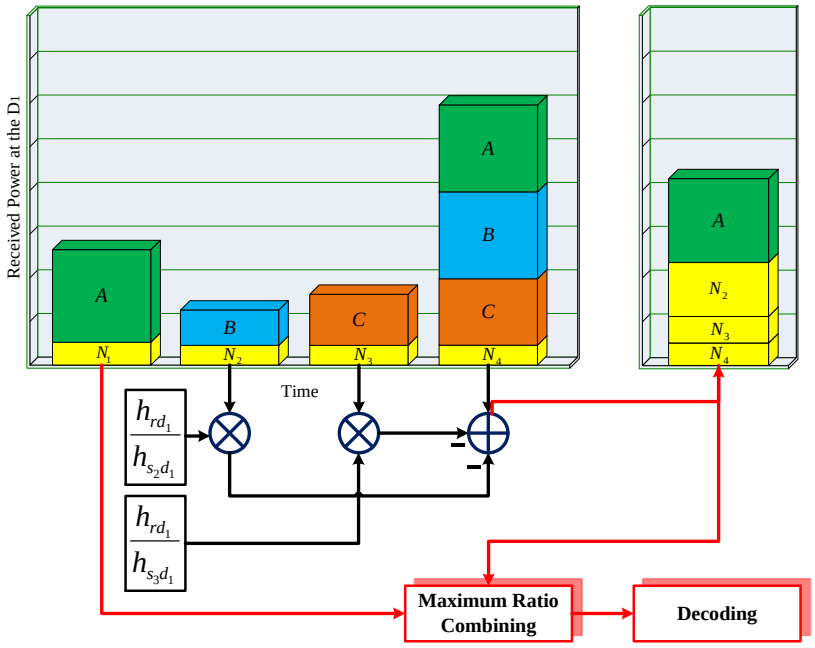

Figure 3.4: Decoding Process of the SPM-NC-CC scheme.

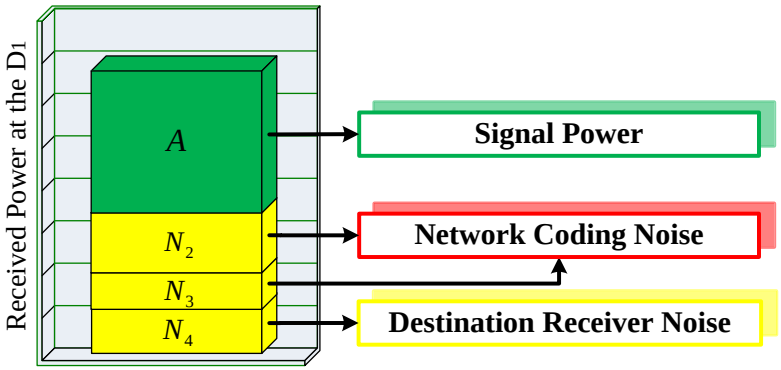

Figure 3.5: Decoding Output of the SPM-NC-CC scheme.

on perfect interference cancellation cannot be generalized to more than two SN-DN pair because the two nodes in the pairs of $\{S_1, D_2\}$ and $\{S_2, D_1\}$ have to be co-located or connected with the aid of perfectly error-free channels.

3.2 Outage Analysis

In this section, we aim for analyzing the per-user OP of the network described in Section 3.1. Assuming that perfect capacity-achieving coding is adopted, an outage is defined as the event, when the achievable rate of the link S_k-D_k is below the transmission rate of S_k. We assume a narrow-band Rayleigh-distributed block fading channel model, where the fading coefficients remain constant for the duration of a

packet and then they are faded independently from one packet to another both in time and space. The receivers are assumed to rely on perfect channel estimation. The additive noise at the receivers is modeled by independent zero-mean circularly symmetric complex Gaussian random variables.

Firstly, we formulate the received SNRs at the DNs and then the outage probability of the network. According to Eq. (3.10), the received SNRs at the DN D_k during the broadcast and relay phases are expressed as follows:

$$\begin{aligned}\gamma_k^1 &= \gamma_{s_k d_k} \\ \gamma_k^2 &= \frac{1}{\frac{1}{\gamma_{rd_k/|F_s|}} + \sum_{S_i \in F_s, i \neq k} \frac{1}{\gamma_{s_i d_k}}},\end{aligned} \tag{3.11}$$

where γ_{ab} is the instantaneous received SNR experienced at node b for the signal transmitted by node a. We denote the instantaneous channel coefficient between node a and b by h_{ab} and the average received SNR by $\bar{\gamma}_{ab}$. Then the instantaneous received SNR may be expressed as $\gamma_{ab} = |h_{ab}|^2 \bar{\gamma}_{ab}$, since we are considering block fading channels. It can be observed in Eq. (3.11) that γ_k^2 decreases, as the number of SNs in the forwarding set increases.

3.2.1 Formulation of Outage Probability

Assuming that the k-th SN S_k transmits to D_k at a data rate R_k, an outage event of the k-th SN-DN pair is defined as the event when the maximum achievable rate is below the target rate [75]. If diversity combining is adopted at the DN, the outage probability may be formulated as follows:

$$\begin{aligned}P_{o,k} =& \Pr\left\{\log_2\left(1+\gamma_k^1\right) < R_k\right\} \Pr\left\{S_k \notin F_s\right\} \\ &+ \Pr\left\{\log_2\left(1+\gamma_k^1+\gamma_k^2\right) < R_k\right\} \Pr\left\{S_k \in F_s\right\},\end{aligned} \tag{3.12}$$

where the first term represents the outage probability, when RN fails to decode the S_k's signal. Therefore D_k relies only on the direct transmission from S_k to recover the message, while the second term represents the outage probability when S_k is successfully decoded by the RN and therefore forwarded to D_k via the SPM composite signal.

For brevity, we define the first term in Eq. (3.12) as $P_{o,k}^{DT}$, which may be formulated as:

$$\begin{aligned} P_{o,k}^{DT} &= \Pr\left\{\log_2\left(1+\gamma_k^1\right) < R_k\right\} \Pr\left\{S_k \notin F_s\right\} \\ &= \Pr\left\{\log_2\left(1+\gamma_{s_k d_k}\right) < R_k\right\} \Pr\left\{\log_2\left(1+\gamma_{s_k r}\right) < R_k\right\} \\ &= \Pr\left\{\gamma_{s_k d_k} < 2^{R_k}-1\right\} \Pr\left\{\gamma_{s_k r} < 2^{R_k}-1\right\} \\ &= \left(1-e^{-\frac{2^{R_k}-1}{\bar{\gamma}_{s_k d_k}}}\right)\left(1-e^{-\frac{2^{R_k}-1}{\bar{\gamma}_{s_k r}}}\right). \end{aligned} \tag{3.13}$$

The second term in Eq. (3.12) indicates the outage probability when S_k is in the forwarding set F_s, which may be expressed as follows:

$$\begin{aligned} &\Pr\left\{\log_2\left(1+\gamma_k^1+\gamma_k^2\right) < R_k\right\} \Pr\left\{S_k \in F_s\right\} \\ =& \sum_{F_s | S_k \in F_s} \Pr\left\{\log_2\left(1+\gamma_k^1+\gamma_k^2\right) < R_k | F_s\right\} \Pr\left\{F_s\right\} \\ \triangleq& \sum_{F_s | S_k \in F_s} P_e\left(F_s\right) \Pr\left\{F_s\right\}, \end{aligned} \tag{3.14}$$

where $P_e\left(F_s\right)$ is the error probability conditioned on the forwarding set F_s, which may be expressed by

$$P_e\left(F_s\right) = \Pr\left\{\log_2\left(1+\gamma_k^1+\gamma_k^2\right) < R_k | F_s\right\}, \tag{3.15}$$

while $\Pr\left\{F_s\right\}$ is the probability that a forwarding set F_s is adopted at the RN, which may be expressed as

$$\begin{aligned} \Pr\left\{F_s\right\} &= \prod_{S_i \in F_s} \Pr\left\{\log_2\left(1+\gamma_{s_i r}\right) \geq R_i\right\} \\ &\quad \times \prod_{S_j \notin F_s} \Pr\left\{\log_2\left(1+\gamma_{s_j r}\right) < R_j\right\} \\ &= \prod_{S_i \in F_s} e^{-\frac{2^{R_i}-1}{\bar{\gamma}_{s_i r}}} \prod_{S_j \notin F_s} \left(1-e^{-\frac{2^{R_j}-1}{\bar{\gamma}_{s_j r}}}\right). \end{aligned} \tag{3.16}$$

Then, using the definitions given above, we may rewrite the outage probability in Eq. (3.12) in a simpler form as:

$$P_{o,k} = P_{o,k}^{DT} + \sum_{F_s | S_k \in F_s} P_e\left(F_s\right) \Pr\left\{F_s\right\}$$

3.2.2 Lower Bounds for Outage Probability

In order to derive $P_e\left(F_s\right)$ in Eq. (3.14), we may have to formulate the probability density function (PDF) of the second-hop received SNR γ_k^2 in Eq. (3.11). However,

the PDF of a reciprocal of the sum of exponential random variables is challenging to formulate for the outage performance analysis. Therefore, instead of pursuing the exact PDF of γ_k^2, we investigate the following inequalities:

$$\begin{aligned}\gamma_k^2 &= \frac{1}{\frac{1}{\gamma_{rd_k/|F_s|}} + \sum_{S_i \in F_s, i \neq k} \frac{1}{\gamma_{s_i d_k}}} \\ &\leq \frac{1}{max_{S_i \in F_s, i \neq k} \left(\frac{1}{\gamma_{rd_k/|F_s|}}, \frac{1}{\gamma_{s_i d_k}} \right)} \\ &= min_{S_i \in F_s, i \neq k} \left(\gamma_{rd_k/|F_s|}, \gamma_{s_i d_k} \right) \triangleq \gamma_{min}. \end{aligned} \tag{3.17}$$

Hence, γ_k^2 is upper-bounded by γ_{min}. The cumulative distribution function (CDF) of γ_{min} may be deduced as follows:

$$\begin{aligned} F_{\gamma_{min}}(\gamma) &= \Pr\left\{ min_{S_i \in F_s} \left(\gamma_{rd_k/|F_s|}, \gamma_{s_i d_k} \right) \leq \gamma \right\} \\ &= 1 - \Pr\left\{ \gamma_{rd_k/|F_s|} > \gamma \right\} \prod_{S_i \in F_s, i \neq k} \Pr\left\{ \gamma_{s_i d_k} > \gamma \right\} \\ &= 1 - \exp\left\{ -\gamma \left(\frac{1}{\bar{\gamma}_{rd_k/|F_s|}} + \sum_{S_i \in F_s, i \neq k} \frac{1}{\bar{\gamma}_{s_i d_k}} \right) \right\}. \end{aligned} \tag{3.18}$$

For brevity, we define

$$\bar{\gamma}_{min} = \left(\frac{1}{\bar{\gamma}_{rd_k/|F_s|}} + \sum_{S_i \in F_s, i \neq k} \frac{1}{\bar{\gamma}_{s_i d_k}} \right)^{-1}.$$

Based on the CDF in Eq. (4.3), we may arrive at the PDF of γ_{min} as:

$$f_{\gamma_{min}}(\gamma) = \frac{dF_{\gamma_{min}}(\gamma)}{d\gamma} = \frac{1}{\bar{\gamma}_{min}} \exp\left(-\frac{\gamma}{\bar{\gamma}_{min}} \right). \tag{3.19}$$

If γ_k^2 is replaced by its upper-bound γ_{min} in Eq. (3.17), the *lower-bound* $P_e^{low}(F_s)$ *of* $P_e(F_s)$ may be attained as follows:

$$\begin{aligned} P_e(F_s) =& \Pr\left\{ \log_2\left(1 + \gamma_k^1 + \gamma_k^2\right) < R_k | F_s \right\} \\ \geq& \Pr\left\{ \log_2\left(1 + \gamma_k^1 + \gamma_{min}\right) < R_k | F_s \right\} \triangleq P_e^{low}(F_s), \\ & P_e^{low}(F_s) \\ =& \Pr\left\{ \gamma_k^1 + \gamma_{min} < 2^{R_k} - 1 \right\} \\ =& \int_0^1 \Pr\left\{ \frac{\gamma_{s_k d_k}}{2^{R_k} - 1} < u \right\} \Pr\left\{ \frac{\gamma_{min}}{2^{R_k} - 1} < (1 - u) \right\} du \\ =& 1 - e^{-\alpha} - \alpha e^{-\mu} \frac{e^{\mu - \alpha} - 1}{\mu - \alpha}, \end{aligned} \tag{3.20}$$

where $\alpha = \frac{2^{R_k}-1}{\bar{\gamma}_{s_k d_k}}$ and $\mu = \frac{2^{R_k}-1}{\bar{\gamma}_{min}}$. Using the relation of $P_e(F_s) \geq P_e^{low}(F_s)$ shown in Eq. (3.20), we may formulate the *lower-bound of the outage probability* as follows:

$$\begin{aligned} P_{o,k} =& P_{o,k}^{DT} + \sum_{F_s|S_k \in F_s} P_e(F_s) \Pr\{F_s\}, \\ P_{o,k} \geq& P_{o,k}^{low} = P_{o,k}^{DT} + \sum_{F_s|S_k \in F_s} P_e^{low}(F_s) \Pr\{F_s\}, \end{aligned} \tag{3.21}$$

where $P_{o,k}^{DT}$, $\Pr\{F_s\}$ and $P_e^{low}(F_s)$ are derived in closed-form as in Eq. (3.13), (3.16) and (3.20), respectively.

3.2.3 Diversity Order Analysis

3.2.3.1 Diversity Order of the Outage Probability Lower-bound

The lower-bound derived in Eq. (3.21) enables us to approximate the exact outage probability in Eq. (3.12). However, the diversity performance is not explicit from Eq. (3.21). Let us now embark on deriving the asymptotic outage probability expression based on Eq. (3.21) for the high-SNR regime, which may offer us insights into the achievable diversity performance. We introduce $\bar{\gamma}_{ij} = u_{ij}\bar{\gamma}$ to take into account the pathloss of the link between node i and j. For simplicity of exposure, we investigate the different components in Eq. (3.21) separately.

For a sufficiently high SNR of $\bar{\gamma} \to +\infty$ with the aid of the series expansion, we may write:

$$\begin{aligned} P_{o,k}^{DT} &= \left(1 - e^{-\frac{2^{R_k}-1}{u_{s_k d_k}\bar{\gamma}}}\right)\left(1 - e^{-\frac{2^{R_k}-1}{u_{s_k r}\bar{\gamma}}}\right) \\ &= \frac{\left(2^{R_k}-1\right)^2}{u_{s_k d_k} u_{s_k r}} \frac{1}{\bar{\gamma}^2} + O\left(\frac{1}{\bar{\gamma}^2}\right), \end{aligned} \tag{3.22}$$

$$\begin{aligned} P_e^{low}(F_s) &= 1 - e^{-\alpha} - \alpha e^{-\mu} \frac{e^{\mu-\alpha}-1}{\mu-\alpha} \\ &= \frac{\left(2^{R_k}-1\right)^2}{2u_{s_k d_k} u_{min}(F_s)} \frac{1}{\bar{\gamma}^2} + O\left(\frac{1}{\bar{\gamma}^2}\right), \end{aligned} \tag{3.23}$$

$$\begin{aligned} \Pr\{F_s\} &= \prod_{S_i \in F_s} e^{-\frac{2^{R_i}-1}{u_{s_i r}\bar{\gamma}}} \prod_{S_j \notin F_s} \left(1 - e^{-\frac{2^{R_j}-1}{u_{s_j r}\bar{\gamma}}}\right) \\ &= \left(\prod_{S_j \notin F_s} \frac{2^{R_j}-1}{u_{s_j r}}\right) \frac{1}{\bar{\gamma}^{M-|F_s|}} + O\left(\frac{1}{\bar{\gamma}^{M-|F_s|}}\right), \end{aligned} \tag{3.24}$$

where $u_{min}(F_s) = \left(\frac{1}{u_{rd_k/|F_s|}} + \sum_{S_i \in F_s, i \neq k} \frac{1}{u_{s_i d_k}}\right)^{-1}$ is conditioned on the forwarding set F_s, and $O\left(\gamma^{-K}\right)$ represents the components having diversity orders higher than K. By substituting Eq. (3.22) to Eq. (3.24) into Eq. (3.21), we may arrive at the *high-SNR expression of the lower-bound*:

$$\begin{aligned} & P_{o,k}^{low} \\ =& \frac{\left(2^{R_k}-1\right)^2}{u_{s_k d_k} u_{s_k r}} \frac{1}{\bar{\gamma}^2} + \frac{\left(2^{R_k}-1\right)^2}{2 u_{s_k d_k} u_{min}(S_t)} \frac{1}{\bar{\gamma}^2} + O\left(\frac{1}{\bar{\gamma}^2}\right). \end{aligned} \tag{3.25}$$

Therefore, we can see that the lower bound of the outage probability is indicative of a the diversity order of 2.

The first term in Eq. (3.25) indicates the high-SNR outage probability contributed by the specific scenario, when RN fails to decode the signal of $S_k (S_k \notin F_s)$, and hence D_k relies purely on the direct link for decoding. The second term in Eq. (3.25) represents the high-SNR outage probability contributed by the particular scenario, when RN successfully decodes the signals received from all the SNs ($F_s = S_t$) and we have

$$u_{min}(S_t) = \left(\frac{M}{u_{rd_k}} + \sum_{i=1, i \neq k}^{M} \frac{1}{u_{s_i d_k}}\right)^{-1}.$$

Therefore, as the number M of SN-DN pairs increases, $u_{min}(S_t)$ decreases and this results in an increased outage probability in Eq. (3.25).

3.2.3.2 Diversity Order of the Outage Probability Upper-bound

We may also derive an upper-bound for the exact outage probability in Eq. (3.12) by using the following inequality,

$$\begin{aligned} \gamma_k^2 &= \frac{1}{\frac{1}{\gamma_{rd_k/|F_s|}} + \sum_{S_i \in F_s, i \neq k} \frac{1}{\gamma_{s_i d_k}}} \\ &\geq \frac{1}{M \times max_{S_i \in F_s, i \neq k}\left(\frac{1}{\gamma_{rd_k/|F_s|}}, \frac{1}{\gamma_{s_i d_k}}\right)} \\ &= \frac{1}{M} \times min_{S_i \in F_s, i \neq k}\left(\gamma_{rd_k/|F_s|}, \gamma_{s_i d_k}\right) = \frac{\gamma_{min}}{M}. \end{aligned} \tag{3.26}$$

By using the relationship of $\gamma_k^2 \geq \frac{\gamma_{min}}{M}$ in Eq. (3.12), we may arrive at the *upper-bound* $P_e^{up}(F_s)$ ***of*** $P_e(F_s)$, which may be expressed as:

$$\begin{aligned} P_e(F_s) =& \Pr\left\{\log_2\left(1 + \gamma_k^1 + \gamma_k^2\right) < R_k | F_s\right\}. \\ P_e(F_s) \leq& P_e^{up}(F_s) = \Pr\left\{\log_2\left(1 + \gamma_k^1 + \frac{\gamma_{min}}{M}\right) < R_k | F_s\right\}. \end{aligned} \tag{3.27}$$

Similar to the derivation of the outage probability lower-bound, we may readily deduce the *high-SNR expression of the outage probability upper-bound* as:

$$P_{o,k}^{up} = \frac{\left(2^{R_k}-1\right)^2}{u_{s_k d_k}} \left(\frac{1}{u_{s_k r}} + \frac{M}{2u_{min}(S_t)}\right) \frac{1}{\bar{\gamma}^2} + O\left(\frac{1}{\bar{\gamma}^2}\right). \tag{3.28}$$

Since both the lower-bound in Eq. (3.25) and the upper-bound in Eq. (3.28) give a diversity order of 2, we may conclude that the exact diversity order is 2.

3.2.4 Discussions

Firstly, regardless of the number of SN-DN pairs in the network, a diversity order of 2 is achieved by the SPM-NC-CC scheme. As the number of SN-DN pairs increases, the spectral efficiency improvement is represented by the $\frac{M+1}{M}$ time slots per user, which approaches 1 TS per user, as in the traditional TDMA scheme, while maintaining the second-order diversity gain.

However, Eq. (3.17) also reveals the fact that the SNR gain achieved during the relaying phase is limited by the quality of the worst overheated link spanning from $S_i (i \neq k)$ to D_k. This effect will be illustrated by simulations in Fig. 3.10 of Section 3.4. Therefore, in order to exploit the spectral efficiency improvements of our SPM-NC-CC scheme, it is important to carefully construct the SPM-NC-CC group for the sake of mitigating the performance loss encountered by the overheard S-D channels. On the other hand, when the group formation has been completed, even though the number of available relays is larger than 1, the achievable diversity order would not improve with the aid of dynamic techniques, such as opportunistic relay selection [16]. This is due to the fact that the SNR gain of the relaying phase would be dominated by the worst overheard links. Therefore, we may adopt a simple relay selection scheme using the analytical outage expressions in Eq. (3.21), which relies on a single relay during the entire session, whilst achieving a diversity order of 2 and maintaining the minimum outage probability.

3.3 Applications: Relay Selection

In this section, we consider a scenario, where multiple SN-DN pairs intend to share a RN for creating a SPM-NC-CC arrangement under the assumption that multiple RNs are available in the region.

The candidate RN set is denoted as $\{R_1, R_2, ..., R_N\}$, where we consider that all the RNs contend during the relay selection stage and the best RN is selected for transmission during the data transmission stage. The criterion for selecting the best RN is that of the minimum sum outage probability of all SN-DN pairs. With the

aid of the analytical lower-bound of the outage probability derived in Eq. (3.21), we may design a low-complexity relay selection method by avoiding time consuming Monte-Carlo simulations for evaluating the sum of the resultant outage probabilities.

The relay selection stage is designed to have two phases: the channel measurement phase and the relay contention phase. During the channel measurement phase, each RN R_n evaluates the sum outage probability, if R_n itself is selected for relaying. In the relay contention phase, a distributed method relying on local timers [16] is adopted. The design of the relay selection stage is detailed in the following sections.

3.3.1 Channel measurement phase

In the channel measurement phase, each RN R_n would evaluate the sum outage probability of $P^n_{o,sum} = \sum_{k=1}^{M} P^n_{o,k}$. According to Eq. (3.21), in order to evaluate the outage probability of the k-th SN-DN pair via R_n, which is denoted as $P^n_{o,k}$, the knowledge of the CSI is required and the related process works as follows:

- The average SNR of the channels between R_n and each SN is denoted as $\bar{\gamma}_{sr_n} = \{\bar{\gamma}_{s_i r_n} | \, i = 1, .., M\}$.
- The average SNR of the channels between R_n and D_k is denoted as $\bar{\gamma}_{r_n d_k}$. Hence, in order to evaluate the sum outage probability, the knowledge of the average SNR of the channels between R_n and each DN, denoted as $\bar{\gamma}_{r_n d} = \{\bar{\gamma}_{r_n d_k} | \, k = 1, ..., M\}$ is required.
- The knowledge of the $\bar{\gamma}_{sd_k} = \{\bar{\gamma}_{s_i d_k} | \, i = 1, .., M\}$ average SNR of the channels between each SN and D_k is necessitated. Hence, in order to evaluate the sum outage probability, the average SNR $\bar{\gamma}_{sd} = \{\bar{\gamma}_{s_i d_k} | \, i = 1, .., M, k = 1, ..., M\}$ of the channels between each SN-DN pair is required .

In order to evaluate the required CSI, the pilot and feedback are designed as follows:

1. Each SN S_i broadcasts a pilot signal in orthogonal time slots, where each RN R_n and each DN D_k would estimate both $\bar{\gamma}_{sr_n}$and $\bar{\gamma}_{sd_k}$, respectively.
2. Each RN R_n broadcasts a pilot signal in orthogonal time slots, where each DN estimates the $\bar{\gamma}_{r_n d_k}$.
3. Each DN D_k broadcasts a feedback signal coupling the information of $\bar{\gamma}_{r_n d_k}, n = 1, ..., N$ and $\bar{\gamma}_{sd_k}$.

Then, each RN R_n becomes capable of acquiring the CSI of $\bar{\gamma}_{sr_n}$,$\bar{\gamma}_{r_n d_k}$and $\bar{\gamma}_{sd}$ and hence it is capable of evaluating the approximate sum outage probability $\hat{P}^n_{o,sum} = \sum_{k=1}^{M} P^{low}_{o,k}$ with the aid of Eq. (3.21).

3.3.2 Relay contention phase

In the relay contention phase, the most suitable RN would be selected. The specific node within the RN set R_{n^*}, which has the minimum sum outage probability $\hat{P}^{n^*}_{o,sum}$

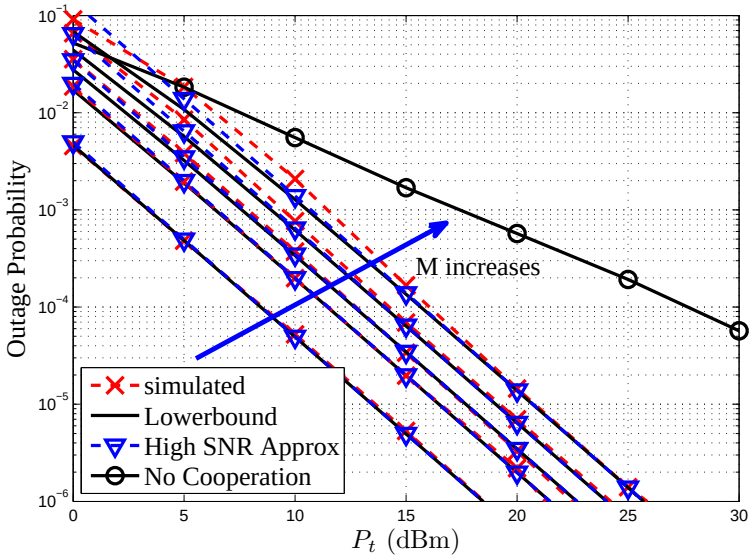

Figure 3.6: Outage probability versus the transmit power for Diversity Combining over block Rayleigh fading channels. The numbers of SN-DN pairs are $M = 1$, 2, 3, 5 and 10.

is selected as the relaying node. This may be implemented without any coordination by a central controller, when the distributed-timer-based technique of [16] is adopted. Specifically, the contention phase begins with a request-to-send (RTS) signal transmitted by a SN, when each RN listens. Upon receiving the RTS signal, each RN R_n starts a local timer having an expiration duration proportional to the sum outage probability $\hat{P}^n_{o,sum}$. Therefore, the timer at R_{n^*} having the minimum $\hat{P}^{n^*}_{o,sum}$ would expire first, which hence broadcasts a clear-to-send (CTS) signal, claiming its occupation of the data transmission stage. Upon receiving the CTS signal by R_{n^*}, the other RNs would remain silent during the data transmission stage.

The relay selection stage may be invoked again, when the topology of the network changes, for example, when some new SN-DN pairs join or leave the SPM-NC-CC group. The performance of the relay selection scheme will be illustrated in Section 3.4.1.

3.4 Simulation Results and Discussions

3.4.1 Outage Probability lower-bound

In this section, we consider both a symmetric and an asymmetric topology. We assume that all nodes in the network use an identical transmit power P_t and transmit rate of $R = 1$bit/sec/Hz. The time-averaged SNR of the SN-DN channel is denoted as $\bar{\gamma}_{s,d} = P_t/(N_0 \times d^{\delta}_{s,d})$, where the noise power N_0 is set to -80 dBm, while β is the channel's pathloss exponent. Therefore, the average SNR of the channel between any

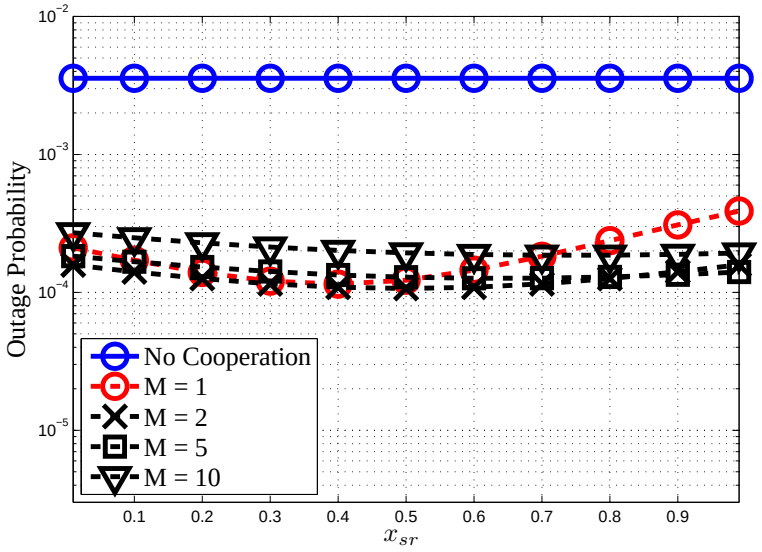

Figure 3.7: Outage probability versus the relay position over block Rayleigh fading channels with identical e2e throughput.

two nodes is $\bar{\gamma}_{i,j} = P_t/(N_0 \times d_{i,j}^{\beta}) = (d_{i,j}/d_{s,d})^{-\beta}\bar{\gamma}_{s,d}$, where $d_{i,j}$ denotes the distance between node i and node j. We assume $\beta = 3$ for our simulations.

3.4.1.1 Symmetric Network

Firstly, we consider a symmetric topology comprising M SN-DN pairs, where the average distance between a SN-DN pair is $d = 200$ meters. A RN is placed halfway along the line between any SN-DN pair. The transmission rate of each SN is set to 2 bits/s/Hz. In Fig. 3.6, we compare the analytical lower-bounds of OP to that acquired by Monte-Carlo simulations. The dashed lines in Fig. 3.6 represent the simulated results, while the solid curves rely on the lower-bounds of Eq. (3.21) derived in this paper. The high-SNR approximations derived in Eq. (3.25) is also illustrated. It is shown that for $M = 1, 2, 3, 5, 10$ SN-DN pairs, the lower-bounds match the simulated results quite closely. Furthermore, it is shown that as the number of sessions or SN-DN pairs simultaneously accessing a RN increases, the performance degrades because of the increased NC noise [43]. However, regardless of the number of cooperative SNs, all SPM-NC-CC schemes achieve a diversity of 2.

In Fig. 3.6, each SN is assumed to have a constant transmission rate R, regardless of the number of the SN-DN pairs in the SPM-NC-CC group. From the perspective of the achievable end-to-end (e2e) throughput, the actual throughput of each SN-DN pair should be $R_{e2e} = \frac{M}{M+1}R$. Therefore, the outage performance comparison of the SPM-NC-CC schemes may be unfair, since they achieve a higher e2e throughput by using less time slots, compared to the traditional scheme relying on $M = 1$.

In this case, we assume that in order to achieve a certain e2e throughput R_{e2e}, the SNs are capable of adjusting the physical layer transmission rate R, according to

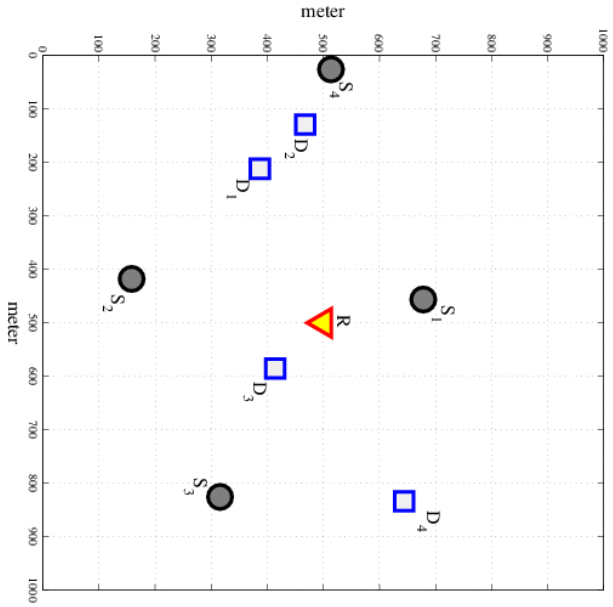

Figure 3.8: Network topology for $M = 4$ SN-DN pairs and a single RN.

the number of SN-DN pairs M. In Fig. 3.7, we fixed $R_{e2e} = 2$ bits/sec/Hz as well as $P_t = 15$ dBm and compared the outage performance of the proposed scheme for different values of M. Fig. 3.7 illustrates the effects of the RN position, which is determined by $x_{sr} = \frac{d_{sr}}{d_{sd}}$.

Based on Fig. 3.7, we may first revisit the outage performance recorded for different values of M for the scenario of $X_{sr} = 0.5$, when the RN is positioned half-way between each SN-DN pair. When $M = 2$, the outage performance becomes better than that of the traditional $M = 1$ scheme operating without SPM-NC-CC, while the outage performance of the $M = 10$ scheme is slightly degraded.

However, observe in Fig. 3.7 that when the RN position changes, the outage performance of $M = 10$ remains almost unaffected and becomes better than that of the $M = 1$ scheme, when the RN is closer to the DN. For the symmetric scenario considered in this example, the $M = 2$ scheme achieves the best outage performance for arbitrary RN positions. Interestingly, the $M = 2$ scheme also exhibits both the lowest implementation complexity and the lowest e2e delay. Therefore, in order to exploit the benefits of the SPM-NC-CC scheme, the RN position and the number of SN-DN pairs should be carefully considered in the light of the analytical results given in Eq. (3.21). As a final remark, compared to the non-cooperation scenario, the proposed schemes achieve significant improvements as a benefit of their increased diversity gain.

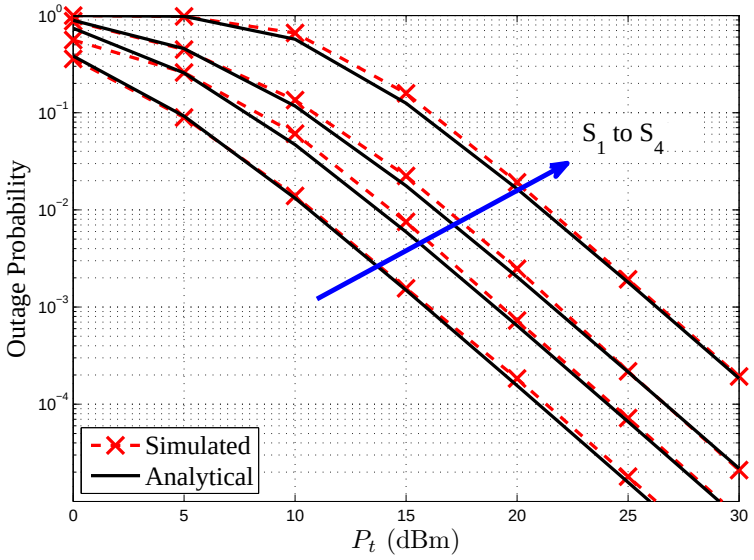

Figure 3.9: Outage probability versus the transmit power for Diversity Combining at the DNs over block Rayleigh fading channels. The network topology is illustrated in Fig. 3.8.

3.4.1.2 Non-Symmetric Network

In order to validate the analytical results in the non-symmetric network topology, we compare the lower-bounds to our simulation results. However, for reasons of space economy, we only consider a simple example topology comprised of $M = 4$ SN-DN pairs, where the nodes are assumed to be placed as in Fig. 3.8. We compare the OP of each SN-DN pair using simulations to the lower bounds derived in Eq. (3.21). It is shown in Fig. 3.9 that the lower-bounds closely match the simulated results for each SN-DN pair, which indicates that the lower-bound deduced is tight. The high-SNR expressions derived in Eq. (3.25) also match with the simulated results quite closely at high SNR, which verifies that the diversity order of 2 is indeed achieved by the SPM-NC-CC scheme.

3.4.1.3 Effects of Overheard Link Quality

In Fig. 3.10 we illustrate that the quality of the the worst overheard link dominates the outage performance. In a network supporting 5 SN-DN pairs, we observe the outage probability of the session S_1-D_1, where we fixed the received SNR of the overheard link spanning from S_2 to D_1 and gradually improve both the other overheard links at D_1 as well as the relaying link, namely, the links spanning from S_3, S_4, S_5 and the RN to D_1. As shown in Fig.3.10, although we improve both the relaying links and the overheard links towards D_1, the outage performance of S_1-D_1 improves only marginally as long as the SNR of the worst overheard link is fixed, indicating that the outage performance is dominated by the quality of the worst overheard link.

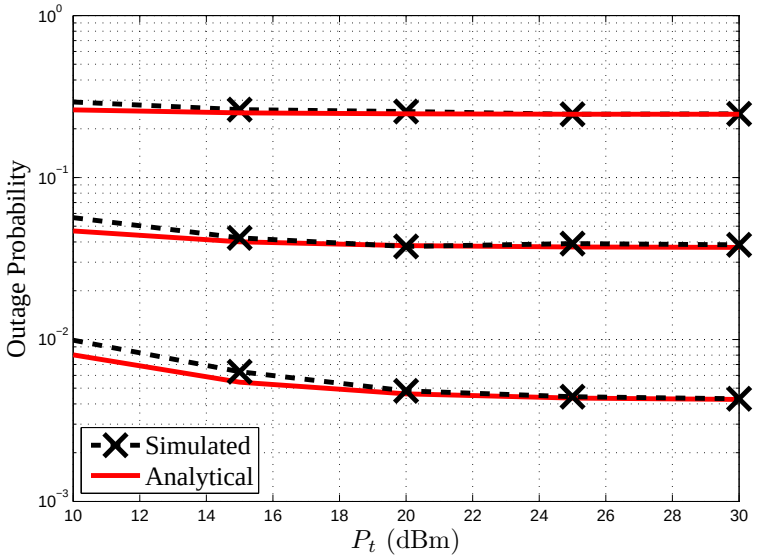

Figure 3.10: Outage probability of $S_1 - D_1$ versus the transmit power. The SNR of the direct link between S_1 and D_1 is fixed to 20dB. The SNR of the link between S_2 and D_1 is fixed to 5dB, 10dB and 15dB, respectively. While the other overheard links and the relaying links are improved gradually by increasing the transmit power.

3.4.1.4 Effects of the Number of RNs

Let us now consider a square-shaped region with an edge-length of 400 meters, where 10 RNs are available. We vary the number of SN-DN pairs and compare the sum outage probability of the proposed relay selection scheme in Section 3.3 to that of a conventional random relay selection scheme, where the RN is chosen randomly. The outage performance was averaged over 100 network instances. Observe in Fig. 3.11 that the proposed relay selection achieves a better outage performance than the benchmark scheme across the entire range of transmit powers. It is also observed that as the number of SN-DN pairs increases, the outage performance degrades.

3.4.2 Comparison with the Spectrum Sharing Scheme of Chapter 2

In Chapter 2, an MUD-SIC-aided scheme is proposed, where multiple SN-RN-DN networks may operate in the same frequency band and hence introduce CCI, while the MUD-SIC detection may be adopted at the RNs and the DN in order to mitigate the CCI. Therefore, the MUD-SIC-aided scheme proposed in Chapter 2 may allow multiple SN-RN-DN networks to share the same spectrum simultaneously. On the other hand, the interference may be resolved by applying the SPM-NC-CC scheme proposed in this chapter, where the spectrum sharing is realised by orthogonal time-division relay-sharing.

Therefore, a comparison between the MUD-SIC based scheme and the relay-sharing based scheme would bring more insights into the design of multi-SN relaying networks. In Fig. 3.12, the outage performance of the spectrum sharing facilitated

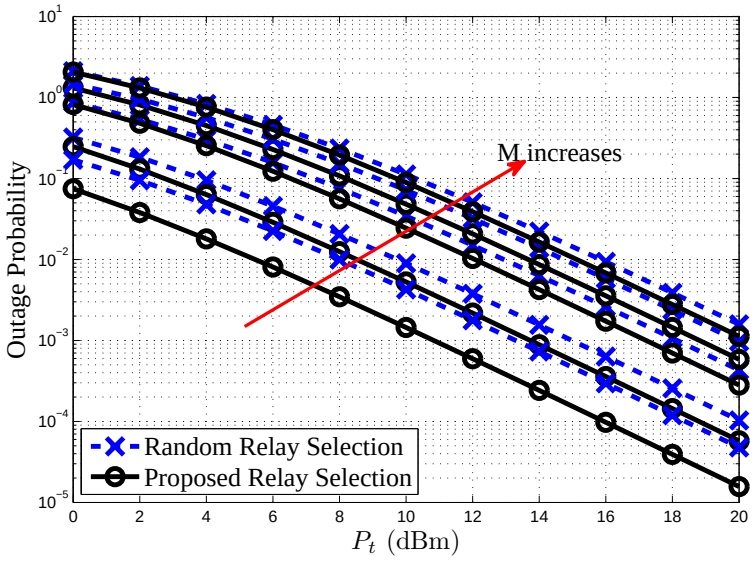

Figure 3.11: Sum outage probability versus the transmit power for different number of SN-DN pairs $M = 1, 2, 4, 6, 8$. The number of available RNs is 10. The outage performance is averaged over 100 network instances.

by MUD-SIC-aided scheme proposed in Chapter 2 is compared with that of the relay sharing based on the SPM-NC-CC scheme used in this chapter.

We consider a symmetric topology comprising M SN-DN pairs, where the average distance between a SN-DN pair is $d = 200$ meters. A RN is placed halfway along the line between any SN-DN pair. The transmission rate of each SN is set to 1.0 bits/s/Hz. It is observed in Fig. 3.12 that for the configuration considered, the MUD-SIC-aided schemes outperform their SPM-NC-CC counterparts of Section 3.1 at arbitrary transmit power, when two SNs share the spectrum. When the number of SNs sharing the spectrum increases, the MUD-SIC-aided scheme would still outperform the SPM-NC-CC counterpart at a low transmit power or a received SNR, because the MUD-SIC-aided scheme does not suffer from any NC noise. However, when the transmit power increases, the outage performance of MUD-SIC-aided scheme would be dominated by the CCI. Meanwhile, the effects of noise become marginal and the SPM-NC-CC scheme becomes capable of achieving a diversity order of $D = 2$. Therefore, at high transmit power, the SPM-NC-CC scheme outperforms the MUD-SIC-aided counterpart of Section 2.2, as shown in Fig. 3.12.

To summarize, we have investigated both the MUD-SIC-aided and the SPM-NC-CC protocols of Section 2.2 and 3.1, which were conceived for allowing multiple SNs to share the same spectrum. Hence the multiplexing loss imposed by half-duplex relaying was compensated. However, neither methods achieve a dominant outage performance advantage in practice, an adaptive scheme may be designed by carefully selecting the scheme having a better outage performance.

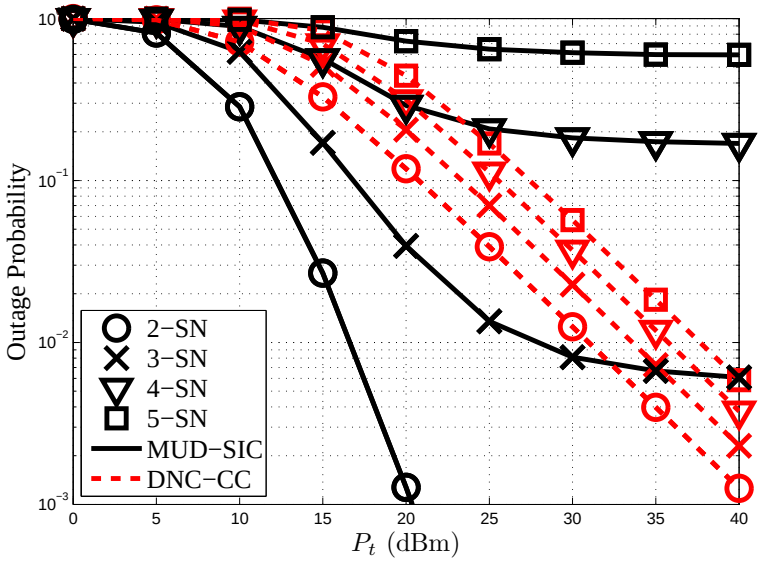

Figure 3.12: OP versus the transmit power for different number of SN-DN pairs $M = 2, 3, 4, 5$. The number of available RNs for each SN is 1. The MUD-SIC-aided schemes adopts spectrum sharing, while the SPM-NC-CC schemes adopts relay sharing. The spectrum efficiency per node is 1.0 bits/sec/Hz.

3.5 Conclusions

In this chapter, we considered a network, where multiple SN-DN pairs share the spectrum by communicating with the aid of a shared RN. The lower bounds of the outage probability were derived, which matches tightly with the simulation results. The results explicitly quantified the detrimental effects of NC noise imposed on SPM-NC-CC schemes. Additionally, we designed a relay selection approach for our SPM-NC-CC scheme using the closed form outage expression derived in Eq. (3.21), which avoids the excessive computational burden required by Monte-Carlo simulations. It is also found that the NC-CC based scheme may not always outperform the conventional MUD-SIC-aided counterparts, which offers valuable insights for the network system designers to select appropriate protocols according the the network topologies and the per-SN transmission rate requirements, as well as the transmit power.

In Table 3.1, we compare the OP of different cooperative schemes. The system configurations are as follows: the average distance between a SN-DN pair is $d = 200$ meters, the e2e transmission rate of each SN-DN pair is $R_{e2e} = 2$bit/sec/Hz. It is shown in Table 3.1 that the SPM-NC-CC schemes as well as the conventional CC scheme outperform the no-cooperation benchmark at $P_{out} = 10^{-2}$ and $P_{out} = 10^{-3}$. However, the OP of SPM-NC-CC schemes is close to that of conventional-CC, when the RN is closer to the SNs, as seen at $x_{sr} = 0.25$ or $x_{sr} = 0.50$ in Table 3.1. However, when the RN is closer to the DN, the OP of the SPM-NC-CC scheme outperforms the conventional-CC counterpart, which experiences a degradation of approximate1.3dB.

Target OP			@10^{-2}			@10^{-3}
RN's position x_{sr}	@0.25	@0.50	@0.75	@0.25	@0.50	@0.75
SPM-NC-CC ($M = 5$)	5.9	5.4	5.5	10.9	10.4	10.5
SPM-NC-CC ($M = 2$)	5.6	5.0	5.2	10.6	10.0	10.2
Conventional-CC ($M = 1$)	5.7	5.4	6.6	10.7	10.4	11.6
No Cooperation			13.8			23.8

Table 3.1: Summary of transmit power P_t in dBm and achievable OP of different schemes.

Therefore, it may be concluded that the SPM-NC-CC schemes may be plausible when the position of the RN is not known or the RN is closer to the DN in order to guarantee the outage performance. It is noted that introducing a number of $M > 2$ SN-DNs in a single SPM-NC-CC group is not recommended in improving the OP. Also, as a higher M imposes higher complexity at the RN and the DN, the conventional CC may be preferred when the RN is close to the SNs.

In both Chapter 2 and this chapter, the spatial diversity gain provided by the RN-DN links was exploited on the second hop for improving the reliability of multi-SN relaying networks. However, there is a further option for providing a spatial diversity gain based on hop-selection. Up to this stage, we have considered time-division multiple access based relaying networks, where the RN receives packets from the SN in one TS and forwards it to the DN in the following TS, whilst relying on a fixed scheduling.

Since in practice, the channel coefficients of the SN-RN hop and the RN-DN hop are independent, a diversity gain may be achieved for improving the outage performance. This may be realised by allowing the RN to dynamically select whether to receive or transmit in each TS, depending on the channel quality of the SN-RN and the RN-DN links. In the next chapter, the spatial diversity gain based on hop-selection will be investigated in the context of multi-SN relaying networks.

Chapter 4

Buffer-Aided Relaying for Multi-User Uplink[1]

In Chapter 2 and 3, the family of classic time-division multiple access (TDMA) based cooperative networks was considered, where the RN receives packets from the SNs during its receive time slot (TS) and forwards it to the DN during the transmit TS for the sake of accommodating the half-duplex nature of conventional transceivers, which indicates that the scheduling of the SN's or the RN's transmission is fixed [11]. However, the attainable performance may be improved if the SN-RN or the RN-DN links are activated to transmit based on their near-instantaneous channel quality (CQ). Recently, buffer-aided relaying (BAR) has received a lot of research attention [87]- [88], demonstrating that it is capable of achieving a higher diversity gain than the traditional relay networks, because the RN is allowed to dynamically opt for either receiving or transmitting in each time slot, depending on the near-instantaneous CQ of the SN-RN and the RN-DN links.

Before reviewing the contributions in the literature, let us start with a simple three-node example in order to highlight the difference between conventional relaying

[1]Part of the work in this chapter has been submitted in the collaborative work: B. Zhang, C. Dong, J. Lei, M. El-Hajjar, L. Yang and L. Hanzo, Buffer Aided Relaying for Multi-user Uplink: Outage Analysis and Power Allocation. 2014

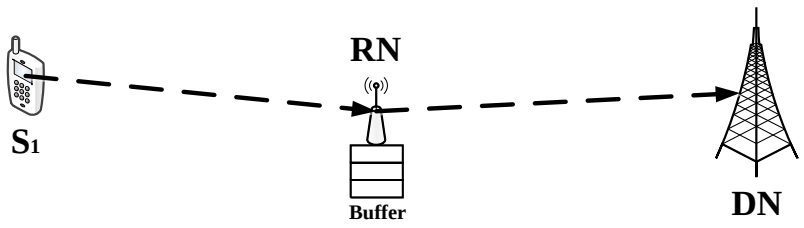

Figure 4.1: System model of a three-node network

	Channel SNR		Conventional Relaying			Buffer-Aided Relaying	
TS Index	SN-RN	RN-DN	b	Activated Channel		b	Activated Channel
1	0.8	0.2	1	S-R (0.8)		1	S-R (0.8)
2	1.2	0.7	0	R-D (0.7)		2	S-R (1.2)
3	1.0	0.8	1	S-R (1.0)		3	S-R (1.0)
4	0.4	1.4	0	R-D (1.4)		2	R-D (1.4)
5	0.8	1.2	1	S-R (0.8)		1	R-D (1.2)
6	0.7	0.3	0	R-D (0.3)		2	S-R (0.7)
.....							

Table 4.1: Example of a three-node network

and BAR. As shown in Fig. 4.1, a SN transmits to a DN with the aid of a RN, which is equipped with a data buffer. In a BAR scheme, the number of packets stored in the RN's buffer is denoted as b. In Table 4.1, the instantaneous channel signal-to-noise-power-ratio (SNR), the number of packets in the buffer b as well as the links activated by both the conventional relaying and the BAR are compared.

As shown in Table 4.1, conventional relaying relies on fixed scheduling, where the SN-RN and RN-DN channels are activated in turn and two TSs would deliver a packet from the SN to RN and from the RN to the DN, respectively. Therefore, the number of packets in the RN's buffer b would be 1 after the SN-RN channel's activation and it would be reduced to 0 after the RN-DN link's activation, and each packet would stay in the RN's buffer for a single TS. By contrast, the BAR facilitates dynamic channel selection, where the channel having a higher channel SNR may be activated during each TS. Therefore, the number of packets in the RN's buffer b may exceed 1. Hence both the channel quality as well as the transmission reliability would be improved compared to the conventional relaying as an explicit benefit of the above-mentioned hop-selection diversity. However, the resultant diversity gain is achieved at the price of a higher packet delay, since some packets may stay in the RN's buffer for more than 1 TS. The associated reliability versus delay tradeoff will be analyzed in Section 4.3.4.

Let us now review the state-of-the-art contributions in the literature in the context of BAR. Assuming a buffer of infinite size at the RN, the authors of [89, 90] demonstrated that a simple two-hop scenario is capable of achieving a diversity order of $D = 2$ in the absence of the direct link, while its multi-hop counterpart attains a diversity order of $D = N$ for the network of $(N - 1)$ intermediate RNs [91–94]. Both the bit error ratio and the outage performance of buffer-aided multi-hop networks relying on a realistic finite-buffer size are analysed in [91,92] for transmissions over Rayleigh channels having identical average signal-to-noise power ratios (SNRs). By contrast in [94] Nakagami-m channels having non-identical average SNRs of the

various hops were analyzed. Then, the corresponding work was extended to adaptive modulation schemes in [95, 96]. The MAC layer protocols of buffer-aided multi-hop networks were proposed in [92, 96], which are also applicable to the regime considered here. Recently, the concept of transmission activation probability space (TAPS) was proposed for a buffer-aided network in [88, 97, 98]. In these contributions, the CQs of all available channels are considered to form a TAPS, which may be partitioned into several regions based on a nonlinear channel space partitioning regime. In each time slot, the near-instantaneous CQ values are mapped to a particular point in the TAPS and the corresponding hop can be activated, unless the CQ is too low. Based on the TAPS concept, the attainable capacity, and the minimum packet-energy-consumption may be obtained. As a further advance, a packet selection scheme was proposed in [99] for the two-hop buffer-aided link relying on AF relaying, where the relay equipped with a buffer is capable of recording the CQ of the source-relay hop and of storing the received packets. In order to satisfy the constraint of equivalent end-to-end SNR, the relay may schedule one of its packets in the buffer for transmission, whilst considering the CQ of both the source-relay hop and of the relay-destination hop. Therefore, by carefully adjusting the packet transmission order of the relay, the outage probability can be reduced by the proposed transmission scheme. Finally, the authors of [100] considered multiple parallel RNs dedicated to a SN in a two-hop scenario, where several buffer-aided relay selection schemes were investigated.

The link activation schemes proposed in the literature consider a single SN, while in this chapter we are interested in a multi-user uplink scenario, where M SNs transmit to a common DN with the aid of a RN. For multi-user cooperative networks, several relay-sharing methods were proposed in [34, 36, 45, 75, 101–104] in order to reduce the multiplexing loss imposed by half-duplex relaying. The basic idea of these contributions is to share a single relay among multiple sources, with the goal of achieving a throughput improvement. However, these relay sharing schemes relied on wireless network coding (NC) [29, 73] at the RNs for the sake of re-encoding multiple SNs' codewords using superposition, while additionally exploiting the direct links between the SNs and the DN in order to cancel the inter-user interference [31, 75, 101, 103, 105]. However, relaying is typically invoked for the sake of improving the uplink's signal quality, when the direct links between the SNs and the DN may be weak [56] and in this scenario, the cooperative-NC based relay sharing schemes perform worse than the conventional cooperative networks [41, 43, 105]. Therefore, we adopt a time-multiplexing cooperative scheme [31, 105], where the RN uses a higher rate for re-encoding the messages received from multiple SNs so that the relaying TS is simultaneously shared among multiple SNs, whilst dispensing with any reliance on the direct links. We allow the system to dynamically activate the highest quality SN-RN and RN-DN hops during each TS. Against this background,

the novel contributions of this chapter are summarized as follows:

1. A hop quality metric (HQM) is designed for the MAC for transmission over the SN-RN hop, which is based on the minimum signal-to-noise power ratio (min-SNR) approximation [105] and supports our novel hop activation regime. We conceive a multi-user buffer-aided-relaying uplink (MU-BR-UL) protocol, which is capable of improving the outage performance of our two-hop system.
2. We analyse the end-to-end (e2e) outage performance of the proposed MU-BR-UL protocol. The lower-bound of the e2e outage probability is found by assuming an infinite buffer size at the RN. Additionally, the closed-form outage performance expressions are derived for a finite buffer size, which is based on the min-SNR approximation and matches closely with the actual outage probability. It is shown that for an infinite buffer size, a diversity order of $D = 2$ may be achieved. By contrast, for a finite buffer, only a diversity order of $D = 1$ is achievable, but nevertheless, a significant outage performance improvement may be attained upon increasing the buffer size. We also analysed the delay of the proposed scheme in terms of its probability mass function (PMF), where as expected, the average delay is shown to increase linearly with the buffer size.
3. Based on the e2e outage probability derived, we formulate a power allocation (PA) problem for the sake of minimizing the e2e outage probability under the constraint of a given total available transmit power. It is shown that compared to the equal-power philosophy, the proposed power allocation scheme is capable of significantly improving the outage performance. For instance, assuming a network of $M = 4$ SNs and a RN equipped with a buffer size of $B = 16$ frames as well as a maximum tolerable OP of $P_{out} = 0.01$, the proposed power allocation regime reduces the required transmit power by 5 dB compared to the equal-power allocation.

The chapter is organised as follows. Our system model and its benchmark system are described in Section 4.1. Then, the proposed MU-BR-UL protocol is detailed in Section 4.2, while both the e2e outage probability and the delay analysis are discussed in Section 4.3. The optimal power allocation regime conceived for minimizing the e2e outage probability is outlined in Section 4.4. Our simulation results are provided in Section 4.5, while our conclusions are offered in Section 4.6.

4.1 System Model and Benchmark System

As shown in Fig. 4.2, we consider a network supporting $(M + 2)$ nodes, where M SNs $\{S_m, 1 \leq m \leq M\}$ transmit their individual information to a common DN with the aid of a single RN. Each node is equipped with a single antenna and operates in a half-duplex mode. We assume a narrow-band Rayleigh block fading channel model, where the fading coefficients remain constant for the duration of a packet

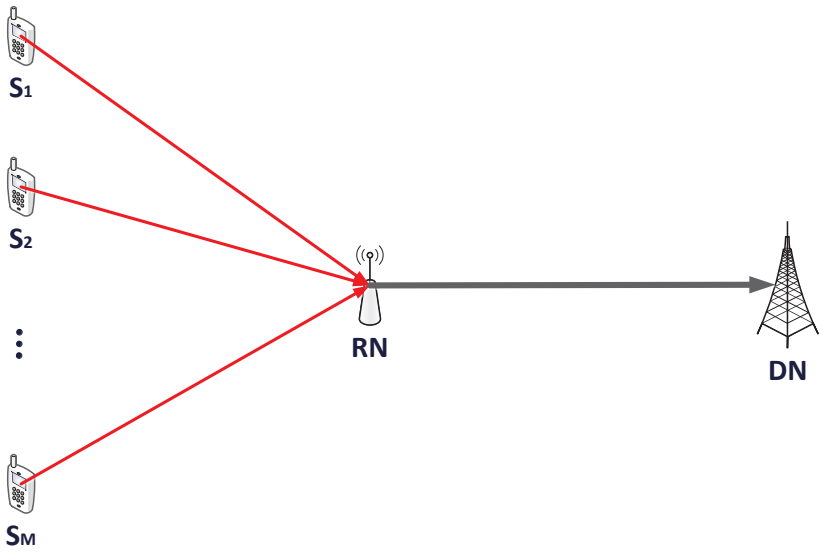

Figure 4.2: System model of the relay-sharing aided multi-user uplink network.

and then they are faded independently from one packet to another both in time and space. The direct links between the SNs and the DN are not considered, since we are interested in the scenario of using relaying for improving the uplink performance of cell-edge users. If the direct link is considered, a diversity order of $D = 2$ may be achieved, but this does not affect the hop activation scheme to be proposed in Section 4.2. The additive noise at the receivers is modeled by independent zero-mean circularly symmetric complex Gaussian random variables.

The receivers are assumed to have perfect channel knowledge and rely on maximum likelihood (ML) detection. The buffer at the RN obeys the first-in-first-out (FIFO) regime, where the frames received first would be transmitted first. Due to the fact that ML detection results in joint detection success or in joint outage events, the packets received from the M SNs are either successfully recovered or corrupted concurrently. Therefore, if the ML detection is successful, all the M detected codewords would be inserted into the RN's buffer, otherwise all the codewords would be discarded. Hence, we consider a buffer storing B M-codeword transmit frames at the RN. We will also appraise the successive interference cancellation (SIC) detector [69, 106] and compare its performance to that of the ML detector with the aid of simulations in Section 4.5.4.

In the conventional two-hop system associated with $B = 1$, the schedule of hop activation obeys a fixed pattern. In the first time slot (TS), all the SNs concurrently transmit their messages at the rate of R, where the RN listens. The SN S_m encodes a bit sequence b_m into a codeword c_m and transmits it to the RN, where the RN jointly detects the codewords received from all the SNs using ML detection. Therefore, the SN-RN hop may be modeled by a MAC and the criterion used for successful decoding

is that of satisfying:

$$\sum_{m\in S} R \leq \log\left(1+\sum_{m\in S}\gamma_{mr}\right), \forall S \subseteq \{S_m, 1\leq m\leq M\}, \tag{4.1}$$

where γ_{mr} represents the instantaneous received SNR of the S_m-RN link. The decoded bit sequences $\{\widetilde{b}_1, \widetilde{b}_2, \ldots, \widetilde{b}_m\}$ would be concatenated and inserted into the buffer as a frame. In the next TS, the RN prepares the frame in its buffer for transmission, re-encodes the messages at the rate of MR and transmits them to the DN, where the criterion to be satisfied for successful decoding is

$$MR \leq \log\left(1+\gamma_{rd}\right), \tag{4.2}$$

with γ_{rd} representing the instantaneous received SNR at the DN.

For the buffer-aided system associated with $B > 1$, the RN either opts for receiving from the SNs or for transmitting to the DN, according to the instantaneous channel quality and to the buffer states in each TS. The proposed hop activation protocol will be described in the following section.

4.2 Buffer-Aided Two-hop Protocol

By introducing a buffer having $B > 1$ at the RN, the proposed MU-BR-UL protocol allows the RN to store a maximum of B frames. In each TS, either the SN-RN hop or the RN-DN hop may be activated for transmission, depending both on their channel qualities as well as on the state of the buffer. In a certain TS, if the SN-RN hop is activated and all the M codewords transmitted over the SN-RN hop are recovered at the RN, then they are entered into the buffer as a frame. If the RN-DN hop is activated for transmission, the specific frame at the top of the buffer is removed from the buffer and transmitted to the DN.

The criterion used for activating a hop in each TS should satisfy the following rules:

1. If the RN's buffer is empty, the SN-RN hop is activated. This is natural, because the RN has no frames to send over the RN-DN hop.
2. If the RN's buffer is full, the RN-DN hop is activated, otherwise the RN's buffer overflows.
3. The SN-RN and RN-DN hop should be activated with equal probability of 50%.

The first two rules are plausible, hence we would focus our attention on justifying the third one. For example, when the number of users is $M = 1$, we always activate the specific hop having the highest instantaneous channel SNR in order to fully exploit the selective diversity potential of the SN-RN and the RN-DN hops. However, assuming

that the average SNR of the SN-RN hop is higher than that of the RN-DN hop, the SN-RN hop would be activated more frequently and therefore the buffer at the RN would overflow. Hence, in order to avoid buffer-overflow, we should activate the SN-RN and RN-DN hop with an equal probability of 50%, relying on an appropriate **hop quality metric (HQM)**, where a hop with a higher HQM would be activated. Therefore, the hop quality metric design is crucial for our system.

For the special case of $M = 1$ and for an unequal channel quality of different hops, the hop activation problem has been addressed in [94], where the cumulative distribution function (CDF) value of the fading is used as our HQM. However, for the scenario of $M > 1$, the hop activation strategy of [94] cannot be used in the multi-user uplink model, because the SN-RN hop is a MAC channel associated with a vector of M instantaneous channel SNR values, while the RN-DN hop is a point-to-point (P2P) channel having a single instantaneous channel SNR value. Hence we are unable to directly estimate and compare the CDF value. Hence, we design a specific HQM for our multiple-user uplink system, where the SN-RN and RN-DN hops are guaranteed to be activated with an equal probability of 50%.

Firstly, let us investigate the error probabilities of the SN-RN hop. If any of the inequalities in Eq. (4.1) is not satisfied, the transmissions over the SN-RN hop are bound to be corrupted. Hence, when the minimum SNR of the M channels spanning from the SNs to the RN, which is defined as $\gamma_{sr}^{min} = \min_{m \in S} \gamma_{mr}$, becomes lower than the threshold of $\gamma_{th}^{sr} = 2^R - 1$ that has to be exceeded for successful decoding, the SN-RN hop becomes erroneous. Therefore, we model the outage performance of the M-user MAC in the context of the SN-RN hop based on the performance of the specific SN-RN link having the minimum SNR γ_{sr}^{min}, *which facilitates a tight approximation of the outage probability.*

In Fig. 4.3, we compare the outage performance of the M-user MAC channel employing ML detection to that of a single link having the minimum SNR γ_{sr}^{min} of the M-user system. As shown in Fig. 4.3, *the outage performance of the two systems characterized by simulation matches the approximated outage probability using our minimum-SNR approach for both symmetric and asymmetric topologies.* In the symmetric topology, the average channel quality spanning from each SN to the RN is identical, while in the asymmetric topology the average channel quality is different, where the SNRs of the $M = 4$ links are 1, 2, 4 and 8 times higher than that in the symmetric topology, respectively. It is shown in Fig. 4.3 that the exact OP of the M-user MAC channel and the predicted OP using the P2P channel associated with the minimum SNR are identical for both topologies. Therefore, γ_{sr}^{min} may be used for quantifying the quality of the SN-RN hop, where γ_{sr}^{min} is a scalar random variable, which may be readily compared to the instantaneous RN-DN channel SNR. Hence, we define the HQM of the SN-RN link as the specific channel-SNR CDF ordinate

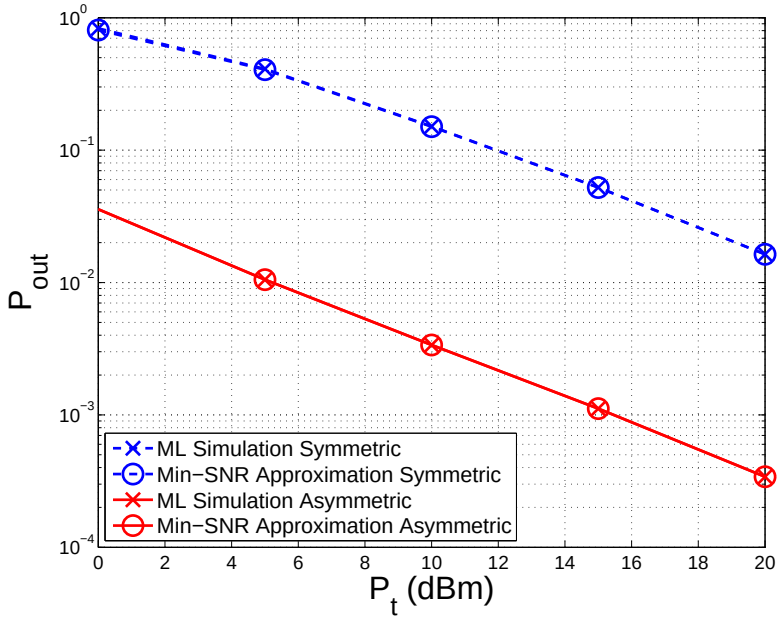

Figure 4.3: The approximation accuracy of the outage probability, when using the minimum SNR of the M SN-RN links as the Hop Quality Metric for $M = 4$, $R = 0.5bps/Hz$. The distance between the SNs and the RN is $d = 100$ meters and the path-loss exponent is $\beta = 3$.

value $F_{SR}\left(\gamma_{sr}^{min}\right)$, which may be formulated as follows:

$$\begin{aligned} F_{SR}\left(\gamma\right) &= \Pr\left\{\min_{m\in S}\gamma_{mr} \leq \gamma_{sr}^{min}\right\} \\ &= 1 - \prod_{m\in S}\Pr\left\{\gamma_{mr} > \gamma_{sr}^{min}\right\} \\ &= 1 - \exp\left[-\gamma_{sr}^{min}/\left(\sum_{m\in S}\bar{\gamma}_{mr}^{-1}\right)^{-1}\right], \end{aligned} \tag{4.3}$$

where $\bar{\gamma}_{mr}$ is the average SNR of the channel between the SN S_m and the RN. For brevity, we use the shorthand of $\bar{\gamma}_{sr}^{min} = \left(\sum_{m\in S}\bar{\gamma}_{mr}^{-1}\right)^{-1}$. Furthermore, we define the HQM of the RN-DN link as the CDF ordinate value of

$$F_{RD}\left(\gamma_{rd}\right) = 1 - \exp\left(-\gamma_{rd}/\bar{\gamma}_{rd}\right). \tag{4.4}$$

In order to satisfy the third rule by activating both the SN-RN and the RN-DN hop with an equal probability [94], when the buffer is neither empty nor full, the SN-RN hop is activated for transmission, provided that the CDF ordinate value of the SN-RN hop is higher than that of the RN-DN hop, which is equivalent to the following condition:$\gamma_{sr}^{min}/\bar{\gamma}_{sr}^{min} > \gamma_{rd}/\bar{\gamma}_{rd}$. By contrast, when $\gamma_{sr}^{min}/\bar{\gamma}_{sr}^{min} \leq \gamma_{rd}/\bar{\gamma}_{rd}$ is satisfied and the buffer is neither full nor empty, then the RN-DN hop is activated

for transmission.

Based on the above hop activation strategy, we design our MU-BR-UL protocol in two stages: the hop activation stage and the data transmission stage. In the hop activation stage, the SNs and DN broadcast pilots for channel estimation in orthogonal TSs, while the RN estimates the instantaneous channel quality over both the SN-RN and the RN-DN channels[2]. Then, the RN calculates the HQM for both the SN-RN and the RN-DN hop according to Eq. (4.3) and Eq. (4.4), where the hop having a higher HQM would be activated for transmission. Finally, the RN would either transmit a clear-to-send (CTS) signal, if the RN-DN hop is selected or a request-to-send (RTS) signal if the SN-RN hop is selected and then the data transmission will be initiated. It is assumed that the duration of the CTS and RTS signal is negligible, when compared to the length of a TS in the data transmission.

The design of the medium access control layer protocol is discussed here. In our previous work [92,96], the medium access control protocol for the buffer-aided multi-hop networks is proposed and in this chapter, we consider the two-hop case. In the network considered in Fig. 4.2, the network has a single RN, which can serve as a central control unit. Based on the hop quality metric and the hop activation strategy proposed in this chapter, the best hop may be activated as follows. In the first M symbol durations, each SN broadcasts the channel-quality estimation pilot over time-orthogonal channels, whereas in the $(M+1)-$th symbol duration, the DN broadcasts the same pilot. The RN may estimate the channel SNR of each the SN–RN and the RN–DN channels and it may choose the hop having a higher HQM. Then, during the $(M+2)-$th symbol duration, the RN transmits an request-to-send signal if the first hop is chosen, whereas it sends a clear-to-send signal if it selects the second hop. Data transmission starts from the $(M+3)-$th symbol duration. Therefore, the selection process requires $(M+2)$ symbol durations. Throughout this chapter and in the following analysis, it is assumed that the channel quality estimation is perfect.

4.3 Performance Analysis

The outage event is defined as the event, when any of the codewords received from the SNs is not correctly recovered at the DN. The e2e outage probability of the two-hop system may be expressed as

$$P_{out} = 1 - (1 - P_{e,SR})(1 - P_{e,RD}), \tag{4.5}$$

where P_{out} represents the e2e outage probability of the outage system, while $P_{e,SR}$ and $P_{e,RD}$ stand for the error probability of the SN-RN and the RN-DN hop, respectively.

[2]Note that the duration of transmitting pilots can be considered negligible compared to the the data transmission duration in the data transmission stage

4.3.1 Outage Probability Lower-bound

We first assume that the buffer at the RN has an infinite size and that there are always packets in the buffer ready to be transmitted. In other words, the buffer is assumed to be neither full nor empty. Therefore, the system is always at liberty to choose between the SN-RN and the RN-DN hops to be activated and hence it benefits from a selective diversity gain. In practice, the buffer size is finite and the buffer may be empty, in which case no selective diversity gain is achieved. Therefore, by relying on the assumption mentioned before, we may derive the lower-bound $P_{out,L}$ of the e2e OP, which may be formulated as follows:

$$P_{out,L} = 1 - \left(1 - P_{e,SR}^{select}\right)\left(1 - P_{e,RD}^{select}\right), \tag{4.6}$$

where $P_{e,SR}^{select}$ and $P_{e,RD}^{select}$ stand for the error probability lower-bound, when benefiting from a hop selection diversity by appropriately activating the SN-RN and the RN-DN hop[3].

According to our analysis provided in Section 4.2, the MAC channel of the SN-RN hop may be modeled by a P2P channel having the minimum received SNR γ_{sr}^{min} amongst all the channels spanning from the SNs to the RN. According to Eq. (4.3), we may also arrive at the probability density function (PDF) of γ_{min} in the form of:

$$f_{\gamma_{sr}^{min}}(\gamma) = \frac{dF_{\gamma_{sr}^{min}}(\gamma)}{d\gamma} = \frac{1}{\bar{\gamma}_{sr}^{min}} \exp\left(-\frac{\gamma}{\bar{\gamma}_{sr}^{min}}\right). \tag{4.7}$$

Therefore, we may formulate $P_{e,SR}^{select}$ using the minimum-SNR approximation as:

$$\begin{aligned} P_{e,SR}^{select} &\approx \Pr\left\{\gamma_{sr}^{min} < \gamma_{th}^{sr} \middle| \frac{\gamma_{sr}^{min}}{\bar{\gamma}_{sr}^{min}} > \frac{\gamma_{rd}}{\bar{\gamma}_{rd}}\right\} \Big/ \Pr\left\{\frac{\gamma_{sr}^{min}}{\bar{\gamma}_{sr}^{min}} > \frac{\gamma_{rd}}{\bar{\gamma}_{rd}}\right\} \\ &= 2\Pr\left\{\gamma_{sr}^{min} < \gamma_{th}^{sr}, \gamma_{sr}^{min} > \gamma_{rd}\frac{\bar{\gamma}_{sr}^{min}}{\bar{\gamma}_{rd}}\right\} \\ &= 2\int_0^{\gamma_{th}^{sr}} \left(\int_0^{x\frac{\bar{\gamma}_{sr}^{min}}{\bar{\gamma}_{rd}}} f_{\gamma_{rd}}(y)\, dy\right) f_{\gamma_{sr}^{min}}(x)\, dx \\ &= 1 + \exp\left(-2\frac{\gamma_{th}^{sr}}{\bar{\gamma}_{sr}^{min}}\right) - 2\exp\left(-\frac{\gamma_{th}^{sr}}{\bar{\gamma}_{sr}^{min}}\right), \end{aligned} \tag{4.8}$$

where we exploited the relation of $\Pr\left\{\frac{\gamma_{sr}^{min}}{\bar{\gamma}_{sr}^{min}} > \frac{\gamma_{rd}}{\bar{\gamma}_{rd}}\right\} = \Pr\left\{\frac{\gamma_{sr}^{min}}{\bar{\gamma}_{sr}^{min}} \leq \frac{\gamma_{rd}}{\bar{\gamma}_{rd}}\right\} = 0.5$.

[3]The error performance of the SN-RN and the RN-DN hop achieves the hop activation diversity, when the buffer is neither full nor empty.

Similarly, we may arrive at

$$P_{e,RD}^{select} = \Pr\left\{\gamma_{rd} < \gamma_{th}^{rd} \middle| \frac{\gamma_{sr}^{min}}{\bar{\gamma}_{sr}^{min}} \leqslant \frac{\gamma_{rd}}{\bar{\gamma}_{rd}}\right\} \Big/ \Pr\left\{\frac{\gamma_{sr}^{min}}{\bar{\gamma}_{sr}^{min}} \leqslant \frac{\gamma_{rd}}{\bar{\gamma}_{rd}}\right\}$$
$$= 1 + \exp\left(-2\frac{\gamma_{th}^{rd}}{\bar{\gamma}_{rd}}\right) - 2\exp\left(-\frac{\gamma_{th}^{rd}}{\bar{\gamma}_{rd}}\right), \tag{4.9}$$

where $\gamma_{th}^{rd} = 2^{MR} - 1$ is the threshold that has to be exceeded for the sake of achieving successful decoding on the RN-DN hop. By substituting Eq. (4.8) and Eq. (4.9) into Eq. (4.6), we arrive at the OP lower-bound for our two-hop system.

4.3.2 Exact Outage Probability

Let us now remove the assumption of having a buffer, which is neither full nor empty as stipulated in the previous section and take into account the scenarios, when the buffer is either empty or full. In these cases, according to the hop activation rules, we have to activate the SN-RN or the RN-DN hops without the benefit of choice and therefore no selective diversity gain is achieved. We define the buffer size as B frames, while b is the number of frames stored in the buffer.

According to our hop activation strategy, we can derive the approximate error probability of $P_{e,SR}$ using the min-SNR approximation and the actual $P_{e,RD}$ as follows:

$$P_{e,SR} \approx \frac{\Pr\{b=0\} P_{e,SR}^{b=0} + \frac{\Pr\{0<b<B\}}{2} P_{e,SR}^{select}}{\Pr\{b=0\} + \frac{\Pr\{0<b<B\}}{2}}$$
$$P_{e,RD} = \frac{\Pr\{b=B\} P_{e,RD}^{b=B} + \frac{\Pr\{0<b<B\}}{2} P_{e,RD}^{select}}{\Pr\{b=B\} + \frac{\Pr\{0<b<B\}}{2}}, \tag{4.10}$$

where $P_{e,SR}^{b=0}$ stands for the error probability of the SN-RN hop, when the buffer is empty, i.e. $b = 0$ and this can be expressed as:

$$P_{e,SR}^{b=0} = 1 - \exp\left(-\frac{\gamma_{th}^{sr}}{\bar{\gamma}_{sr}^{min}}\right). \tag{4.11}$$

On the other hand, $P_{e,RD}^{b=B}$ stands for the error probability of the RN-DN hop, when the buffer is full, i.e. $b = B$ and we can express $P_{e,RD}^{b=B}$ as:

$$P_{e,RD}^{b=B} = 1 - \exp\left(-\frac{\gamma_{th}^{rd}}{\bar{\gamma}_{rd}}\right). \tag{4.12}$$

In order to derive $P_{e,SR}$ and $P_{e,RD}$, we have to derive the probability of $\Pr\{b=0\}$ as well as of $\Pr\{b=B\}$ and hence we adopt the state-transition analytical tools proposed in [92]. We first define the state V_b as the specific state, in which the

number of frames stored in the buffer is b, $0 \leq b \leq B$. Then we arrive at the state transition matrix T, where the specific element T_{ij} in the $i-$th row and the $j-$th column stands for the transition probability from the state V_i to V_j. For example, the transition matrix T of the $B = 3$ scenario is:

$$T = \begin{bmatrix} 0 & 1 & 0 & 0 \\ 0.5 & 0 & 0.5 & 0 \\ 0 & 0.5 & 0 & 0.5 \\ 0 & 0 & 1 & 0 \end{bmatrix}. \tag{4.13}$$

When the buffer size B increases, the dimension of T is as large as $(B+1) \times (B+1)$, but it is easy to construct:

1. For the 1-st row, the current state V_0 stands for the empty buffer. It evolves to state V_1 with a probability of 1.
2. For the $(B+1)-$th row, the current state V_B stands for the full buffer. It has to evolve to V_{B-1} with a probability of 1, because the RN-DN hop is activated and the first frame of the buffer would be removed and sent to the DN.
3. For the rest of the rows, the current state V_b represents neither empty nor full buffer. When the RN-DN hop is selected, V_b traverses to V_{b-1} with a probability of 0.5. When the SN-RN hop is activated, V_b traverses to V_{b+1} with a probability of 0.5.

When the buffer state is steady, the state probabilities π may be computed using [92]

$$\pi = T^T \pi, \tag{4.14}$$

where $\pi = \begin{bmatrix} \pi_0 & \pi_1 & ... & \pi_B \end{bmatrix}^T$ and $\pi_i = \Pr\{b = i\}$ is the steady state probability that the buffer is at state V_i. Therefore, we may derive the probability of $\pi_0 = \Pr\{b = 0\} = 1/2B$ and $\pi_B = \Pr\{b = B\} = 1/2B$. With the aid of Eq. (4.11) and Eq. (4.12), we can rewrite the closed-form error probability of $P_{e,SR}$ using minimum-SNR approximation as well as the $P_{e,RD}$ formulated in Eq. (4.10) as follows:

$$\begin{aligned} P_{e,SR} &\approx 1 - \frac{2B-1}{B} \exp\left(-\frac{\gamma_{th}^{sr}}{\bar{\gamma}_{sr}^{min}}\right) + \frac{B-1}{B} \exp\left(-\frac{2\gamma_{th}^{sr}}{\bar{\gamma}_{sr}^{min}}\right) \\ P_{e,RD} &= 1 - \frac{2B-1}{B} \exp\left(-\frac{\gamma_{th}^{rd}}{\bar{\gamma}_{rd}}\right) + \frac{B-1}{B} \exp\left(-\frac{2\gamma_{th}^{rd}}{\bar{\gamma}_{rd}}\right), \end{aligned} \tag{4.15}$$

which can be substituted into Eq. (4.5) in order to arrive at the exact OP for an arbitrary buffer size B as follows:

$$P_{out} \approx 1 - \left[\frac{2B-1}{B}\exp\left(-\frac{\gamma_{th}^{sr}}{\bar{\gamma}_{sr}^{min}}\right) - \frac{B-1}{B}\exp\left(-\frac{2\gamma_{th}^{sr}}{\bar{\gamma}_{sr}^{min}}\right)\right] \left[\frac{2B-1}{B}\exp\left(-\frac{\gamma_{th}^{rd}}{\bar{\gamma}_{rd}}\right) - \frac{B-1}{B}\exp\left(-\frac{2\gamma_{th}^{rd}}{\bar{\gamma}_{rd}}\right)\right]. \quad (4.16)$$

4.3.3 Diversity Analysis

The expression of the exact OP in Eq. (4.16) is somewhat complex, while further insights may be offered by its high-SNR approximations. Firstly, using the Taylor series expansion, we may formulate the per-hop exact error probability of $P_{e,SR}$ and $P_{e,RD}$ as follows:

$$\begin{aligned} P_{e,SR} &\approx \frac{1}{B}\frac{\gamma_{th}^{sr}}{\bar{\gamma}_{sr}^{min}} + \frac{2B-3}{2B}\left(\frac{\gamma_{th}^{sr}}{\bar{\gamma}_{sr}^{min}}\right)^2 + O\left(\bar{\gamma}^{-2}\right) \\ &= \frac{1}{B}\frac{\gamma_{th}^{sr}}{\bar{\gamma}_{sr}^{min}} + O\left(\bar{\gamma}^{-1}\right) \quad (4.17) \\ P_{e,RD} &= \frac{1}{B}\frac{\gamma_{th}^{rd}}{\bar{\gamma}_{rd}} + \frac{2B-3}{2B}\left(\frac{\gamma_{th}^{rd}}{\bar{\gamma}_{rd}}\right)^2 + O\left(\bar{\gamma}^{-2}\right) \\ &= \frac{1}{B}\frac{\gamma_{th}^{rd}}{\bar{\gamma}_{rd}} + O\left(\bar{\gamma}^{-1}\right), \quad (4.18) \end{aligned}$$

where $O\left(\bar{\gamma}^{-k}\right)$ denotes the components associated with a diversity order higher than k. For a finite buffer size of B, the error probability is dominated by the first terms in Eq. (4.17) and Eq. (4.18), since they are associated with a diversity order of $D = 1$, showing that the buffer-aided system fails to achieve a diversity gain at high SNRs. However, compared to the traditional scheme associated with $B = 1$, the OP of the proposed protocol at high SNRs may be reduced by a factor B as seen below:

$$\begin{aligned} P_{out} &= P_{e,SR} + P_{e,RD} - P_{e,SR}P_{e,RD} \\ &= \frac{1}{B}\left(\frac{\gamma_{th}^{sr}}{\bar{\gamma}_{sr}^{min}} + \frac{\gamma_{th}^{rd}}{\bar{\gamma}_{rd}}\right) + O\left(\bar{\gamma}^{-1}\right). \quad (4.19) \end{aligned}$$

Therefore, as the buffer size B increases, the outage performance improves by a factor of B. In the extreme case of $B = \infty$, the OP would no longer be dominated by the components associated with the diversity order of $D = 1$ at high SNRs, where a diversity order of $D = 2$ may be achieved as the lower-bound, which is given by:

$$P_{out,L} = \left(\frac{\gamma_{th}^{sr}}{\bar{\gamma}_{sr}^{min}}\right)^2 + \left(\frac{\gamma_{th}^{rd}}{\bar{\gamma}_{rd}}\right)^2 + O\left(\bar{\gamma}^{-2}\right). \quad (4.20)$$

4.3.4 End-to-end Transmission Delay

In conventional two-hop systems, the frame received by the RN may be readily retransmitted immediately in the following TS of the same frame, which results in a constant delay of 2 TSs. The outage performance improvement of the proposed BAR system arises from the selective diversity gain achieved by activating the better of the SN-RN hop or the RN-DN hop, relying on the RN's ability to store the frames for a certain number of TSs, before retransmitting them to the DN.

For the buffer-aided two-hop system, the minimum delay for a frame is 2 TSs and the maximum delay for a frame is $2B$ TS. The minimum delay corresponds to the scenario, when the frame is received by the RN in a TS and then immediately transmitted to the DN in the following TS. On the other hand, the maximum delay of $2B$ TSs is related to the specific case, when a frame X is received by the RN in TS 1 and hence it is inserted at the bottom of the buffer. Then it waits for $(B-1)$ TSs for all the previous received frames stored already in the buffer to be transmitted, followed by another $(B-1)$ TSs for $(B-1)$ newly received frames to be inserted in the buffer, until the frame X reaches the top of the full buffer. Then, it is transmitted to the DN using another single TS.

Even though a certain frame may experience a longer delay than that in the conventional two-hop system, the overall delay for a block of M frames is $2M$, which is identical to that in the conventional system. This is because in a certain time slot, a frame is moving forward by one hop, either on the SN-RN or the RN-DN hop.

Let us now consider the PMF of the delay for characterizing the delay distribution of the frames, which are successfully delivered to the DN. We define the delay PMF as $P_{del} = \begin{bmatrix} p_2 & p_3 & \dots & p_{2B} \end{bmatrix}$, where p_k stands for the probability that a frame is received at the DN at $TS = k$. We first assume that the system is in its steady state at $TS = 0$ and therefore the probability of the current buffer state is characterized by $\pi = \begin{bmatrix} \pi_0 & \pi_1 & \dots & \pi_B \end{bmatrix}^T$ as in Eq. (4.14). Then we assume that a hypothetical *test frame* of M packets is transmitted from the SNs to the RN. We define a position-state matrix W of size $(B+1)\times(B+1)$, where the specific element in the i-th row and j-th column is the probability that the *test frame* is at the $(i-1)$-th position in the buffer and the buffer is at the state of V_{j-1}, while the element in the 1-st row indicates the probability that the *test frame* has left the buffer and it is being transmitted to the DN. For brevity, we define the state $E_{i,j}$, $i > 1$ and $j > 1$, as the specific state that the test frame is at the $(i-1)$-th position in buffer and the buffer state is V_{j-1}. In other words, $W_{i,j}(k)$ corresponds to the probability of the system being in state $E_{i,j}$ at $TS = k$.

Since we assume that the buffer is in its steady state before the test frame arrives, we can initialize the matrix $W(1)$ at $TS = 1$ by setting its i-th diagonal elements to $W_{i,i}(1) = \pi_{i-1} T_{i-1,i}$, while the remaining elements are set to 0. Furthermore, we

have to normalize $W(1)$ to ensure that the sum of the elements in $W(1)$, namely the sum of the probabilities of all pairs equals to 1.

Then, in the next time slot of $TS = k$ associated with $k > 1$, we initialize $W(k)$ as a zero-matrix. For each state $E_{i,j}$ associated with $i > 1$ and $j > 1$, the following four events may be encountered and the corresponding elements in $W(k)$ have to be updated:

1. If the SN-RN hop is activated and a new frame is inserted into the buffer, then the test frame stays at its current position and the buffer state changes from V_{j-1} to V_j. Then we have $W_{i,j+1}(k) = W_{i,j+1}(k) + T_{j,j+1}W_{i,j}(k-1)$.
2. If the SN-RN hop is activated, but the SN-RN hop is in error, then the test frame stays at its current position and the buffer state stays at V_{j-1}. Then we have $W_{i,j}(k) = W_{i,j}(k) + T_{j,j}W_{i,j}(k-1)$.
3. If the RN-DN hop is activated and the current frame at the top of the buffer is transmitted to the DN, then the test frame moves up, or it is removed from the buffer, and hence the buffer state changes from V_{j-1} to V_{j-2}. Then we have $W_{i,j-1}(k) = W_{i,j-1}(k) + T_{j,j-1}W_{i,j}(k-1)$.
4. Finally, the 1-st row of $W(k)$ represents the probabilities that the test frame has left the buffer and was sent to the DN. By adding these probabilities together, we arrive at $p_k = \sum_{j=1}^{B+1} W_{1,j}(k)$. Then, the elements of the $1-$st row of $W(k)$ are set to zero.

By iteratively carrying out these four steps until the maximum delay of $2B$ is achieved, we arrive at the delay PMF for the two-hop system. The average frame delay $\bar{d}$ can then be expressed as

$$\bar{d} = \sum_{k=1}^{2B} p_k k. \tag{4.21}$$

Alternatively, according to Little's law [107], the average time duration that a frame is stored in the buffer is given by

$$\bar{d} = \bar{b}/A, \tag{4.22}$$

where $A = 0.5$ is the average arrival rate experienced in terms of frames per TS, while $\bar{b}$ is the average queue length, which can be expressed as

$$\bar{b} = \sum_{i=0}^{B} i \Pr\{b = i\}. \tag{4.23}$$

Upon solving Eq. (4.14), we arrive at $\Pr\{b = B\} = \Pr\{b = 0\} = 1/2B$ and $\Pr\{b = i\} = 1/B, \forall i \in [1, B-1]$. By substituting these probabilities into Eq. (4.23), we arrive at $\bar{b} = B/2$ and the average time duration that a frame is stored in the buffer therefore

becomes B TSs. While 1 TS is required for transmitting the frame from the RN to the DN, the average frame delay becomes $(B+1)$ TSs, indicating that the average frame delay increases linearly with the buffer size B.

As derived in Section 4.3.2, when the buffer size B increases, the e2e outage probability decreases by a factor of B. Therefore, the outage-versus-delay trade-off should be considered in a practical design. In the next section, we aim for improving the e2e outage probability by finding the optimal power allocation among the SNs and the RN. By fixing the buffer size, the optimal power allocation improves the e2e outage performance without increasing the delay. On the other hand, the optimal power allocation may be capable of reducing the delay, while maintaining the same e2e outage performance, as an equal-power allocation scheme.

4.4 Optimal Power Allocation

In this section, we design a PA algorithm for minimizing the e2e outage probability of the proposed BAR system subject to the constraint of a total power budget given by $P_A = (M+1)P_t$, where P_t is the average power assigned to a transmit node among the SNs and the RN. The maximum power per transmit node is given by $P_{max} = KP_t$ and K satisfies $1 \leq K \leq (M+1)$. The problem is formulated as the following maximization problem:

$$\begin{aligned} \max \quad & 1 - P_{out} \\ s.t. \quad & \sum_{m=1}^{M} P_m + P_r = P_A \\ & P_m \leq P_{max}, \quad m = 1, \ldots, M \\ & P_r \leq P_{max}, \end{aligned} \tag{4.24}$$

where $P_1, P_2, \ldots, P_M$ denotes the transmitted power of the SNs, while P_r represents the transmitted power of the RN. The average SNR of the link between node i and j is $\bar{\gamma}_{ij} = G_{ij}P_i$, where $G_{ij} = (N_0 \times d_{sd}^{\beta})^{-1}$ captures the effect of both the pathloss and of the noise power.

Here, we adopt the Lagrange multiplier based maximization method by ignoring the constraints of the maximum power per transmit node [108], where the Lagrange function can be expressed as

$$L = (1 - P_{out}) + \lambda \left(\sum_{m=1}^{M} P_m + P_r - P_A \right). \tag{4.25}$$

By substituting the exact formulation of P_o from Eq. (4.16) into Eq. (4.25) and setting the partial derivative of L to 0 with respect to P_m and P_r, the optimal power

allocation can be obtained as:

$$\begin{cases} P_r^* & = P_A \frac{K(P_s^*,P_r^*)G_{rd}^{-1/2}}{\sum_{m=1}^{M} G_{mr}^{-1/2}+K(P_s^*,P_r^*)G_{rd}^{-1/2}} \\ P_i^* & = (P_A - P_r^*)\frac{G_{ir}^{-1/2}}{\sum_{m=1}^{M} G_{mr}^{-1/2}}, \quad i = 1,\ldots,M \end{cases}, \tag{4.26}$$

where $K(P_s, P_r)$ is defined as

$$K(P_s, P_r) = \sqrt{\frac{(2B-1)\exp\left(-\frac{\gamma_{th}^{sr}}{\bar{\gamma}_{sr}^{min}}\right) - 2(B-1)\exp\left(-\frac{2\gamma_{th}^{sr}}{\bar{\gamma}_{sr}^{min}}\right)}{(2B-1)\exp\left(-\frac{\gamma_{th}^{rd}}{\bar{\gamma}_{rd}}\right) - 2(B-1)\exp\left(-\frac{2\gamma_{th}^{rd}}{\bar{\gamma}_{rd}}\right)}\frac{\gamma_{th}^{sr}}{\gamma_{th}^{rd}}}. \tag{4.27}$$

The solution in Eq. (4.27) is not in closed-form. However, it may be solved by the successive approximation method using the iteration of $\left[P_1^{k+1}, \ldots P_M^{k+1}, P_r^{k+1}\right] = f\left(\left[P_1^k, \ldots P_M^k, P_r^k\right]\right)$, where $f(\cdot)$ is defined by the right hand side of Eq. (4.27) and the initial solution in iteration $k = 1$ is assumed to be a uniform allocation of $P_r = P_1 = \ldots = P_M = P_t$. If the solution of Eq. (4.27) violates the constraints of the maximum affordable power per node, clipping is applied by assigning the maximum power P_{max} to each node in the set N_V comprising the violating nodes. Then we re-optimize the modified problem by changing the first constraint in Eq. (4.24) as $\sum_{n \notin N_V} P_n = P_A - |N_V| P_{max}$.

4.5 Simulation Results

In this section, we evaluate the achievable performance of the proposed buffer-aided two-hop system in terms of the associated e2e outage probability and transmission delay. We consider the impact of different buffer sizes, user numbers and relay positions. The noise power is set to $N_0 = -80$ dBm, while the channel's pathloss exponent to $\beta = 3$ for our simulations. Note that in this section, the theoretical e2e outage probability is evaluated from the formulas derived in Section 4.3. The theoretical transmission delay is obtained by the algorithms detailed in Section 4.3.4. In all the results provided, the curves represent the theoretical results, while the markers denote our simulation results.

4.5.1 Impact of the Buffer Size

The impact of the buffer size B on the e2e outage performance of the proposed two-hop system is illustrated in Fig. 4.4. In the examples shown in Fig. 4.4, we assume the distance between each SN and the RN to be $d_{sr} = 80$ meters, while the distance between the RN and the DN to be $d_{rd} = 120$ meters. The number of SNs is $M = 4$ and the transmission rate of each SN is $R = 1 bps/Hz$.

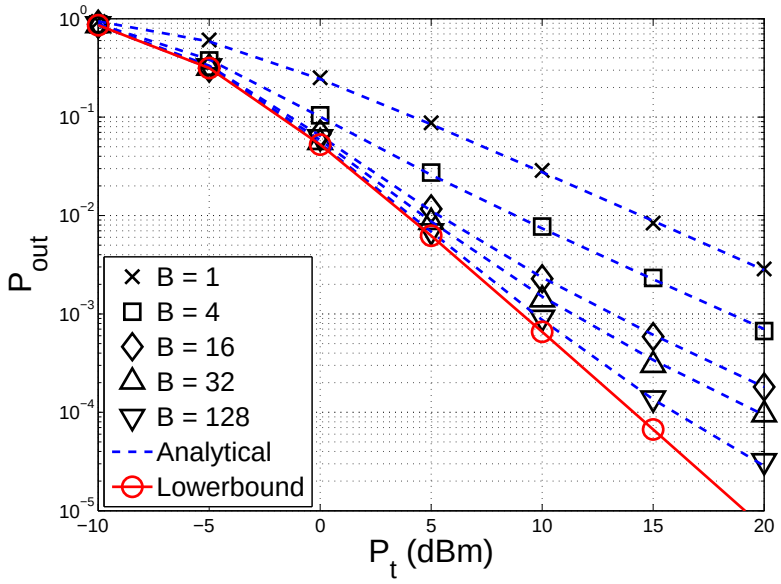

Figure 4.4: Outage performance of the proposed system for different buffer sizes.

Fig. 4.4 illustrates that the e2e outage performance improves gradually as the buffer size increases and approaches the lower-bound of Eq. (4.6), which assumes having an infinite buffer size and that the RN always has frames to send. It is shown that the simulation results match the analytical expressions derived in Eq. (4.16), while an increased gap is observed between the exact e2e outage performance and the lower-bound as the SNR increases. This is because the buffer may be full or empty, and the diversity order achieved is $D = 1$ as derived in Eq. (4.19), while the lower-bound is associated with a diversity order of $D = 2$ as shown in Eq. (4.20). Compared to the conventional scheme, even though the diversity order of the proposed scheme is not improved, the scheme advocated substantially reduces the OP, namely, by a factor of B as shown in Eq. (4.19). For example, a significant gain of 10 dB is achieved compared to the conventional scheme by the proposed buffer-aided protocol at $P_{out} = 0.01$ for a buffer size of $B = 16$, as shown in Fig. 4.4.

Fig. 4.5 compares the e2e outage performance of the proposed MU-BR-UL protocol using both equal-power sharing and the optimal power allocation of Section 4.4. It is shown in Fig. 4.5 that a beneficial gain of approximately 5 dB may be achieved with the aid of the proposed optimal power allocation regime over the equal-power allocation aided system, regardless of the buffer size.

The impact of the buffer size on the delay's PMF is illustrated in Fig. 4.6, where the transmission power is set to $P_t = 5$ dBm. It is observed in Fig. 4.6 that the PMF of the two-hop systems having a buffer size of B spreads over the delay range of $[2, 2B]$, with a fairly flat distribution across the range of $[0, B]$, followed by a peak and a gradual decay beyond $2B$. Furthermore, as the buffer size B increases, the average frame delay is also increased. Furthermore, observe in Fig. 4.6 that the simulation

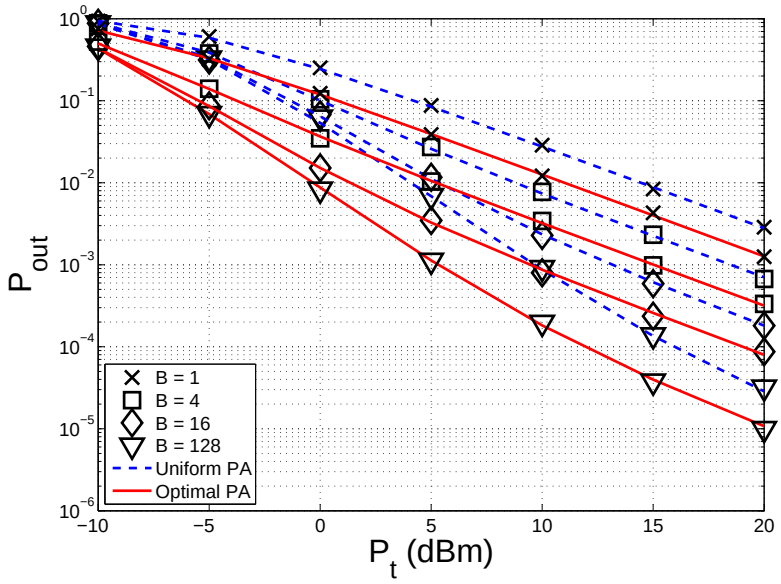

Figure 4.5: Outage performance of the proposed system using the proposed power allocation.

results and the analytical results match closely, which validates our method proposed in Section 4.3.4.

Therefore, based on Fig. 4.4 and Fig. 4.6, we may conclude that by increasing the buffer size, the e2e outage performance is improved at the cost of an increased e2e delay, which allows us to strike an outage-versus-delay tradeoff in the system design. On the other hand, by using the proposed power allocation, the e2e outage performance improves without increasing the buffer size, hence this does not affect the delay.

4.5.2 Impact of the Number of Users

The impact of the number of SNs M on the e2e outage performance is illustrated in Fig. 4.7. In the examples shown in Fig. 4.7, we assume $d_{sr} = 80$ meters and $d_{rd} = 120$ meters, while the transmission rate of each SN is $R = 1bps/Hz$.

As the number of SNs M increases, it is observed in Fig. 4.7 that the outage performance degrades. The reasons for the performance degradation are two-fold. Firstly, the average minimum SNR $\bar{\gamma}_{sr}^{min} = \left(\sum_{m\in S} \bar{\gamma}_{mr}^{-1}\right)^{-1}$ on the SN-RN hop decreases, which results in a higher error probability over the SN-RN hop, as derived in Eq. (4.15). Secondly, as the number of SNs increases, a higher rate of MR is achieved over the RN-DN hop, which results in a higher decoding threshold of $\gamma_{th}^{rd} = 2^{MR} - 1$ and a higher error probability over the RN-DN hop.

It is also observed in Fig. 4.7 that the proposed MU-BR-UL protocol using $B > 1$ improves the outage performance, regardless of the number of SNs involved. In the example illustrated in Fig. 4.7, an SNR gain of approximately 8 dB may be achieved

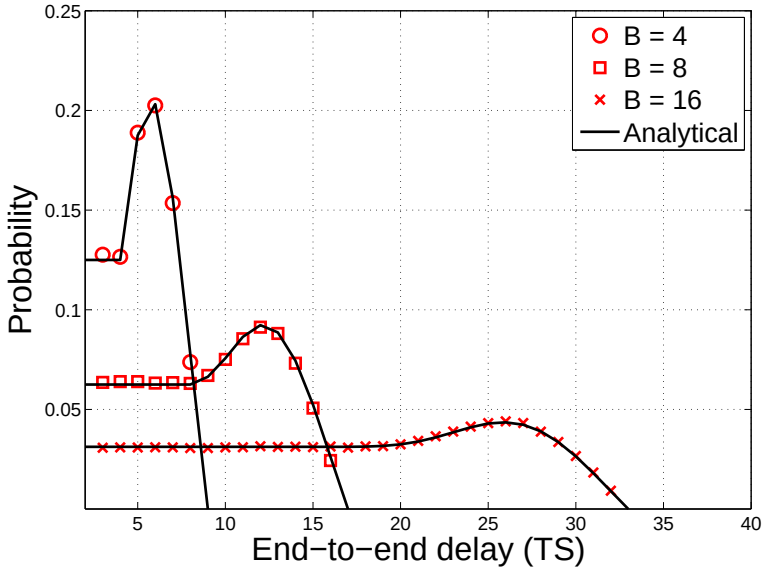

Figure 4.6: Delay probability mass function of the proposed system for different buffer sizes.

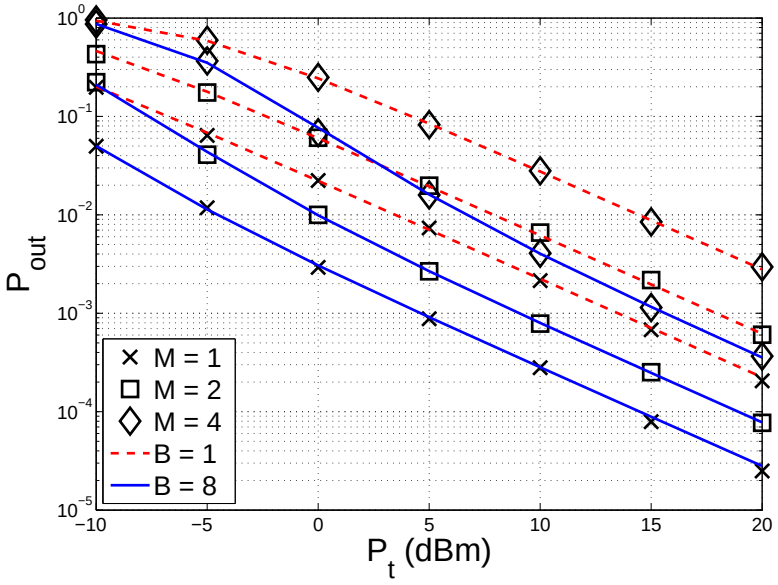

Figure 4.7: Outage performance for different number of SNs.

by the proposed protocol with a buffer size $B = 8$, when compared to a conventional two-hop system having a buffer size $B = 1$ for a system supporting $M = 4$ users.

4.5.3 Impact of the Relay Position

Let us now investigate the impact of the RN position on the outage performance. In the example illustrated in Fig. 4.8, we assume that the SNs, the RN and the DN are placed in a straight line and the distance between a SN and the DN is $d_{sd} = 200$ meters. In order to quantify the position of the RN, we introduce the normalized position of $X_{sr} = \frac{d_{sr}}{d_{sd}} \in [0, 1]$. The transmission rate of each SN is $R = 1bps/Hz$ and

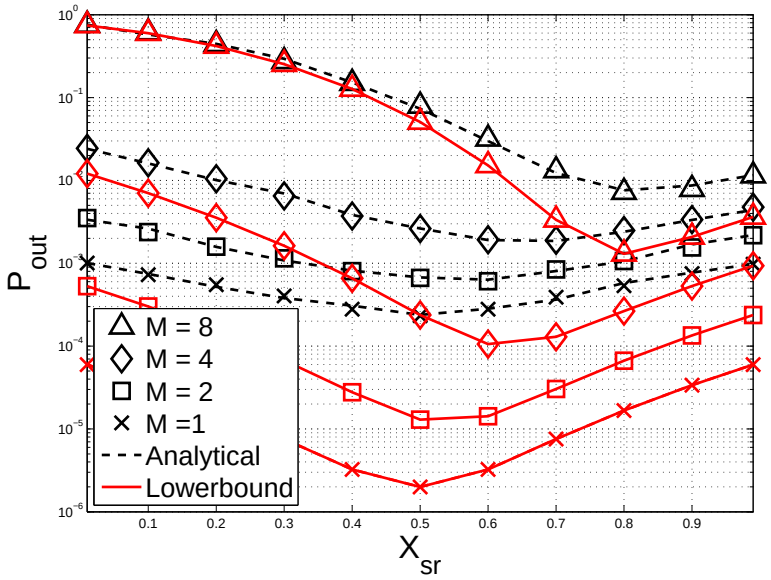

Figure 4.8: Outage performance of the proposed system for different RN positions.

the transmission power of each node is $P_t = 10$ dBm, while the buffer size at the RN is $B = 8$.

Observe in Fig. 4.8 that when the number of SNs increases, the e2e outage performance degrades, as also seen in Fig. 4.7. The optimal RN position quantified in terms of the minimum e2e outage performance moves from the SNs closer to the DN, because a higher rate of MR is transmitted over the RN-DN hop. Therefore, from a network design perspective, the results may provide guidance on the optimal RN deployment or the number of SNs in the same transmission group. It is observed that for the two-hop system, the optimal RN position for $M = 1$ is exactly in the middle of the SN-DN. Furthermore, in the example of Fig. 4.8, the buffer size is set to $B = 8$, albeit an increased buffer size may further improve the achievable outage performance as shown in the results of Fig. 4.4.

The impact of power allocation is illustrated in Fig. 4.9 for different RN positions, where it is shown that for arbitrary RN positions, the optimal power allocation scheme outperforms its equal-power allocation counterpart. Specifically, it is observed in Fig. 4.9 that the outage performance is less sensitive to the RN positions with the assistance of the optimal power allocation, while the outage improvement of optimal power allocation over uniform power allocation is more significant, when the RN is closer to the SNs or when the number of SNs increases. It is also observed that for specific RN positions, the outage performance results of the optimal power allocation and of the equal-power allocation are similar, because in these cases, the solutions of the optimal power allocation regime is close to the equal-power allocation.

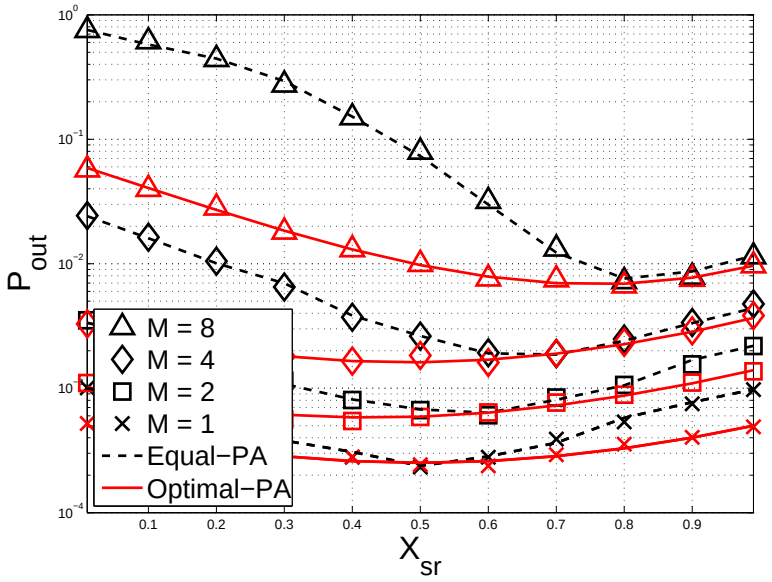

Figure 4.9: Outage performance of the proposed system for different RN positions using both optimal power allocation and equal-power allocation.

4.5.4 Impact of the Detection Method

In all our previous analysis and simulations, the MU-BR-UL protocols proposed for two-hop systems assume ML detection at both the RN and the DN. In practice, when the number of SNs increases, the ML detection may impose an excessive implementation complexity. Additionally, the ML detector treats the packets transmitted by the SNs in a TS as a single frame, where the frame is discarded, whenever an error is detected in any of its packets.

As an attractive design alternative, the reduced-complexity successive interference cancellation (SIC) detection [4] may be adopted. As a further benefit, the SIC detector may be capable of recovering the packet of a SN, even if the other SNs' packets in the same frame may be erroneous. Therefore, the per-user outage performance using SIC may be better than that of the ML detection [69], which is shown in Fig. 4.10, when the number of SNs is $M = 4$ and the transmission rate of each SN is $R = 0.4bps/Hz$.

However, for fixed-rate applications, the performance of ML detection improves monotonically, as the SNR or transmit power P_t increases, while that of the SIC detector may exhibit an interference-limited region at high SNRs, if the rate required for each user is higher than a predefined value [69]. In this case, the outage performance of SIC is dominated by its signal-to-interference power ratio and hence it does not improve, as P_t increases. As seen in Fig. 4.11, when the number of SNs is $M = 4$ and the transmission rate of each SN is $R = 0.5bps/Hz$, the e2e outage performance exhibits an error floor at $P_{out} = 0.01$ and it does not improve, as the SNR increases.

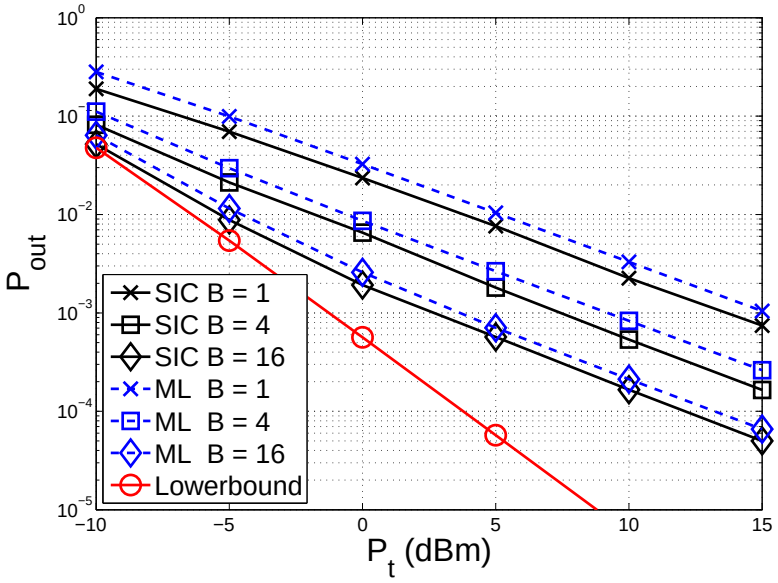

Figure 4.10: Per-user outage performance of the proposed system using ML and SIC detection in conjunction with $M = 4$, $R = 0.4bps/Hz$.

The distances of SN-RN and RN-DN are $d_{sr} = 100$ meters in both Fig. 4.10 and Fig. 4.11,

Hence, for the fixed rate applications considered in this chapter, the adoption of SIC detection should take into account both the number of users as well as the required per-user rate. By contrast, if online rate adaptation is adopted, the SIC detection is capable of avoiding the interference-limited region [4]. However, given our limited space, the MU-BR-UL protocol design conceived for rate-adaptive applications is beyond the scope of this contribution and would be investigated in our future work.

4.6 Conclusions

In this chapter, we have proposed and investigated a multi-user buffer-aided-relaying uplink protocol conceived for two-hop systems. With the aid of the min-SNR approximation technique, we analysed the e2e outage probability and the transmission delay of the proposed protocol. Our analysis and simulation results showed that by exploiting the selection diversity of the SN-RN and the RN-DN hops, significant outage improvements may be achieved compared to the conventional systems, albeit this is attained at the expense of an increased end-to-end delay. The optimal power allocation scheme was also conceived, which achieved a better end-to-end outage performance than the equal-power allocation scheme.

In Table 4.2, we summarize the required transmit power P_t expressed in dBm in order to achieve the target OP. The proposed BAR schemes associated with different buffer sizes B as well as the effects of the power allocation strategies are shown.

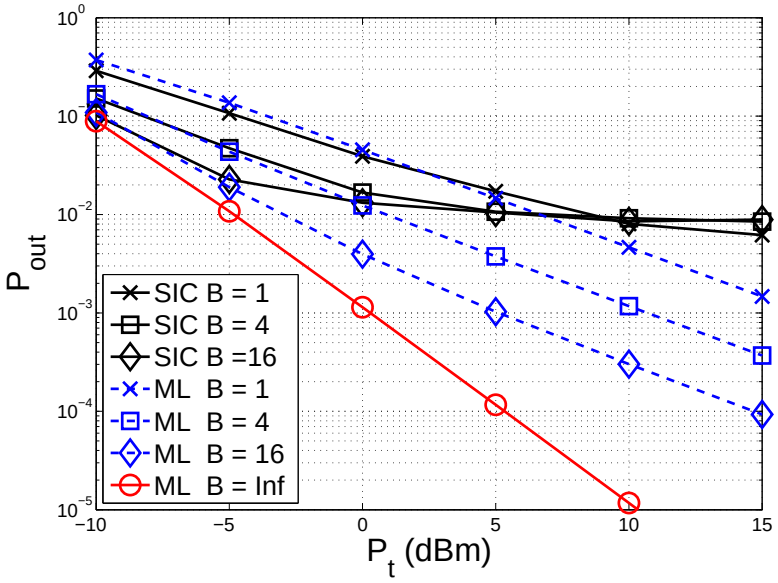

Figure 4.11: Per-user outage performance of the proposed system using ML and SIC detection in conjunction with $M = 4$, $R = 0.5bps/Hz$.

	Target OP	@10^{-2}	@10^{-3}
Conventional Relaying ($B = 1$)	Equal PA	14.4	24.8
	Optimal PA	11.2	21.0
Buffer-Aided Relaying	$B = 4$ Equal PA	8.8	18.6
	$B = 4$ Optimal PA	5.2	15.0
	$B = 128$ Equal PA	4.1	9.8
	$B = 128$ Optimal PA	-0.4	5.4
	$B = \infty$ Equal PA	3.8	9.0
	$B = \infty$ Optimal PA	-0.8	4.0

Table 4.2: Summary of the transmit power P_t in dBm and of the target OP of different buffer sizes and power allocation strategies. The distance between each SN and the RN was set to $d_{sr} = 80$ meters, while that between the RN and the DN to $d_{rd} = 120$ meters. The number of SNs is $M = 4$ and the transmission rate of each SN is $R = 1bps/Hz$.

The conventional relaying regime may be viewed as a special case of BAR, when the buffer size is $B = 1$. Firstly, it is plausible that increasing size of the buffer at the RN would gradually improve the OP. However, the maximum achievable improvement will be bounded by that of the scenario, when we assume an infinite buffer size at the RN, namely that $B = \infty$. Furthermore, the OP improvement is achieved at the price of an increased packet delay, which is analyzed in Section 4.3.4. For example, recall from Table 4.2, when $B = 4$ is adopted, a 5.6dB gain may be achieved at $P_{out} = 10^{-2}$ over the conventional relaying scheme, which is attained at a price of four times higher average packet delay. Finally, compared to the equal PA scheme,

the optimal PA scheme is capable of improving the OP without increasing the packet delay, where a 3.6dB gain may be achieved by optimal PA for $B = 4$ at $P_{out} = 10^{-2}$.

In the context of spectrum sharing between multiple SNs supported by relaying networks, we have proposed the MUD-SIC-aided schemes of Chapter 2, the SPM-NC-CC schemes of Chapter 3 as well as the BAR schemes of this chapter, respectively. The proposed schemes are capable of improving the OP by exploiting the spatial diversity provided by relaying. In the above mentioned schemes, all the SNs and RNs were assumed to have a constant power supply. However, in a practical scenario they tend to be battery-powered, as exemplified by mobile phones and sensors.

Instead of relying on the battery, the nodes may also be capable of harvesting energy from the environment, for example in form of solar power in order to increase the recharge-period. In this scenario, relying on a constant power supply may not be optimal in terms of OP. Therefore, in the next chapter, we eliminate the assumption that the nodes have a constant power supply and assume that the nodes have an energy-harvesting capability, which motivates us to investigate the design of an energy usage policy for the sake of improving the OP.

Chapter 5

Outage Analysis and Optimization for Energy Harvesting Networks[1]

Chapter 2, 3 and 4 considered the scenario, where all the SNs and RNs in the networks rely on battery-powered energy sources for providing constant power supply. In practical scenario like wireless sensor networks, it is challenging or difficult to replace the nodes, the network is energy-constrained and has a limited lifetime [7]. One way of circumventing this problem is allowing the nodes to harvest energy from the environment. According to the authors of [7]: "*Energy harvesting refers to harnessing energy from the environment or other energy sources (body heat, foot strike, finger strokes) and converting it to electrical energy*". The harnessed electrical energy may then be used for powering wireless transceivers. If a harvested energy source is permanently available, the transceiver can be powered perpetually, which fundamentally changes the wireless system design compared to the classic energy-constrained design relying on an energy source storing a limited amount energy in batteries. Furthermore, based on the periodicity and magnitude of harvested energy arrival rate, the transceiver may adjust its energy usage policy (EUP) in order to improve certain network performance metrics, for example, throughput or OP, etc. Since a node is energy-limited until the next harvesting opportunity, it may optimize its EUP for the sake of maintaining a certain performance during this interval, which is defined as the *recharge cycle* [7], or *the duration of a fading block of the energy arrival rate* in this treatise. For example, a wireless sensor node may increase its sampling frequency or its duty-cycle in order to increase its sensing reliability, which relies on an increased data transmission rate [7, 8, 56], or increase of transmission power to improve the attainable outage performance [55–57].

In this chapter, we investigate the effects of random energy arrival and EUP design on the outage performance in energy harvesting wireless networks. Recently,

[1]Part of the work in this chapter is collaborative work with Dr. Chen Dong, and will be submitted for publication

the EUP design of EH networks has become a hot research area. Hence various schemes have been proposed in the literature [8, 52] [55–57, 109, 110] in order to improve certain performance metrics in a particular network topology, relying on different assumptions of the energy arrival rates as well as on the knowledge available at the wireless transceivers for optimization. Before delving into our own work, the similar research contributions found in the literature are reviewed.

5.1 Research Contributions in EH Aided Network Design

In this section, the contributions on EH aided wireless network design will be reviewed for different network topologies, ranging from point-to-point (P2P) networks to multiple access and relay-aided networks. Since the scope of this treatise is that of analyzing and optimizing the outage performance of EH networks, the most relevant contributions are reviewed in this specific context, while those focusing on analyzing and optimizing other performance metrics will only be touched upon.

5.1.1 P2P-EH Networks

Under the idealized simplifying assumption of having both the non-causal channel state information (CSI) and the energy harvesting information (EHI) characterizing the energy arrival rate at the transmitter, in [8, 52][2] the optimal offline EUPs were designed using either the throughput maximization or the completion-time minimization file-transfer objective function. With the aid of the classic stochastic dynamic programming technique [111], the optimal online policies were determined based on the stochastic fading and energy arrival processes with the aid of causal CSI feedback [8, 112].

When the instantaneous CSI at the transmitter is not available, a fixed rate strategy can be adopted. Accordingly, the outage performance of the P2P-EH networks was investigated in [55–57, 109, 110]. The analysis and optimization techniques of the outage performance may be categorized into two subclasses according to the knowledge of the energy arrival rates and the mathematical frameworks they adopt, as described in the following:

1. *The first category of contributions recommends time-variant policies [57, 109, 110]. These authors followed the same mathematical framework as proposed in [8, 112], which adopted the directional waterfilling algorithms with EH-causality*

[2]The authors of [8, 52] used the terminology of "transmission policy" to represent the policy of using the harvested energy in the energy buffer. However, the transmission policy may stand for more widely used schemes, such as rate adaptation, multiple access policy. Therefore, in order to avoid ambiguity, we use the terminology of "EUP" throughout this treatise.

constraints[3] *for offline EUP design and the stochastic dynamic programming in online EUP design. The time-variant policy is named after the fact that the energy usage would be adapted according to the apriori-knowledge of the instantaneous energy arrival rates.* In [57, 109], the authors considered the average outage probability (OP) minimization problem over a finite horizon of a certain number of EH recharge cycles, this problem was shown to be non-convex for a large class of practical fading channels. Then, the globally optimal "offline" power allocation was obtained by a forward search algorithm with the aid of at most N one-dimensional searches. For the special case of $N = 1$, the classic outage capacity of fading channels may be revisited under uniform power allocation. In [110], the authors addressed the optimal transmission scheduling problem of a hybrid energy supply system, in which the transmitter is equipped with a primary battery and an energy harvester. In practical scenarios, the offline policy as well as the optimal online policy mainly served as a benchmark due to their high computation complexity. As the computation complexity of finding the optimal EUPs increases linearly or exponentially with the number of transmission slots, the methods proposed in [8, 57, 109, 110, 112] may not be applicable in scenarios requiring a long transmission duration. However, one of the most attractive features of EH networks is their long network lifetime. An important application of the EH techniques is found in wireless sensor networks (WSNs), in which the sensors may have to operate at a low power and hence only may tolerate a low computational complexity [7].

2. *The second category of the EUP recommends time-invariant policies for long transmission durations, routinely encountered in WSNs, which exhibit negligible computational complexities [55, 56]. The terminology of a time-invariant policy reflects the fact that it does not rely on the knowledge of the instantaneous energy arrival rate, regardless whether the energy usage is designed according to the statistical information of the energy arrival [56] or not [55].* Specifically, the authors of [55] proposed the best-effort EUP, where each EH-powered transmitter uses up the available energy in the energy buffer for each of its transmissions. Hence, the best-effort policy does not exploit the energy buffer to store harvested energy for future usage. Therefore, a system adopting the best-effort policy is equivalent to the 'harvest-and-use' architecture as defined in [7]. The authors of [55] analysed the outage performance of the point-to-point (P2P) networks with a EH-powered transmitter and compared it to its counterparts relying on a classic constant-power supply. It was shown that the performance discrepancy between the non-EH and the EH systems

[3] *The EH-causality constraint refers to the fact that at any time, the transceivers can only utilize the energy that was harvested during the past and the energy not harvested yet, hence it was unavailable for usage. Taking into account the causality constraints imposed on the energy usage, the energy can only be saved and used in the future. Therefore, the waterfilling algorithm is redesigned as a directional one, which allows the energy flow only to take place from the past to the future.*

may be huge, and the OP would include both the channel-induced outage and the EH-induced circuit outage, where the circuit outage is specific to EH-aided network, which is imposed by their random power supply [55]. By contrast, the authors of [56] proposed the asymptotic-optimal EUP, which allows the EH-powered transmitter to store the harvested energy in the energy buffer for future usage. For an infinite energy buffer, the asymptotic-optimal policy minimises the OP by allowing the EH-SN to transmit at a constant power, which is equal to the average energy arrival rate supplied by the EH-source, when sufficient energy is stored in the energy buffer. If insufficient energy is stored in the energy buffer, the SN would switch to the best-effort policy and used up the residual energy. When the size of the energy buffer approaches infinity, it was shown in [56] that the outage performance of the EH system adopting the asymptotic-optimal policy would approach that of the non-EH system assuming an energy source that was capable of providing a constant energy supply.

In this treatise, we aim to fill the gap between the high-complexity time-variant EUPs and the low-complexity state-of-the-art time-invariant policies, in the scenarios having a practical finite energy buffer. Hence, we propose a range of meritorious methods that fall into the time-invariant category in order to impose a low computation complexity by relying merely on the statistical information of the energy arrival rate. By effectively exploiting the statistics of the energy arrival rates, the proposed methods achieve a significantly better performance than the state-of-the-art benchmarks of [55, 56], which either do not exploit the statistics of the energy arrival rate [55] or only exploit the first-order statistics, i.e. its expectation as in [56]. Specifically, we adopt the discrete Markov chain (DMC) model for characterizing the energy buffer relying on the probability distribution function (PDF) of the energy arrival rate.

It should be noted that the DMC or Markov decision process (MDP) is not a new concept in the EH research area, hence there are recent contributions using this mathematical tool as detailed in [113, 114] and in the references therein. Specifically, the authors of [113] formulate the rate maximization problem as a discrete-time and continuous-state Markov decision process. In order to avoid the potentially prohibitive complexity imposed by promptly updating the associated utility function associated with the continuous states, the authors of [113] introduced an approximate closed-form concave utility function, which is then used for finding the a near-optimal solution of the power allocation for both the finite- and infinite-horizon scenarios. The authors of [114] considered the scenario, in which the RNs harvest energy via radio frequency radiation from the SN into finite energy buffers, which is then used for forwarding the SN's message, where a single best RN is selected to forward the SN's message, while the remaining RNs harvest energy simultaneously. Since RF power transfer is adopted, the instantaneous harvested energy arrival rate is highly correlated with the instantaneous channel fading, and the authors of [114] developed

a MDP to capture the variation of the energy buffer states, and derived the OP. In this treatise, we assume that the energy arrival rate is independent from the channel fading, which is common for EH sources like solar and wind sources [7].

To the best of our knowledge, the outage minimization problem considering a finite energy-buffer has not been investigated in the literature, which is hence our novel contributions in the context of P2P-EH networks. In the next section, the state-of-the-art contributions to the field of multiple access EH networks will be reviewed.

5.1.2 Multiple Access EH Networks

As an evolution of research in the subject-area of P2P-EH networks, the recent contributions on EH strategy design here covered numerous aspects of generalized multiple-source EH networks [53, 55, 115–117]. In [53], the authors investigated the optimal packet scheduling problem in the context of a *two-user fading multiple access channel*. The objective in [115] was to minimize the time by which all packets from both users are delivered to the destination by optimizing both the transmission powers and transmission rates of both users. The authors of [115] addressed the analysis and design of multiple access EH networks by focusing on conventional medium access control (MAC) protocols, namely on time division multiple access (TDMA), on framed-ALOHA and on dynamic-framed-ALOHA, where the interplay between delivery efficiency and time efficiency of the data collection rate at the fusion center was investigated using Markov models. In [116], the author considered an ad hoc network supporting multiple pairs of EH-SN and DN, in which all SN-DN pairs compete for the same channel relying on a random access protocol and a distributed opportunistic scheduling framework using a save-then-transmit scheme, which is potentially capable of achieving a 75% throughput gain over the method of best-effort EUP. In [117], the authors developed optimal energy scheduling algorithms for a *generalized M-user fading multiple-access channel* relying on energy harvesting in order to maximize the network's sum-rate, assuming that the side information of both the channel states and energy harvesting states are known for a certain number of time slots, where both the battery capacity and the maximum energy consumption in each time slot are finite. The authors of [55] considered a multiple-access network, where the EH source nodes (SNs) access the channel using the classic orthogonal TDMA protocol and with the goal of delivering independent or common data to a single DN. However, only the symmetric setup is considered, in which the channels spanning from every EH-SN to the DN are independent and identically distributed. Therefore the TDMA network can be readily decomposed into multiple P2P links, which are mutually independent in terms of optimizing their EUP. However, the methods detailed in [55] cannot be directly applied to the *M-user fading multiple-access channel*,

where the outage events of the EH-SNs are correlated, hence the joint optimization of the EUPs of all the EH-SNs may be required.

To the best of our knowledge, the *OP minimization problem of a generalized M-user fading multiple access channel* is an open problem. Hence in this treatise, we solve this problem with the aid of our proposed 2D-search and 1D-search algorithms, whilst relying on a distributed EUP optimization (DEUPO) protocol. In the next section, the family of more sophisticated relay-aided EH networks will be investigated with reference to the relevant contributions in the literature.

5.1.3 Relay-Aided EH Networks

The EUP optimization of EH wireless networks became a hot topic, especially in the context of relay-aided EH networks [50, 114, 118–123]. According to their network topologies, we classified the contributions the works into two categories: three-node networks and relay selection aided EH networks.

- Three-node networks: A three-node network is constituted of a SN, a RN and a DN. In [54], the authors investigated the classic three-node Gaussian relay channel in conjunction with a single EH-SN and a single EH-RN using the decode-and-forward relaying strategy. Assuming that the energy arrival time and the harvested amount of energy are known prior to transmission, the throughput maximization problem over a finite time-horizon of N transmission blocks was solved in [54]. The authors of [121] also considered the same system model, and investigated both the short-term throughput maximization and the transmission completion time minimization problems.
- Relay selection aided EH networks: If multiple RNs are available for relaying the SN's messages, relay selection is adopted for achieving a maximum attainable diversity order, while minimizing the synchronization overhead [50]. The authors of [50] first adopted the EH-nodes as cooperative RNs and considered a cooperative system in which the EH-RNs volunteer to serve as amplify-and-forward RNs whenever they have sufficient energy for transmission. The achievable symbol error rate was analyzed in [50]. suggesting that the energy usage at an EH-RN depends not only on the RN's energy harvesting capability, but also on its transmit power setting as well as on the other RNs in the system.

Meanwhile, since relaying offers a new way of sharing power via power transfer between the transmitters and energy harvesting receivers, there are a lot of recent contributions on power transfer aided relay networks [114, 118–120, 122–124]. For example, the authors of [122] considered the sum-rate maximization problem in a multi-user uplink relay sharing EH network. As a further contribution, the authors of [123] invoked power allocation for minimizing the outage probability for multiple SN-DN pairs communicating with each other via an EH-RN.

To the best of our knowledge, the *outage probability minimization problem of generalized M-user relay sharing EH networks* has not been investigated in the open literature. Hence, in this chapter, we designed the distributed protocols for SDMA-EH networks, where we jointly optimize the position of the RN and the EUPs of both the SNs and of the RN for minimizing the end-to-end (e2e) outage probability.

5.1.4 Contributions of this Treatise

Against the background, the novel contributions in this chapter are as follows:

1. An analytical framework is proposed for investigating the outage performance of a EH-P2P network, in which a EH-SN equipped with a finite energy buffer transmits to a DN. Given the energy buffer's size and assuming a certain probability distribution function (PDF) for the energy arrival rate, the OP is derived for arbitrary EUPs. Specifically, the DMC is adopted for modeling the time-varying states of the energy buffer. In our case study we assume that the energy arrival rate is block-faded over time and obeys the exponential distribution [55, 56]. However, it should be noted that the proposed analytical framework may be applied to other energy arrival rate PDFs. As for the channel model, a simple block Rayleigh fading channel is adopted in our case study. If the closed-form expressions of the outage-probability of non-EH networks communicating over other fading channels are tractable, our DMC framework may be directly applied for deriving the closed-form OP expression of the corresponding EH networks.
2. We investigate the optimal EUP conceived for minimizing the OP of a P2P-EH network. Based on our proposed analytical framework, we show that constructing an exhaustive search for finding the optimal EUP for minimizing the OP is impractical owning to its excessive complexity, because it scales with $(L_{\max})!$, where $L_{\max}$ is the number of states in the DMC. Therefore, a heuristic two-dimensional-search (2D-search) algorithm is proposed for finding a plausible policy. It turns out that the proposed algorithm is potentially capable of finding the optimal policy at a manageable complexity[4].
3. The 2D-search algorithm conceived still exhibits a high complexity, hence we also propose a low-complexity one-dimensional-search (1D-search) algorithm. We will demonstrate that the OP of the 1D-search algorithm is close to that

[4]

- When the Markov-chain model has $L_{\max} \leq 10$ states and the number of cost function evaluations is smaller than10!, the exhaustive searching may be implemented and therefore may serve as the benchmark for our proposed algorithm. However, for $L_{\max} > 10$ the complexity becomes excessive, which prevents us from verifying, whether the 2D-search algorithm is capable of matching the optimal policy. On the other hand, it is challenging to mathematically prove the optimality of a search algorithm in the context of a non-convex problem involving high-dimensional matrices. Therefore, this open problem will be further detailed in our discussions and it will be investigated in our future work.

of the 2D-search counterpart, which may be attractive for applications relying on low-cost hardware, such as mobiles and wireless sensors.

4. We also extend the proposed DMC framework to more general non-orthogonal EH-networks, where a spatial-division-multiple-access (SDMA) network and a SDMA-aided two-hop relay sharing network are investigated, as specific case studies. In contrast to the P2P and to the orthogonal division multiple access networks, the outage events of the different EH-SNs are correlated. In the context of SDMA networks, we first investigate the OP of ML detection. Explicitly, we decompose the joint OP of SDMA into multiple independent outage probabilities, each of which corresponds to a simple P2P EH-network sub-problem. Then, we propose a distributed EUP optimization (DEUPO) protocol, in which each EH-SN is capable of optimizing its own policy using both the local statistics of the fading channel and the related energy arrival model.
5. We apply the proposed DEUPO protocol to the SDMA-aided two-hop relay sharing network, and derive the end-to-end (e2e) OP for an arbitrary number of EH-SNs and relay positions. Finally, with the aid of the proposed 1D-search and 2D-search algorithms as well as the DEUPO protocol, we are ready to optimize the position of the relay node (RN) using the objective function of minimizing the e2e OP.

The rest of this chapter is organized as follows. In Section 5.2 we first discuss the EUPs found in the literature and then invoke the DMC for modelling the energy buffer's state. Based on this model, we consider the OP minimization problem and propose the 2D-search and 1D-search algorithms conceived for finding the optimal EUPs. In Section 5.3, we investigate the EUP design of SDMA-EH networks, and we propose the above-mentioned distributed DEUPO protocol. The DEUPO protocol is then investigated in the context of an SDMA-aided relay-sharing EH network. Finally, our conclusion are presented in Section 5.4.

5.2 P2P-EH Network Design

5.2.1 System Model and OP Formulation

We first consider a simple P2P network constituted by a source node (SN) and a destination node (DN), which is shown in Fig. 5.1. As suggested in [7], the energy harvesting techniques may be divided into two classes, harvest-and-use as well as harvest-store-and-use. In the harvest-and-use architecture, the energy is harvested just in time for usage. By contrast, an energy buffer is introduced in the harvest-store-and-use architecture to store the harvested energy for future usage. In this treatise, we only consider the harvest-store-and-use architecture. As shown in Fig. 5.1, a primary energy buffer and a secondary energy buffer is required in practice [7,55]. In

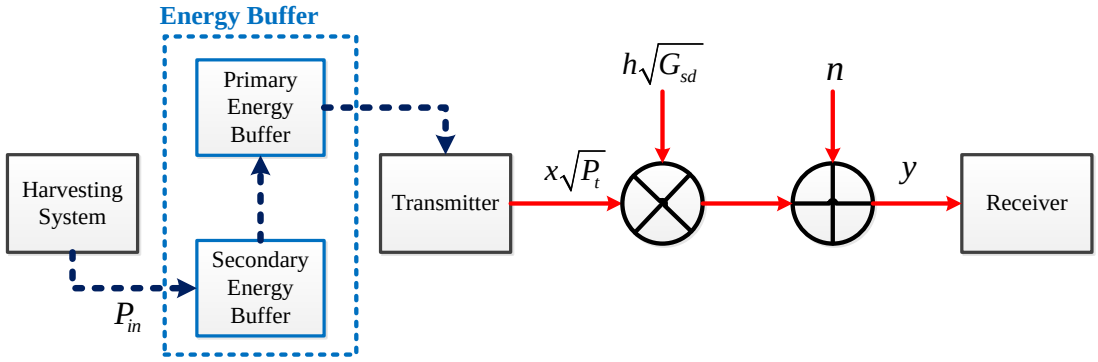

Figure 5.1: System model of the point-to-point energy harvesting network.

[7], the secondary storage is a backup storage invoked for situations, when the primary storage is exhausted. In [55], the authors assumed that the rechargeable energy storage devices cannot charge and discharge simultaneously, hence the transmitter is powered by the primary energy buffer for data transmission, while the secondary energy buffer is connected to the harvesting system and charges up. At the end of a recharge cycle, the secondary energy buffer would be charged by the secondary energy buffer. We assume that the charging time of the primary energy buffer is negligible[5] and the charging efficiency is assumed to be 100%[6]. Therefore, the primary and the secondary energy buffers may be represented by a single energy buffer, which is represented by the dashed-line box seen in Fig. 5.1. This buffer is assumed to be capable of powering the transmitter, while being charged by the harvesting system simultaneously. We did not make any assumptions on what harvesting system is adopted, which may be solar cells, a wind anemometer, etc as discussed in [7].

We assumed that the energy buffer at the SN has a finite energy buffer size, where the harvested energy is stored and used for transmission. We assumed furthermore that the average energy arrival rate P_{in} obeys a certain probability distribution with an expectation of $\overline{P}_{in}$, and it remains constant over a time slot of duration T_E, while changing independently over the subsequent time slots, where a time slot is a recharge cycle. We assume that instantaneous energy arrival rate is unknown and cannot be used during the current time slot of T_E, because the secondary energy buffer is not allowed to charge and discharge simultaneously, as shown in Fig. 5.1. In order to focus our attention on the EUP conceived for wireless transmission, we assume that the circuit power consumption at the SN is negligible and that the energy conversion

[5]In practice, this may be realized by a supercapacitor-based storage system, such as for example the everlast solar system introduced in [7].

[6]In practice, the charging efficiency of the secondary energy buffer may not reach 100%, hence, it may be multiplied by an efficiency factor $\eta_{buffer} \in [0, 1]$, which may be equivalently considered to be a reduced energy arrival rate and hence it does not affect any of our analysis.

efficiency between the energy buffer and the transmit power is 100%[7].

Let us now consider the channel modelling of the wireless communication links. We assume experiencing a narrow-band block-fading channel model, where the fading coefficients remain constant for the duration of a transmission packet denoted as T_C and then they are faded independently from one packet to another over the time dimension. Please note that we make no assumptions conceiving the specific channel model as well as the distribution of the channel gain. We also assume there are always data packets buffered at the SN for transmission. The signal received at the DN is represented by

$$y = h\sqrt{P_t G_{sd}}x + n, \tag{5.1}$$

where h is the channel coefficient capturing the effects of fading, while P_t is the transmit power, x is the transmitted signal and n is the additive noise at the receiver, which is modeled by independent standard circularly symmetric complex Gaussian random variables having a zero mean and a variance of 1. In Eq. (5.1), the average processing gain of $G_{sd} = (N_0 \times d_{sd}^{\beta})^{-1}$ between the SN and the DN captures the effect of the pathloss and of the noise, where N_0 is the noise power at the receiver, d_{sd} is the distance between the SN and the DN, while β is the pathloss exponent.

An outage is defined as the event, when the instantaneous received signal-to-noise power ratio (SNR) γ at the receiver is below a predefined threshold γ_{th} that has to be exceeded for successful decoding. If perfect capacity-achieving coding is assumed, we have $\gamma_{th} = 2^R - 1$, where R is the data transmission rate [4]. Then, the OP of the single-hop EH network may be expressed as follows:

$$\begin{aligned} P_{out} &= \Pr\left\{P_t |h|^2 G_{sd} < \gamma_{th}\right\} \\ &\triangleq \Pr\left\{P_t |h|^2 < P_{th}\right\}, \end{aligned} \tag{5.2}$$

where P_t is the transmit power and h is the normalised channel coefficient capturing the fading effects. In Eq. (5.2), we define $P_{th} = \gamma_{th}/G_{sd}$ in order to focus our attention on the effects of transmit power P_t and of the channel's fading coefficient h.

In the conventional transmission scheme relying on conventional constant-power supply, the transmit power P_t is a constant and the corresponding OP over narrow-band block fading channels was quantified in [4]. However, in the EH networks,

[7] In practice, the power consumption of the circuits may be non-negligible. We may assume that the harvesting system is capable of providing sufficient circuit power, while additionally providing a non-negative transmit power. When the energy harvesting system is not capable of supplying sufficient circuit power, the transmitter may be switched off. On the other hand, the energy conversion efficiency η_{TX} from the energy buffer to the transmitter cannot reach 100% in practice. Hence, we may simply multiply the energy arrival rate at the transmitter by an efficiency coefficient $\eta_{TX} \in [0, 1]$, which does not affect any of our analysis.

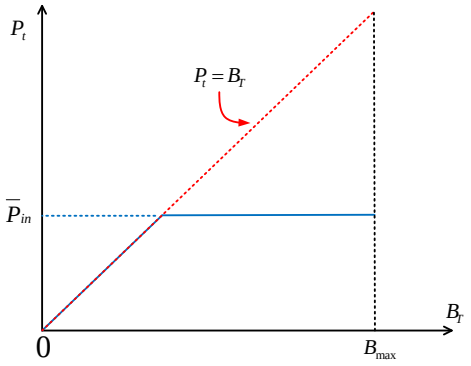

Figure 5.2: EUP illustrated as the function of P_t versus B_T.

the instantaneous transmit power P_t is a time-variant, which is constrained by the amount of the energy available in the energy buffer, which in turn is a random variable depending on the energy arrival rate. The energy arrival rate is assumed to exhibit a block-fading nature, which remains constant over a time slot (TS) of duration T_E and changes independently over subsequent TSs. During a TS with duration of T_E, the amount of energy harvested $P_{in}T_E$ is independent of that harvested in the previous TS and the energy consumed P_tT_E during transmission is determined by the energy buffer state B_T at the beginning of the current TS.

We define the energy buffer state as $B_T = B_E/T_E$, where B_E is the amount of energy available in the energy buffer, while T_E is the duration of the recharge cycle. The physical interpretation of B_T is the maximum average transmit power that may be supported by the amount of energy stored in the buffer during the current recharge cycle[8]. *The EH-causality constraint [8] is interpreted as follows: the instantaneous transmit power P_t cannot exceed the maximum power B_T that may be supported by the current energy buffer state, i.e. we have $P_t \leq B_T$, explicitly indicating that the energy consumed for transmission cannot exceed the amount of energy harvested.* We may model the EUP by the transmit power as a function of the energy buffer state:

$$P_t(B_t),\ B_T \in [0, B_{max}], \tag{5.3}$$

where the energy buffer state B_T is upper-bound by $B_{\max}$ defined as the energy buffer capacity divided by the recharge cycle T_E. In Fig. 5.2, the EH-causality constraint is shown in dashed lines as $P_t(B_T) = B_T$, which models the best-effort policy proposed in [55], where all harvested energy in the buffer is used up for transmission. On the other hand, the asymptotic-optimal policy proposed in [56] is illustrated by the solid line in Fig. 5.2, where the SN aims for to transmitting at a power of $P_t = \overline{P}_{in}$.

[8] When the knowledge of the instantaneous CSI during a period is unavailable at the transmitter, transmitting at a constant transmit power would achieve the minimum OP [4]. Therefore, a constant transmit power is adopted during each recharge cycle and B_T is the upper-bound.

In the asymptotic-optimal policy, when the remaining energy in the energy buffer is capable of supporting a higher transmit power than the average energy arrival rate $\overline{P}_{in}$, the transmitter conserves the energy for its future usage. If the remaining energy in the energy buffer is insufficient for supporting $P_t = \overline{P}_{in}$, the SN switches to the best-effort policy.

We may formulate the OP of the single-hop EH network as:

$$P_{out}\left(P_t\right) = \int_0^{B_{\max}} \Pr\left\{P_t(x)\left|h\right|^2 < P_{th}\right\} f_{B_T}(x)dx, \tag{5.4}$$

where $f_{B_T}(x)$, $x \in [0, B_{\max}]$ is the PDF of the energy buffer state B_T. Therefore, in order to derive the OP in Eq. (5.4), the PDF of the energy buffer state B_T has to be modeled, relying on the specific EUP adopted. Furthermore, because both P_t and B_T are continuous variables, the number of feasible EUPs is infinite and since different policies would result in different energy buffer state PDF, finding the optimal policy for minimizing the OP in Eq. (5.4) may be quite challenging. Hence we will investigate this problem in the next section.

5.2.2 Discrete Markov Chain Model for energy buffer State

As the energy arrival rate P_{in} is assumed to be constant over a recharge cycle T_E and then changes independently over the subsequent recharge cycles, the energy buffer state $B_T(k)$ at the end of k-th ($k \geq 1$) recharge cycle relies only on the state of $B_T(k-1)$, on the amount of energy consumed for transmission $P_t[B_T(k)]$, as well as on current energy arrival rate P_{in}, which obeys a certain PDF and it is statistically independent from its previous samples. Therefore, B_T may be modeled by a continuous Markov process.

However, the domain of $B_T \in [0, B_{max}]$ is continuous, hence the set of the states is uncountable and challenging to manage [125]. Therefore, given the EUP, deriving the PDF of B_T is quite challenging, except for certain special cases, such as the best-effort policy combined with the condition, when the transmit power is equal to the instantaneous energy arrival rate, which may be modeled by the exponential distribution [55]. Even for the asymptotic-optimal policy [56], where P_t is a simple function determined by a combination of the best-effort policy and of the constant power supply, the PDF of B_T cannot be readily derived in closed-form, hence the asymptotic optimality relies on the fact that the probability of $\Pr\left\{B_T < P_t = \overline{P}_{in}\right\} \to 0$, when the energy buffer size obeys $B_{\max} \to \infty$.

In order to quantify and minimize the OP in Eq. (5.4), we approximate the continuous-state Markov process by a finite-state Markov chain [118] in order to model the energy buffer state B_T and to derive the PDF of B_T. Specifically, the energy buffer size $B_{\max}$ is discretized as $L_{\max} = \lfloor B_{\max}/\varepsilon_P \rfloor$, where ε_P is the step size

of the power. Therefore, $l = \lfloor B_T/\varepsilon_P \rfloor$ may take a value from $l \in \{0, 1, ..., L_{\max}\}$ and has a state space size of $(L_{\max} + 1)$. The instantaneous energy harvesting rate P_{in} and the decoding threshold P_{th} are also discretized with a unit of ε_P as

$$\begin{aligned} L_{in} &= \lfloor P_{in}/\varepsilon_P \rfloor \\ L_{th} &= \lfloor P_{th}/\varepsilon_P \rfloor . \end{aligned} \tag{5.5}$$

Hence, L_{th} is a discrete constant when P_{th} is given, while l and L_{in} are discrete random variables and their probability mass functions (PMFs) may be generated from the PDFs of B_T and P_{in} as follows:

$$\begin{aligned} \Pr\{l = x\} &= \int_{x\varepsilon_P}^{(x+1)\varepsilon_P} f_{B_T}(u)\, du \\ \Pr\{L_{in} = x\} &= \int_{x\varepsilon_P}^{(x+1)\varepsilon_P} f_{P_{in}}(u)\, du. \end{aligned} \tag{5.6}$$

Although the variables B_T, P_{in} and P_t may assume any continuous non-negative value, the discrete Markov chain may be capable of sufficiently accurately capturing the buffer's behaviour as long as the discretization step size ε_P is small enough. Finally, we may discretize the EUP formulated in Eq. (5.3) as

$$P_t(l) = P_t(\lfloor B_T/\varepsilon_P \rfloor),\ l \in \{0, 1, ..., L_{\max}\}, \tag{5.7}$$

where the discrete EUP is defined as

$$L_t(l) = \lfloor P_t(l)/\varepsilon_P \rfloor . \tag{5.8}$$

Then, we may construct the state transition matrix T of the energy buffer states, where the specific element in the i-th row and j-th column is given by

$$\begin{aligned} T_{i,j} &= \Pr\{l(k+1) = j \mid l(k) = i\} \\ &= \begin{cases} \Pr\{j = i + L_{in} - L_t(i)\} & , 0 \le j < L_{\max} \\ \Pr\{j \le i + L_{in} - L_t(i)\} & , j = L_{\max} \end{cases} . \end{aligned} \tag{5.9}$$

T we arrive at the steady state probability vector $\pi = \begin{bmatrix} \pi_0 & \pi_1 & ... & \pi_{L_{max}} \end{bmatrix}^T$ using the relationship of

$$\pi = T^T \pi, \tag{5.10}$$

where the physical interpretation of Eq. (5.10) is that the state probability vector π converges and remains constant. Then, we may formulate the OP as

$$P_{out}\left(L_t(l)\right) = \sum_{l=0}^{L_{\max}} \Pr\left\{L_t(l)\left|h\right|^2 < L_{th}\right\}\pi(l) \triangleq \sum_{l=0}^{L_{\max}} P_e(l)\pi(l), \tag{5.11}$$

which is the discrete version of Eq. (5.4). It should be noted that in Eq. (5.11), the OP component of $P_e(l) \triangleq \Pr\left\{L_t(l)\left|h\right|^2 < L_{th}\right\}$ is not only determined by the EUP defined by $L_t(l)$, $l \in [0, L_{\max}]$, but also relies on the statistical channel model determining the distribution of $\left|h\right|^2$. For example, if a narrow-band Rayleigh block fading channel is assumed, then $\left|h\right|^2$ follows the exponential distribution in conjunction with the parameter of 1. In this case, the OP component $P_e(l)$ may be expressed as

$$P_e(l) = \Pr\left\{L_t(l)\left|h\right|^2 < L_{th}\right\} = 1 - e^{-\frac{L_{th}}{L_t(l)}}. \tag{5.12}$$

5.2.3 Two-Dimensional Search Algorithm

Given a certain EUP represented by $L_t\left(l\right), l \in [0, L_{\max}]$ and a specific statistical channel model, we are now capable of quantifying the OP of a certain EUP with the aid of Eqs. (5.7)-(5.11). The optimal EUP $L_t\left(l\right), l \in [0, L_{\max}]$ may be formulated by using the physically meaningful objective function (OF) minimizing the OP as follows:

$$\min_{L_t(l)} P_{out}[L_t(l)]. \tag{5.13}$$

However, the inverse of the mapping in Eq. (5.11) from the OP $P_{out}[L_t(l)]$ to the specific EUP $L_t(l)$ cannot be readily evaluated. In other words, given a certain $P_{out}[L(l)]$, it is not possible to derive the EUP $L_t\left(l\right)$ adopted. Naturally, this hinders the inverse-mapping and hence the closed-form derivation of the optimal EUP is not possible. Although the transition matrix T of Eq. (5.9) may be readily determined, given the EUP $L_t(l)$ according to Eq. (5.9), the resultant steady state probability vector $\pi = \left[\begin{array}{cccc} \pi_0 & \pi_1 & ... & \pi_{L_{max}} \end{array}\right]^T$ is a solution of Eq. (5.10), which is a high-dimensional system of linear equations. Furthermore, given a certain steady state probability vector π, it is not possible to derive the transition matrix T and hence we cannot uniquely and unambiguously determine the discrete EUP $L_t(l)$.

5.2.3.1 Design Motivations

When using discrete Markov modelling, the EUP is represented by a vector of $L_t\left(l\right), l \in [0, L_{\max}]$, *which has* $(L_{\max}+1)$ *legitimate elements over the first dimension, where*

the l-th element in $L_t(l)$ may be assigned any discrete value spanning from 0 to l over a second dimension, hence the search is over a two-dimensional (2-D) space. The above fact motivates us to design a search algorithm. The most conceptually straightforward way of finding the optimal EUP $L_t(l)$, $l \in [0, L_{\max}]$ is to invoke an exhaustive search, which evaluates every feasible EUPs and selects the one having the minimum OP. As illustrated in Fig. 5.2, an EUP $L_t(l)$ is physically feasible as long as the instantaneous transmit power P_t is non-negative and does not exceed the maximum power B_T that may be supported by the current energy buffer state $P_t \leq B_T$, which is equivalent to the following discrete form:

$$0 \leq L_t(l) \leq l, \forall l \in [0, L_{\max}]. \tag{5.14}$$

This simple feasibility constraint results in a large number of feasible energy policies, where the complexity of searching for the optimal policy that minimizes the OP may be excessive. Quantitatively, there are a number of $N_f = (L_{\max}+1)!$ feasible functions of $L_t(l)$, given the condition in Eq. (5.14). For example we have $L_{\max} > 11$, the number of feasible functions becomes $N_f > 10^8$. Therefore, the exhaustive search method of finding the optimal policy is not practically feasible. Therefore, we have to design search algorithms having a practically tolerable complexity, which are detailed in the following sections.

5.2.3.2 2D-Search Algorithm Design

In the algorithms proposed in this treatise, the design guidelines we adopted for controlling the complexity are summarized as follows:

- **Guideline 1:** *The optimal EUP $L_t(l)$, $l \in [0, L_{\max}]$ is a non-decreasing function of the energy buffer state l, namely $\forall k \in [0, L_{\max}-1]$, $L_t(k+1) - L_t(k) \geq 0$.* The physical interpretation of this guideline can be summarized as follows. If the amount of energy available in the energy buffer is increased, the transmitter should not use a lower transmit power. The reason behind this guideline is two-folds: Firstly, the transmitter has no knowledge of the energy arrival rate in the future, therefore it cannot decide whether conserving the harvested energy in the energy buffer for future usage is beneficial. Secondly, the transmitter has no knowledge of the instantaneous channel gain, therefore it cannot decide how to control the transmit power.
- **Guideline 2:** *The increasement of the optimal EUP $L_t(l)$, $l \in [0, L_{\max}]$ is no higher than one unit of energy with respect to the energy buffer state l, namely $\forall k \in [0, L_{\max}-1]$, $L_t(k+1) - L_t(k) \leq 1$.* Let us assume that there are two feasible EUPs L_t and $\hat{L}_t$, which satisfy $L_t(k+1) - L_t(k) \geq 2$, $\hat{L}_t(k+1) - \hat{L}_t(k) \leq 1$ and $\hat{L}_t(k+1) + \hat{L}_t(k) = L_t(k+1) + L_t(k)$. When the OP versus the transmit power is a convex function, the algorithm should choose $\hat{L}_t$, because it would

achieve a lower OP than L_t according to Eq. (5.11), provided that the steady state probability vector π is assumed to be fixed. However, it was shown in [57] that the OP functions with respect to the transmit power are non-convex in the low transmit power region, i.e. when $P_{out} > 0.1$. However, in most practical scenarios, a better OP is required, in which case the OP functions are convex. In this scenario, evenly allocating transmit power to state k and $(k+1)$ may achieve a lower OP than an unequal allocation of power, given a fixed total amount of transmit power. Therefore, we judiciously opt for EUPs satisfying $L_t(k+1) - L_t(k) \leq 1$.

Although the above-mentioned pair of design guidelines may be interpreted physically in a simple manner, it is challenging to prove the optimality of *Guideline 1* rigorously, while *Guideline 2* is applied in relatively high transmit power associated with a good channel quality, when the OP is a convex function of the transmit power [57]. When relying on the proposed pair of design guidelines, the number of OP evaluations is reduced from $N_f = (L_{\max})!$ to $N_{2D} = 2^{N_{\max}}$, which may still be excessive. Quantitatively, when $N_{\max} > 30$, the number of evaluations obeys $N_{2D} > 10^9$. Therefore, we conceive a third guideline for controlling the complexity, at the cost of potentially resulting in a local optimal solution, which is detailed as follows:

- **Guideline 3:** *When the search does not find an EUP resulting in a reduced OP, it is terminated.* This is a widely used early-stopping technique employed in heuristic optimization algorithms [126]. Albeit its global optimality is not guaranteed without further information about the search space, it is capable of substantially reducing the complexity.

Since *Guideline 3* may result in locally optimal solutions, multiple initial solutions may be chosen for the search algorithm. However, through our extensive numerical evaluations conducted for $N_{\max} < 12$, when the exhaustive search algorithm is still feasible, our numerical results have shown that Algorithm 5.1 is capable of finding the globally optimal policy. Algorithm 5.1 uses the best-effort policy as the initial solution, and then the above three guidelines are followed throughout the rest of the design. Therefore, it may be concluded that even though the optimality may not be shown mathematically, the proposed heuristic 2D-search algorithms are effective for practical applications, whilst imposing a much lower complexity than the exhaustive search.

5.2.4 One-Dimensional Search Algorithm

In the previous section, the optimal EUP was investigated and a search algorithm was proposed. However, the algorithm relies on searching in a two-dimensional domain and hence it is quite involved, as it will be demonstrated in Section 5.2.5. In this section, motivated by the fact that the asymptotic-optimal policy is characterized by

Algorithm 5.1 2D-Search Algorithm

$L_t(l) = l,\ l \in [0, L_{\max}]$; //**Start as the best-effort policy**
$P_{out,\min} \leftarrow 1$;
$N_I \leftarrow 0$;
$I_U \leftarrow 1$;
while $I_U == 1$ **do**
  $N_I \leftarrow N_I + 1$; //record the number of searches
  for $l = L_{max}$ to 0 **do**
    $\widetilde{L}_t \leftarrow L_t$; //store the current policy
    if $L_t(l) > 0$ **then**
      $L_t(l) \leftarrow L_t(l) - 1$; //**remove the top tile only (guideline 2).**
    end if
    for $i = 0$ to l **do**
      $L_t(i) \leftarrow \min(L_t(i), L_t(l))$; //**ensure policy is non-decreasing (guideline 1).**
    end for
    $P_{out} = P_{out}(L_t)$;
    if $P_{out} < P_{out,\min}$ **then**
      $P_{out,\min} \leftarrow P_{out}$;
    else
      $L_t \leftarrow \widetilde{L}_t$; //recover the stored policy
    end if
    $L_t[N_I] \leftarrow L_t$;
    if $L_t[N_I] == L_t[N_I - 1]$ **then**
      $I_U \leftarrow 0$; //**terminate if the iteration (guideline 3).**
    end if
  end for
end while

a constant desired transmit power [56], we formulate a 1D-search based EUP and aim for minimising the OP using one-dimensional search, which will be shown in Section 5.2.5 to exhibit a significantly lower complexity than the 2D-search algorithm.

5.2.4.1 Design Motivations

Our proposed 1D-search policy is motivated by the asymptotic-optimal policy proposed in [56], which is illustrated in Fig. 5.2. The suboptimal EUP considered is based on a combination of the constant power policy and the best-effort policy. Specifically, given a desired constant transmit power P_d, when the remaining energy in the energy buffer satisfies $B_t \geq P_d$, the transmitter opts for transmitting at a power of $P_t = P_d$ and conserves the rest of the energy for its future usage. Otherwise, when

$B_t < P_d$, the transmitter switches to the best-effort policy and transmits at a power of $P_t = B_T$. The suboptimal policy is represented by a fixed $P_t(B_T)$ of:

$$P_t\left(B_T\right) = \begin{cases} B_T & , \ B_T < P_d \\ P_d & , \ B_T \geq P_d \end{cases}, \tag{5.15}$$

while its discrete version represented by $L_t\left(l\right)$, $l \in [0, L_{\max}]$ is:

$$L_t\left(l\right) = \begin{cases} l & , \ l < L_d \\ L_d & , \ l \geq L_d \end{cases}, \tag{5.16}$$

where we define $L_d = \lfloor P_d/\varepsilon_P \rfloor$. Compared to the generalized representation $L_t\left(l\right)$, $l \in [0, L_{\max}]$, which requires $(L_{\max}+1)$ variables for fully characterizing the policy, the proposed EUP may be characterized by a single variable L_d. Therefore, L_d is also the only variable that may be optimized in order to minimize the OP. However, the 1D-search policy may be expected to result in a degraded OP.

A special case of the proposed EUP is to set $P_d = \overline{P}_{in}$ or equivalently $L_d = \overline{L}_{in}$. The asymptotic-optimal EUP proposed in [56] was shown to achieve the performance of its constant-power counterpart operating at $P_t = \overline{P}_{in}$, based on the assumption of an infinite energy buffer size of $B_{max} \to \infty$ [56]. In this case, the probability of an energy buffer overflow is 0, and the probability of $\Pr\left\{B_T < P_d\right\} = \Pr\left\{l < L_d\right\} \to 0$. It is plausible that the performance of the classic non-EH system constitutes the OP lower-bound that may be achieved by any EH system relying on a random energy arrival rate. Naturally, achieving the performance of the asymptotic-optimal EUP is desirable [56].

However, when the energy buffer size is finite, the asymptotic-optimal policy would be sub-optimal, because a finite energy buffer may overflow with a non-negligible probability, when the instantaneous energy arrival rate is high and cannot be stored for future usage. Meanwhile, the choice of $L_d = \overline{L}_{in}$ may not be optimal, since a choice of $L_d \neq \overline{L}_{in}$ may reduce both the probability of energy buffer overflow and the OP. However, the optimal choice[9] of P_d is not obvious, because the relationship between the OP P_{out} and the energy usage function L_t is quantified by Eq. (5.9) (5.10) and (5.11), which makes the direct derivation of the optimal P_d quite challenging.

By comparison, as shown in Eq. (5.7-5.11), given a specific value of P_d, the numerical evaluation of P_{out} may be straightforward, according to the OP expression provided in Eq. (5.11). This motivates us to design a search algorithm, which

[9]The optimal choice is in the context of selecting P_d for the 1D-search algorithm, which may still result in inferior OP compared to the exhaustive search and the 2D-search algorithms.

searches for the optimal P_d based on the numerical evaluation of P_{out}, instead of using an analytical derivation to get the optimal P_d directly.

In the next section, we would first derive the OP for the 1D-search based EUP given a specific L_d, then propose the search algorithm for finding the optimal L_d in order to minimize the OP.

5.2.4.2 1D-Search Algorithm Design

Upon invoking the 1D-search based EUP represented in Eq. (5.16), we may simplify the OP expression of Eq. (5.11) specifically for the 1D-search policy as follows:

$$\begin{aligned} P_{out} =& \Pr\{l \geq L_d\} \Pr\left\{L_d |h|^2 < L_{th}\right\} \\ &+ \Pr\{l < L_d\} \Pr\left\{l |h|^2 < L_{th} | l < L_d\right\}, \end{aligned} \tag{5.17}$$

where the first line represents the OP, when the energy in the energy buffer is capable of supporting transmitting at the desired level of L_d. The second line in Eq. (5.17) represents the OP, when the energy in the energy buffer is insufficient for transmitting at the power level of $L_t = L_d$, and the transmitter consumes all the energy in the energy buffer, while transmitting at a power level of $L_t = l$.

Then we construct the state transition matrix T of the energy buffer state according to Eq. (5.9), and when the energy buffer state is steady, the state probability vector π may be formulated as:

$$\pi = T^T \pi,$$

where $\pi = \begin{bmatrix} \pi_0 & \pi_1 & \ldots & \pi_{L_{max}} \end{bmatrix}^T$. Given the desired power level represented by L_d and the OP expression in Eq. (5.17), we have

$$\Pr\{l \geq L_d\} = \sum_{l=L_d}^{L_{max}} \pi_l. \tag{5.18}$$

If we assume furthermore that the channel obeys Rayleigh fading, the other terms in Eq. (5.17) can be derived as follows:

$$\Pr\left\{L_d |h|^2 < L_{th}\right\} = 1 - \exp\left(-\frac{L_{th}}{L_d}\right), \tag{5.19}$$

and

$$\begin{aligned} & \Pr\{l < L_d\} \Pr\left\{l |h|^2 < L_{th} | l < L_d\right\} \\ =& \sum_{l=0}^{L_d-1} \pi_l \Pr\left\{l |h|^2 < L_{th}\right\} \\ =& \sum_{l=0}^{L_d-1} \pi_l \left[1 - \exp\left(-\tfrac{L_{th}}{l}\right)\right]. \end{aligned} \tag{5.20}$$

By substituting the terms of Eq. (5.18), (5.19) and (5.20) into Eq. (5.17), we may arrive at the analytical OP for transmission over block Rayleigh fading channels in the single-hop EH network of Fig. 5.1. If a different statistical channel model is adopted, we may change Eq. (5.19) and Eq. (5.20) accordingly. Throughout this chapter, we use the block Rayleigh fading channel as a case study, although our proposed OP analysis and the search algorithms conceived for OP minimisation are sufficiently general and for arbitrary channel models. The effects of other wireless channel models will be investigated in our future research.

Therefore, given a specific value of L_d, the numerical evaluation of P_{out} is straightforward, according to the OP expression provided in Eq. (5.17). Since it relies on the single parameter L_d and hence a 1D-search algorithm may be designed for finding the optimal L_d, instead of searching over a 2D space, as in Section 5.2.3. This 1D-search procedure is detailed in Algorithm 5.2, which is much simpler than the 2D-search algorithm of Section 5.2.3. Specifically, in Algorithm 5.2 there are a total number of $(L_{\max}+1)$ candidate EUPs, namely $L_d \in \{0, 1, ..., L_{\max}\}$. For each candidate EUP, the OP is evaluated using Eq. (5.17), where the one achieving the minimum OP is selected.

Algorithm 5.2 1D-Search Algorithm

$L_{d,opt} \leftarrow 0$;
$P_{out,\min} \leftarrow 1$;
for $L_d = 0$ to $L_{\max}$ **do**
  $P_{out} = P_{out}(L_d)$;
  if $P_{out} < P_{out,\min}$ **then**
    $P_{out,\min} \leftarrow P_{out}$;
    $L_{d,opt} \leftarrow L_d$;
  end if
end for

Specifically, the 1D-search procedure of Algorithm 5.2 requires $(L_{\max}+1)$ evaluations of the OP, which is significantly lower than that of the 2D-search of Algorithm 5.1 or the exhaustive search methods, as we will demonstrate quantitatively in Section. 5.2.5. The low-complexity of Algorithm 5.2 accrues from the fact that the EUP functions $L_t(l)$ investigated may be characterized by a single scalar L_d, as shown in Eq. (5.16). Therefore, the OP may be expressed as a function of a scalar L_d rather than as a vector $\overrightarrow{L_t} \triangleq \{L_t(l) | \, l \in [0, L_{\max}]\}$. In the next section, we will compare the OP of the proposed 2D-search and 1D-search Algorithms 5.1 and 5.2 to a pair of state-of-the-art EUPs found in the literature, namely, to the best-effort policy [55] and to the asymptotic-optimal policy [56].

A conceptual example is illustrated in Fig. 5.3, where we have $L_{\max} = 3$ and therefore there are $N_f = 4! = 24$ feasible functions of $L_t(l)$. The exhaustive search

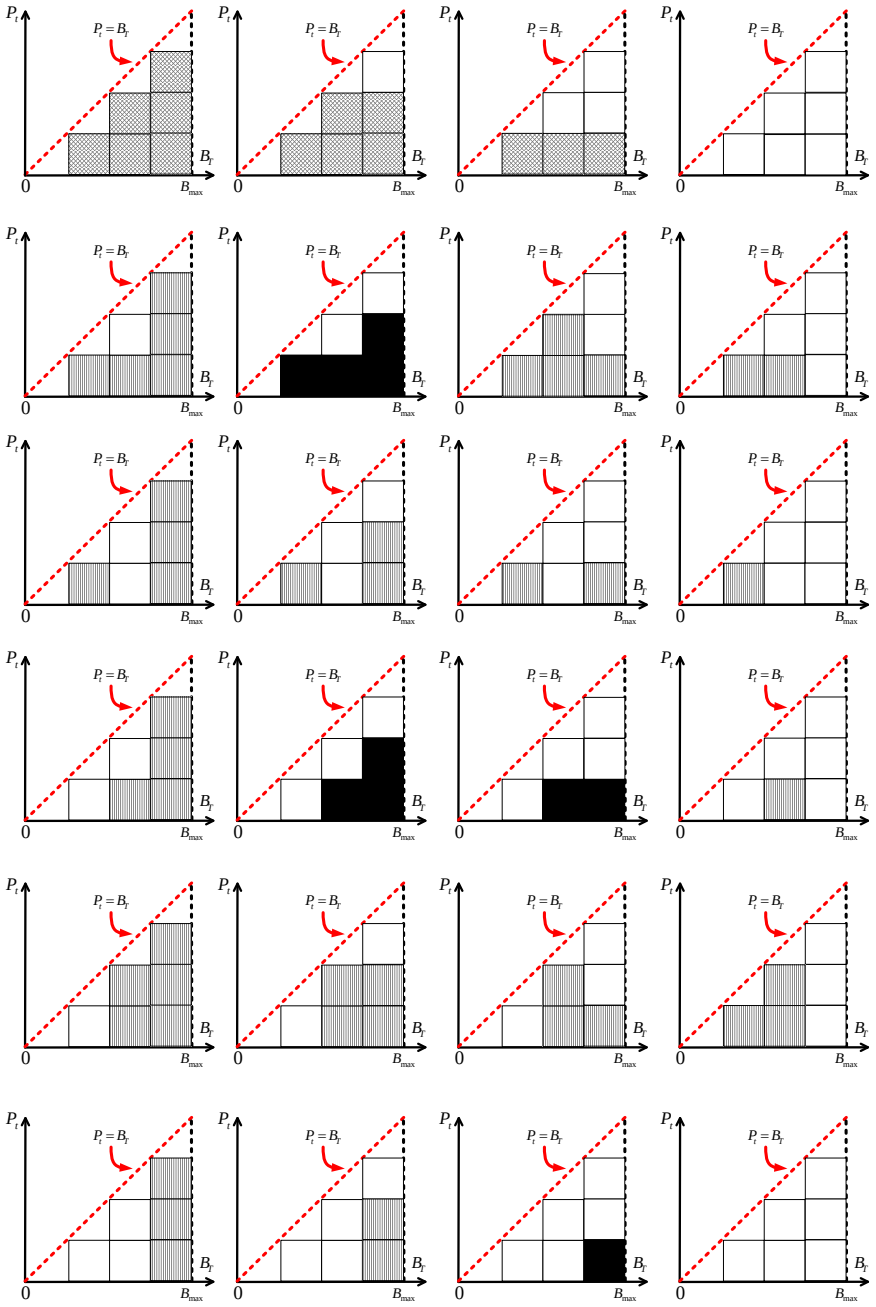

Figure 5.3: Search space of the different search algorithms for $L_{\max} = 3$.

algorithm would evaluate the OP for each of the 24 functions and selects the one having the minimum OP. According to Guideline 1 and 2, the 2D-search algorithm would select from a set of $N_{2D} = 8$ functions, which are represented by black tiles as well as the 1-st row of Fig. 5.3. By contrast, the 1D-search algorithm selects from a set of $L_{\max} = 4$ functions from the 1-st row of Fig. 5.3.

5.2.5 Numerical Results for P2P Networks

As detailed in Sections 5.2.3 and 5.2.4, the OP relies on the following system parameters:

- **Statistics of the Energy Arrival Rates** include the average energy arrival rate $\bar{P}_{in}$ and the recharge cycle T_E. The distribution of the fading energy arrival directly affects its rate, assumed to be exponentially distributed, as in [55, 56] in order to facilitate our comparisons with the state-of-the-art benchmarkers proposed in these references.
- **Statistics of the wireless information-transfer channels:** the wireless channel spanning from the SN to the DN is assumed to obey block Rayleigh fading, although our analysis technique can be applied to arbitrary channel models.
- **Parameters of the EH-SN:** the energy buffer size $B_{\max}$ and the data transmission rate R.

In this section, the dependence of the OP on the aforementioned system parameters will be investigated. In the context of the P2P-EH networks, the distance between the SN and the DN is set to $d_{sd} = 100$ meters and the pathloss exponent to $\beta = 3$, while the noise power at the receiver is assumed to be $N_0 = -80$dBm. The data transmission rate is set to $R = 1$ bits/second/Hertz. In this section, the analytical results are represented by the dashed curves, while the simulation results are shown by the symbols. It should be noted that the discrete step size ε_P for quantifying the OP and for searching for the feasible EUP sets are different. For OP evaluations, ε_P is set for ensuring that $L_{\max} = 6400$ in order to guarantee a high accuracy of quantifying the OP, while we have ε_P is set to $L_{\max} = 200$, when searching for the EUP using Algorithm 5.1 and Algorithm 5.2 in order to control the search complexity. We will demonstrate that the analytical results represented by the dashed curves closely match the simulation results, which indicates that the DMC based analytical framework is capable of accurately predicting the OP of the P2P-EH networks for all of the EUPs considered.

The different EUPs are illustrated in Fig. 5.4. It is shown that the best-effort policy proposed in [55] exhibits a slope of 1, indicating that the currently harvested amount of energy in the energy buffer will be used up for transmission. The x-axis l represents the discrete maximum power that may be supplied given the amount of energy in the energy buffer for a period of T_E. The asymptotic-optimal policy is based on a combination of two trends: when the amount of energy in the energy buffer satisfies $B_t < \bar{P}_{in}$, the EH-SN transmits by employing the best-effort EUP, otherwise the EH-SN opts for a constant power strategy by choosing a fixed transmit power $P_t = \bar{P}_{in}$. When the energy buffer size tends to infinity, the asymptotic-optimal policy would approach the constant power policy, indicating that a large energy buffer is capable of converting a EH system into an equivalent non-EH system having a constant transmit power of $P_t = \bar{P}_{in}$ [56]. However, when the energy buffer size is finite, the asymptotic-optimal policy is no longer optimal in terms of minimizing the OP, as shown in Fig. 5.5.

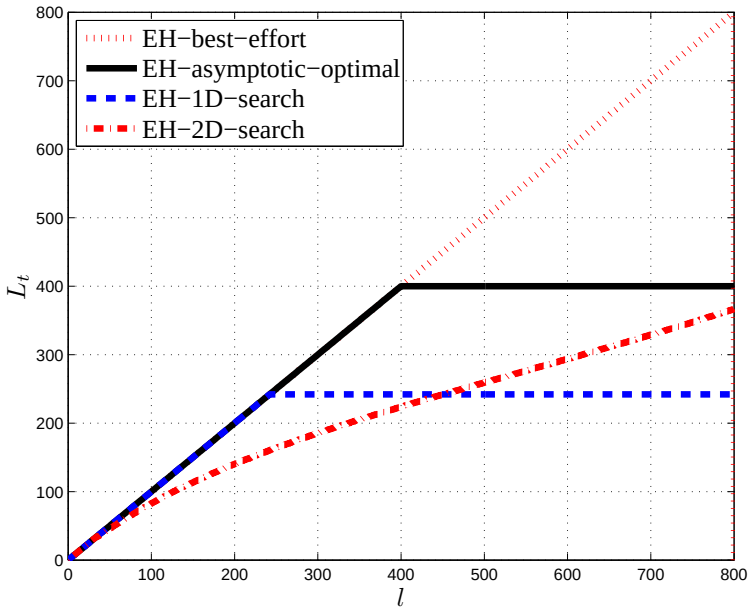

Figure 5.4: Illustration of different EUPs for the P2P network. The average energy arrival rate is $\bar{P}_{in} = 10$dBm, while the energy buffer size is $B_{max} = 16\bar{P}_{in}$, while $R = 1$ bits/sec/Hz and $T_E = 8T_C$.

In Fig. 5.5, the performance of the EUPs found by the proposed 2D-search and 1D-search Algorithms 5.1 and 5.2 are compared to that of the best-effort policy as well as to the asymptotic-optimal policy proposed in [55] and [56], respectively. It is shown that for the given configurations, the OP achieved by the proposed algorithms tends to be better than those achieved by the benchmarkers. Specifically, the 2D-search Algorithm 5.1 performs close to its non-EH counterpart, which serves as the lower-bound of the OP for the EH systems [56]. At $P_{out} = 0.01$, the EUP found by the 2D-search Algorithm 5.1 achieves a 3dB gain over the asymptotic-optimal policy and a 6dB gain over the best-effort policy. Therefore, if an EH-SN adopts the asymptotic optimal policy, it requires twice the average energy arrival rate harvested from the environment, compared to an EH-SN equipped with the proposed 2D-search algorithm, while maintaining the same level of reliability at $P_{out} = 0.01$. This ratio would in fact be further increased to four, if the benchmark EH-SN adopts the best-effort policy.

We may conclude that the 2D-search algorithm is capable of significantly improving the EH-SN's capability to exploit the harvested energy most efficiently, or to substantially simplify the hardware required for harvesting the energy from the environment, which is very important for applications such as WSNs [7]. For example, the best-effort policy requires a four times higher average energy arrival rate for maintaining an identical outage performance as that using the 2D-search algorithm. Equivalently, as the amount of power harvested by the solar panel increases linearly

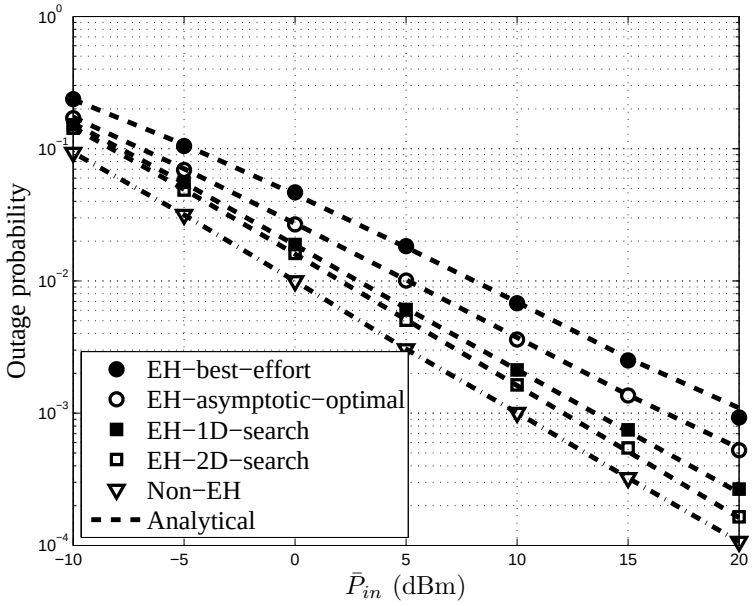

Figure 5.5: OP versus average energy arrival rate $\bar{P}_{in}$ using different EUPs for the P2P network. The energy buffer size is $B_{max} = 16\bar{P}_{in}$ and $R = 1$ bits/sec/Hz, $T_E = 8T_C$. The analytical results were evaluated from Eq. (5.11).

with the area of the solar panel [7], hence requiring a four times larger solar-panel. In other words, the 2D-search Algorithm 5.1 allows us to design a sensor node having a solar panel of much smaller size, which has 25% of the area necessitated by the best-effort policy. Furthermore, as shown in Fig. 5.5, when the reliability requirement are more stringent, the performance improvements of the proposed EUPs would be more significant in terms of requiring a lower energy arrival rate or a smaller solar-panel. Finally, the 1D-search Algorithm 5.2 is inferior to the 2D-search Algorithm 5.1, since it exhibits a modest performance degradation of 0.9dB at $P_{out} = 10^{-2}$. From an alternative perspective, an EH-SN adopting the 1D-search Algorithm 5.2 may require 1.23 times higher energy arrival rate, which is the price paid for reducing the computational complexity. Therefore, in a WSN application scenario having sensor nodes which have a low computational capability, the 1D-search Algorithm 5.2 or the simple asymptotic-optimal policy may be preferred.

The fundamental reason for the OP improvements of the proposed 2D-search and 1D-search Algorithms 5.1 and 5.2 may be inferred from Fig. 5.6, which represents the probability mass function (PMF) of the discrete energy buffer state l for different EUPs. It is observed that all EUPs resulted in relatively near-constant PMF values, apart from the peaks at the states, when the energy buffer was full at $l = L_{\max}$. Compared to the PMF of the best-effort and the asymptotic-optimal policy, the 2D-search and 1D-search Algorithm 5.1 and 5.2 may be capable of reducing the PMF when the energy buffer is small, which reduces the weights π_l for the relatively large OP components of $P_e(l) = \Pr\left\{L_t(l)\,|h|^2 < L_{th}\right\}$ in Eq. (5.11), when the discrete

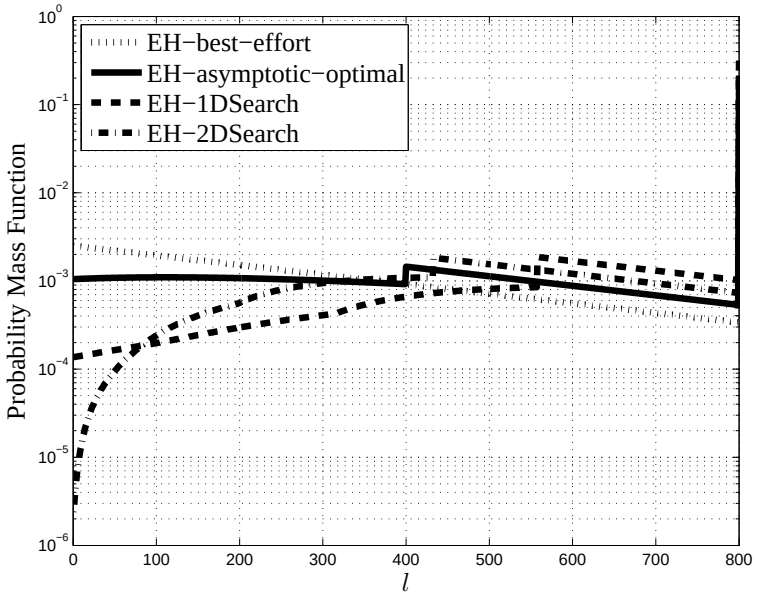

Figure 5.6: Probability Mass Function (PMF) of the energy buffer states for the P2P network. The average energy arrival rate is $\bar{P}_{in} = 10$dBm, while the energy buffer size is $B_{max} = 16\bar{P}_{in}$ and $R = 1$ bits/sec/Hz, $T_E = 8T_C$. The results were evaluated via simulations.

transmit power L_t is low. Therefore, reshaping the PMF by reducing the contribution of the high OP components and increasing the weights of the low OP components, the overall OP may be beneficially reduced, which is confirmed by the results of Fig. 5.5.

In Fig. 5.7, the relationship between the OP and the desired transmit power P_d required by the 1D-search Algorithm 5.2 is illustrated. As the desired transmit power P_d increases, the OP decreases monotonically, until its minimum value is achieved, and then increases monotonically, ultimately converging to that of the best-effort policy. It is also shown that the 1D-search Algorithm 5.2 may be capable of finding an EUP, which performs close to the 2D-search Algorithm 5.1, despite its lower complexity, as seen in Fig. 5.8.

More explicitly in Fig. 5.8, the relationship between the number of the OP evaluations and the discrete energy buffer size $L_{\max}$ is illustrated for both the 2D-search Algorithm 5.1 and 1D-search Algorithm 5.2. Observe that the 1D-search Algorithm 5.2 drastically reduces the complexity of 2D-search counterparts, albeit at the cost of an OP increase as shown in Fig. 5.7. Quantitatively, when the discrete energy buffer size is $L_{\max} = 400$, the 1D-search Algorithm 5.2 imposes as little as 0.46% of the computational complexity compared to that of its 2D-search based counterpart, while imposing a 0.9dB loss at $P_{out} = 10^{-2}$, as shown in Fig. 5.5. On the other hand, from an overall energy consumption point of view, the energy required for computation the EUP also dissipates a non-negligible portion of the

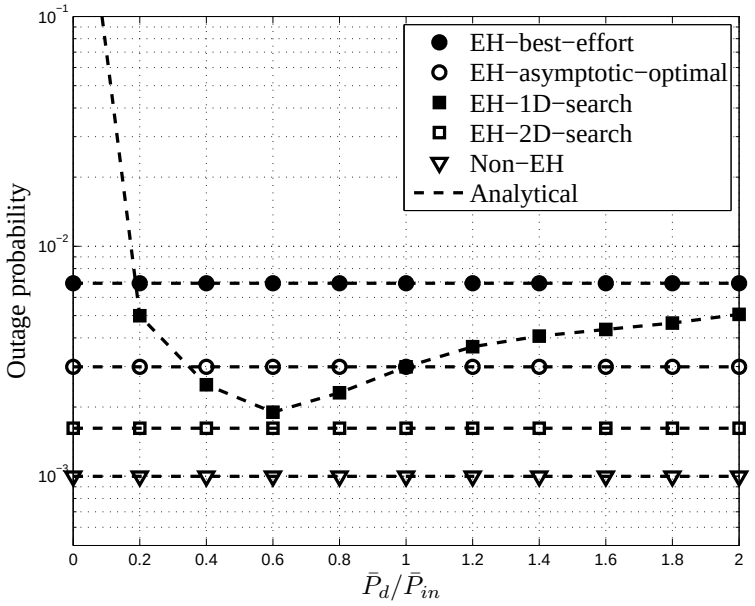

Figure 5.7: OP versus the desired transmit power P_d divided by $\bar{P}_{in}$ for 1D-search Algorithm 5.2 for the P2P network considered. The average energy arrival rate is $\bar{P}_{in} = 10$dBm and $R = 1$ bits/sec/Hz, $T_E = 8T_C$. The analytical OP results were evaluated from Eq. (5.11).

energy, especially for users relying on low-end devices. Therefore, the 1D-search Algorithm 5.2 may be deemed attractive for applications relying on hardware having a low computational capability, such as mobiles and wireless sensors.

In Fig. 5.9, the impact of energy buffer size $B_{\max}$ is investigated. The horizontal axis is $B_{\max}/\bar{P}_{in}$. It is shown in Fig. 5.9 that when the energy buffer size increases, the OP of the both the asymptotic-optimal policy proposed in [56] and of the EUP relying on our 2D-search Algorithm 5.1 improves, and they would converge to that of their conventional non-EH counterparts. However, as the energy buffer size B_{max} increases, the EUP found by the 2D-search Algorithm 5.1 may achieve a much better OP, when the energy buffer size is small, and it may converge to that of its non-EH counterpart. This confirms the superiority of the proposed search algorithms conceived for EH systems having a finite energy buffer, especially when the available size of the energy buffer is severely limited.

5.3 SDMA-EH Network Design

In the previous section the EUPs conceived for minimizing the OP of P2P networks were investigated. In this section, we continue by investigating the EUP design of more generalized multiple access EH-SNs. Let us consider non-orthogonal-multiple-access (N-ODMA) EH-networks, where a spatial-division-multiple-access (SDMA) network and a SDMA-aided two-hop relay sharing network are investigated. There are two challenges in optimizing the EUPs in SDMA networks, which are as follows:

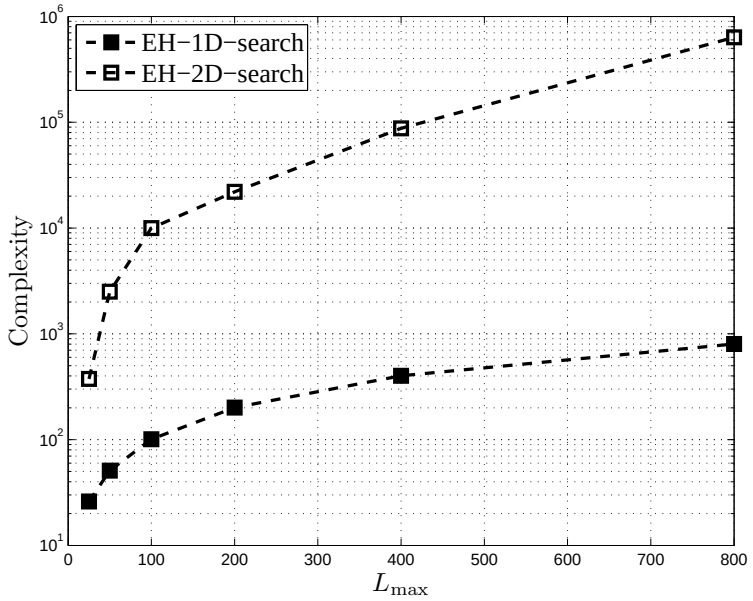

Figure 5.8: Computational complexity in terms of the number of OP evaluations versus the discrete energy buffer size $L_{\max}$ for the 1D-search and the 2D-search algorithms for the P2P network. The results were evaluated via simulations.

- Compared to the P2P network, the outage events of different EH-SNs are correlated, but a centralized optimization would impose an excessive formidable complexity. Even if a sub-optimal one-dimensional search space is adopted for each EH-SN, a M-dimensional search space is required for a SDMA network of M EH-SNs, which is generally not practical. Furthermore, the global knowledge of the channel quality between each EH-SN and the DN as well as the statistical distribution of the energy arrival rates should be available at a central controller node, which also imposes a high complexity.
- For traditional non-EH SDMA networks, the closed-form OP expressions are not available in the open literature for generalized SDMA networks having M SNs. Therefore, to derive the closed-form OP expressions for EH SDMA networks is quite challenging.

Against this background, in this section, our novel contributions on optimizing the EUPs are as follows:

1. *We embark on the OP analysis of an SDMA network relying on ML detection and use the minimum-signal-to-noise-ratio (min-SNR) approximations as in Chapter 3 and Chapter 4 in order to arrive at the approximate OP of our SDMA networks, which has been documented in [105,127]. It will be shown that the min-SNR approximations are accurate in predicting the OP of the SDMA networks.*
2. *Given an SDMA network comprised of M EH-SNs and a DN, we decompose the approximate joint OP of SDMA into a product of M mutually-independent*

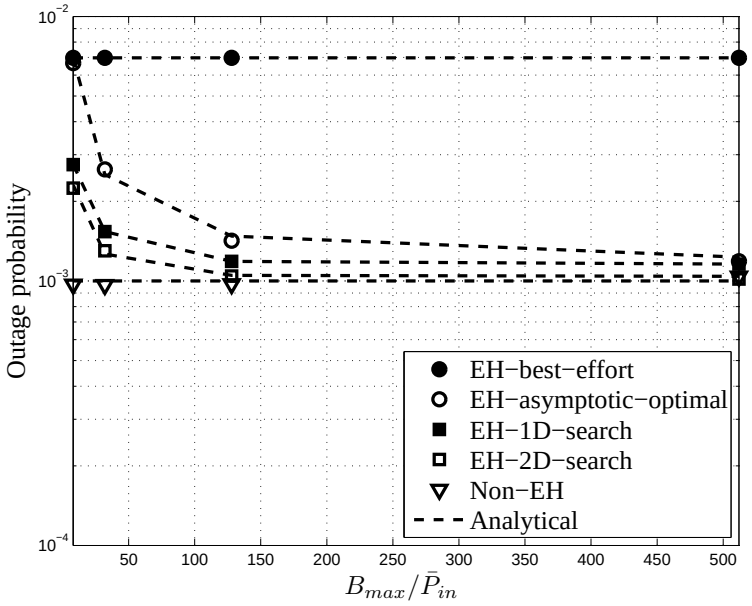

Figure 5.9: OP versus the energy buffer size $B_{\max}$ using different energy policies for the P2P network considered. The average energy arrival rate is $\bar{P}_{in} = 10$dBm, and $R = 1$ bits/sec/Hz,$T_E = 8T_C$. The analytical OP results were evaluated from Eq. (5.11).

OP components, each of which corresponds to a P2P EH-network counterpart. Then we propose a distributed EUP optimization protocol, in which each EH-SN is capable of optimizing its own EUP based on the 2D-search and 1D-search algorithms of Section 5.2, using the statistics of its own uplink channel and its own energy arrival rates, indicating that only local knowledge is required.

3. *As a further application of our distributed EUP optimization protocol, we investigate an SDMA-aided two-hop relay-sharing network. We derive the end-to-end (e2e) OP for an arbitrary number of EH-SNs and an arbitrary relay position when communicating over Rayleigh block fading channels. With the aid of the min-SNR approximation and the 2D-search and 1D-search algorithms of Section 5.2, we may optimize the position of the relay node (RN) for minimizing the e2e OP.*

5.3.1 System Model and OP Formulation

We consider a network of $(M + 1)$ nodes, where M SNs $\{S_m, 1 \leq m \leq M\}$ transmit their individual information to a common DN and each SN is equipped with a harvesting system and an energy buffer, as shown in Fig. 5.1. We assume a narrowband Rayleigh block fading channel model, where the fading coefficients remain constant for the duration of a packet and then they are faded independently from one packet to another both in time and space. The additive noise imposed by the receivers is

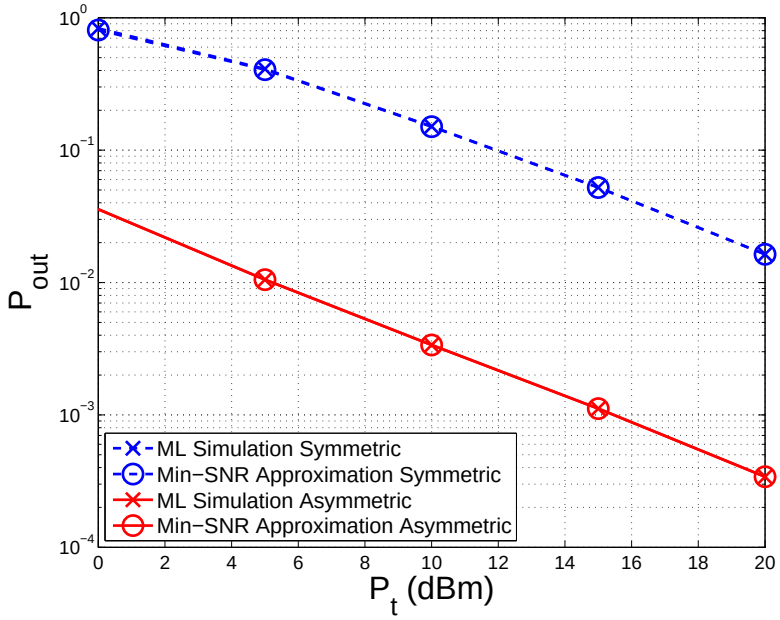

Figure 5.10: The accuracy of the OP evaluation using the min-SNR approximations for $M = 4$, $R = 0.5$bps/Hz. The distance between the SNs and the DN is $d_{sd} = 100$ m and the path-loss exponent is $\beta = 3$.

modeled by independent zero-mean circularly symmetric complex Gaussian random variables with a variance of unity.

The DN is assumed to have perfect channel knowledge and adopts maximum likelihood (ML) detection. All the SNs transmit their messages concurrently at the rate of R. The SN S_m encodes a bit sequence into a codeword and transmits it to the DN, where the DN jointly decodes the codewords received from all the SNs. Therefore, the SN-DN hop may be modeled by a multiple access channel (MAC) and the criterion used for successful decoding is to satisfy

$$\sum_{m\in S} R \leq \log\left(1+\sum_{m\in S}\gamma_{md}\right), \forall S \subseteq \{S_m, 1 \leq m \leq M\}, \tag{5.21}$$

where γ_{md} represents the instantaneous received SNR of the S_m-DN link. There are $(M! - 1)$ inequalities in Eq. (5.21) and if any of the inequalities in Eq. (5.21) are not satisfied, the transmission over the SN-DN hop becomes erroneous. Hence, when the minimum SNR of the M channels spanning from the SNs to the RN, defined as $\gamma_{sd}^{min} = \min_{m\in S}\gamma_{md}$ is smaller than the threshold $\gamma_{th}^{sd} = 2^R - 1$ to be exceeded for successful decoding, an outage event occurs. Therefore, we aim for modelling the OP of the M-user MAC on the SN-RN hop with the aid of the specific SN-RN link having the minimum SNR γ_{sd}^{min}. We have evaluated the accuracy of the min-SNR approximations in Chapter 4, but we repeat the comparison here in Fig. 5.10 for readers' convenience.

Specifically in Fig. 5.10 we compare the OP of the M-user MAC channel using ML detection to that of a single link having the minimum SNR γ_{sd}^{min} of the M-user system. As shown in Fig. 5.10, the OP of the two systems obtained by simulation are perfectly matching for both symmetric and asymmetric topologies. In the symmetric topology, the average channel quality of the link spanning from each SN to the DN is identical, while in the asymmetric topology the average channel quality is different. It is shown in Fig. 5.10 that for both topologies, the exact OP of the M-user MAC channel and the predicted OP using the P2P channel associated with the min-SNR are identical. Hence the OP using the min-SNR approximation may be expressed as:

$$\begin{aligned} P_{out,SD} &\approx \Pr\left\{\min_{m\in S}\gamma_{md} < \gamma_{th}^{sd}\right\} \\ &= 1 - \Pr\left\{\min_{m\in S}\gamma_{md} \geq \gamma_{th}^{sd}\right\} \\ &= 1 - \prod_{m\in S}\Pr\left\{\gamma_{md} > \gamma_{th}^{sd}\right\} \\ &\triangleq 1 - \prod_{m\in S}\left(1 - P_{out,md}\right). \end{aligned} \tag{5.22}$$

5.3.2 Distributed EUP Optimization Protocol

With the aid of the min-SNR approximation, we may now formulate the OP minimization problem for the SDMA-EH network as:

$$\min_{L_{t,1}(l),L_{t,2}(l),...,L_{t,m}(l)} \quad P_{out,SD}\left[L_{t,1}(l), L_{t,2}(l), ..., L_{t,m}(l)\right], \tag{5.23}$$

where $L_{t,1}(l), L_{t,2}(l), ..., L_{t,m}(l)$ corresponds to the discrete EUPs at the SNs. Equivalently, the minimization problem defined in Eq. (5.23) may be expressed by

$$\max_{L_{t,1}(l),L_{t,2}(l),...,L_{t,m}(l)} \quad 1 - P_{out,SD}\left(L_{t,1}, L_{t,2}, ..., L_{t,m}\right). \tag{5.24}$$

Let us now investigate the formulation of $1 - P_{out,SD}\left(L_{t,1}, L_{t,2}, ..., L_{t,m}\right)$ in detail. By using the min-SNR approximation of Eq. (5.22), we have

$$1 - P_{out,SD}\left(L_{t,1}, L_{t,2}, ..., L_{t,m}\right) \approx \prod_{m\in S}\left[1 - P_{out,md}\left(L_{t,m}\right)\right]. \tag{5.25}$$

In order to maximize the objective function in Eq. (5.24), we may maximize each component of $\left[1 - P_{out,md}\left(L_{t,m}\right)\right]$ since they are mutually independent or equivalently, minimizing each component $P_{out,md}\left(L_t\right)$. This is an beneficial, because the m-th component $P_{out,md}\left(L_{t,m}\right)$ corresponds to the OP of a P2P-EH link spanning from the m-th EH-SN to the DN, while it is independent of both the channel quality as well as the EUPs adopted by other EH-SNs.

Therefore, we may design a distributed EUP optimization (DEUPO) protocol, in which each EH-SN optimizes its own EUP relying on the proposed 1D-search and 2D-search algorithms proposed for a P2P link in Section 5.2. Specifically, we design the medium-access-control (MAC) protocol as follows:

- **Acquiring the Energy Arrival Rate and Channel Statistics:** In practical applications, the system designer may choose appropriate EHI and CSI estimation algorithms, through which the system may detect the changes, generate a trigger and decide when to activate its EUP optimization. This is a widely used event-triggered protocol [128, 129]. A simpler solution is to periodically invoke the EUP optimization, according to the instantaneous estimated statistics of the energy arrival rates as well as the channels. This is however beyond the scope of this work. Instead, we focus our attention on the issue of deciding the EUP, whenever the optimization is activated. In our analysis we assume that both the estimated energy arrival rate and the channel statistics are perfectly estimated. Hence each EH-SN has perfect knowledge of the statistics of energy arrival rate, while the DN has the knowledge of the statistics of the uplink (UL) channels spanning from each EH-SN. In practice this knowledge is acquired with the aid of pilot based channel estimation mechanism and/or prediction methods.
- **Local EUP Optimization Phase:** Each SN sends a request-to-send (RTS) packet to the DN. The DN would send M clear-to-send (CTS) packets to the M SNs and the channel statistics between the m-th EH-SN and the DN would be conveyed in each CTS packet, which is assumed to be perfectly recovered at the EH-SNs. Then, each EH-SN may adopt the 2D-search of Section 5.2.3 or the 1D-search of Section 5.2.4 to find the approximate EUP for our P2P-EH network. As discussed in the context of Eq. (5.25), our design objective is to minimize the approximate OP of the SDMA-EH network considered.
- **Data Transmission Phase:** Each EH-SN commence its session by transmitting to the DN by relying on its locally optimized EUP.

In the next section, we will apply our DEUPO protocol to SDMA-aided relay sharing EH networks, while a numerical results characterizing the SDMA-EH networks and the SDMA-aided relay sharing EH networks are provided in Section 5.3.3.

5.3.3 Numerical Results

In Fig. 5.11, the OP of our SDMA-EH network is investigated and the EUPs found by the proposed 2D-search and 1D-search algorithms of Section 5.2 are compared to that of the best-effort policy and asymptotic-optimal policy. It is shown that for the given configurations, the OPs achieved by the proposed algorithms are better than those of the benchmarks. Furthermore, it is shown that the analytical results represented by dashed curves closely match the simulation results, which indicates

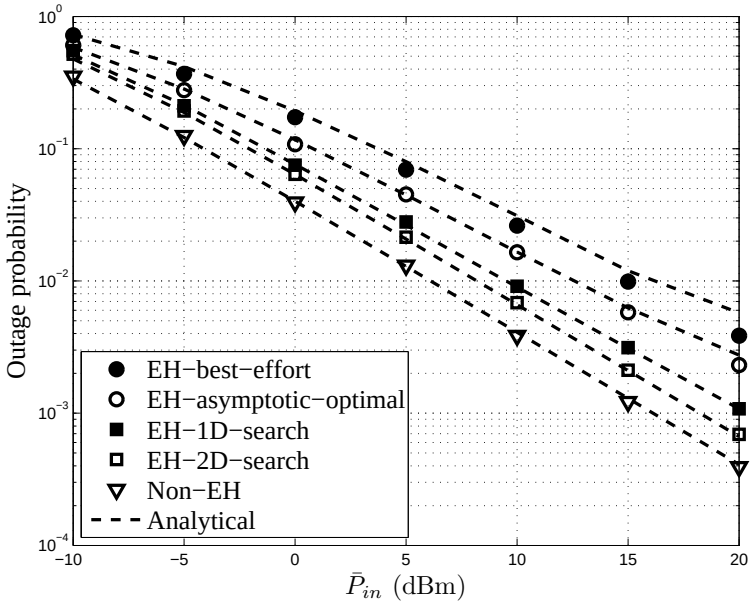

Figure 5.11: OP versus average energy arrival rate $\bar{P}_{in}$ using different energy policies for the SDMA network associated with $M = 4$ SNs. The energy buffer size $B_{max} = 16\bar{P}_{in}$, $R = 1$ bits/sec/Hz, $T_E = 8T_C$. The analytical OP results were evaluated from Eq. (5.22).

that the proposed min-SNR approximation as well as the DMC based analytical framework are accurate.

Specifically, the 2D-search algorithm performs within 2 dB from its non-EH counterpart at $P_{out} = 10^{-2}$, which serves as the lower-bound of the OP for EH systems [56]. At $P_{out} = 10^{-2}$, the EUP found by the 2D-search algorithm achieves a 4.6dB gain compared to the asymptotic-optimal policy and an 8dB gain compared to the best-effort policy. Therefore, if an EH-SN adopts the asymptotic-optimal EUP, it requires $10^{4.6/10} \approx 2.9$ times higher average energy arrival rates harvested from the environment, compared to an EH-SN equipped with the proposed 2D-search algorithm at $P_{out} = 10^{-2}$. This ratio would be further increased to a factor of 6.3, if the benchmark EH-SN adopts the best-effort policy. The 1D-search algorithm is sub-optimal, hence it exhibits a performance degradation of 1.4dB compared to that of the 2D-search algorithm at $P_{out} = 10^{-3}$. From a different perspective, an EH-SN adopting our 1D-search algorithm may require 1.4 times higher energy arrival rate, which is the price paid for its reduced computational complexity. In our future work we will jointly consider the optimization of the energy arrival rate and of the power savings of the reduced-complexity algorithms. This might in fact favor the 1D algorithm over its 2D counterpart. The resultant EUPs are illustrated in Fig. 5.12, which shows similar results to those of the P2P-EH networks, because the DEUPO protocol actually decomposes the SDMA-EH network into M P2P-EH sub-networks.

Similar to the trends observed in Fig. 5.13 for P2P-EH networks, in a SDMA-EH

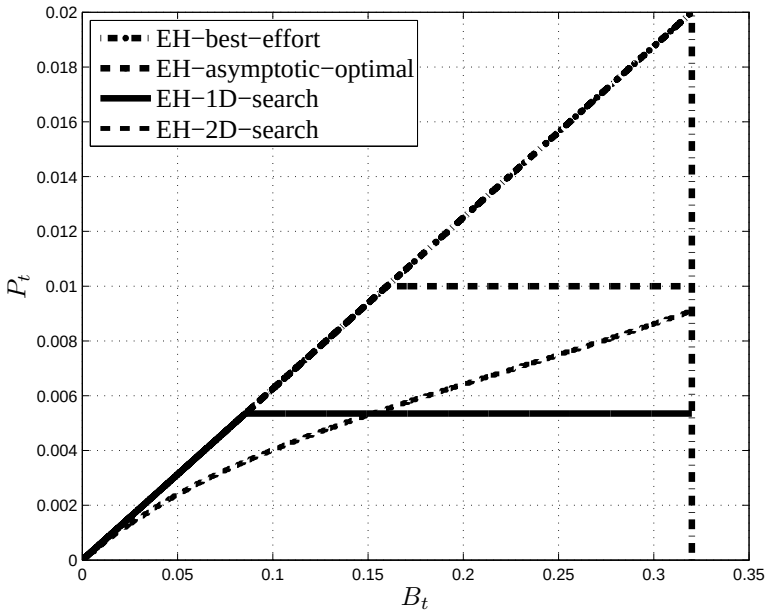

Figure 5.12: Illustration of different EUPs for the SDMA network. The average energy arrival rate $\bar{P}_{in} = 10$dBm, while the energy buffer size is $B_{max} = 16\bar{P}_{in}$, and the $R = 1$ bits/sec/Hz, $T_E = 8T_C$. The results were evaluated via simulations.

networks, the OP of both the asymptotic-optimal EUP proposed in [56] and that of the EUP found by the 2D-search algorithm improves, when the energy buffer size at the EH-SNs increases, and they would both converge to their non-EH counterparts. The superiority of the proposed 2D-search algorithms is retained for SDMA-EH systems having a finite energy buffer size, especially when the size of the energy buffer is small, as demonstrated in Fig. 5.13.

Finally, we investigate the effects of the number of EH-SNs on the OP in SDMA-EH networks. It is shown in Fig. 5.14 that as the number of SNs M increases, the OP of all EUPs is reduced. However, the EUPs found by the proposed 2D-search and 1D-search algorithms always outperform both the asymptotic-optimal policy and the best-effort policy. The results allow the SDMA-EH network to accommodate more users, while maintaining the same reliability. For example, if a maximum OP of $P_{out} = 10^{-2}$ is tolerable in the SDMA-EH network, both the best-effort policy and the asymptotic policy may be capable of supporting $K = 2$ and 4 users, while the 1D-search and the 2D-search algorithms support more than $K = 8$ users simultaneously.

To conclude, given the proposed 1D-search and 2D-search algorithms, a receiver is capable of simultaneously offering reliable UL services for significantly more EH-users. We exploit this benefit in the SDMA-aided relay-sharing network considered, where a EH-RN is serving multiple EH-SNs by relaying their messages to a common DN.

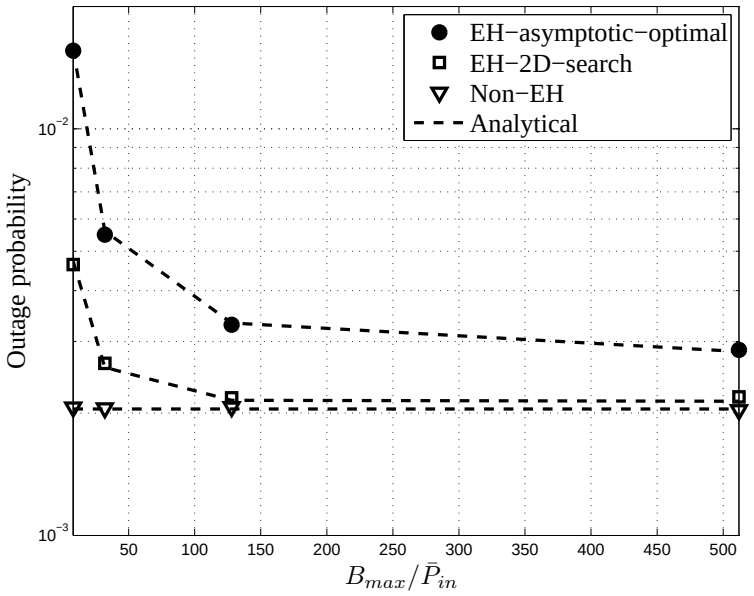

Figure 5.13: OP versus the energy buffer size $B_{t,\max}$ using different EUPs for the SDMA network associated with $M = 4$ SNs. The average energy arrival rate is $\bar{P}_{in} = 10$dBm, and $R = 1$ bits/sec/Hz, $T_E = 8T_C$. The analytical OP results were evaluated from Eq. (5.22).

5.3.4 SDMA-aided Relay Sharing EH Network Design

In this section, the DEUPO protocol is applied to SDMA-aided relay sharing EH networks, such as that depicted in Fig. 5.15. In addition to the EUP of each EH-SN, that of the EH-RN as well as the specific effects of the RN's position are optimized. First, the system model will be described in Section 5.3.4.1, followed by the OP minimization in Section 5.3.4.2.

5.3.4.1 System Model

As shown in Fig. 5.15, we consider a network supporting $(M + 2)$ nodes, where M EH-SNs $\{S_m, 1 \leq m \leq M\}$ transmit their individual information to a common DN with the aid of a single EH-RN. The SN-RN hop is a EH-SDMA network associated with M EH-SNs, while the RN-DN hop is a EH-P2P network. Each node is equipped with a harvesting system, a finite energy buffer as well as a transmitter, as shown in Fig. 5.1. The transmitter is equipped with a single antenna and operates in a half-duplex mode. We assume a narrow-band Rayleigh block fading channel model, where the fading coefficients remain constant for the duration of a packet and then they are faded independently from one packet to another both in time and space. The direct links between the SNs and the DN are to be weak, hence we rely on relaying for improving the UL performance of the SNs. The additive noise at the receivers is modeled by independent zero-mean circularly symmetric complex Gaussian random variables.

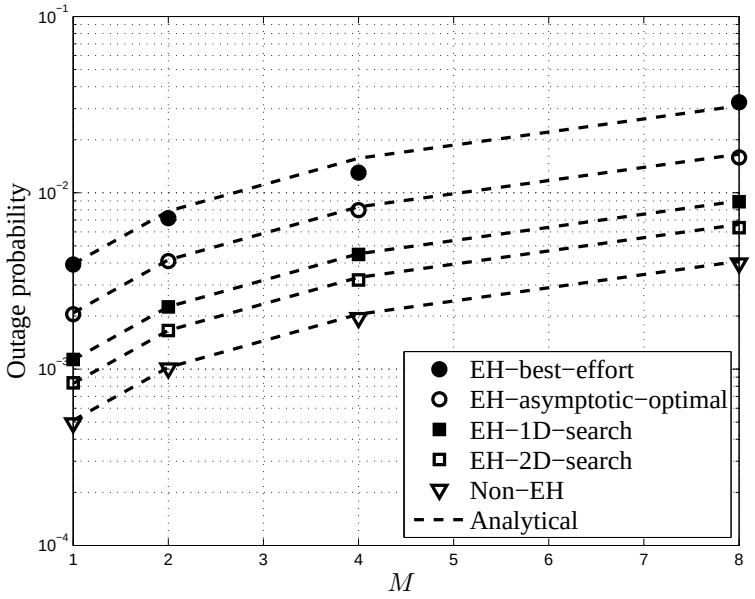

Figure 5.14: OP versus average energy arrival rate $\bar{P}_{in}$ using different energy policies for the SDMA network associated with different number of SNs $M = 1, 2, 4, 8$. The average energy arrival rate is $\bar{P}_{in} = 10$dBm, the energy buffer size is $B_{max} = 16\bar{P}_{in}$ and $R = 1$ bits/sec/Hz, $T_E = 8T_C$. The analytical OP results were evaluated from Eq. (5.22).

The receivers are assumed to have perfect channel knowledge and adopt ML detection. Due to the fact that ML detection results in joint success or outage events, the packets received from the M SNs are either all successfully recovered or corrupted concurrently. Therefore, if the ML detection is successful, all the M codewords are stored in the RN's data buffer, otherwise all the codewords are discarded. We consider a traditional relay-sharing network operating without hop selection, which may be left for our future work. In the first TS, all the SNs transmit their messages concurrently at the rate of R, where the RN listens. The SN S_m encodes a bit sequence b_m into a codeword c_m and transmits it to the RN, where the RN jointly decodes the codewords received from all the SNs. Therefore, the SN-RN hop may be modeled by a multiple access channel and the criterion used for successful decoding is to satisfy

$$\sum_{m\in S} R \leq \log\left(1 + \sum_{m\in S} \gamma_{mr}\right), \forall S \subseteq \{S_m, 1 \leq m \leq M\}, \tag{5.26}$$

where the γ_{mr} represents the instantaneous received SNR of S_m-RN link. The decoded bit sequences $\{\widetilde{b}_1, \widetilde{b}_2, \ldots, \widetilde{b}_m\}$ are concatenated and inserted into the data buffer as a frame. In the next TS, the RN fetches the frame from the data buffer, re-encodes the messages at the rate of MR and transmits them to the DN, where the criterion

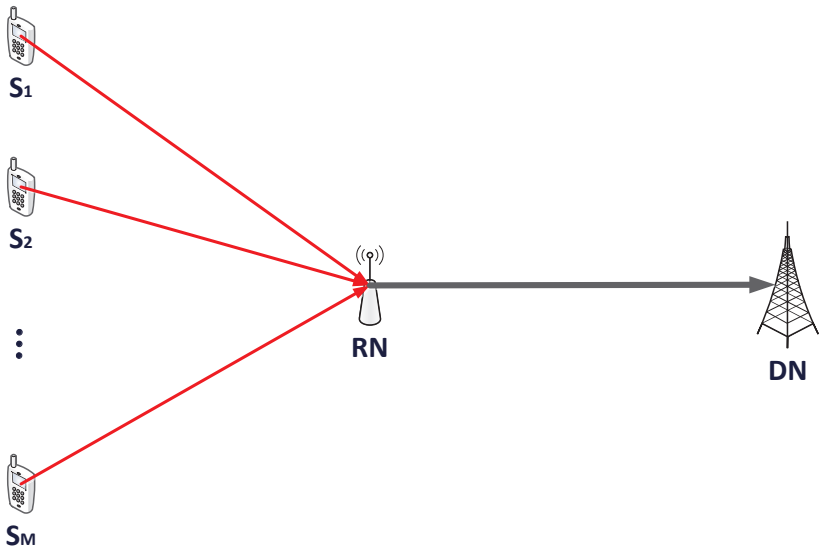

Figure 5.15: System model of an SDMA-aided Relay Sharing EH Network.

for successful decoding is to satisfy

$$MR \leq \log\left(1+\gamma_{rd}\right), \tag{5.27}$$

where γ_{rd} represents the instantaneous received SNR at the DN. This formulation assumes perfect capacity-achieving coding.

5.3.4.2 OP Minimization

An outage event is defined as the event, when any of the codewords from the SNs is incorrectly recovered at the DN. The e2e OP of the two-hop system may be expressed as

$$P_{out,e2e} = 1-\left(1-P_{out,SR}\right)\left(1-P_{out,RD}\right), \tag{5.28}$$

where the $P_{out,e2e}$ represents the e2e OP of the entire system, while $P_{out,SR}$ and $P_{out,RD}$ stand for the OP over the SN-RN and of the RN-DN hop, respectively.

Since the OP of the RN-DN hop $P_{out,RD}$ is independent of that of the SN-RN hop $P_{out,SR}$, the EUP at the EH-RN may be optimized locally, using the statistics of the energy arrival rate at the EH-RN as well as at the RN-DN channel, which is a P2P-EH network design problem and can be optimized using the 2D-search and 1D-search solutions proposed in Section 5.2. On the other hand, the SN-RN hop may be modeled as a SDMA-EH network and hence the DEUPO protocols proposed in Section 5.3.4.2 may be invoked for optimizing the EUP of each EH-SN. It may be concluded that the OP minimization problem of SDMA-aided relay sharing EH networks can be decomposed into $(M+1)$ independent sub-problems, where each EH-SN and the RN may optimize the EUP based on local knowledge of both the

energy arrival rate and of the channel statistics. Compared to that of the SDMA-EH and P2P-EH networks, the number of SNs as well as the location of the RN plays an important role in the SDMA-aided relay sharing EH networks considered. Specifically, the number of SNs directly affects the OP $P_{out,SR}$ of the SN-RN hop. Furthermore, it determines the transmission rate required by the RN, which increases linearly with the number of SNs and it substantially affects the OP $P_{out,RD}$ of the RN-DN hop. Similarly, the RN location substantially affects the quality of both the SN-RN as well as of the RN-DN hops. However, it is quite a challenge to optimize the RN locations, when the channel quality of the links obeys different statistics. Finally, the e2e OP may be dominated by the RN-DN hop, because the RN is shared among multiple SNs.

5.3.4.3 Results for the SDMA-aided Relay Sharing EH network

In this section, the numerical results characterizing our SDMA-aided relay sharing EH networks are shown. In Fig. 5.16, the OP of the SDMA-aided relay sharing EH network is investigated. It is shown that for the given configurations, the OPs achieved by the proposed 1D-search and 2D-search algorithms are better than those achieved by the best-effort and asymptotic-optimal policy. These improvements are plausible according to our previous observations made in the context of P2P-EH networks and the SDMA-EH networks, which build up the second and the first hop in the SDMA-aided relay sharing EH network, respectively. In Fig. 5.17, the superiority of the proposed algorithms is retained, regardless of the relay positions. It is shown that the analytical results represented by dashed curves closely match the simulation results, which indicate that the proposed min-SNR approximation as well as the DMC based analytical framework are accurate.

Let us now investigate the effects of the number of EH-SNs on the OP of our SDMA-aided relay sharing EH networks. It is shown in both Fig. 5.18 and Fig. 5.19 that as the number of SNs M increases, the OP of all the EUPs is increased. The superiority of the proposed 2D-search and 1D-search algorithms is retained, which is in line with our observation made both for our P2P-EH networks and the SDMA-EH networks.

However, observe by comparing Fig. 5.14 and Fig. 5.18, the SDMA-aided relay sharing EH networks is inferior to that observed in the SDMA-EH network. For example, it may be seen in Fig. 5.14 a maximum OP of $P_{out} = 10^{-2}$ is tolerable in the SDMA-EH network, the best-effort policy and the asymptotic policy may support $K = 2$ and $K = 4$ users, while the 1D-search and the 2D-search algorithms are capable of supporting $K = 8$ users simultaneously. By comparison, the SDMA-relay sharing network is only capable of accommodating at most 2 users, even when the most powerful 2D-search algorithm is adopted. These observations are not surprising, on the basis of our experience concerning the relay-sharing mechanisms offered in

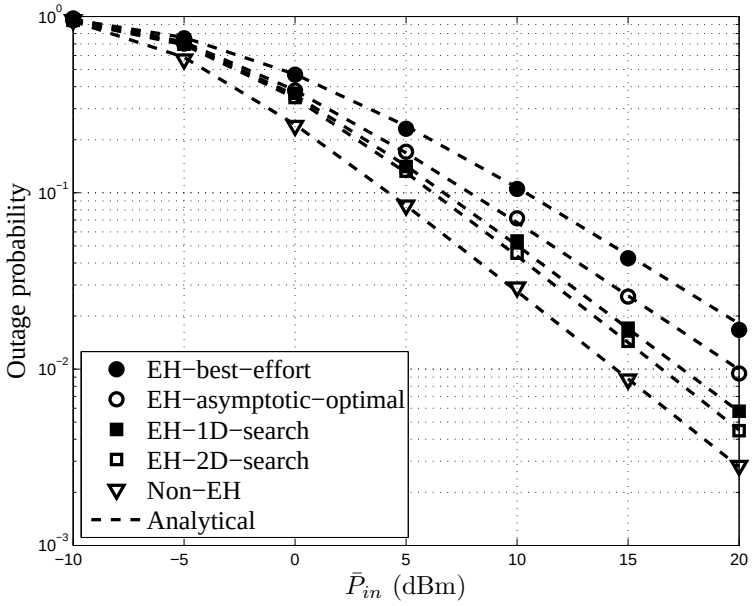

Figure 5.16: OP versus average energy arrival rate $\bar{P}_{in}$ using different EUPs for the SDMA-aided relay sharing network associated with $M = 4$ SNs, the energy buffer size is $B_{max} = 16\bar{P}_{in}$, and $R = 1$ bits/sec/Hz, $T_E = 8T_C$. The analytical OP results were evaluated from Eq. (5.28).

Chapter 3 and Chapter 4 for non-EH networks. As for the relay-sharing EH networks, the bottleneck is constituted by the second hop, where the P2P-EH link in the RN-DN hop incapable of accommodating a data rate that increases linearly according to $R_{RD} = MR$. The fundamental reason for this observation is as follows:

According to Shannon's theorem, the maximum achievable rate may be expressed as $R = \log(1+\frac{P_t G}{N_0})$ *bits/sec/Hz, where* P_t *is the transmission power,* G *is the channel gain and* N_0 *is the noise power. The logarithmic capacity function suggest that if the RN-DN hop is expected to accommodate a data rate that increases linearly, the required transmission power* P_t *should increase exponentially, which is excessive. This trend may be circumvented with the aid of MIMO techniques, which are potentially capable of increasing the throughput linearly at the cost of a linear power increase. Hence it is promising to combine EH techniques with MIMO techniques. Ultimately, the performance of EH systems is always bounded by their non-EH counterparts, in both conventional SISO and in the more power-efficient MIMO scenarios [56]. The main benefit of EH techniques lies in the fact that by harvesting energy from the environment, the network lifetime of wireless systems can be extended.*

5.4 Conclusions

In this chapter, we summarized the state-of-the-art EUP design aiming for minimizing OP of P2P-EH networks based on the literature and proposed two novel algorithms, which are capable of exploiting the harvested energy stored in a finite energy

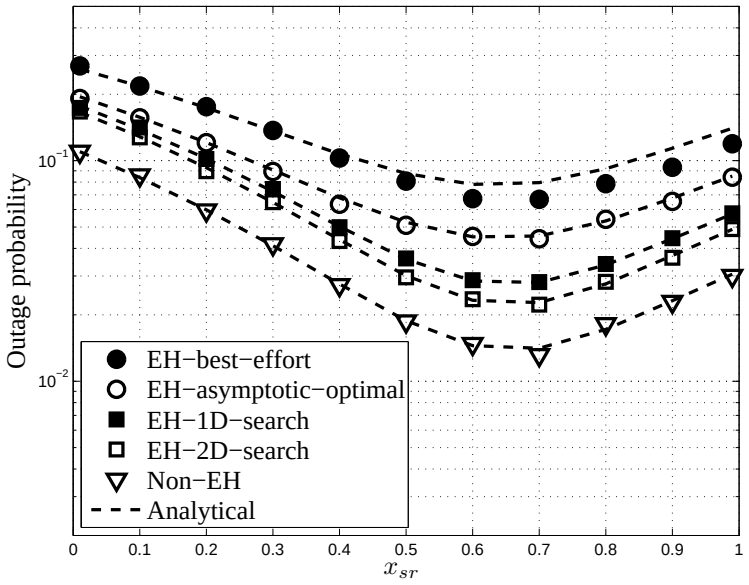

Figure 5.17: OP versus the RN position for different EUPs in the SDMA-aided relay sharing network associated with $M = 4$ SNs, the energy buffer size is $B_{max} = 16\bar{P}_{in}$, and $R = 1$ bits/sec/Hz, $T_E = 8T_C$. The analytical OP results were evaluated from Eq. (5.28).

Target OP		@10^{-1}	@10^{-2}	@10^{-3}
$\bar{P}_{in}$(dBm) of	Best-Effort [55]	-4.8	8.1	20.1
	Asymptotic-Optimal [56]	-6.8	5.1	16.8
	1D-Search	-7.8	2.9	13.6
	2D-Search	-8.0	2.0	12.0
	Non-EH	-10.0	0.0	10.0

Table 5.1: Summary of average energy arrival rate $\bar{P}_{in}$ in dBm at different OPs for the different EUPs for transmissions over P2P channels, which is extracted from Fig. 5.5.

buffer. Upon invoking the min-SNR approximation of Section 5.3.2, the proposed algorithms of Section 5.2 were invoked for SDMA-EH networks and the distributed EUP optimization protocol of Section 5.3.2 was designed.

In Table 5.1, the performance of the different EUPs is summarized. Given the target OP, the required average energy arrival rate $\bar{P}_{in}$ is quantified for different EUPs. The energy buffer size was set to $B_{max} = 16\bar{P}_{in}$ and the transmission rate was $R = 1$ bits/sec/Hz, while the energy arrival fading duration T_E was 8 times the channel's fading duration T_C. Observe in Table 5.1 that the OP of the EUPs based on the proposed 2D-search and 1D-search algorithms of Section 5.2.3 and 5.2.4 is better than that of the benchmarks of [56] and [55]. Furthermore, the EUP optimized by the 2D-search algorithm achieves the lowest OP and performs within about 2 dB of its

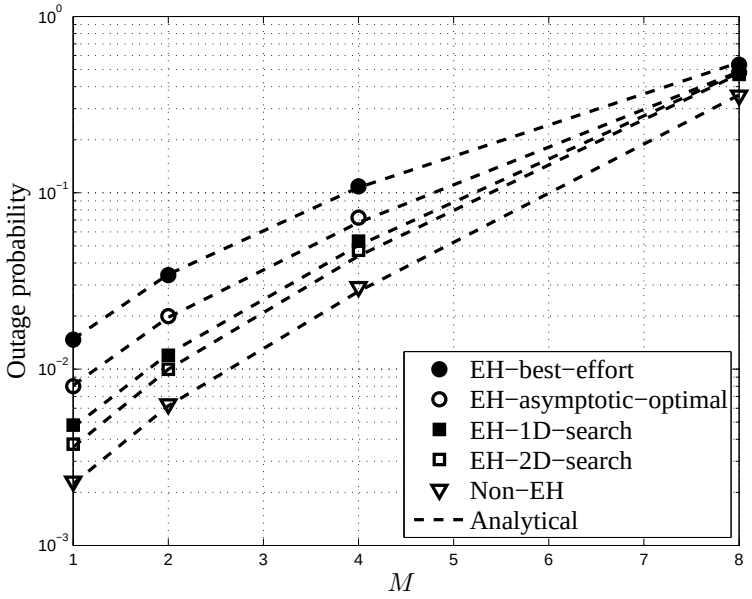

Figure 5.18: OP versus average energy arrival rate $\bar{P}_{in}$ using different EUPs for the SDMA-aided relay sharing network associated with different number of SNs $M = 1, 2, 4, 8$. The average energy arrival rate is $\bar{P}_{in} = 10$dBm, the energy buffer size is $B_{max} = 16\bar{P}_{in}$ and $R = 1$ bits/sec/Hz, $T_E = 8T_C$. The analytical OP results were evaluated from Eq. (5.28).

Target OP		@10^{-1}	@10^{-2}	@10^{-3}
$\bar{P}_{in}$(dBm) of	Best-Effort [55]	3.8	16.0	28.1
	Asymptotic-Optimal [56]	0.9	12.7	24.1
	1D-Search	-1.3	9.4	20.4
	2D-Search	-2.1	8.1	18.1
	Non-EH	-4.1	6.1	16.1

Table 5.2: Summary of average energy arrival rate $\bar{P}_{in}$ in dBm at different OPs for the different EUPs for transmissions over SDMA channels, which is extracted from Fig. 5.11.

the non-EH counterpart, which represents the OP lower-bound for EH systems. The EUP optimized by the 1D-search algorithm performs within about 2.9 dB and 3.6 dB of the non-EH benchmarks, albeit their discrepancy increases at lower target OP. However, the 1D-search algorithm imposes a lower computational complexity than its 2D-search based counterparts. Overall, the EUPs optimized by the proposed 2D-search algorithm significantly outperform the EH benchmarks found in the open literature. Quantitatively, our solutions attain gains up to 3 dB at $P_{out} = 10^{-2}$ and this gain will increase even further at lower target OPs.

With the advent of the DEUPO protocols proposed in this chapter, the proposed 1D- and 2D-search algorithm requires a significantly lower energy arrival rate at a

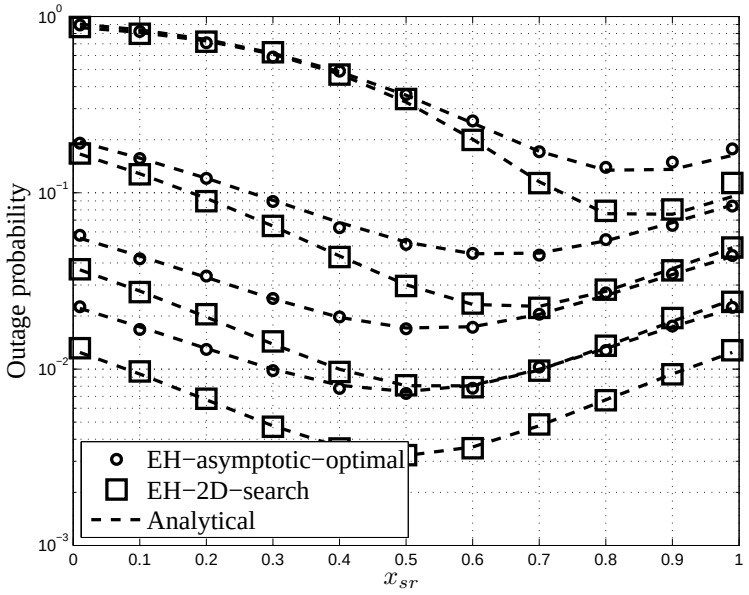

Figure 5.19: OP versus the RN position for different number of SNs $M = 1, 2, 4, 8$ in the SDMA-aided relay sharing network. The energy buffer size is $B_{max} = 16\bar{P}_{in}$ and $R = 1$ bits/sec/Hz, $T_E = 8T_C$. The analytical OP results were evaluated from Eq. (5.28).

given target OP. The results recorded for $M = 4$ SNs are summarized in Table 5.2. The EUPs found by the proposed 2D-search algorithm outperform the EH benchmarks provided of [56] and [55] in excess of 4 dB at $P_{out} = 10^{-2}$.

Chapter 6

Conclusions and Future Works

Firstly, we summarise the main findings of our research in Section 6.1. Then, our design guidelines are presented in Section 6.2. Finally, a range of ideas concerning our future research is presented in Section 6.3.

6.1 Conclusions

In this thesis, we have investigated spectrum-sharing techniques in multi-source relaying networks for the sake of enhancing the achievable outage probability (OP). More specifically, we proposed several spectrum-sharing schemes, where interference-cancellation (IC) techniques were adopted at the destination nodes (DNs) and/or the relay nodes (RNs). Table 6.1 summarizes the basic characteristics of all the multi-source relaying schemes proposed in this thesis.

1. In Chapter 2, in order to characterize the systems contaminated by co-channel interference (CCI), in Section 2.2.2 we investigated the OP of relay networks in the presence of CCI, when the RNs adopt either SUD or MUD-SIC receivers. Then, in Section 2.2.3 we proposed an outage-optimal BED-ORS for both systems based on a best-effort detection criterion. The proposed systems were shown in Fig. 2.5 -2.9 to outperform both the non-cooperative system and the system employing SUD receivers at the DN, while the MUD-SIC-aided system achieved a significant OP performance improvement with the aid of the BED-ORS of Section 2.2.3. Additionally, an optimised BED-ORS scheme was designed in Section 2.2.4, which was shown in Fig. 2.10 to have an improved robustness against a degraded CSI accuracy imposed by outdated CSI.
2. Although the proposed BED-ORS schemes of Section 2.2.3 significantly reduce the OP of relay networks, the CCI imposed a BER/FER floor in the high SNR region of Fig. 3.12. In order to mitigate this performance erosion, in Chapter 3 we adopt the network coding (NC) scheme, where CCI effects were mitigated with the aid of relay sharing, while simultaneously enhancing the

Design Options	MAC Protocol		Relay Processing	
	Hop Activation	Source Access	Receiver Processing	Transmitter Processing
Chapter 2	Fixed	SDMA	DF, MUD-SIC or SUD	Spatial Division
Chapter 3	Fixed	TDMA	DF, SUD	Network Coding
Chapter 4	Dynamic	SDMA	DF, ML or MUD-SIC	Time-Division Multiplexing
Chapter 5	Fixed	SDMA	DF, ML	Time-Division Multiplexing

Table 6.1: Summary of Design Options for Multi-Source Relaying Networks

throughput of both multi-user multi-unicast networks as evidenced by Fig. 3.2. Specifically, in Section 3.1 we considered a network supporting multiple SN-DN pairs communicate with the aid of a single RN. In Section 3.2 a closed-form OP expression was derived, which was verified our simulation results in Fig. 3.6 and Fig. 3.9. The results explicitly quantified the detrimental effects of NC noise imposed on NC-CC schemes. As the number of source nodes (SNs) increases, the attainable throughput improvement saturates owning to having an increased NC noise, which results in a degraded OP as seen in Fig. 3.6 and 3.7. In Section 3.3, the analytical expressions were applied to relay selection schemes conceived for network-coded relay-sharing scenario.

3. In Chapter 4, we have proposed and investigated a multi-user buffer-aided-relaying uplink protocol conceived for a two-hop system. When the direct links between the SNs and the DN may be weak and negligible, relaying is introduced for improving the uplink. It was shown in Fig. 3.7 the NC based relay-sharing schemes may in fact perform worse than the conventional cooperative networks dispensing with NC. Hence in Section 4.1, we adopted a time-multiplexing-aided relay-sharing scheme, where the RN uses a higher rate for re-encoding the message from multiple SNs, so that the relaying phase is shared among multiple SNs, whilst dispensing with the direct links. In Section 4.3 we analysed both the end-to-end OP and the transmission delay of the proposed protocol. Our analysis and simulation results in Fig. 4.4, 4.7 and 4.8 showed that by exploiting the selection diversity of the SN-RN and the RN-DN hops, significant OP improvements may be achieved at the expense of an increased end-to-end frame delay. The corresponding optimal power allocation scheme was proposed in Section 4.4, which was shown to achieve a better end-to-end OP in Fig. 4.5 and 4.9 than the uniform power allocation scheme.
4. In Chapter 5, we summarized the state-of-the-art energy-usage policies (EUPs) designed for minimizing the OP of P2P-EH networks based on the literature and in Section 5.2 we proposed a pair of novel algorithms, which are capable of exploiting the harvested energy stored in a finite energy buffer. Upon invoking the min-SNR approximation of Section 5.3.1, the proposed algorithms were invoked for SDMA-EH networks and in Section 5.3.2 a distributed EUP optimization protocol was designed. The OP of the EUPs based on the proposed 2D-search and 1D-search algorithms were showed in Fig. 5.5, 5.11 and 5.16 to outperform that of the benchmarks provided by [55] and [56]. The EUP optimized by the 2D-search algorithm of Section 5.2.3 achieves the minimum OP, which provides the OP lower-bound for EH systems. By contrast, the 1D-search algorithm of Section 5.2.4 imposes a lower computational complexity than its 2D-search based counterpart at the cost of a degraded OP. In the scenario of multi-source relaying networks, the distributed-energy-usage-policy-optimization (DEUPO) protocol of Section 5.3.2 was proposed based

on the 1D-search and the 2D-search algorithms, which requires a significantly lower energy arrival rate, given a specific maximum OP.

6.2 Design Guidelines

When designing a multi-source relaying network, we can identify three basic design steps, which are given below:

1. Determining the design specifications, which may be reliability metrics such as the OP or bit/symbol/frame error ratio, or spectrum-efficiency metrics such as the achievable rate or goodput. The complexity metrics also have to be taken into account.
2. Determining the medium access control (MAC) and the relay processing options. We have designed multiple candidate schemes in this thesis, which are summarized in Table 6.1.
3. Evaluating the performance of each solution provided and determining the solution for the system according to the system parameters based on theoretical analysis.

The design steps may be detailed as follows:

- In any wireless transmission system, the design objective plays a vital role, which was the OP in this thesis considered in the context of fixed-rate applications. However, the OP may only be improved at the cost of a reduced network throughput/increased delay/increased complexity, where the specific design trade-off should be carefully defined by considering multiple metrics. For example, although the SUD-aided relaying scheme of Chapter 2 was inferior compared to the MUD-SIC-aided counterpart in terms of the OP, the complexity imposed at the RNs was substantially reduced, especially when the number of sources sharing the spectrum is high. If the maximum tolerable processing complexity at the RN is low, the SUD-aided relaying scheme may be preferred, even though its OP seen in Fig. 2.9 is sub-optimal.
- After determining the design objective, we may propose multiple candidate schemes. First, we may consider the choice of MAC protocols. Specifically, we may first define a particular hop activation scheme and then define the MAC supporting the SNs. Firstly, the link/hop activation schemes may be categorize into fixed and dynamic activation regime. In Chapter 2, Chapter 3 and Chapter 5, we opt for the classic fixed activation scheme, in which the SNs and the RNs take turns to transmit in the adjacent time slots, while in Chapter 4, we proposed a dynamic activation regime, in which the buffer-aided relaying achieves a beneficial hop-selection diversity and hence improve the OP at the cost of an increased delay. Secondly, we define the MAC supporting

the SN-RN hop. For example, in Chapter 3 the classic time-division-multiple-access (TDMA) was adopted, while in Chapter 2, Chapter 4 and Chapter 5, spatial-division-multiple-access (SDMA) was advocated. We may also opt for frequency-division multiple access (FDMA) and code-division-multiple-access (CDMA), etc. Furthermore, a beneficial multi-user diversity may be achieved.

- After defining the MAC protocol, the specific relay signal processing technique should be defined, which is divided into two steps, namely receiver processing and transmitter processing. The relay's receive processing may opt for conventional decode-and-forward (DF) or amplify-and-forward (AF) relaying, where the DF regime is potentially capable of flawlessly recover the received signals at the cost of a higher processing complexity and delay, compared to its low-complexity AF counterpart. It should be noted that if the MAC of SNs relies on non-orthogonal SDMA, the detection technique may choose either from maximum-likelihood (ML) or successive interference cancellation (SIC) in order to facilitate DF relaying.
- Then, in order to facilitate the multiplexing of multiple SNs, the relay's transmitter processing may opt for time-division multiplexing, as adopted in Chapter 4 and Chapter 5, or for network-coding based multiplexing, as advocated in Chapter 3. Another way of simplifying the relay's transmitter processing is to forward the recovered information without multiplexing, while leaving the IC task to the DN, as adopted in Chapter 2.
- After defining both the MAC protocol and the relay processing, the DN's signal processing is designed for recovering the signals gleaned from multiple SNs. If the RN relies on time-division multiplexing, the DN may adopt single-user-detection methods, as exemplified in Chapters 4 and 5. Otherwise, CCI is imposed and the DN should adopt MUD methods as discussed in Chapters 2 and 3.
- When completing the previous steps, we may arrive at several candidate schemes relying on different MAC, relay processing and destination processing options. As shown in our previous chapters, the attainable OP relies on the transmission rate requirements and on the network topology, namely, on the number and the location of the nodes. Therefore, the OP of different candidate schemes may be evaluated analytically as exemplified, in Chapters 3-5 or numerically in Chapter 2. Finally, the scheme having the best OP may be selected.

According to the above design steps, we summarize the design options for each scheme of this thesis in Table 6.1.

6.3 Future Works

In the context of multi-source relaying networks, there are several open problems, which are detailed as follows:

6.3.1 Theoretical Analysis of MUD-SIC

When the SN's access relies on non-orthogonal SDMA and IC is invoked at the RNs or DNs, the outage events of multiple SNs tend to be correlated. In this thesis, both the ML and the MUD-SIC detection schemes were considered. Specifically, in Chapter 4 and Chapter 5, ML detection was adopted at the RN for detecting the signals received from multiple SNs and the OP may be approximated with the aid of min-SNR techniques. However, as we observed in Chapter 2, when the MUD-SIC is adopted at the DN, the OP of ORS has not been derived in a closed form in Section 2.2.2. Furthermore, as discussed in Chapter 4, when the MUD-SIC is adopted at the RN, the modeling of the data buffer's state at the RN has not been found in a closed form. In this thesis, the OP of the schemes involving MUD-SIC of Section 2.2 and Section 4.1 was evaluated by simulations. Hence, the theoretical OP analysis for MUD-SIC-aided schemes have to be carried out.

6.3.2 Node-Grouping for Spectrum Sharing

In this thesis, our benchmark was the conventional orthogonal multi-source relaying scheme, where the spectrum is shared orthogonally among all SNs. In this case, no CCI is introduced and hence the RNs and DNs may adopt SUD techniques. In order to improve the attainable bandwidth efficiency, we investigated the family of non-orthogonal multi-source relaying schemes, when the SNs in the network access the spectrum either simultaneously using SDMA as in Chapters 2, 4 or adopt network coding as in Chapter 3. In both cases, CCI is introduced, hence more sophisticated MUD techniques such as ML and MUD-SIC methods have to be adopted.

However, the complexity of ML detection increases exponentially with the number of SNs, while the OP of the MUD-SIC may not improve, when the number of co-channel SNs increases, as shown in Fig. 3.12 at high SNRs. Therefore, when there is a large number of SNs in the network, it is not necessarily beneficial for all the SNs to share the spectrum non-orthogonally. This motivated us to divide the SNs, RNs and the DNs into multiple groups, where the spectrum was accessed orthogonally among the groups, while within each group, the non-orthogonal multi-source relaying scheme was adopted for improving the spectrum efficiency. Hence, the node-grouping design has to be studied in detail.

6.3.3 Theoretical Analysis for Amplify-and-Forward Scheme

Although we briefly considered the options of both DF and AF in the context of multi-source relaying networks, we only investigated the DF option in specific detail. If AF is adopted at the relay, the RNs cannot invoke IC, which should be invoked at the DN. The signal model of the system should be modified, where we have to re-design our analytical tools.

6.3.4 Energy Harvesting Based Power Supply

First of all, when EH-based nodes are considered, the schemes proposed for constant power supply should be re-designed for the sake of taking into account of the random power supply provided by the EH system. We have explored a scheme in Chapter 5, as shown in Table 6.1, but there are still numerous open problems. We may apply our discrete-Markov-model based analysis framework to orthogonal-division-multiple-access (ODMA) networks such as TDMA, FDMA and CDMA, in which the EH-SNs access the channel in orthogonal time-frequency-coding resource blocks. In TDMA networks, when the average energy arrival rate is constant and the number of EH-SNs is equal to M, the resulted equivalent average energy arrival rate is effectively increased by a factor of M, since each EH-SN is only occupying a $1/M$ fraction of the time, but may harvest energy for the entire duration. However, in FDMA and CDMA networks, the equivalent average energy arrival rate is still equal to the actual energy arrival rate, since each EH-SN relies on the entire time duration for its transmission.

Bibliography

[1] L. Hanzo, *Near-Capacity Multi-Functional MIMO Systems*. Wiley, 2009.

[2] D. J. Costello and G. D. Forney, "Channel coding: the road to channel capacity," *Proceedings of the IEEE*, vol. 95, pp. 1150–1177, June 2007.

[3] F. Boccardi, R. W. Heath, A. Lozano, T. L. Marzetta, and P. Popovski, "Five disruptive technology directions for 5G," *IEEE Communications Magazine*, vol. 52, pp. 74–80, Feb. 2014.

[4] D. Tse and P. Viswanath, *Fundamentals of wireless communication*. Cambridge University Press, 2005.

[5] A. Nosratinia and T. Hunter, "Cooperative communication in wireless networks," *IEEE Communications Magazine*, no. October, pp. 74–80, 2004.

[6] J. Laneman, D. Tse, and G. Wornell, "Cooperative diversity in wireless networks: efficient protocols and outage behavior," *IEEE Transactions on Information Theory*, vol. 50, pp. 3062–3080, Dec. 2004.

[7] S. Sudevalayam and P. Kulkarni, "Energy harvesting sensor nodes: survey and implications," *IEEE Communications Surveys & Tutorials*, vol. 13, no. 3, pp. 443–461, 2011.

[8] O. Ozel, K. Tutuncuoglu, J. Yang, S. Ulukus, and A. Yener, "Transmission with energy harvesting nodes in fading wireless channels: optimal policies," *IEEE Journal on Selected Areas in Communications*, vol. 29, pp. 1732–1743, Sept. 2011.

[9] D. Gunduz, K. Stamatiou, N. Michelusi, and M. Zorzi, "Designing intelligent energy harvesting communication systems," *IEEE Communications Magazine*, vol. 52, pp. 210–216, Jan. 2014.

[10] L. Hanzo, M. El-Hajjar, and O. Alamri, "Near-capacity wireless transceivers and cooperative communications in the MIMO era: evolution of standards, waveform design, and future perspectives," *Proceedings of the IEEE*, vol. 99, pp. 1343–1385, Aug. 2011.

[11] J. Laneman and G. Wornell, "Distributed space-time-coded protocols for exploiting cooperative diversity in wireless networks," *IEEE Transactions on Information Theory*, vol. 49, pp. 2415–2425, Oct. 2003.

[12] A. Stefanov and E. Erkip, "Cooperative coding for wireless networks," *IEEE Transactions on Communications*, vol. 52, pp. 1470–1476, Sept. 2004.

[13] B. Zhao and M. Valenti, "Practical relay networks: a generalization of hybrid-ARQ," *IEEE Journal on Selected Areas in Communications*, vol. 23, pp. 7–18, Jan. 2005.

[14] K. Azarian, H. El-Gamal, and P. Schniter, "On the achievable diversity-multiplexing tradeoff in half-duplex cooperative channels," *IEEE Transactions on Information Theory*, vol. 51, pp. 4152–4172, Dec. 2005.

[15] Y. Zhao, R. Adve, and T. Lim, "Improving amplify-and-forward relay networks: optimal power allocation versus selection," *IEEE Transactions on Wireless Communications*, vol. 6, pp. 3114–3123, Nov. 2007.

[16] A. Bletsas, H. Shin, and M. Z. Win, "Cooperative communications with outage-optimal opportunistic relaying," *IEEE Transactions on Wireless Communications*, vol. 6, pp. 3450–3460, Sept. 2007.

[17] Y. Jing and H. Jafarkhani, "Single and multiple relay selection schemes and their achievable diversity orders," *IEEE Transactions on Wireless Communications*, vol. 8, pp. 1414–1423, Mar. 2009.

[18] A. Sendonaris, E. Erkip, and B. Aazhang, "User cooperation diversity-part I: system description," *IEEE Transactions on Communications*, vol. 51, pp. 1927–1938, Nov. 2003.

[19] A. Sendonaris, E. Erkip, and B. Aazhang, "User cooperation diversity-part II: implementation aspects and performance analysis," *IEEE Transactions on Communications*, vol. 51, pp. 1939–1948, Nov. 2003.

[20] M. Janani, A. Hedayat, T. Hunter, and A. Nosratinia, "Coded cooperation in wireless communications: space-time transmission and iterative decoding," *IEEE Transactions on Signal Processing*, vol. 52, pp. 362–371, Feb. 2004.

[21] T. Hunter and A. Nosratinia, "Diversity through coded cooperation," *IEEE Transactions on Wireless Communications*, vol. 5, pp. 283–289, Feb. 2006.

[22] T. Hunter, S. Sanayei, and A. Nosratinia, "Outage analysis of coded cooperation," *IEEE Transactions on Information Theory*, vol. 52, pp. 375–391, Feb. 2006.

[23] A. Bletsas, A. Khisti, D. Reed, and A. Lippman, "A simple cooperative diversity method based on network path selection," *IEEE Journal on Selected Areas in Communications*, vol. 24, pp. 659–672, Mar. 2006.

[24] I. Krikidis, J. Thompson, S. Mclaughlin, and N. Goertz, "Max-min relay selection for legacy amplify-and-forward systems with interference," *IEEE Transactions on Wireless Communications*, vol. 8, pp. 3016–3027, June 2009.

[25] C. Zhong, S. Jin, and K.-K. Wong, "Dual-hop systems with noisy relay and interference-limited destination," *IEEE Transactions on Communications*, vol. 58, pp. 764–768, Mar. 2010.

[26] D. Lee and J. H. Lee, "Outage probability for dual-hop relaying systems with multiple interferers over Rayleig fading channels," *IEEE Transactions on Vehicular Technology*, vol. 60, pp. 333–338, Jan. 2011.

[27] H. Yu, I.-h. Lee, and G. L. Stuber, "Outage probability of decode-and-forward cooperative relaying systems with co-channel interference," *IEEE Transactions on Wireless Communications*, vol. 11, pp. 266–274, Jan. 2012.

[28] R. Zhang and L. Hanzo, "Cochannel interference mitigation: active and passive techniques," *IEEE Vehicular Technology Magazine*, vol. 5, pp. 31–39, Dec. 2010.

[29] S. Katti, H. Rahul, W. Hu, D. Katabi, M. Médard, and J. Crowcroft, "XORs in the air: practical wireless network coding," in *Proceedings of the ACM conference on Applications, technologies, architectures, and protocols for computer communication (SIGCOMM)*, vol. 36, (New York, New York, USA), p. 243, ACM Press, Aug. 2006.

[30] S. Katti, S. Gollakota, and D. Katabi, "Embracing wireless interference: analog network coding," in *Proceedings of the ACM conference on Applications, technologies, architectures, and protocols for computer communication (SIGCOMM)*, (New York, New York, USA), p. 397, ACM Press, 2007.

[31] T. Fuja, J. Kliewer, and D. Costello, "A network coding approach to cooperative diversity," *IEEE Transactions on Information Theory*, vol. 53, pp. 3714–3722, Oct. 2007.

[32] E. Larsson, "Collaborative transmit diversity with adaptive radio resource and power allocation," *IEEE Communications Letters*, vol. 9, pp. 511–513, June 2005.

[33] S. Zhang, S. C. Liew, and P. P. Lam, "Hot topic: physical-layer network coding," in *Proceedings of the annual international conference on Mobile computing and networking (MOBICOM)*, vol. 1, (New York, New York, USA), p. 358, ACM Press, 2006.

[34] T. Wang and G. Giannakis, "Complex field network coding for multiuser cooperative communications," *IEEE Journal on Selected Areas in Communications*, vol. 26, pp. 561–571, Apr. 2008.

[35] J. Zheng, N. Ansari, V. Li, X. Shen, H. Hassanein, and B. Zhang, "Network coding for wireless communication networks," *IEEE Journal on Selected Areas in Communications*, vol. 27, pp. 577–581, June 2009.

[36] M. Xiao and M. Skoglund, "Multiple-user cooperative communications based on linear network coding," *IEEE Transactions on Communications*, vol. 58, pp. 3345–3351, Dec. 2010.

[37] J. a. L. Rebelatto, B. F. Uchoa-Filho, Y. Li, and B. Vucetic, "Multiuser cooperative diversity through network coding based on classical coding theory," *IEEE Transactions on Signal Processing*, vol. 60, pp. 916–926, Feb. 2012.

[38] E. Larsson and B. Vojcic, "Cooperative transmit diversity based on superposition modulation," *IEEE Communications Letters*, vol. 9, pp. 778–780, Sept. 2005.

[39] Y. Chen, S. Kishore, and L. Jing, "Wireless diversity through network coding," in *IEEE Wireless Communications and Networking Conference, 2006. WCNC 2006.*, vol. 00, pp. 1681–1686, IEEE, 2006.

[40] T. Ho, M. Medard, R. Koetter, D. Karger, M. Effros, J. Shi, and B. Leong, "A random linear network coding approach to multicast," *IEEE Transactions on Information Theory*, vol. 52, pp. 4413–4430, Oct. 2006.

[41] S. Sharma, Y. Shi, J. Liu, Y. T. Hou, and S. Kompella, "Is network coding always good for cooperative communications?," in *Proceedings of the Conference on Information Communications (INFOCOM)*, vol. 4, pp. 1–9, IEEE, Mar. 2010.

[42] H. V. Nguyen, S. X. Ng, and L. Hanzo, "Performance bounds of network coding aided cooperative multiuser systems," *IEEE Signal Processing Letters*, vol. 18, pp. 435–438, July 2011.

[43] S. Sharma, Y. Shi, J. Liu, Y. T. Hou, S. Kompella, and S. F. Midkiff, "Network coding in cooperative communications: friend or foe?," *IEEE Transactions on Mobile Computing*, vol. 11, pp. 1073–1085, July 2012.

[44] B. Nazer and M. Gastpar, "Compute-and-forward: harnessing interference through structured codes," *IEEE Transactions on Information Theory*, vol. 57, pp. 6463–6486, Oct. 2011.

[45] V. T. Muralidharan and B. S. Rajan, "Physical layer network coding for the K-user multiple access relay channel," *IEEE Transactions on Wireless Communications*, vol. 12, pp. 3107–3119, June 2013.

[46] Z. Chen, P. Fan, and K. B. Letaief, "Compute-and-forward: optimization over multi-source-multi-relay networks," *IEEE Transactions on Vehicular Technology*, vol. 9545, no. c, pp. 1–1, 2014.

[47] M. Di Renzo, "On the achievable diversity of repetition-based and relay selection network-coded cooperation," *IEEE Transactions on Communications*, vol. 62, pp. 2296–2313, July 2014.

[48] J. Lei, R. Yates, and L. Greenstein, "A generic model for optimizing single-hop transmission policy of replenishable sensors," *IEEE Transactions on Wireless Communications*, vol. 8, pp. 547–551, Feb. 2009.

[49] V. Sharma, U. Mukherji, V. Joseph, and S. Gupta, "Optimal energy management policies for energy harvesting sensor nodes," *IEEE Transactions on Wireless Communications*, vol. 9, pp. 1326–1336, Apr. 2010.

[50] B. Medepally and N. B. Mehta, "Voluntary energy harvesting relays and selection in cooperative wireless networks," *IEEE Transactions on Wireless Communications*, vol. 9, pp. 3543–3553, Nov. 2010.

[51] H. Li, N. Jaggi, and B. Sikdar, "Relay scheduling for cooperative communications in sensor networks with energy harvesting," *IEEE Transactions on Wireless Communications*, vol. 10, pp. 2918–2928, Sept. 2011.

[52] J. Yang and S. Ulukus, "Optimal packet scheduling in an energy harvesting communication system," *IEEE Transactions on Communications*, vol. 60, pp. 220–230, Jan. 2012.

[53] J. Yang and S. Ulukus, "Optimal packet scheduling in a multiple access channel with energy harvesting transmitters," *Journal of Communications and Networks*, vol. 14, pp. 140–150, Apr. 2012.

[54] C. Huang, R. Zhang, and S. Cui, "Throughput maximization for the Gaussian relay channel with energy harvesting constraints," *IEEE Journal on Selected Areas in Communications*, vol. 31, pp. 1469–1479, Aug. 2013.

[55] S. Luo, R. Zhang, and T. J. Lim, "Optimal save-then-transmit protocol for energy harvesting wireless transmitters," *IEEE Transactions on Wireless Communications*, vol. 12, pp. 1196–1207, Mar. 2013.

[56] N. Zlatanov, R. Schober, and Z. Hadzi-Velkov, "Asymptotically optimal power allocation for energy harvesting communication networks," pp. 1–40, Aug. 2013.

[57] C. Huang, R. Zhang, and S. Cui, "Optimal power allocation for outage probability minimization in fading channels with energy harvesting constraints," *IEEE Transactions on Wireless Communications*, vol. 13, pp. 1074–1087, Feb. 2014.

[58] J. Xu and R. Zhang, "Throughput optimal policies for energy harvesting wireless transmitters with non-ideal circuit power," *IEEE Journal on Selected Areas in Communications*, vol. 32, pp. 322–332, Feb. 2014.

[59] D. Lee and J. H. Lee, "Outage probability of decode-and-forward opportunistic relaying in a multicell environment," *IEEE Transactions on Vehicular Technology*, vol. 60, pp. 1925–1930, May 2011.

[60] F. Etezadi, K. Zarifi, A. Ghrayeb, and S. Affes, "Decentralized relay selection schemes in uniformly distributed wireless sensor networks," *IEEE Transactions on Wireless Communications*, vol. 11, pp. 938–951, Mar. 2012.

[61] C.-H. Yu and O. Tirkkonen, "Opportunistic multiple relay selection with diverse mean channel gains," *IEEE Transactions on Wireless Communications*, vol. 11, pp. 885–891, Mar. 2012.

[62] C. Gong, A. Tajer, and X. Wang, "Group decoding for multi-relay assisted interference channels," *IEEE Journal on Selected Areas in Communications*, vol. 30, pp. 1489–1499, Sept. 2012.

[63] J. Vicario, A. Bel, J. Lopez-Salcedo, and G. Seco, "Opportunistic relay selection with outdated CSI: outage probability and diversity analysis," *IEEE Transactions on Wireless Communications*, vol. 8, pp. 2872–2876, June 2009.

[64] M. Chen, T. C.-K. Liu, and X. Dong, "Opportunistic multiple relay selection with outdated channel state information," *IEEE Transactions on Vehicular Technology*, vol. 61, pp. 1333–1345, Mar. 2012.

[65] S. Kim, S. Park, and D. Hong, "Performance analysis of opportunistic relaying scheme with outdated channel information," *IEEE Transactions on Wireless Communications*, pp. 1–12, 2013.

[66] Y. Li, Q. Yin, W. Xu, and H.-m. Wang, "On the design of relay selection strategies in regenerative cooperative networks with outdated CSI," *IEEE Transactions on Wireless Communications*, vol. 10, pp. 3086–3097, Sept. 2011.

[67] I. Stanojev, O. Simeone, Y. Bar-Ness, and C. You, "Performance of multi-relay collaborative hybrid-ARQ protocols over fading channels," *IEEE Communications Letters*, vol. 10, pp. 522–524, July 2006.

[68] J. Si, S. Member, Z. Li, and Z. Liu, "Outage probability of opportunistic relaying in Rayleigh fading channels with multiple interferers," *IEEE Signal Processing Letters*, vol. 17, pp. 445–448, May 2010.

[69] V. Lau, "Per-user packet outage analysis in slow multiaccess fading channels with successive interference cancellation for equal rate applications," *IEEE Transactions on Wireless Communications*, vol. 7, pp. 1754–1763, May 2008.

[70] T. H. Cormen, C. Stein, R. L. Rivest, and C. E. Leiserson, *Introduction to algorithms*, vol. 7. McGraw-Hill Higher Education, 2nd ed., 2001.

[71] L. Li, R. G. Maunder, B. M. Al-Hashimi, and L. Hanzo, "A low-complexity turbo decoder architecture for energy-efficient wireless sensor networks," *IEEE Transactions on Very Large Scale Integration (VLSI) Systems*, pp. 1–9, 2011.

[72] A. Nuttall, "Some integrals involving the Q function," *IEEE Transactions on Information Theory*, vol. 21, pp. 95–96, Jan. 1975.

[73] R. Ahlswede, S.-Y. Li, and R. Yeung, "Network information flow," *IEEE Transactions on Information Theory*, vol. 46, pp. 1204–1216, July 2000.

[74] X. Bao and J. Li, "Adaptive network coded cooperation (ANCC) for wireless relay networks: matching code-on-graph with network-on-graph," *IEEE Transactions on Wireless Communications*, vol. 7, pp. 574–583, Feb. 2008.

[75] C. Peng, S. Member, Q. Zhang, and M. Zhao, "On the performance analysis of network-coded cooperation in wireless networks," *IEEE Transactions on Wireless Communications*, vol. 7, pp. 3090–3097, Aug. 2008.

[76] L. Kong, P. Chen, and L. Wang, "Outage probability analysis of a space-time block coding physical-layer nertwork coding," in *International Conference on Wireless Communications & Signal Processing (WCSP)*, pp. 2–7, 2012.

[77] Z. Yi, M. Ju, and I.-m. Kim, "Outage probability and optimum power allocation for analog network coding," *IEEE Transactions on Wireless Communications*, vol. 10, pp. 407–412, Feb. 2011.

[78] R. Louie, Y. Li, and B. Vucetic, "Practical physical layer network coding for two-way relay channels: performance analysis and comparison," *IEEE Transactions on Wireless Communications*, vol. 9, pp. 764–777, Feb. 2010.

[79] A. Pandharipande, "Adaptive two-way relaying and outage analysis," *IEEE Transactions on Wireless Communications*, vol. 8, pp. 3288–3299, June 2009.

[80] Z. Ding, K. K. Leung, D. L. Goeckel, and D. Towsley, "On the study of network coding with diversity," *IEEE Transactions on Wireless Communications*, vol. 8, pp. 1247–1259, Mar. 2009.

[81] G. Wang, W. Xiang, J. Yuan, and T. Huang, "Outage analysis of non-regenerative analog network coding for two-way multi-hop networks," *IEEE Communications Letters*, vol. 15, pp. 662–664, June 2011.

[82] X. Jia, H. Fu, L. Yang, and L. Zhao, "Superposition coding cooperative relaying communications: Outage performance analysis," *International Journal of Communication Systems*, vol. 24, pp. 384–397, Mar. 2011.

[83] A. Zhan, C. He, and L.-G. Jiang, "Outage behavior in wireless networks with analog network coding," *IEEE Transactions on Vehicular Technology*, vol. 61, pp. 3352–3360, Sept. 2012.

[84] S. Sharma, Y. Shi, Y. Hou, H. Sherali, and S. Kompella, "Optimizing network-coded cooperative communications via joint session grouping and relay node selection," in *Proceedings of the conference on Information communications (INFOCOM)*, pp. 1898–1906, IEEE, Apr. 2011.

[85] L. Wang, L. Kong, S. X. Ng, and L. Hanzo, "Code-rate-optimized differentially modulated near-capacity cooperation," *IEEE Transactions on Communications*, vol. 59, pp. 2185–2195, Aug. 2011.

[86] Z. Mobini, P. Sadeghi, M. Khabbazian, and S. Zokaei, "Power allocation and group assignment for reducing network coding noise in multi-unicast wireless systems," *IEEE Transactions on Vehicular Technology*, vol. 61, pp. 3615–3629, Oct. 2012.

[87] N. Zlatanov, A. Ikhlef, T. Islam, and R. Schober, "Buffer-aided cooperative communications: opportunities and challenges," *IEEE Communications Magazine*, vol. 52, pp. 146–153, Apr. 2014.

[88] C. Dong, L.-L. Yang, J. Zuo, S. X. Ng, and L. Hanzo, "Minimum average end-to-end packet energy dissipation of a buffer-aided three-node network relying on opportunistic routing," *Submitted to IEEE Transactions on Communications.*

[89] N. Zlatanov, Z. Hadzi-Velkov, G. K. Karagiannidis, and R. Schober, "Cooperative diversity with mobile nodes: capacity outage rate and duration," *IEEE Transactions on Information Theory*, vol. 57, pp. 6555–6568, Oct. 2011.

[90] N. Zlatanov, R. Schober, and P. Popovski, "Buffer-aided relaying with adaptive link selection," *IEEE Journal on Selected Areas in Communications*, vol. 31, pp. 1530–1542, Aug. 2013.

[91] L.-L. Yang, C. Dong, and L. Hanzo, "Multihop diversity - a precious source of fading mitigation in multihop wireless networks," in *IEEE Global Telecommunications Conference (GLOBECOM)*, pp. 1–5, IEEE, Dec. 2011.

[92] C. Dong, L.-L. Yang, and L. Hanzo, "Performance analysis of multihop-diversity-aided multihop links," *IEEE Transactions on Vehicular Technology*, vol. 61, pp. 2504–2516, July 2012.

[93] C. Dong, L.-L. Yang, and L. Hanzo, "Multihop diversity for fading mitigation in multihop wireless networks," in *IEEE Vehicular Technology Conference (VTC'11-Fall), San Francisco, CA, USA*, pp. 1–5, Sept. 2011.

[94] C. Dong, L.-L. Yang, and L. Hanzo, "Multi-hop diversity aided multi-hop communications: a cumulative distribution function aware approach," *IEEE Transactions on Communications*, vol. 61, pp. 4486–4499, Nov. 2013.

[95] C. Dong, L.-L. Yang, J. Zuo, S. Ng, and L. Hanzo, "Maximum throughput adaptive rate transmission scheme for multihop diversity aided multihop links," in *IEEE International Conference on Communications (ICC'14), Syndey, Australia*, pp. 1–5, Jun. 2014.

[96] C. Dong, L.-L. Yang, and L. Hanzo, "Adaptive modulation for multihop communications exploiting multihop diversity," *Submitted to IEEE Transactions on Wireless Communications*.

[97] C. Dong, J. Zuo, L.-L. Yang, Y. Huo, S. Ng, and L. Hanzo, "Energy-efficient buffer-aided relaying relying on non-linear channel probability space division," in *IEEE Wireless Communications and Networking Conference (WCNC'14), Istanbul, Turkey*, pp. 1–5, Apr. 2014.

[98] C. Dong, J. Zuo, L.-L. Yang, Y. Huo, S. X. Ng, and L. Hanzo, "On buffer-assisted opportunistic routing relying on linear transmission activation probability space partitioning for relay-aided networks," in *IEEE Vehicular Technology Conference (VTC'14-Fall), Vancouver, Canada*, pp. 1–5, Sep. 2014.

[99] G. Li, C. Dong, J. Zuo, D. Liu, G. Li, and Y. Zhang, "Outage analysis of dual-hop transmission with buffer aided amplify-and-forward relay," in *IEEE Vehicular Technology Conference (VTC'14-Fall), Vancouver, Canada*, pp. 1–5, Sep. 2014.

[100] I. Krikidis, T. Charalambous, and J. S. Thompson, "Buffer-aided relay selection for cooperative diversity systems without delay constraints," *IEEE Transactions on Wireless Communications*, vol. 11, pp. 1957–1967, May 2012.

[101] Z. Ding and K. K. Leung, "On the combination of cooperative diversity and network coding for wireless uplink transmissions," *IEEE Transactions on Vehicular Technology*, vol. 60, pp. 1590–1601, May 2011.

[102] H. V. Nguyen, C. Xu, S. X. Ng, and L. Hanzo, "Non-coherent near-capacity network coding for cooperative multi-user communications," *IEEE Transactions on Communications*, vol. 60, pp. 3059–3070, Oct. 2012.

[103] M. Dai, H. Y. Kwan, and C. W. Sung, "Linear network coding strategies for the multipale access relay channel with packet erasures," *IEEE Transactions on Wireless Communications*, vol. 12, pp. 218–227, Jan. 2013.

[104] M. Di Renzo, M. Iezzi, and F. Graziosi, "Error performance and diversity analysis of multi-source multi-relay wireless networks with binary network coding and cooperative MRC," *IEEE Transactions on Wireless Communications*, vol. 12, pp. 2883–2903, June 2013.

[105] B. Zhang, M. El-Hajjar, and L. Hanzo, "Opportunistic relay selection for cooperative relaying in co-channel interference contaminated networks," *IEEE Transactions on Vehicular Technology*, pp. 1–1, 2014.

[106] Z. Han, X. Zhang, and H. Poor, "High performance cooperative transmission protocols based on multiuser detection and network coding," *IEEE Transactions on Wireless Communications*, vol. 8, pp. 2352–2361, May 2009.

[107] J. D. C. Little, "A proof for the queuing formula: L = λW," *Operations Research*, vol. 9, no. 3, pp. 383–387, 1961.

[108] M. Hasna and M.-S. Alouini, "Optimal power allocation for relayed transmissions over Rayleigh-fading channels," *IEEE Transactions on Wireless Communications*, vol. 3, pp. 1999–2004, Nov. 2004.

[109] C. Huang, R. Zhang, and S. Cui, "Outage minimization in fading channels under energy harvesting constraints," *IEEE International Conference on Communications (ICC)*, pp. 5788–5793, June 2012.

[110] Y. Mao, G. Yu, and Z. Zhang, "On the optimal transmission policy in hybrid energy supply wireless communication systems," *IEEE Transactions on Wireless Communications*, vol. XX, no. XX, pp. 1–1, 2014.

[111] M. Sniedovich, *Dynamic Programming: Foundations and Principles*. Taylor & Francis, 2010.

[112] C. K. Ho and R. Zhang, "Optimal energy allocation for wireless communications with energy harvesting constraints," *IEEE Transactions on Signal Processing*, vol. 60, pp. 4808–4818, Sept. 2012.

[113] Z. Wang, V. Aggarwal, and X. Wang, "Power allocation for energy harvesting transmitter with causal information," vol. 10027, pp. 1–29, Jan. 2014.

[114] K.-h. Liu, "Selection cooperation using RF energy harvesting relays with finite energy buffer," in *IEEE Wireless Communications and Networking Conference (WCNC)*, vol. 00, pp. 2186–2191, 2014.

[115] F. Iannello, O. Simeone, and U. Spagnolini, "Medium access control protocols for wireless sensor networks with energy harvesting," *IEEE Transactions on Communications*, vol. 60, pp. 1381–1389, May 2012.

[116] H. Li, C. Huang, S. Cui, and J. Zhang, "Distributed opportunistic scheduling for wireless networks powered by renewable energy sources," in *IEEE International Conference on Computer Communications (Infocom)*, 2014.

[117] Z. Wang, V. Aggarwal, and X. Wang, "Iterative dynamic water-filling for fading multiple-access channels with energy harvesting," vol. 10027, pp. 1–34, Jan. 2014.

[118] I. Krikidis, S. Timotheou, and S. Sasaki, "RF energy transfer for cooperative networks: data relaying or energy harvesting?," *IEEE Communications Letters*, vol. 16, pp. 1772–1775, Nov. 2012.

[119] K. Ishibashi, H. Ochiai, and V. Tarokh, "Energy harvesting cooperative communications," in *IEEE 23rd International Symposium on Personal, Indoor and Mobile Radio Communications - (PIMRC)*, pp. 1819–1823, IEEE, Sept. 2012.

[120] A. A. Nasir, X. Zhou, S. Durrani, and R. A. Kennedy, "Relaying protocols for wireless energy harvesting and information processing," *IEEE Transactions on Wireless Communications*, vol. 12, pp. 3622–3636, July 2013.

[121] Y. Luo, J. Zhang, and K. B. Letaief, "Optimal scheduling and power allocation for two-hop energy harvesting communication systems," *IEEE Transactions on Wireless Communications*, vol. 12, pp. 4729–4741, Sept. 2013.

[122] K. Tutuncuoglu and A. Yener, "Cooperative energy harvesting communications with relaying and energy sharing," *2013 IEEE Information Theory Workshop (ITW)*, pp. 1–5, Sept. 2013.

[123] Z. Ding, S. M. Perlaza, I. Esnaola, and H. V. Poor, "Power allocation strategies in energy harvesting wireless cooperative networks," *IEEE Transactions on Wireless Communications*, vol. 13, pp. 846–860, Feb. 2014.

[124] B. Gurakan, O. Ozel, J. Yang, and S. Ulukus, "Energy cooperation in energy harvesting communications," *IEEE Transactions on Communications*, vol. 61, pp. 4884–4898, Dec. 2013.

[125] R. Gallager, *Discrete Stochastic Processes*. MIT OpenCourseWare: Massachusetts Institute of Technology, 2011.

[126] V. Kulkarni, A. Forster, and G. Venayagamoorthy, "Computational intelligence in wireless sensor networks: A survey," *Communications Surveys & Tutorials, IEEE*, vol. 13, no. 99, pp. 1–29, 2011.

[127] B. Zhang, C. Dong, J. Lei, M. El-hajjar, L.-l. Yang, and L. Hanzo, "Buffer-aided relaying for the multi-user uplink : outage analysis and power allocation." 2014.

[128] C. Intanagonwiwat, R. Govindan, D. Estrin, J. Heidemann, and F. Silva, "Directed diffusion for wireless sensor networking," *IEEE/ACM Transactions on Networking*, vol. 11, pp. 2–16, Feb. 2003.

[129] Y. Hou, H. Sherali, and S. Midkiff, "On energy provisioning and relay node placement for wireless sensor networks," *IEEE Transactions on Wireless Communications*, vol. 4, pp. 2579–2590, Sept. 2005.

Author Index

Subject Index